

**LA-14018**

*Approved for public release;  
distribution is unlimited.*

**Safeguards Science and Technology  
Group NIS-5**

**Nonproliferation and International  
Security Division**

# **Application Guide to Gamma-Ray Isotopic Analysis Using the FRAM Software**

Edited by Heather L. Edwards, Weirich and Associates, for Group IM-1

Los Alamos National Laboratory, an affirmative action/equal opportunity employer, is operated by the University of California for the United States Department of Energy under contract W-7405-ENG-36.

This report was prepared as an account of work sponsored by an agency of the United States Government. Neither the Regents of the University of California, the United States Government nor any agency thereof, nor any of their employees make any warranty, express or implied, or assume any legal liability or responsibility for the accuracy, completeness, or usefulness of any information, apparatus, product, or process disclosed, or represent that its use would not infringe privately owned rights. Reference herein to any specific commercial product, process, or service by trade name, trademark, manufacturer, or otherwise does not necessarily constitute or imply its endorsement, recommendation, or favoring by the Regents of the University of California, the United States Government, or any agency thereof. The views and opinions of authors expressed herein do not necessarily state or reflect those of the Regents of the University of California, the United States Government, or any agency thereof. Los Alamos National Laboratory strongly supports academic freedom and a researcher's right to publish; as an institution, however, the Laboratory does not endorse the viewpoint of a publication or guarantee its technical correctness.

LA-14018  
Issued: September 2003

---

Application Guide  
to Gamma-Ray  
Isotopic Analysis  
Using the FRAM Software

Thomas E. Sampson  
Thomas A. Kelley  
Duc T. Vo



## CONTENTS

ABSTRACT .....	1
I. INTRODUCTION .....	2
A. Purpose of This Application Guide.....	2
B. Isotopic Analysis Applications in Nondestructive Assay .....	2
1. Calorimetry.....	2
2. Neutron Coincidence Counting.....	3
3. Other Bulk Measurement Techniques.....	4
4. Process Control .....	5
5. Treaty Verification.....	5
6. Confirmation Measurements .....	5
II. BASIC PRINCIPLES OF GAMMA-RAY ISOTOPIC ANALYSIS FOR THE ARBITRARY SAMPLE	6
A. Methods for Obtaining Isotopic Fractions Using Gamma Rays .....	6
B. Calibrated Absolute Measurements.....	6
C. Ratio Measurements for the Arbitrary Sample—Without Efficiency Corrections.....	7
D. The Intrinsic Self-Calibration Technique.....	8
1. Isotopic Ratio Measurement.....	8
2. Assumption of Isotopic Homogeneity.....	9
E. The Relative Efficiency Concept .....	10
F. Relative Efficiency Models.....	11
1. Piecewise Linear.....	11
2. Spline Fitting .....	13
3. Polynomial Least-squares Fitting .....	13
4. Physical Model (Gunnink).....	13
5. Physical Model (Vo).....	14
6. Heterogeneous Relative-Efficiency Models .....	15
III. ISOTOPIC ANALYSIS DEVELOPMENT AT THE LOS ALAMOS NATIONAL LABORATORY ...	16
IV. FRAM DEVELOPMENT .....	18
A. Factors Influencing Development.....	18
1. Interferences .....	18
2. Heterogeneous Am/Pu .....	18
3. Additional Versatility .....	18
4. Existing Approaches and Development.....	19
B. VAX Version of FRAM.....	19
C. PC/FRAM Development.....	21
1. Single Detector System.....	22
2. Choice of Detector Types .....	22
3. Shielded Samples .....	22
4. Uranium Isotopic Analysis.....	23
D. Version/Feature History of PC/FRAM .....	23
1. Version 1.....	23
2. Version 2.....	23
3. Version 3.....	24
4. Version 4.....	25

V.	HOW FRAM WORKS.....	27
A.	Obtain Data.....	27
B.	Perform Analysis .....	27
	1. Internal Calibrations .....	27
	2. Analysis of Spectral Data.....	29
VI.	PARAMETER FILES, THE KEY TO FRAM'S VERSATILITY.....	33
A.	What are Parameter Files?.....	33
B.	The Change Parameter Utility.....	33
C.	Analysis Parameters.....	35
	1. Fitting Parameters .....	35
	2. Gamma-Ray Peak Data.....	37
	3. Analysis Region Definition .....	39
	4. Isotope Information .....	40
	5. Application Constants.....	40
VII.	FRAM USER INTERFACE.....	45
A.	FRAM Main Menu .....	45
B.	Main Menu Options.....	45
	1. File .....	45
	2. Edit .....	45
	3. Measure .....	46
	4. Options .....	48
	5. Help .....	49
C.	Password Protection .....	49
D.	Dual Language Capability.....	50
VIII.	FRAM COMPUTER REQUIREMENTS.....	51
IX.	FRAM PERFORMANCE .....	52
A.	Measurement Precision or Repeatability .....	52
	1. Definitions .....	52
	2. Influencing Factors.....	53
	3. Prediction of Precision in the FRAM Code .....	60
	4. Examples of FRAM's Statistical Precision .....	63
B.	Measurement Bias .....	67
	1. Introduction .....	67
	2. Plutonium Measurement Bias .....	68
	3. Uranium Measurement Bias .....	71
	4. MOX Measurement Bias .....	73
C.	Intercomparison Exercises .....	75
	1. The PIDIE Exercise .....	75
	2. Uranium Enrichment Measurement Exercise, IRMM 1996 .....	75
	3. The Pu-2000 Exercise.....	76
D.	Factors Influencing Measurement Bias.....	78
	1. Sample Composition Characteristics .....	78
	2. Branching Ratios .....	78
	3. Coincidence Summing .....	78
	4. Peak Area Determination .....	79

E.	<b>Bias Correction .....</b>	<b>82</b>
1.	<b>Adjustment of Branching Ratios .....</b>	<b>82</b>
2.	<b>Branching Ratio Values .....</b>	<b>82</b>
3.	<b>Observation of Peak Area Biases .....</b>	<b>82</b>
4.	<b>Least-Squares Adjustment of Branching Ratios .....</b>	<b>83</b>
5.	<b>Use of Standards .....</b>	<b>84</b>
X.	<b>MAKING MEASUREMENTS FOR FRAM ANALYSIS .....</b>	<b>85</b>
A.	<b>Choice of Detector .....</b>	<b>85</b>
B.	<b>Choice of Energy Range .....</b>	<b>86</b>
C.	<b>Collection of Pulse Height Spectra .....</b>	<b>88</b>
1.	<b>Electronics.....</b>	<b>88</b>
2.	<b>Electronics Interconnections and Settings.....</b>	<b>89</b>
3.	<b>Counting Rate Considerations .....</b>	<b>91</b>
4.	<b>Pulse Pileup.....</b>	<b>93</b>
5.	<b>Filtering .....</b>	<b>94</b>
6.	<b>Shielding.....</b>	<b>96</b>
XI.	<b>MODIFYING PARAMETER FILES FOR SPECIAL CASES .....</b>	<b>99</b>
A.	<b>Standard Parameter Files .....</b>	<b>99</b>
B.	<b>General Approach to Parameter File Modification .....</b>	<b>99</b>
1.	<b>Start With Existing Parameter File .....</b>	<b>99</b>
2.	<b>Set Energy Calibration Defaults and Isotopes for Analysis .....</b>	<b>99</b>
3.	<b>Select Gamma-Ray Peaks for Analysis .....</b>	<b>100</b>
4.	<b>Select Regions for Analysis .....</b>	<b>100</b>
5.	<b>Select Peaks for Internal Calibrations .....</b>	<b>100</b>
6.	<b>Edit Application Constants.....</b>	<b>101</b>
C.	<b>Discussion of Special Cases .....</b>	<b>101</b>
1.	<b>Very Low Plutonium-240 .....</b>	<b>101</b>
2.	<b>Very High Plutonium-240 .....</b>	<b>102</b>
3.	<b>Very High Neptunium-237 .....</b>	<b>103</b>
4.	<b>Very High Americium-241 .....</b>	<b>105</b>
5.	<b>Heterogeneous Am/Pu .....</b>	<b>106</b>
6.	<b>Plutonium with Cs-137 Interference.....</b>	<b>107</b>
7.	<b>Uranium with Cs-137 Interference.....</b>	<b>108</b>
8.	<b>Heat Source Grade Pu-238.....</b>	<b>108</b>
9.	<b>Uranium-Plutonium Mixed Oxide (MOX) .....</b>	<b>109</b>
10.	<b>Am-243–Np-239 .....</b>	<b>110</b>
11.	<b>Physically, Spatially, and Isotopically Heterogeneous Waste .....</b>	<b>110</b>
XII.	<b>DIFFICULT MEASUREMENT SITUATIONS .....</b>	<b>112</b>
A.	<b>Using FRAM With Rate-Loss Correction Sources.....</b>	<b>112</b>
B.	<b>Simultaneous FRAM/AWCC Measurements .....</b>	<b>112</b>
C.	<b>Measurements Through Thick Shielding .....</b>	<b>113</b>
1.	<b>Steel Shielding .....</b>	<b>113</b>
2.	<b>Lead Shielding .....</b>	<b>116</b>
3.	<b>9975 Shipping Container.....</b>	<b>117</b>
D.	<b>Measurements on Am-Be Neutron Sources .....</b>	<b>119</b>

XIII. FRAM APPLICATION WITH CADMIUM TELLURIDE (CDTE) DETECTORS .....	120
XIV. FRAM APPLICATIONS IN AUTOMATED SYSTEMS .....	123
A. ROBOCAL .....	123
1. Intelligent Isotopic Unit Autoanalysis.....	123
2. Intelligent Isotopic Unit Hardware.....	124
B. ARIES NDA System .....	125
REFERENCES.....	128
APPENDIX A .....	134
APPENDIX D .....	149
APPENDIX E .....	161
APPENDIX F.....	162

## List of Abbreviations and Acronyms

ADC	analog-to-digital Converter	MC&A	measurement control and accounting.
ARIES	Advanced Retirement and Integrated Extraction System	MeV	million electron volts
ASTM	American Society for Testing and Materials	MGAU	multi group analysis, uranium
AWCC	active well coincidence counter	MOX	mixed oxide
CRM	certified reference material	mfp	mean free path
DEC	Digital Equipment Corporation	MS	mass spectroscopy
DOE	Department of Energy	MUDPI	Multiple Detector Plutonium Isotopic System
ESARDA	European Safeguards Research and Development Agency	NDA	nondestructive assay
FRAM	Fixed energy, Response function Analysis with Multiple efficiencies. Also a Scandinavian word meaning “forward” or “onward.” The name of the Los Alamos gamma-ray isotopic analysis software.	NIM	nuclear instrumentation module
		PIDIE	Plutonium Isotopic Determination Intercomparison Exercise
		PANDA	passive nondestructive assay of nuclear materials
		ppm	parts per million
		R&D	research and development
FWHM	full width at half maximum	RF	Russian Federation
HEU	highly enriched uranium	ROBOCAL	Robotic Calorimetry and Gamma Ray Isotopic System
HPGe	high-purity germanium	ROI	region of interest
IAEA	International Atomic Energy Agency	RSD	relative standard deviation
IIU	intelligent isotopic unit	SAI	solution assay instrument
IRMM	Institute of Reference Materials and Measurements	SGS	segmented gamma scanner
keV	kilo electron volts	SNM	special nuclear material
LAPIS	Los Alamos Plutonium Isotopic System	TASTEX	Tokai Advanced Safeguards Exercise
LA-UR	Los Alamos unlimited release	TCPA	transmission-corrected passive assay
LANL	Los Alamos National Laboratory	TGS	tomographic gamma scanner
LLNL	Lawrence Livermore National Laboratory	UMCBI	universal multichannel buffer interface
MBA	material balance area	US	United States
MCA	multichannel analyzer	WIPP	Waste Isolation Pilot Plant
MCB	multichannel buffer		



# **Application Guide to Gamma-Ray Isotopic Analysis Using the FRAM Software**

Thomas E. Sampson, Thomas A. Kelley, and Duc T. Vo

## **ABSTRACT**

The FRAM Application Guide discusses in detail the development, performance, and application of the PC/FRAM gamma-ray isotopic analysis code.

After discussing the basic principles of gamma-ray isotopic analysis, we describe the development of gamma-ray isotopic analysis at Los Alamos and the conditions that led to the development of PC/FRAM. The version and feature history of all four (as of this writing) versions of FRAM is outlined and is followed by a detailed discussion of how FRAM works.

We document the performance of FRAM (measurement bias and measurement precision and repeatability) for isotopic analysis of gamma ray spectra from a wide range of plutonium and uranium samples. Because good performance can only arise from high-quality data, we also describe and recommend measurement conditions and practices to assure the best possible data for FRAM analysis.

We also discuss the parameter file structure of the FRAM software and describe in detail how the experienced spectroscopist can tailor FRAM to essentially any isotopic analysis application.

The FRAM Application Guide concludes by describing automated systems, FRAM application to CdTe detector spectra, and the extreme measurement analysis problems successfully completed by FRAM.

### I. INTRODUCTION

#### A. Purpose of This Application Guide

This application guide is written to provide information and guidance to the users of the FRAM\* gamma-ray isotopic analysis software, used in many nondestructive assay (NDA) and materials control and accounting (MC&A) applications. This guide will cover all aspects of the FRAM software, including usage, development history, algorithms, parameter files, performance, and measurement applications.

The Department of Energy (DOE), National Nuclear Security Administration, Office of Policy Integration and Technical Support (SO-13) is the sponsor for this application guide.

#### B. Isotopic Analysis Applications in Nondestructive Assay

##### 1. Calorimetry.

A calorimeter (Likes 91a, Likes 91b, Bracken 02, ASTM 00) measures the heat produced by a sample of special nuclear material (SNM), the heat arising primarily from the alpha decay of the isotopes making up the SNM. Calorimetry is most widely used to quantify plutonium and americium in plutonium-bearing items. Elemental plutonium almost always contains a mixture of isotopes, with  $^{238}\text{Pu}$ ,  $^{239}\text{Pu}$ ,  $^{240}\text{Pu}$ ,  $^{241}\text{Pu}$ ,  $^{242}\text{Pu}$ , and  $^{241}\text{Am}$  present in most plutonium-bearing items. Each isotope produces a characteristic amount of heat proportional to its decay rate and decay energy. This decay heat, when quantified per gram of isotope, is called the specific power, has the customary units of watts/gram isotope, and is denoted by  $P_i$ . The specific powers can be calculated from fundamental principles and can also be directly measured from pure isotopes. The accepted values for the specific powers of the plutonium isotopes and  $^{241}\text{Am}$  are given in Table I-1 (ASTM 00).

Table I-1. Specific Power Values for the Isotopes of Plutonium.

Isotope	Half Life (yr)	Specific Power (mW/g isotope)	Standard Deviation (mW/g isotope)
$^{238}\text{Pu}$	87.74	567.57	0.26
$^{239}\text{Pu}$	24119	1.9288	0.0003
$^{240}\text{Pu}$	6564	7.0824	0.002
$^{241}\text{Pu}$	14.348	3.412	0.002
$^{242}\text{Pu}$	376300	0.1159	0.0003
$^{241}\text{Am}$	433.6	114.2	0.42

---

\* FRAM is the name of the gamma-ray isotopic analysis software developed over the years in the Safeguards Science and Technology Group, NIS-5, at the Los Alamos National Laboratory (LANL). FRAM is a word of Scandinavian origin meaning "forward" or "onward". It is also an acronym of the general features of the code, Fixed energy, Response function Analysis with Multiple efficiencies.

## I. INTRODUCTION

---

The total power  $W$  from a mixture of isotopes is the sum of the power from each heat-producing isotope.

$$W = \sum_i m_i P_i \quad . \quad (I-1)$$

Here  $m_i$  is the mass of the  $i$ th isotope and  $P_i$  is the specific power of the  $i$ th isotope with the sum taken over all heat-producing isotopes, most usually those in Table I-1. Now, define  $R_i$  as the mass fraction  $m_i/M$  where  $M$  is the total mass of all the plutonium isotopes; Eq. I-1 becomes

$$W = M \sum_i R_i P_i \quad . \quad (I-2)$$

This equation allows us to define the effective specific power  $P_{eff}$  in units of watts/gram of plutonium by

$$P_{eff} = \sum_i R_i P_i \quad . \quad (I-3)$$

$P_{eff}$  is the important factor required to convert the watts measured by the calorimeter to grams of elemental plutonium. In terms of  $P_{eff}$ , the mass of elemental plutonium (all the heat-producing isotopes) is given by

$$M = W / P_{eff} \quad (I-4)$$

where  $W$  is the measured watts from the calorimeter, and  $P_{eff}$  in units of watts/gram of plutonium is the effective specific power.

$P_{eff}$  is most often determined from knowledge of the plutonium isotopic composition and  $^{241}\text{Am}$  content of the measured item. The isotopic composition information can come from destructive mass spectrometry measurements or from nondestructive gamma-ray isotopic analysis measurements. The latter method is one of the principal applications of FRAM. The characteristics and errors involved in the measurement of  $P_{eff}$  by FRAM will be discussed in detail in other sections of this guide.

### 2. Neutron Coincidence Counting.

The even isotopes of plutonium ( $^{238}\text{Pu}$ ,  $^{240}\text{Pu}$ , and  $^{242}\text{Pu}$ ) have large spontaneous fission yields that dominate the spontaneous fission neutron output from plutonium. The spontaneous fission neutron yields of the plutonium isotopes are shown in Table I-2 (Ensslin 91a).

Table I-2. Spontaneous Fission Neutron Yields from the Isotopes of Plutonium.

Isotope	Spontaneous Fission Yield (n/s-g)
$^{238}\text{Pu}$	$2.59 \times 10^3$
$^{239}\text{Pu}$	$2.18 \times 10^{-2}$
$^{240}\text{Pu}$	$1.02 \times 10^3$
$^{241}\text{Pu}$	$5 \times 10^{-2}$
$^{242}\text{Pu}$	$1.72 \times 10^3$

Spontaneous fission neutron emission, in conjunction with sensitive neutron-coincidence counting systems, provides a widely used measurement technique (Ensslin 98, Reilly 91). All three of the even

## I. INTRODUCTION

---

isotopes contribute to the response of a neutron-coincidence counter. The contribution from  $^{240}\text{Pu}$  dominates, however, for most plutonium-bearing materials. For this reason it is customary to define the effective  $^{240}\text{Pu}$  mass by

$$^{240}\text{Pu}_{\text{eff}} = 2.52 * ^{238}\text{Pu} + ^{240}\text{Pu} + 1.68 * ^{242}\text{Pu} \quad (\text{I-5})$$

where  $^{240}\text{Pu}_{\text{eff}}$  is the mass of  $^{240}\text{Pu}$  that would give the same coincidence response as that observed from the actual measured item.

Clearly, if we know  $^{240}\text{Pu}_{\text{eff}}$  mass from a coincidence counting measurement, we also need to know the isotopic distribution of the plutonium to determine the elemental plutonium mass. Therefore, we define the effective  $^{240}\text{Pu}$  fraction in an analogous fashion by

$$\text{fract}^{240}\text{Pu}_{\text{eff}} = 2.52 * \text{fract}^{238}\text{Pu} + \text{fract}^{240}\text{Pu} + 1.68 * \text{fract}^{242}\text{Pu} . \quad (\text{I-6})$$

The isotopic fractions are obtained from either destructive analysis (mass spectrometry) or from nondestructive gamma-ray isotopic analysis. This yields the elemental plutonium mass in a fashion completely analogous to calorimetry as

$$M = \text{grams } ^{240}\text{Pu}_{\text{eff}} / \text{fract}^{240}\text{Pu}_{\text{eff}} \quad (\text{I-7})$$

where grams  $^{240}\text{Pu}_{\text{eff}}$  comes from the neutron-coincidence counting measurement of the bulk item and  $\text{fract}^{240}\text{Pu}_{\text{eff}}$  comes from the isotopic analysis measurement. In addition to the isotopic information required in computing  $\text{fract}^{240}\text{Pu}_{\text{eff}}$ , coincidence counting also requires knowledge of the complete isotopic distribution, including  $^{241}\text{Am}$ , for computing sample  $(\alpha, n)$  rates for multiplication corrections.

### 3. Other Bulk Measurement Techniques.

#### a. Active Well Coincidence Counter.

The active well coincidence counter (AWCC) uses AmLi neutron sources mounted above and below the assay chamber in a coincidence counter body to induce fissions in isotopes not having significant spontaneous fission activity. The induced-fission neutrons are quantified with standard coincidence counting techniques. The primary use of this detector is for measuring  $^{235}\text{U}$  and, as with nearly all bulk NDA techniques, the AWCC is only sensitive to a particular isotope or isotopes, not the entire element. Thus, for application to  $^{235}\text{U}$  in the AWCC, we require knowledge of the  $^{235}\text{U}$  isotopic fraction. Nondestructive gamma-ray isotopic analysis can provide this information for most measured items. The FRAM software was the first gamma-ray isotopic analysis code to demonstrate measurements on uranium (Sampson 90) and today is the most versatile code, being able to analyze more types of uranium materials than any other software.

#### b. Segmented Gamma Scanner.

The segmented gamma scanner (SGS) uses transmission-corrected passive assay techniques (Parker 91) to quantify individual isotopes (usually  $^{239}\text{Pu}$  or  $^{235}\text{U}$ ) in items of scrap and waste. Because only individual isotopes are measured, we require knowledge of the isotopic composition to convert the isotope measurement to elemental mass. The isotopic composition measurement is especially needed if the measured streams have variable isotopic composition. In other cases, such as streams of weapons-grade plutonium or highly enriched uranium (HEU), isotopic measurements can be avoided and the well-known stream average values can be used instead.

## I. INTRODUCTION

---

The tomographic gamma scanner (TGS) (Prettyman 93, Mercer 02) is a three-dimensional analog to the SGS and requires the same type of isotopic information (Mercer 99) as does the SGS.

### c. Solution Assay Instrument.

The solution assay instrument (SAI) also uses transmission-corrected passive assay techniques to quantify individual isotopes in solution samples. The use of the information provided by isotopic composition measurements is similar to that in the application of the SGS.

### 4. Process Control

There are numerous applications of gamma-ray isotopic analysis in providing information necessary for the control of various fabrication processes. Isotopic analysis may be required any time material from two different batches is mixed to produce a product that must meet designated specifications.

One example might be that of blending materials with different  $^{240}\text{Pu}$  fractions to meet a given "weapons grade" specification. Another application is blending plutonium from different batches to produce mixed-oxide (MOX) fuel. In this case, the important parameter is usually the  $^{239}\text{Pu}$  fraction. These operations are facilitated if the requisite isotopic analysis measurements can be made nondestructively. The accuracy and precision of the NDA measurement relative to alternative techniques such as mass spectrometry must be weighed against its convenience and the requirements of the blending specification.

### 5. Treaty Verification.

Arms control and plutonium disposition negotiations between the United States (US) and the Russian Federation (RF) are considering the disposition of plutonium from dismantled Russian nuclear weapons. The treaties and agreements arising from these negotiations contain requirements to verify the amount and isotopic composition of the plutonium declared as coming from dismantled weapons. A problem that arises is that in Russia the isotopic composition of the plutonium used in Russian weapons is classified. The US and the RF have agreed to declare plutonium with a  $^{240}\text{Pu}/^{239}\text{Pu}$  ratio of less than 0.1 as "weapons grade." Nondestructive gamma-ray isotopic analysis techniques are applied behind an information barrier to verify this ratio without revealing the detailed isotopic composition.

The Russian Weapons Plutonium Conversion Line will take plutonium from dismantled weapons, mix it with fuel grade plutonium and produce  $\text{PuO}_2$  for MOX fuel with, again, a  $^{240}\text{Pu}/^{239}\text{Pu}$  ratio of less than 0.1. Gamma-ray isotopic analysis will be used to determine the proper mixing ratios and also to verify the isotopic composition of the output  $\text{PuO}_2$ .

### 6. Confirmation Measurements

The US DOE regulations often require confirmation measurements when materials are moved between material balance areas (MBAs) or between facilities. These measurements are not meant to quantify the SNM but to measure attributes of the item to confirm that it contains the type of material specified.

The isotopic composition of the plutonium in the item is one important attribute that is often measured. These measurements often place exacting requirements on the gamma-ray isotopic analysis software because most facilities want to do these measurements rapidly and without removing the items from the shipping container. This leads to requirements to measure items through the walls of various shipping containers. Fortunately, measurements of this type usually do not have to be as precise as accountability or verification measurements. Isotopic verification measurements are usually quite straightforward with the use of appropriate isotopic analysis software and an appropriate detector.

### II. BASIC PRINCIPLES OF GAMMA-RAY ISOTOPIC ANALYSIS FOR THE ARBITRARY SAMPLE

#### A. Methods for Obtaining Isotopic Fractions Using Gamma Rays

Gamma-ray isotopic analysis methods rely on straightforward application of basic gamma-ray spectrometry principles by relating photopeak areas to isotope activity and hence to isotopic fractions. Early methods used absolute counting principles requiring strict control of the sample and measurement geometry. The next advance made use of ratio measurements of neighboring gamma-ray lines from different isotopes, reducing the requirement for sample and geometry control. The most modern techniques correct the isotopic ratios for efficiency differences between the energies of the peaks forming the isotopic ratio. The following sections in this chapter discuss each of these methods in more detail.

#### B. Calibrated Absolute Measurements

Some of the very first gamma-ray isotopic analysis measurements were developed starting in the mid-1970s at the Lawrence Livermore National Laboratory (LLNL) for application to solution samples. These measurements were made with small, approximately 1-cm<sup>3</sup> planar high-purity germanium (HPGe) detectors with resolution of about 530–550 eV at 122 keV. The procedures developed by LLNL used a highly controlled geometry that placed a plutonium-bearing solution sample right in front of the detector. (Gunnink 74) The method used absolute counting techniques in the energy region from 40–60 keV for solutions separated from <sup>241</sup>Am and <sup>237</sup>U and similar techniques in the 100-keV region for aged plutonium solutions.

The methods used to analyze the spectral data grew out of the computerized methods developed by Gunnink and coworkers in the early 70s for generalized radionuclide counting. (Gunnink 71). The solution-sample isotopic analysis work was one of the first applications of the response function fitting of x-rays in the 100-keV region (Gunnink 76). In general, these early methods were very successful for the specialized problem they were designed to solve. Their application was for in-line monitoring of solution isotopic composition with a short (10–15 minutes) measurement time. They also quantified <sup>241</sup>Am and exhibited <sup>240</sup>Pu measurement precision and bias of under 1% [1 relative standard deviation (RSD)] for a 10-minute measurement.

This type of absolute measurement presented many challenges. Two types of calibrations were used on early applications (Gunnink 74). The first was a separate measurement to calibrate the peak shape required for the response function fitting in the 100-keV region. The second was an absolute efficiency calibration using solutions of known isotopic composition. For solution samples with a concentration differing from the calibration solutions, one must also make attenuation corrections to correct for self-absorption by the plutonium in the cell. The attenuation corrections are small for low concentrations of plutonium but had to be more carefully considered for concentrations in the 200-g/L range especially if the plutonium concentration is unknown. Finally, detector and electronic instabilities presented some difficulties. This is not surprising for the electronic systems of two to three decades ago.

These isotopic analysis techniques for solutions were fielded at the Savannah River Plant and also at the Tokai-mura reprocessing plant of the Power Reactor and Nuclear Fuel Development Corporation in Japan [Tokai Advanced Safeguards Exercise (TASTEX)] (Gunnink 81).

Gunnink's early work at LLNL pioneered the development of some of the isotopic analysis techniques, especially in the area of photopeak analysis, that are still used today both in FRAM and other isotopic analysis software.

## II. BASIC PRINCIPLES OF GAMMA-RAY ISOTOPIC ANALYSIS FOR THE ARBITRARY SAMPLE

### C. Ratio Measurements for the Arbitrary Sample—Without Efficiency Corrections

The measurement of the isotopic composition of plutonium in an arbitrary sample is an entirely different problem from the fixed-sample, fixed-geometry measurements just described. An “arbitrary sample” is the name given to items that have no constancy in their mass, chemical composition, physical composition, physical dimensions, packaging materials, and container characteristics. The lack of uniformity of the vast majority of items encountered in plutonium processing, makes it impractical and in many cases, impossible, to apply absolute counting techniques. The magnitude of the problem required a new approach to isotopic composition measurements.

A very simple expression can be developed for the ratio of the number of atoms of isotope  $i$  ( $N_i$ ) to the number of atoms of a given isotope, assume  $^{239}\text{Pu}$ ,  $N_{239}$  using measured gamma-ray intensities.

The intensity of a gamma-ray peak from isotope  $i$  is given as a proportionality by

$$I_i \approx N_i * \lambda_i * B_i, \quad (\text{II-1})$$

where  $I_i$  is the intensity of the gamma-ray photopeak from isotope  $i$  in the recorded spectrum,  $\lambda_i$  is the decay constant of isotope  $i$  ( $\lambda_i = \ln 2 / T_{1/2}$ ) with  $T_{1/2}$  being the half life of isotope  $i$ , and  $B_i$  is the branching intensity of the recorded gamma ray. When the peak intensity of a gamma ray from isotope  $i$  is compared to the intensity of a gamma ray from  $^{239}\text{Pu}$ , the expression for the atom number ratio of isotope  $i$  to  $^{239}\text{Pu}$  can be simply written as

$$N_i / N_{239} = K * I_i / I_{239} \quad (\text{II-2})$$

where the constant  $K$  contains the known half lives of the of the two isotopes and the known branching intensities of the selected gamma rays.

This expression incorporates the important assumption that the two recorded gamma rays are close enough in energy that the differences in sample self-attenuation, absorption in the packaging materials, and detector efficiency can be neglected between the two gamma-ray energies. The early applications of this technique at the Mound Laboratory (Haas 74) recommended using gamma-ray pairs with energy spacing less than 10 keV. Earlier references to this technique dating back to 1970 are reported in Haas (Haas 74).

The assumption of equal detection efficiency for the two gamma rays limited the pairs of gamma rays that could be used for this method to those close in energy. Efficiency differences even with closely spaced peak pairs can be significant and were the cause of some of the biases observed with this early method. Table II-1 demonstrates the magnitude of the bias that can be caused by neglecting efficiency and absorption differences. In Table II-1 we document the combined efficiency differences for measurements on 454 g of  $\text{PuO}_2$  when measured with a 16-mm-diam. by 13-mm-deep planar detector and a 25% relative-efficiency coaxial detector. The efficiency differences are tabulated for the energies of commonly used, “closely spaced” peak pairs. These biases will change with detector and sample and are meant to be illustrative, only.

## II. BASIC PRINCIPLES OF GAMMA-RAY ISOTOPIC ANALYSIS FOR THE ARBITRARY SAMPLE

Table II-1. Bias Magnitude From Neglecting Efficiency Differences.

Peak Pairs Isotope1(keV)/Isotope2(keV)	Planar Detector	Coaxial Detector
<sup>240</sup> Pu(160.3)/ <sup>241</sup> Pu(148.6)	1.23	1.38
<sup>240</sup> Pu(160.3)/ <sup>241</sup> Pu(164.6)	0.94	0.90
<sup>241</sup> Pu(208.0)/ <sup>239</sup> Pu(203.5)	1.03	1.06

### D. The Intrinsic Self-Calibration Technique

Parker and Reilly (Parker 74) at Los Alamos proposed the first practical method for measuring the isotopic composition of an arbitrary (size, shape, composition, and measurement geometry) plutonium sample via analysis of its gamma-ray spectrum. The key to their method was the incorporation of an internal or intrinsic self-determination of the relative efficiency curve from the gamma-ray spectrum of each unknown sample. No longer was it necessary to use closely spaced peak pairs or to assume equal detection efficiency. Their approach is developed below.

#### 1. Isotopic Ratio Measurement

We can write an expression for the photopeak counts from a specific gamma ray, emitted from a given isotope in a sample of arbitrary configuration, as

$$C(E_j^i) = \lambda^i \times N^i \times BR_j^i \times \varepsilon(E_j), \quad (\text{II-3})$$

where

- $C(E_j^i)$  = photopeak area of gamma ray  $j$  with energy  $E_j$  emitted from isotope  $i$ ,
- $\lambda^i$  = decay constant of isotope  $i$ ,  $\lambda^i = \ln 2 / T_{1/2}^i$  where  $T_{1/2}^i$  is the half life of isotope  $i$ ,
- $N^i$  = number of atoms of isotope  $i$ ,
- $BR_j^i$  = branching ratio (gamma rays/disintegration) of gamma ray  $j$  from isotope  $i$ ,
- $\varepsilon(E_j)$  = total efficiency for photopeak detection of a gamma ray with energy  $E_j$ . This includes detector efficiency, geometry (solid angle), sample self-absorption, and attenuation in packaging and materials between the sample and the detector.

In an entirely analogous fashion, we can write the expression for the photopeak counts in terms of the mass of the isotope present as

$$C(E_j^i) = M^i \times \gamma_j^i \times \varepsilon(E_j) \quad (\text{II-4})$$

where

- $M^i$  = mass of isotope  $i$ , and
- $\gamma_j^i$  = photon emission rate of gamma ray  $j$  from isotope  $i$  (gammas/s·g isotope).

## II. BASIC PRINCIPLES OF GAMMA-RAY ISOTOPIC ANALYSIS FOR THE ARBITRARY SAMPLE

Writing the expression for photopeak counts (Eq. II-3) for gamma ray  $l$  from isotope  $k$  and combining it with the expression for gamma ray  $j$  from isotope  $i$  gives the expression for the atom ratio of isotope  $i$  to isotope  $k$  from measurement of a gamma ray with energy  $E_j$  from isotope  $i$  and  $E_l$  from isotope  $k$  as

$$\frac{N^i}{N^k} = \frac{C(E_j^i)}{C(E_l^k)} \times \frac{T_{1/2}^i}{T_{1/2}^k} \times \frac{BR_l^k}{BR_j^i} \times \frac{RE(E_l)}{RE(E_j)} \quad (\text{II-5})$$

Equation II-4 can also be cast in this form; however, we will use Eq. II-5 as the standard expression for obtaining isotopic ratios from a gamma-ray spectrum. We do this because the variables in Eq. II-5 are more commonly published and available than is the photon emission rate per gram in Eq. II-4.

In going from Eq. II-3 to Eq. II-5 the total efficiency has been rewritten in terms of the relative efficiency, RE. The geometric factors associated with the total efficiency cancel in the ratio in Eq. II-5. Also, now the RE includes the effects of sample self-absorption, attenuation in materials between the sample and the detector, and detector efficiency. The half lives,  $T_{1/2}$ , and the branching ratios,  $BR$ , are known nuclear data.

The  $C(E)$  term is determined from the gamma-ray spectral data, leaving only the ratio of the relative detection efficiencies to be determined. The need for only an efficiency ratio removes the problems associated with the geometric and sample reproducibility associated with absolute measurements and makes the method applicable to samples of arbitrary size, shape, and composition.

For every sample, we can determine the ratio of the relative efficiency at the selected energies from the measured gamma-ray spectrum of that sample. From Eq. II-3, considering a series of gamma rays from a single isotope, we see that the quotient of the photopeak counts at energy  $E_j^i$  and the branching ratio  $BR_j^i$  is proportional to the efficiency at energy  $E_j$ :

$$\frac{C(E_j^i)}{BR_j^i} \propto \left[ \frac{N^i \ln 2}{T_{1/2}^i} \right] \varepsilon(E_j) \quad (\text{II-6})$$

Thus, this quotient defines the shape of the relative efficiency as a function of energy for that particular measurement. Because we use isotopic ratios, only the shape (variation with energy), not the absolute magnitude, of the relative efficiency curve is important. In practice, the values for  $C(E_j^i)$  are obtained from analysis of the gamma-ray spectrum of the sample under study. The  $BR_j^i$  are tabulated nuclear constants. Gamma rays from several isotopes may be used to define the relative efficiency as long as all the isotopes used have the same physical distribution. The curves from different isotopes with the same physical distribution have the same shape and differ only in their amplitude, the term in brackets in Eq. II-6.

The development above of Parker and Reilly (Parker 74) forms the basis for nearly all isotopic analysis by gamma-ray spectrometry applications that are in use today, including the FRAM code.

### 2. Assumption of Isotopic Homogeneity

While the above development is very general, there is one very important assumption built into the formalism. This assumption is that all the measured isotopes in the sample are homogeneous with respect to each other. Another way of saying this is that gamma rays of the same energy from different isotopes must suffer the same average attenuation as they escape from the sample. This must not be confused with physical or chemical homogeneity. A sample may be highly heterogeneous physically and chemically and still satisfy the isotopic homogeneity assumption. Consider a plutonium-bearing solution with undissolved plutonium oxide and undissolved pieces of plutonium metal in it. If all of the plutonium

## II. BASIC PRINCIPLES OF GAMMA-RAY ISOTOPIC ANALYSIS FOR THE ARBITRARY SAMPLE

---

(solution, oxide, metal) has the same isotopic content and same  $^{241}\text{Am}$  concentration, then this technique works, regardless of the physical or chemical heterogeneity. However, if the plutonium metal has a different isotopic composition than the plutonium in solution, then the technique fails because the average attenuation of a gamma ray of energy  $E$  escaping from the metal is different than the average attenuation of a gamma ray of the same energy escaping from the solution. This situation is called isotopic heterogeneity.

### a. Pyrochemical Residues

A very real example of isotopic heterogeneities occurs in pyrochemical plutonium processing applications. The pyrochemical process produces pure plutonium metal with americium and uranium removed. The waste americium and uranium that have been separated reside as a chloride salt along with small amounts of residual plutonium as metal fines in the salt residue stream. The proper quantification of the plutonium in this residue stream is complicated by the isotopic heterogeneity of the plutonium and americium present.

The calorimetric assay technique (section I. B. 1.) requires the accurate determination of the  $^{241}\text{Am}/\text{Pu}$  ratio in the sample. The gamma rays from  $^{241}\text{Am}$  suffer attenuation predominately in a low- $Z$  chloride salt matrix while the plutonium gamma rays suffer attenuation characteristic of the high- $Z$  plutonium metal fines. The relative efficiency curve for gamma rays from  $^{241}\text{Am}$  is different than that from plutonium. The isotopic ratio expression of Eq. II-5 does not work in this instance. We will discuss later a method for improving the isotopic analysis results from these isotopically heterogeneous pyrochemical residues.

### b. Waste Drums

Another application that often encounters isotopically heterogeneous items is that of analysis of 200-L drums of waste. Waste drums may contain several different smaller packages. Each of the smaller packages may have a different plutonium isotopic composition and  $^{241}\text{Am}$  content. While the attenuations may be similar for gamma rays from the two elements (often not true), the different geometrical distributions, relative to the detector, of the individual, isotopically different, smaller packages will affect the relative contributions of the individual package contents. This is often more of a geometric problem, but the result is the same—the relative efficiencies are different for the individual packages and a single measurement cannot assure that they are weighted properly. Scanning and rotation are usually used to minimize this problem.

## E. The Relative Efficiency Concept

The concept of the intrinsically determined self-calibration of the measurement's relative efficiency is the key feature of modern gamma-ray isotopic analysis methods. Equation II-6 is used to determine the relative efficiency at the gamma-ray energies used in the peak pair ratio expression of Eq. II-5.

The relative efficiency is viewed as a function of energy. Almost any variable that perturbs the absorption or relative intensity of gamma rays emitted from the sample can affect the shape or energy dependence of the relative efficiency curve. The following are examples:

- The size, configuration, and efficiency of the HPGe detector
- The mass of plutonium in the sample
- The areal density of plutonium in the sample
- The density and absorption properties of any matrix material
- Material properties and thickness of the container(s)
- Absorbers between the sample and the detector

## II. BASIC PRINCIPLES OF GAMMA-RAY ISOTOPIC ANALYSIS FOR THE ARBITRARY SAMPLE

Figures II-1 and II-2 show the effects of some of these variables. Figure II-1 shows the overall effect seen as the sample gets larger, which also usually means thicker. The curves in Fig. II-1 are normalized to unity at their maximum value. The mean free path increases as energy increases, therefore, an isotopic measurement will “see” farther into the sample and hence more sample volume and mass at high energy than at low energy. This means that relative to low energies, more high-energy gamma rays than low-energy gamma rays escape from large samples and the relative efficiency tends to increase with increasing energy more strongly than for small samples. This is illustrated numerically in Table II-2 for plutonium at low density approximating that of PuO<sub>2</sub>. The “thickness” of the plutonium in a sample must be several mean free paths in magnitude to take full advantage of the intensity available at a specific measurement energy.

Table II-2. Mean Free Path for Various Gamma Rays in Plutonium of Density 3.0 g/cm<sup>3</sup>.

Pu238	$\lambda$ (cm)	Pu239	$\lambda$ (cm)	Pu240	$\lambda$ (cm)
152 keV	0.13	129 keV	0.083	104 keV	0.19
766 keV	3.0	414 keV	1.2	160 keV	0.15
				642 keV	2.4

Figure II-1 shows that the user can get qualitative information on the plutonium areal density in comparably packaged samples just by examination of the shape of the relative efficiency curve.

Figure II-2 compares the relative efficiency for the same sample measured on two different detectors. The planar detector was a 16-mm-diam. by 13-mm-deep detector while the coaxial detector was small, (about 50 mm diam. by 40 mm thick). The two curves are normalized at 414 keV. The higher detection efficiency of the coaxial detector compared to the detection efficiency of the planar detector causes the relative efficiency of the coaxial detector above 250 keV to keep increasing where the planar efficiency falls off.

### F. Relative Efficiency Models

After the relative efficiency has been determined for a specific measurement from Eq. II-6, we have a series of relative-efficiency energy points that might appear to look like Fig. II-3. We then need to find relative efficiency values for energies not defined by a specific relative efficiency point and also, sometimes, even outside the range defined by the relative efficiency points. This requirement has led to the development of several models to parameterize the relative efficiency curve.

#### 1. Piecewise Linear

This simple model assumes that the efficiency is linear between any two adjacent points. It obviously works best where the efficiency itself is linear and requires closely spaced points for best results. This method was used in the early Los Alamos codes preceding FRAM (Sampson 80, Hsue 80, Sampson 82, Sampson 83).

## II. BASIC PRINCIPLES OF GAMMA-RAY ISOTOPIC ANALYSIS FOR THE ARBITRARY SAMPLE

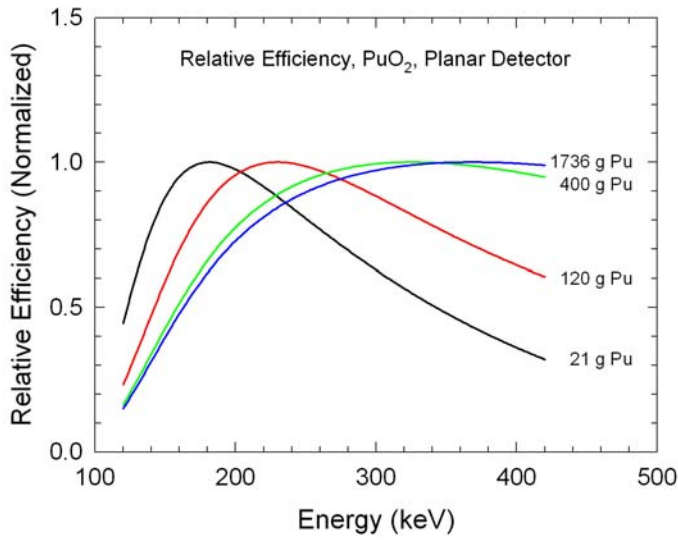


Fig. II-1. Relative efficiency variation for different size samples using the same 16-mm-diam. by 13-mm-deep planar detector. The curves are normalized at their maximum value.

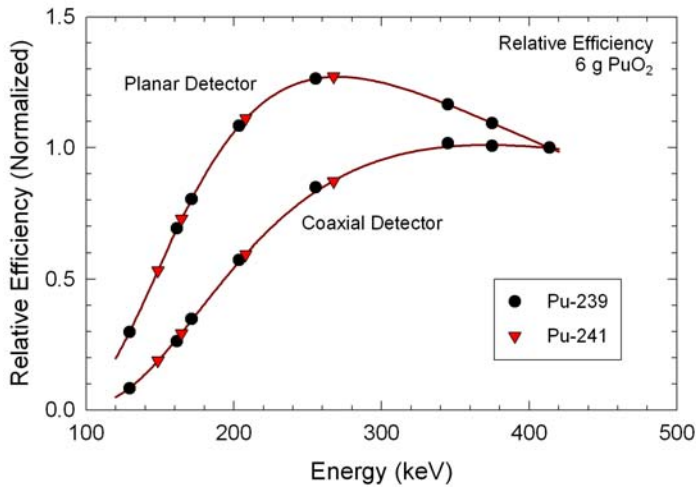


Fig. II-2. Relative efficiency variation for the same sample for a planar and coaxial HPGe detector. The curves are normalized at 414 keV.

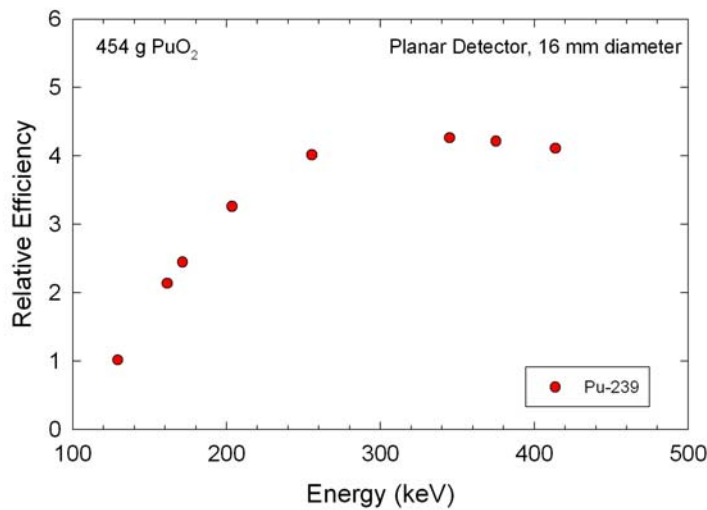


Fig. II-3. "Raw" relative efficiency points from <sup>239</sup>Pu for a specific measurement.

## II. BASIC PRINCIPLES OF GAMMA-RAY ISOTOPIC ANALYSIS FOR THE ARBITRARY SAMPLE

Its advantage is computational simplicity and it worked very well in the framework of the early analysis software as long as it was applied within the range of definition of the data points.

### 2. Spline Fitting

Spline fitting could also be used to interpolate between the individual relative-efficiency points. This form would not extrapolate well outside the range of definition of the data points.

### 3. Polynomial Least-squares Fitting

Linear least-squares fitting of polynomial expressions in  $\ln E$  were used by Fleissner (Fleissner 81) and Ruhter (Ruhter 84) in the early 1980s to parameterize the relative efficiency vs energy relationship.

Fleissner in his GRPAUT software (Fleissner 81a) used the form

$$\ln \varepsilon_i = a_0 + \sum_{j=1}^2 (a_j E_i^{-j}) + \sum_{j=1}^3 (a_{j+2} (\ln E_i)^j) + a_6 \delta_6 + a_7 \delta_7 \quad (\text{II-7})$$

in the energy range from 120 keV to above 450 keV, with points from  $^{239}\text{Pu}$ ,  $^{241}\text{Pu}$  and  $^{241}\text{Am}$ . The delta function terms,  $a_6$  and  $a_7$ , normalize the  $^{241}\text{Pu}$  and  $^{241}\text{Am}$  data points to the  $^{239}\text{Pu}$  data points.

Ruhter's form (Eq. II-8) was similar and was used to fit from 120 keV to 210 keV if the data were limited to that range, or from 120 keV to 380 keV if the data included the 375-keV region. His expression was simpler because it was used on a system with limited computing resources:

$$\ln \varepsilon_i = a_0 + a_1 \delta_1 + \sum_{j=1}^{2 \text{ or } 3} (a_{j+1} (\ln E_i)^j) \quad (\text{II-8})$$

The delta function term,  $a_1$ , normalizes the  $^{241}\text{Pu}$  data points to the  $^{239}\text{Pu}$  data points. Ruhter did not use any points from  $^{241}\text{Am}$  to determine efficiency.

All versions of FRAM use or have available an empirical relative-efficiency curve of essentially the same polynomial form (Sampson 89). FRAM's empirical relative efficiency is

$$\ln \varepsilon_i = C_1 + C_2 E_i^{-2} + \sum_{j=1}^3 (C_{j+2} (\ln E_i)^j) + \sum_{k=1}^m C_{k+5} \delta_{k+5} + \sum_{l=1}^n C_{l+5+m} \delta_{l+5+m} E_i^{-1} \quad (\text{II-9})$$

where the  $k$  summation is the normalization for each isotope after the first and the  $l$  summation is the normalization for each additional relative-efficiency curve. The FRAM empirical relative-efficiency curve is not limited with regard to the number of isotopes, nor is it limited to the number of different relative-efficiency curves applied for isotopic heterogeneity (more on this later).

All applications of this empirical, polynomial-based relative-efficiency curve work very well over the range of definition but can run into trouble if extrapolated outside its range of definition or if the relative-efficiency data is statistically poor. In these cases, the cubic nature of most of the forms may give rise to unphysical behavior.

### 4. Physical Model (Gunnink)

A physics-based relative-efficiency model has been widely used by Gunnink and coworkers at the Lawrence Livermore National Laboratory (Gunnink 90).

## II. BASIC PRINCIPLES OF GAMMA-RAY ISOTOPIC ANALYSIS FOR THE ARBITRARY SAMPLE

$$\varepsilon_j = \exp(-\mu_j^{Cd} * x_{Cd}) * \frac{1}{\mu_j^{Pu} * x_{Pu}} (1 - \exp(-\mu_j^{Pu} * x_{Pu})) * eff_j * (1 + bE_j + cE_j^2), \quad \text{II-10}$$

where

- $\mu_j^{Cd}$  = mass absorption coefficient of cadmium for peak  $j$ ,
- $\mu_j^{Pu}$  = mass absorption coefficient of plutonium for peak  $j$ ,
- $x_{Cd}$  = thickness (g/cm<sup>2</sup>) of cadmium absorber,
- $x_{Pu}$  = thickness (g/cm<sup>2</sup>) of plutonium in the sample,
- $eff_j$  = detector efficiency for peak  $j$  from a “generic” efficiency curve,
- $b, c,$  = coefficients in a quadratic function to account for small deviations in the efficiency from the generic value as well as other slowly varying effects, such as absorption from low  $Z$  matrix materials.

This model explicitly accounts for self-absorption in the plutonium in the sample, absorption in a cadmium filter between the sample and detector, and the intrinsic detector efficiency. It has been used very successfully in the region from 59 keV to 300 keV with a planar detector. The variables are determined by iterative nonlinear least-squares techniques. Because the model is based on physical principles, it can give valid results outside its range of definition in cases where empirical polynomials fail.

### 5. Physical Model (Vo)

Duc Vo at Los Alamos has implemented a very versatile physical model for relative efficiency that allows for multiple absorbers and multiple efficiency curves and uses a wide-ranging correction factor for slowly varying effects (Sampson 99):

$$\begin{aligned} \varepsilon = & \frac{1}{\mu_{Pu} * x_{Pu}} (1 - \exp(-\mu_{Pu} * x_{Pu})) \\ & * \exp(-\mu_{Cd} * x_{Cd}) * \exp(-\mu_{Fe} * x_{Fe}) * \exp(-\mu_{Pb} * x_{Pb}) \\ & * (I_i) * \exp\left(\frac{c_j}{E}\right) * (Det\ Eff) * (Correction\ Factor) \end{aligned} \quad \text{(II-11)}$$

The first term is self-absorption in the plutonium; the second line is the absorption in up to three different materials (out of a choice of seven—aluminum, iron, cadmium, erbium, lead, water, and concrete);  $I_i$  is the activity of isotope  $i$ ;  $Det\ Eff$  is a generic detector efficiency parameterized in the software; and  $Correction\ Factor$  corrects for variations of the actual detector efficiency, nuclear material, and matrix from those specified in the model. The  $Correction\ Factor$  is a modified Hoerl function.

$$Correction\ Factor = \left( E^b * c^{\frac{1}{E}} \right) \quad \text{(II-12)}$$

This physical efficiency function is available in FRAM version 4 and will be discussed later in this document.

### 6. Heterogeneous Relative-Efficiency Models

Section II.D.2 discussed the basic assumption of isotopic homogeneity built into the fundamental isotopic ratio expression, Eq. II-5. We say we have isotopic heterogeneity whenever the isotopes are not physically distributed in the same manner; hence, gamma rays of the same energy from different isotopes suffer different attenuations. The two principal cases previously mentioned are those of pyrochemical separation residues and drums of scrap and waste.

Fleissner is credited with first applying a method to correct for isotopic heterogeneities in pyrochemical residues (Fleissner 83). He added an additional term to his relative-efficiency expression (Eq. II-7) to account for the different absorption in the isotopically heterogeneous isotope. This term was proportional to  $\exp(\beta/E)$ . The so-called "beta" term, fitted during the relative-efficiency determination, is a measure of the heterogeneity. The overall shape of the function modeled the difference in shape between the plutonium and americium relative-efficiency curves for pyrochemical residues. The heterogeneity term decreases as the energy  $E$  increases, allowing the correction to become smaller at higher energies. This models the observation that mass absorption coefficients of the elements decrease and tend to become independent of  $Z$  above 1000 keV.

Los Alamos adopted the Fleissner heterogeneous relative-efficiency correction for FRAM (Sampson 89), and this term is shown in the FRAM empirical relative-efficiency expression in Eq. II-9.

Testing of this heterogeneous model has involved comparison of isotopic measurements on heterogeneous pyrochemical residues with destructive chemical analysis of the entire item (Longmire 90, Fleissner 83, Sampson 89). These destructive chemical analysis studies are very lengthy and extremely expensive, so comparison data is limited. The most important parameter determined in the isotopic measurement is the effective specific power,  $P_{\text{eff}}$  in mW/gPu. This is used directly to convert a calorimetry measurement of total sample power to grams elemental plutonium. With the heterogeneous relative-efficiency model of Fleissner, both Fleissner's GRPAUT code and the Los Alamos FRAM code determined  $P_{\text{eff}}$  with a bias that usually did not exceed 5%. Analysis of the same data without using the heterogeneous relative-efficiency correction yielded biases from 10% to 200%.

#### III. ISOTOPIC ANALYSIS DEVELOPMENT AT THE LOS ALAMOS NATIONAL LABORATORY

Several isotopic analysis systems, using a computerized implementation of the principles developed by Parker and Reilly, were completed at Los Alamos National Laboratory starting in 1980 (Sampson 80, Hsue 80, Sampson 82).

The computer systems used online control of data acquisition and analysis with PDP/11 computers and the RT-11 operating system. The analysis featured simple region-of-interest (ROI) summation to obtain peak areas (Reilly 91a). Small, planar (16-mm-diam. by 10–13-mm-deep), HPGe detectors were used for data collection with 4096 channels spanning the energy range from 10–420 keV. Detector resolution was typically approximately 500 eV at 122 keV. The specific peak ratios to be calculated in the 120–420 keV region were fixed in the code.

A system using multiple detectors to measure multiple samples simultaneously, with a single multichannel analyzer and computer, was implemented at the Los Alamos Plutonium Facility in 1981. The MUDPI (MULTiple Detector Plutonium Isotopic system) was used for all nondestructive isotopic measurements at Los Alamos until the late 1980s. The MUDPI system is pictured in Fig. III-1.



*Fig. III-1. The MUDPI plutonium isotopic analysis system implemented at the Los Alamos TA-55 Plutonium Facility in the early 1980s.*

A similar system with a single detector was fielded at the Savannah River site in 1981. This system, called LAPIS (Los Alamos Plutonium Isotopic System), is pictured in Fig. III-2. It was fielded in an air-conditioned instrument rack and the sample, placed on the platform above the up-looking detector, and surrounded with a shielding clamshell to reduce the radiation dose to the operator.



*Fig. III-2. The LAPIS plutonium isotopic analysis system implemented at the Savannah River Plant.*

Sampson (Sampson 83) describes both of these systems, including the data acquisition equipment, isotopic ratio algorithms, software user interface, and data from the initial operation of the systems. These systems used conventional analog nuclear instrumentation module (NIM) electronics with the amplifier time constant set at 3  $\mu$ s and a maximum recommended counting rate of 15 kHz. The measurement precision, or repeatability, for the effective specific power under these counting conditions was approximately 0.5% for a 2-hour count on a 500-g plutonium sample. The precision for  $^{240}\text{Pu}$  for the same conditions fell into the range from 2%–4%, [1 relative standard deviation (RSD)].

The MUDPI system performed very well at Los Alamos throughout most of the 1980s. However, by the mid-1980s it became apparent that improvements were needed to address two measurement problems. The first problem was the presence of interference isotopes in some samples. Gamma rays from these interfering isotopes ( $^{235}\text{U}$ ,  $^{243}\text{Am}$ - $^{239}\text{Np}$ ,  $^{237}\text{Np}$ ) were not accounted for in the simple ROI analysis leading to analysis error when gamma rays from these isotopes overlapped a peak or background ROI. A second problem arose from the analysis of residue samples from pyrochemical processes. These processes produce residues consisting of americium in low Z chloride matrix with plutonium metal fines suspended in the matrix. For these samples, gamma rays from americium suffer different attenuation than plutonium gamma rays of the same energy. This violated the isotopic homogeneity assumption of the analysis method and especially led to errors in the  $^{241}\text{Am}/\text{Pu}$  measurement (see section II.D.2) and hence to errors in  $P_{\text{eff}}$ .

### IV. FRAM DEVELOPMENT

#### A. Factors Influencing Development

Starting in the mid-1980s, the development of FRAM was driven primarily by the needs and requirements for measurements at the Los Alamos Plutonium Facility. We have just discussed the general features of the first isotopic analysis codes implemented at Los Alamos. The details of the improvements are presented below.

##### 1. Interferences

The MUDPI system (Sampson 83) used fixed ROIs to extract its peak areas. Some of the important regions for the analysis covered the energy ranges 140–165 keV, 203–208 keV, 330–345 keV, 375 keV, and 414 keV.

If  $^{235}\text{U}$  is present it will produce interferences at 143, 163, 202, and 205 keV. Neptunium-237 will interfere at 375 and 415 keV while  $^{243}\text{Am}$ - $^{239}\text{Np}$  has interferences at 209 and 334 keV. These interferences would invalidate a measurement when they were present in a spectrum because the simple ROI peak area extraction method was not designed to handle overlapping peaks. All three interferences can be present in the many materials processed at the Los Alamos Plutonium Facility. A peak area extraction method capable of handling multiple overlapping peaks was needed to solve this problem.

##### 2. Heterogeneous Am/Pu

The previous sections, Assumption of Isotopic Homogeneity (II.D.2.a) and Heterogeneous Relative-Efficiency Models (II.F.6), have provided an introduction to this problem.

At the Los Alamos Plutonium Facility, a major isotopic analysis problem arose in the calorimetric assay of pyrochemical residues. This problem came about for several reasons involving the MUDPI software's inability to correctly determine  $^{241}\text{Am}$  for these residues. Americium determination for pyrochemical residues is important for calorimetric assay because of americium's high specific power (114.2 mW/g compared to 1.9288 mW/g for  $^{239}\text{Pu}$ ), especially as it is concentrated in the residues, often at levels exceeding 5% or 50,000 ppm. This concentration of  $^{241}\text{Am}$  in normal weapons grade plutonium produces over 70% of the total power produced by the sample.

The simple piecewise linear relative-efficiency model used in MUDPI used several "coenergetic" peaks (peaks with  $^{241}\text{Pu}$  and  $^{241}\text{Am}$  contributions at the same energy)—164, 208, and 267 keV—in its relative-efficiency determination. The correction for the  $^{241}\text{Am}$  content of these peaks was made assuming isotopic homogeneity. The homogeneity assumption overestimated the actual concentration of the americium because gamma rays from the americium in a low-Z matrix were not absorbed as strongly as the gamma rays from the plutonium metal fines in the sample. Since americium was overestimated,  $P_{\text{eff}}$  was too large, and the total plutonium was underestimated. These errors could be 10%–100%.

##### 3. Additional Versatility

The Los Alamos Plutonium Facility handled a very wide variety of plutonium-bearing materials in its research and development (R&D) and production missions. There were many special materials for which isotopic analysis was needed that could not be handled with MUDPI because the code was highly "hard-wired."

As an example, the first software implementation of the Parker and Reilly method involved software to determine isotopic ratios in research materials containing very high concentrations of  $^{242}\text{Pu}$ . This measurement required a separate hard-wired program for this unique analysis, a program that could not be used for any other purpose (Sampson 80).

### 4. Existing Approaches and Development

The requirement that isotopic analysis must have the capability to analyze a wider variety of materials was becoming apparent in the early 1980s. At that time there were two other implemented codes available that provided approaches to parts of the problem. The first was the LLNL “Blue Box” (Ruhter 84) and the second was GRPAUT (Fleissner 81, Fleissner 81a). Our overall approach was to use readily available developments when feasible and develop our own approaches in areas that needed new thinking.

The Blue Box software used the response function approach to determine peak areas while GRPAUT used iterative, nonlinear least-squares techniques for its peak area determination. The response function approach was appealing for several reasons:

- The Blue Box software used linear least-squares fitting techniques that were significantly faster than the nonlinear methods used in GRPAUT.
- The Blue Box software characterized all the energy variation of the peak shapes at the beginning of the analysis. Multiple peak parameters were predetermined before the analysis.
- Response function fitting is more robust for fitting multiple peaks, especially those containing peaks with large intensity ratios.

We chose response function analysis as the method for obtaining peak areas in FRAM.

At this time Fleissner had already developed a heterogeneous relative-efficiency model for analysis of pyrochemical residues (II.F.6). This proven model significantly improved the analysis of these residues. We adopted it for FRAM.

We also made a conscious choice to restrict the range of analysis to energies above 120 keV; that is, we chose not to pursue analysis of the 100-keV x-ray region that was being developed at Livermore (Gunnink 81a). The entire energy range above 120 keV provided more opportunities for analysis of the widest possible range of materials than did the narrower energy range from 100 keV to 300 keV. Also, at that time LANL did not have the experience in fitting the x-ray line shapes in the 100-keV region that LLNL had and we did not want to “reinvent the wheel.”

Over the years, the Los Alamos approach was very successful. Most recently, the approach has been expanded further to encompass analysis areas not previously used. The Los Alamos FRAM code now has the capability to analyze the 100-keV x-ray region for both uranium and plutonium, as well as the 40-keV region for plutonium.

### B. VAX Version of FRAM

The first version of FRAM, running on Digital Equipment Corporation (DEC) MicroVAX computers, was fielded in 1988 at the Los Alamos Plutonium Facility. The FRAM code represented a major advance in measurement flexibility as it was designed to address the shortcomings of the MUDPI/LAPIS software and also included significant upgrades in the measurement and analysis hardware to the state of the art at that time. The features and characteristics of the FRAM code included the following:

- MicroVAX computer and VMS operating system with software written in FORTRAN 77
- The response function analysis for peak area determination allowed fitting of multiple overlapping peaks
- Heterogeneous Am/Pu analysis capability using separate relative-efficiency curves for heterogeneous isotopes
- Capability to select any or all spectral peaks to contribute to analysis via least-squares resolution of isotopic ratios

## IV. FRAM DEVELOPMENT

---

- User-editable analysis parameters controlled all facets of the analysis allowing the user to cope with arbitrary interference peaks, variable energy calibrations, different detector types, and the widest possible variety of matrix conditions

The editable analysis parameters feature of the FRAM code is its most important characteristic, allowing FRAM to successfully analyze a wider range of materials than any other single code available. This characteristic is described in detail later in this document.

FRAM was installed at the Los Alamos Plutonium Facility at TA-55 in 1988 and was put into operation in 1989. Figure IV-1 shows the FRAM system that was in use until 1997. This system used two planar-HPGe-detectors allowing two samples to be measured simultaneously. The samples were placed on a scanning table in front of the detector and were rotated and translated vertically during the measurement. Scanning was performed primarily to improve measurements on the isotopically heterogeneous pyrochemical residues. The scanning mechanism was completely shielded to reduce operator exposure from the sample. The detector table and detector shield (hidden behind the shielded scanning mechanisms in Fig. IV-1) could be manually positioned to vary the sample-detector distance and hence the detector counting rate. Improvements in detectors and electronics permitted measurements at throughput rates significantly higher than those used with MUDPI/LAPIS. Triangular shaping with a 1  $\mu$ s time constant allowed a maximum recommended counting rate of 40 kHz.



*Fig. IV-1. Testing a FRAM system before installation at TA-55.*

In addition to implementing the capability improvements mentioned above, FRAM also allowed more rapid data collection that significantly improved precision in a shorter counting time.. Table IV-1 displays the summary results for Los Alamos from the DOE Calorimetry Exchange Program for the years 1988 to 2000, spanning the change over from MUDPI to FRAM. The DOE Calorimetry Exchange Program tabulates the results from the facility's measurements of a standard PuO<sub>2</sub> sample containing 400 g Pu with about 6% <sup>240</sup>Pu content. Each facility collects data in a manner suitable for their own operations. The Los Alamos data in Table IV-1 were collected in the same manner as routine unknown samples were

## IV. FRAM DEVELOPMENT

measured and tabulates the precision or repeatability of a single measurement derived from the distribution of measurements over a period of a year. The data is tabulated for the  $^{240}\text{Pu}$  isotope and the effective specific power (mW/gPu) derived from the entire isotopic distribution.

Table IV-1. Los Alamos Calorimetry Exchange Results: 454 g  $\text{PuO}_2$  Calorimetry Exchange Standard, 5.86%  $^{240}\text{Pu}$ , Measurement Repeatability.

Year	# of Meas.	% RSD Single Measurement		Code*	Ct. Time (h)
		$^{240}\text{Pu}$	$P_{\text{eff}}$		
1988	40	3.49	0.36	MP	2
1989	67	4.26	0.56	MP	2
1990	46	2.77	0.41	F	1
1991	42	2.07	0.28	F	1
1992	40	1.64	0.24	F	1
1993	44	1.73	0.20	F	1
1994	36	1.29	0.22	F	1
1995	51	1.58	0.25	F	1
1996	44	1.33	0.27	F	1
1997	68	1.60	0.25	F	1
1998	92	1.69	0.25	F	1
1999	65	1.92	0.23	F	1
2000	88	2.00	0.25	F	1

\* MP = MUDPI, F = FRAM

Table IV-1 shows not only a decrease in the counting time from 2 hours to 1 hour but also a simultaneous improvement in precision of about a factor of two during the gradual switch over from MUDPI to FRAM. The precision continued to improve as the operators gained experience with the FRAM code. The improvement in precision arose from the following:

- The ability to use more gamma-ray peaks in the analysis; a typical FRAM analysis uses over 60 peaks while MUDPI used about 20
- Improved detectors and data acquisition electronics allowed data collection at higher count rates and shorter time constants yielding greater throughput

The average bias in these measurements was unchanged in moving from MUDPI to FRAM. The bias of less than 0.1% for  $P_{\text{eff}}$  and less than 0.3% for  $^{240}\text{Pu}$  is about at the limit expected for the technique.

### C. PC/FRAM Development

By the early 1990s computer hardware and software developments made the VAX/VMS-based FRAM system obsolete. The program was recoded in C to operate on a PC under Windows 3.1. This advance was necessary to open up the applications for the FRAM code (now called PC/FRAM) at other facilities that did not support the previous VAX system. This change has resulted in FRAM becoming commercially available through several vendors and now being used worldwide.

PC/FRAM has preserved all of the principal features of the VAX FRAM code while adding significant new capabilities (Sampson 95, Kelley 95).

### 1. Single Detector System

Like all previous Los Alamos isotopic analysis systems, PC/FRAM uses only a single detector to acquire its data. We have made a conscious choice to keep FRAM a single detector system because single detector systems are inherently

- more versatile,
- easier to use,
- more reliable,
- less expensive, and
- occupy less facility space.

### 2. Choice of Detector Types

PC/FRAM is the only isotopic analysis system that can obtain a complete isotopic analysis using either a single planar-HPGe-detector, a single coaxial-HPGe-detector, or a single CdTe-detector with the same code. When using the traditional single planar-detector, PC/FRAM has most often been used to collect and analyze data in the 120–420 keV range, although it is not limited to this range. Indeed, PC/FRAM has been used with a single planar detector to measure uranium isotopic composition in the energy range from 120–1024 keV. The most widely used mode of operation for plutonium or uranium using a single coaxial detector is to acquire a single spectrum in the range from 0 to 1024 keV. Various analysis modes can then be used with this wide data range. If the region between 120 and 200 keV is available for plutonium, PC/FRAM often works best analyzing in an energy range from 120–450 keV. When sample shielding or thick-walled sample containers preclude analysis of plutonium below 200 keV, PC/FRAM can still obtain a complete isotopic analysis using only gamma rays above 200 keV from a single coaxial-detector spectrum. A complete analysis of plutonium (all measurable isotopes) using only gamma rays above 300 keV is also possible. Uranium analyses are carried out using the entire 0–1024 keV spectrum.

The optimum choice of planar or coaxial detectors is made only after all possible measurement applications are considered. The planar detector is usually the detector of choice if all measured items are unshielded or contained in “thin” containers. If shielded containers, thick-walled containers or a mixture of thin and thick/shielded containers are encountered, then a single coaxial detector system is optimum. PC/FRAM is the only available isotopic analysis method using a coaxial detector in the energy range from 120–300 keV.

The CdTe detector application is new as this report is being prepared (Vo 02). This detector collects data for analysis in the 125–414 keV range, just like a planar HPGe detector. The CdTe application is discussed in more detail in chapter XIII.

### 3. Shielded Samples

Most isotopic analysis codes (including the original FRAM) require the presence of spectral peaks in the region below 200 keV, regardless of whether they acquire data from one or two detectors. Some isotopic analysis codes may not function when the sample is shielded to lower radiation exposure or because the sample is inside a very heavy walled container precluding the use of the lower-energy gamma rays. PC/FRAM was the first code to demonstrate the ability to make measurements through thick walled containers or on shielded samples. Any software that obtains its results from gamma rays and x-rays in the region around 100 keV is easily defeated by as little as a few tenths of a millimeter of lead or approximately 10 mm of steel. FRAM measurements have been made through as much as 25 mm (1 in.) of lead and very easily through 25 mm of steel. These are examples only and do not exhaust the full range of capabilities in this area.

### 4. Uranium Isotopic Analysis

Up until 1990 the isotopic analysis techniques originally proposed by Parker and Reilly were applied only to plutonium analysis. There was always the need for uranium isotopic analysis but the features of the uranium gamma-ray spectrum precluded the easy application of the “peak pair” ratio method that was used initially.

The uranium gamma-ray spectrum is essentially divided into two regions below 1 MeV. The low energy region up to about 200 keV contains gamma rays from  $^{235}\text{U}$  with the major  $^{235}\text{U}$  gamma rays at 143.76, 163.33, 185.72, 202.11, and 205.31 keV. The sole visible gamma ray from  $^{234}\text{U}$  above 100 keV is at 120.90 keV and  $^{236}\text{U}$  does not have any measurable gamma rays. Uranium-238 gamma rays arise from its  $^{234\text{m}}\text{Pa}$  daughter with energies of 742.81, 766.36, 786.27, and 1001.03 keV (Sampson 72) for the most intense lines. The wide separation between  $^{235}\text{U}$  and  $^{238}\text{U}$  gamma rays stymied the application of the early arbitrary-sample isotopic analysis techniques to uranium.

The formalism of the FRAM software does not require closely spaced peak pairs for analysis. Thus, in the late 1980s we applied the original VAX version of FRAM to analysis of uranium. This required the use of a coaxial detector and data analysis in the 120–1200 keV region. We demonstrated FRAM’s ability to measure, *without any modifications to the code*, the  $^{238}\text{U}/^{235}\text{U}$  ratio in samples of arbitrary physical and chemical composition, geometry, and mass, containing only uranium (Sampson 90).

In PC/FRAM uranium analysis was expanded to include  $^{234}\text{U}$  and in the latest version we include a correlation to predict  $^{236}\text{U}$  as well as a correction for cases where the  $^{234\text{m}}\text{Pa}$  daughter is not in equilibrium.

### D. Version/Feature History of PC/FRAM

#### 1. Version 1

Version 1.0 of PC/FRAM was released in September of 1994 followed by version 1.1 in December of the same year. These versions were implemented at the Los Alamos Plutonium Facility and at the Atomic Weapons Establishment at Aldermaston, United Kingdom.

Parameter files were provided with version 1.1 for the following:

- Plutonium, planar detector, Am/Pu homogeneity, 10-420 keV
- Plutonium, planar detector, Am/Pu heterogeneity, 10-420 keV
- Plutonium, coaxial detector, Am/Pu homogeneity, 0-1024 keV
- Plutonium, shielded sample, coaxial detector, Am/Pu homogeneity, 200-1024 keV
- Uranium,  $^{238}\text{U}/^{235}\text{U}$  ratio, coaxial detector, 0-1200 keV
- MOX, planar detector,  $^{235}\text{U}/\text{Pu}$  ratio < 0.3, 10-420 keV

#### 2. Version 2

Version 2 of PC/FRAM incorporated many changes, improvements, and capability enhancements. Versions 2.1, 2.2, and 2.3 were the first widely available versions with version 2.3 being customized for and licensed to ORTEC. Version 2 ran under either Windows 3.1 or Windows 95 and was first released in 1997. A computer with a 486-class processor was recommended. Over 20 major enhancements and new features are documented for versions 2.1 and 2.2 in the software user manual (Kelley 98). Some of these are highlighted below.

##### Version 2.1

- **Combined Acquisition and Analysis.** The Measure Sample option allowed the user to control the data acquisition in the MCA and automatically analyze the data after completion of the acquisition.
- **Plutonium-242 Correlation.** A general model for the  $^{242}\text{Pu}$  correlation was introduced.

## IV. FRAM DEVELOPMENT

---

$${}^{242}\text{Pu} = A * ({}^{238}\text{Pu})^B * ({}^{239}\text{Pu})^C * ({}^{240}\text{Pu})^D * ({}^{241}\text{Pu} + {}^{241}\text{Am})^E$$

- **Password Protection.** Password protection enabled for parameter changes.
- **ISOPOW.** A stand-alone plutonium decay correction program was incorporated as a menu option.
- **Plot Relative-Efficiency Curve.** A new option allows the user to view a plot of the relative-efficiency curve.
- **Display Analysis Results.** The analysis results can be viewed on the terminal in the same form they appear on the printed output.
- **Uranium Analysis Output.** A separate output is specifically formatted for uranium (only) isotopic results.
- **MCA Support.** Support for control of Canberra S100, ORTEC ADCAM, and LANL M<sup>3</sup>CA.
- **Plotting Spectral Data.** Spectral data can be plotted on the computer monitor with full zoom and scroll features from within FRAM. There is no need to have an MCA emulator present for detailed spectral viewing.
- **Plotting Fits.** The fits of the response functions to the data can be viewed with zoom and scroll control from within FRAM.
- **FWHM Calibration.** Improvements were made in the way the internal calibration of FWHM vs Energy is carried out.
- **Backgrounds.** Improvements in the calculation of the background underneath a peak region.
- **Dates.** Versatile date template allows display of date in all common formats.

### Version 2.2

- **Acquire Data.** FRAM's built-in MCA emulator displays the spectrum on the screen as it is being accumulated in the MCA.
- **Plotting Response Functions.** The individual response functions for the fit of a multiplet can be viewed and plotted.
- **MCA Choice.** Control of ORTEC MCAs updated to use their universal multichannel buffer interface (UMCBI) routines.

Version 2.3 of FRAM, customized and licensed to ORTEC, was functionally the same as version 2.2. The only difference was that support for Canberra S100 MCA was not included.

### 3. Version 3

While the new features in version 3 are not numerous, they represent a very major upgrade to the overall capability and utility of PC/FRAM.

#### Version 3.2

- **32-bit Code.** Version 3 was upgraded to 32-bit code from the old 16-bit code of version 2. It is designed to run under Windows 95, Windows 98, and Windows NT.
- **New User Interface.** The user interface is new, having a three-dimensional (3-D) look and feel similar to that of Windows 95.

## IV. FRAM DEVELOPMENT

---

- **New Measure Menu.** There is a new option under the Measure menu called Analyze Data. This combines and replaces the old **Analyze | Single Spectrum** and **Analyze | Autocycle** options.
- **Bi-lingual Support.** There is a new option called Language under the Options menu. It allows the user to choose one of two languages to be used when displaying information on the screen or printer. The character strings to be displayed are stored in one of two language files. Currently we support English and Russian as the two languages. This can be easily extended to other European languages.
- **New Database Format.** The analysis parameters are stored in a database using a new format. This format is not compatible with previous versions of FRAM. The distribution kit does not contain an “empty” database as it did for version 2.2. The new version of PC/FRAM creates the necessary files when it is first executed.

Version 3 exists in three variants. Version 3.2 is the standard version used at Los Alamos and contains MCA support for both ORTEC and Canberra MCAs. Version 3.3 is functionally equivalent and is licensed to ORTEC and ANTECH with only ORTEC MCA support. Version 3.4 is also functionally equivalent and is licensed to Canberra with only Canberra MCA support.

### 4. Version 4

The new features and upgrades in version 4 mainly concern enhancements to the physics algorithms, new measurement capabilities, and a new structure to make derivative applications easier to implement.

#### Version 4.2

- **Relative Efficiency.** This version incorporates a new physical model for calculating the relative-efficiency curve. See II.F.5.
- **Analysis Engine.** The analysis algorithms have been split out from FRAM proper and placed in their own library. This makes it easier for licensees and other users to adapt FRAM for their own applications.
- **New Menus for Uranium Analysis.** There are separate dialog boxes for measuring plutonium and uranium. There are separate dialog boxes for analyzing plutonium and uranium data files.
- **Intelligence.** There is a selectable capability of automatically switching, in a limited way, from one parameter set to another depending on the results of the analysis.
- **Canberra MCA Enhancements.** There is now support for the control of Canberra MCA's as well as the reading and writing of spectral data to and from their CAM files. This is done in conjunction with the Genie 2000 software package from Canberra.
- **Uranium Analysis Enhancements.** Enhancements for uranium analysis include 1) correction for  $^{234}\text{Th}$  nonequilibrium, 2) isotopic correlation to predict  $^{236}\text{U}$ , and 3) corrections for coincidence summing effects (Vo 99a).
- **Data Formats.** The MMCA and MCRS systems of the International Atomic Energy Agency (IAEA) and the Green Star SBS-60 systems are now supported.
- **CdTe.** FRAM now has the capability for complete plutonium analysis from spectra taken with a CdTe detector in the 120–414 keV energy range (Vo 02).
- **100-keV Region Analysis.** FRAM version 4 has complete capability for plutonium analysis in the 100-keV region (Vo 01, Vo 01a).

#### IV. FRAM DEVELOPMENT

---

- **40-keV Region Analysis.** FRAM version 4 has complete capability for plutonium analysis in the 40-keV region (Vo 99, Vo 01a).

### V. HOW FRAM WORKS

This section of the FRAM Application Guide describes the process by which FRAM obtains the isotopic composition from a gamma-ray spectrum.

#### A. Obtain Data

FRAM can analyze data from a number of sources. There are two basic types of sources of data for FRAM.

1) “Live” data from a multichannel analyzer (MCA) acquisition of a gamma-ray spectrum from a high-resolution detector (usually HPGe). FRAM can control the data acquisition from several commercially available multichannel analyzer families. The ORTEC line of multichannel buffers (MCB) operating with Maestro can all be controlled via FRAM. Canberra MCAs operating under Genie 2000 can be controlled from FRAM. Note that this control is limited to the basic functions of preset count time, start, stop, and readout to a disk file. The user must invoke the appropriate commercial MCA emulator, e.g., Maestro for ORTEC and Genie 2000 for Canberra, to perform functions involving MCA and data acquisition (high voltage, amplifier gain, etc.) setup.

The analysis of the data acquired in a “live” data acquisition under FRAM control proceeds automatically without operator intervention after the acquisition terminates.

2) Data from a disk file. FRAM can read and analyze data from disk files recorded in several different data formats. These data formats include, for version 4, the following formats:\*

- NIS-5 standard
- Canberra S100
- Ortec ‘chn’
- Ortec ‘spc’
- Canberra CAM
- IAEA MCRS
- IAEA MMCA
- Green Star
- ASCII

#### B. Perform Analysis

The analysis of a gamma-ray pulse height spectrum by the PC/FRAM code can be described in two parts, 1) Internal Calibration, and 2) Analysis of the Spectral Data.

##### 1. Internal Calibrations

The internal calibration uses selected peaks in the spectrum under analysis to provide a calibration of energy vs channel, full width at half maximum (FWHM) vs channel, and peak shape (tailing parameters) vs channel. These calibrations are done internally on the spectrum under analysis so the analysis does not depend on parameters determined from other measurements that may have been taken with different conditions of count rate, resolution, or electronic adjustment.

---

\* Proprietary Information: If FRAM is purchased from a licensee it will not contain the full range of control and format features outlined above. Only the control and data formats appropriate to the vendor’s own products or that are publicly available are likely to be present. In a version of FRAM from Los Alamos, the user will have access to everything that was current at the version release date. The user will have to purchase and install the appropriate commercial MCA emulator to control the electronics setup of the MCA and to make full use of all the file formats.

## V. HOW FRAM WORKS

---

There may be cases where the spectral quality or type is such that there are insufficient peaks to be able to use the unknown spectrum for its own peak calibrations. In these cases one can fix the peak calibration parameters to their initial values in the parameter set. The appropriate portion of the internal calibration is bypassed in this case.

### a. Energy Calibration

The first portion of the internal calibration procedure calibrates energy vs channel number from a list of peaks, usually strong single peaks, in the parameter set. A piecewise linear calibration between pairs of peaks is used for the energy calibration. The peaks are located using the default gain (keV/ch) and default zero (keV at channel 0) in the parameter set. The algorithm locates the peak at the maximum count found in a region of 10 channels on either side of the default peak position, which is located using the default gain and zero. With this algorithm FRAM is not constrained to any particular energy calibration. Within the general constraints of spectral quality, FRAM can analyze spectra at any gain, if the energy calibration is known a priori well enough to find the internal energy calibration peaks within a  $\pm 10$  channel window.

The peak centroid is found using a least-squares fit of a quadratic function to the logarithm of the counts. If there is an error in the calculation the peak is not used in the calibration. Calibration outside the range of peaks defined in the energy calibration list is extrapolated from the nearest two points.

### b. Initial Background

A background is then calculated for all peak regions defined in the parameter set. The background is calculated using the specific background functional shape for each region as specified in the parameter set.

### c. FWHM Calibration

The parameter set contains a user-editable list of peaks for use in the internal calibration of FWHM vs energy. The FWHM of the peaks in this list is calculated from the net data after a channel-by-channel subtraction of the initial background. The FWHM is calculated from a least-squares fit of a quadratic equation to the logarithm of the net counts. The fit is over a range of channels in which the counts exceed 75% of the peak maximum on the low-energy side and exceed 25% of the peak maximum on the high-energy side (for CdTe detectors, because of their larger tails, the fit starts from 85% on the low-energy side). This fit also yields the peak centroid, and if there is a match with an energy calibration peak (very likely) the centroid of the energy calibration peak is updated.

The FWHM as a function of energy that is used in calculating the response function for an arbitrary fitted peak is found from a least-squares fit to the function

$$FWHM(E) = SQRT \left[ A_1 + (A_2 * E) + \left( \frac{A_3}{E} \right) \right] \quad (V-1)$$

The first two terms are physics-based and the third term is incorporated to account for the empirical observation that, for some detectors, the FWHM tends to “level out” at low energies.

### d. Peak Shape/Tailing Calibration

The gamma-ray peak shape is described by a central Gaussian component with a single exponential tail on the low-energy side of the peak.

$$Y(J) = Ht * \exp[\alpha * (J - x_0)^2] + Tail(J) \quad (V-2)$$

## V. HOW FRAM WORKS

---

where

$$\begin{aligned} Y(J) &= \text{Net counts in channel } J \\ Ht &= \text{Peak height at the peak centroid } x_0 \\ \alpha &= 2.77259/\text{FWHM}^2 \text{ is the peak width parameter} \end{aligned}$$

and the tailing parameter Tail(J) is given by

$$\text{Tail}(J) = Ht * \exp[(T1 + T2 * E) + (T3 + T4 * E) * (J - x_0)] * [1 - \exp(-0.4 * \alpha * (J - x_0)^2)] . \quad (\text{V-3})$$

Both the amplitude and slope of the tailing function are permitted to be a function of energy. However, in practice we set T4 to zero, reducing the number of unknowns to three. After subtracting the Gaussian portion of the peak (known because we have calibrations for energy and FWHM), we determine the slope and amplitude constants from a least-squares fit of the data from all the FWHM peaks (using the net channel contents on the low-energy side of the peak from 0.5 to 1.5 FWHMs from the peak center).

At this point we have completed the internal calibration and have all the parameters necessary to calculate the shape of a gamma-ray peak at any location in the spectrum.

### 2. Analysis of Spectral Data

After the internal calibration is complete the analysis proceeds on a region-by-region basis in the order that the regions are presented in the parameter set. The program makes three passes or iterations through all the regions. While the regions are generally analyzed in order of increasing energy, if a region has a peak fixed to a second peak outside of the region, it is desirable to analyze the second region before the first so all peaks fit in a given region use the most current data. This ordering is done when constructing the regions in the parameter set.

The analysis starts by subtracting the background to get the net counts in a region. The background for the first iteration is available from the initial background calculation, which was done during the calibration phase. Below we describe the steps taken during each iteration of the analysis.

#### a. Calculate Peak Areas Using Response Functions

For each of the regions defined in the parameter set, FRAM does the following:

- Establishes the start and end of the region and the number of peaks in the region.
- Subtracts background for the region using the most current information.
- Allocates dynamic memory for the least-squares fitting of the response functions. Sets the values of the output array to the net counts in the region.
- Constructs a set of response functions, one for each isotope with a free peak in the region. Each response function has the form

$$\sum_i f_i R_i(x), \quad (\text{V-4})$$

where each  $R_i$  is a unit area function describing the shape of a photopeak and  $f_i$  is the associated area factor. One of the terms in this sum will correspond to a given free peak: its area factor is set to one. The other terms in the sum will correspond to peaks, which are fixed to this free peak. If peak  $i$  is fixed to peak  $j$ , the area factor will be

$$f_i = \left( \frac{BR_i}{BR_j} \right) * \left( \frac{RE_i}{RE_j} \right) * \left( \frac{RA_i}{RA_j} \right) \quad (V-5)$$

where BR = branching ratio, RE = relative efficiency, and RA = relative activity. This defines the ratio of the area of peak *i* to the area of peak *j*. The relative activity is the ratio of the activity of the given isotope to that of the first isotope in the parameter set's isotope list. The relative activity ratio is set to unity for the first iteration.

If a peak in the region is fixed to another peak outside the region, its photopeak function  $R_i(x)$  is multiplied by the product of the area factor and the previously determined area of the other peak. These values are then subtracted from the values in the output array. Thus, this peak is effectively stripped off or removed from the spectrum.

- Performs the weighted least-squares fitting of the response function for the free peaks to the adjusted (adjusted for stripped peaks) net counts. If the areas of any of the peaks turn out to be negative, perform another least-squares analysis, forcing them to be zero. The coefficients resulting from the analysis will be the areas of the free peaks.
- Calculates the predicted responses and saves them for display and output.
- Calculates the areas of all the peaks from the coefficients and determines appropriate values for their errors. If this is not the final iteration, use the results at this point to update the background offsets.

#### b. Calculate Relative Efficiencies

- Obtain the number of peaks to be used from the relative-efficiency peak list in the parameter set.
- Determine the number of isotopes, *N*, and the number of efficiency functions, *M*, represented by these peaks. The number of parameters used in the least-squares analysis for the empirical model relative-efficiency curve will be  $5 + (N - 1) + (M - 1)$ .
- The model for the empirical relative-efficiency curve is

$$\ln\left(\frac{Area}{BR}\right) = c_1 + \frac{c_2}{E^2} + c_3(\ln E) + c_4(\ln E)^2 + c_5(\ln E)^3 + c_i + \frac{c_j}{E} \quad (V-6)$$

where the energy *E* is in MeV. Each  $c_i$  is associated with isotopes beyond the first one, and *i* ranges in value from 6 to  $5 + (N-1)$ . Each  $c_j$  is associated with an efficiency function beyond the first one; *j* ranges in value from  $6 + (N-1)$  to  $5 + (N-1) + (M-1)$ .

- Perform the least-squares analysis.
- Compute the relative efficiency for every peak in the relative-efficiency peak list using the first  $5 + (N-1)$  terms in the above model. In addition, if a peak is associated with an isotope that is assigned an efficiency function other than one, compute its heterogeneity factor,  $h = \exp(c_j/E)$ , then multiply its relative efficiency by *h*.
- The model for the physical relative-efficiency curve is

$$\begin{aligned} \varepsilon = & \frac{1}{\mu_{Pu} * x_{Pu}} \left( 1 - \exp(-\mu_{Pu} * x_{Pu}) \right) \\ & * \exp(-\mu_{Cd} * x_{Cd}) * \exp(-\mu_{Fe} * x_{Fe}) * \exp(-\mu_{Pb} * x_{Pb}) \\ & * (I_i) * \exp\left(\frac{C_j}{E}\right) * (Det\ Eff) * (Correction\ Factor) \end{aligned} \quad (V-7)$$

This model has been discussed in II.F.5 above. The relative-efficiency function is fit to the selected relative-efficiency data points by nonlinear least-squares using the Levenberg-Marquardt method.

### c. Calculate Relative Activities

The model used to calculate the relative activities is  $Area_i = \sum_j A_j (BR_{ij})(RE_i)$  where  $A_j$  is the activity ratio for the  $j$ th isotope,  $BR_{ij}$  is the branching ratio for the gamma ray emitted by the  $j$ th isotope contributing to the area of the  $i$ th photopeak, and  $RE_i$  is the relative efficiency at the energy of the  $i$ th peak. In this formula, the sum ranges over the isotopes contributing to the area of the  $i$ th photopeak. The sum will have more than one term if a peak was “summed” with another peak.

The estimates for the relative activities can be calculated via a weighted linear least-squares algorithm, the weights being based on the errors involved with the peak areas. The problem is that there are significant errors associated with both the areas and the relative efficiencies, whereas this linear model assumes that the independent variables are known precisely. In addition, there is sometimes a wide range of weights assigned spanning many orders of magnitude, and this causes difficulties in the calculations.

So the calculation proceeds in two steps. First the data for each isotope, where none of its peaks are “summed” with any other peak, are extracted from the model. Suppose that the  $j$ th isotope can be uncoupled from all the other isotopes. For each photopeak used, we calculate  $Z_k = \frac{Area_k}{(BR_{kj})(RE_k)}$  and propagate the error involved with the relative efficiency. The estimate for the relative activity of this isotope is computed as the weighted average  $\frac{\sum_k Z_k w_k}{\sum_k w_k}$  where  $w_k$  is the reciprocal of the square of the error associated with  $Z_k$ . In the second step, the remaining isotopes are collected into a smaller set of equations that is then subjected to a weighted least-squares calculation. The weights used in the calculations are the errors associated with the peak areas, but these are inflated according to the largest error associated with the relative efficiencies appearing in the sum.

The relative masses for each isotope are calculated from the relative activities, the half lives, and atomic masses of the isotopes.

### d. Calculate Isotopic Fractions

After the third iteration is complete the final relative masses (relative to the first isotope in the isotope list) are combined to give the absolute isotopic fractions for the directly measured isotopes. The fractions are renormalized accounting for  $^{242}\text{Pu}$  ( $^{236}\text{U}$ ) computed by correlation or fixed by operator entry. Nonplutonium (uranium) isotopes are quantified relative to total plutonium (uranium). For samples containing no plutonium or uranium, the final results are the relative masses themselves.

Auxiliary results such as the effective specific power and effective  $^{240}\text{Pu}$  fraction are computed from the plutonium isotopic fractions and the appropriate constants in the isotope list in the parameter set.

## V. HOW FRAM WORKS

---

### Calculate Isotopic Correlation for $^{242}\text{Pu}$ and $^{236}\text{U}$

Plutonium-242 and  $^{236}\text{U}$  cannot be measured directly with gamma-ray spectroscopy techniques. It is customary to introduce an empirical isotopic correlation (Gunnink 80, Bignan 95) to predict their concentrations from the measured ratios for the other isotopes.

FRAM predicts the value for  $^{242}\text{Pu}$  by

$$^{242}\text{Pu} = A \times \left[ \left( ^{238}\text{Pu} \right)^B \times \left( ^{239}\text{Pu} \right)^C \times \left( ^{240}\text{Pu} \right)^D \times \left( ^{241}\text{Pu} + ^{241}\text{Am} \right)^E \right] \quad (\text{IV-4})$$

where the five constants, A–E are user-editable values in the parameter file.

In a similar manner, Vo has developed a correlation to predict  $^{236}\text{U}$  in uranium-bearing samples (Sampson 95). It is of the form

$$^{236}\text{U} = A \times \left[ \left( ^{235}\text{U} \right)^B \times \left( ^{238}\text{U} \right)^C \right] . \quad (\text{IV-5})$$

The constants in Eq. IV-5 have been determined from mass spectrometry values for US uranium produced by the gaseous diffusion process and are user-editable values in the parameter file.

### VI. PARAMETER FILES, THE KEY TO FRAM'S VERSATILITY

#### A. What are Parameter Files?

The FRAM code has been structured to give the user as much control as desired over the analysis to increase the versatility and applicability of FRAM. This is accomplished via the use of the Parameter File (or Parameter Set) mechanism. A Parameter File (or Parameter Set) contains the all the parameters required to carry out an analysis on a gamma-ray spectrum. This includes information on the isotopes to be analyzed; the specific gamma-ray peaks to use; the nuclear data for the isotopes and gamma-ray peaks; data acquisition conditions such as gain, zero, number of channels, and regions of the spectrum for analysis; and diagnostic test parameters.

A complete group of these parameters resides in a single, custom-designed database within the FRAM program. The complete group of parameters in the database is called a Parameter Set. This database can accommodate multiple parameter sets (limited only by computer memory). A separate utility, called the Change Parameter Utility, accessed from the FRAM program, gives the user access to all the parameter sets. The Change Parameter Utility allows the user to augment the database with a new parameter set, delete a parameter set from the database, or modify the values in any parameter set. The utility also allows the user to export the information in a parameter set to a text file on disk and subsequently to import this information back into the database. This allows parameter sets to be shared among different FRAM systems. The text file on disk is called a Parameter File. Formally our terminology of a "parameter set" refers to the information residing in the database in computer memory. The terminology of a "parameter file" refers to the information in a text file residing on a disk. We often ignore this distinction when discussing this concept. The Change Parameter Utility is password protected.

The amount of accessible information in a parameter set can be daunting. "How am I ever going to be able to run this code?" is a question that occurs in many new users' minds. This question is easily answered in almost every case because FRAM is delivered with a variety of parameter sets suitable for nearly all routine analyses. These parameter sets usually do not need any editing or changes for first-time use. Routine FRAM analyses can be started with as few as three clicks of the mouse.

#### B. The Change Parameter Utility

The Change Parameter Utility is entered under password protection (valid User Name and Password required) from the FRAM main menu. The password protection option will be illustrated later in this document.

The Change Parameter Utility has two menu options, File and Edit, illustrated below in Fig. VI-1, which shows the options active after entering the utility.

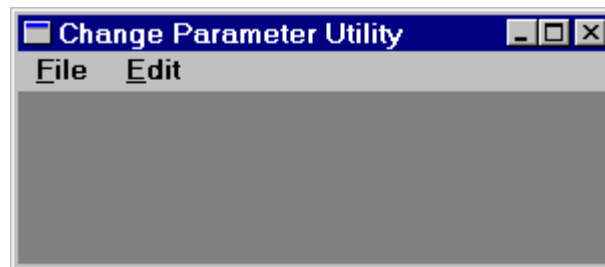


Fig. VI-1. The Change Parameter Utility window.

## VI. PARAMETER FILES, THE KEY TO FRAM'S VERSATILITY

---

The **File** menu governs the manipulation of parameter sets in the parameter database. The dropdown menu (see Fig. VI-2) shows the options available for manipulation of parameter sets in the parameter database. Greyed options become active after a parameter set has been opened.

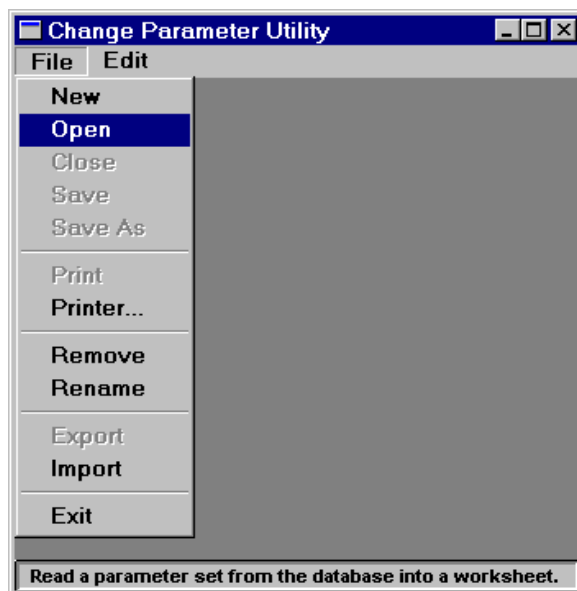


Fig. VI-2. Options under the File menu in the Change Parameter Utility.

A parameter set from the parameter database is read into a worksheet area in memory by invoking the **Open** option. The parameters may then be edited using the **Edit** menu. The **Edit** menu (see Fig. VI-3) allows the user to edit values in the parameter set in five main categories: 1) fitting parameter values and defaults, 2) peak information, 3) region information, 4) isotope information, and 5) application constants governing diagnostic tests. The **Postpone editing** option allows the user to experiment with new parameters without actually modifying the data in the database.

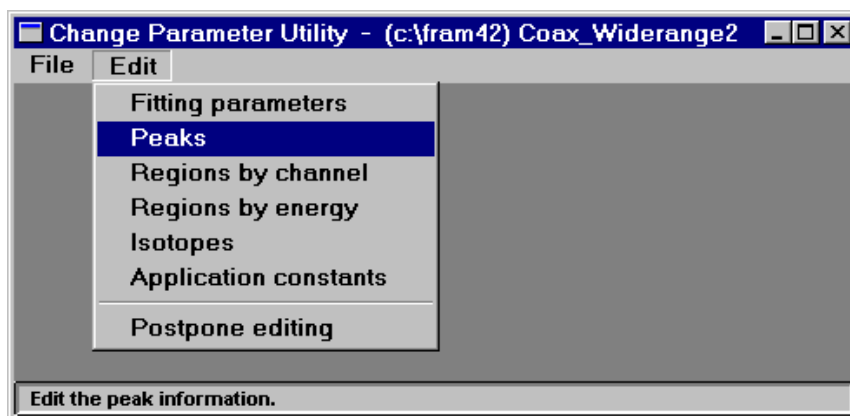


Fig. VI-3. Options under the Edit menu in the Change Parameter Utility.

The next section discusses the parameter groups that may be edited with the Edit option in the Change Parameter Utility.

## C. Analysis Parameters

## 1. Fitting Parameters

Selecting **Edit | Fitting Parameters** brings up the menu below (Fig. VI-4).

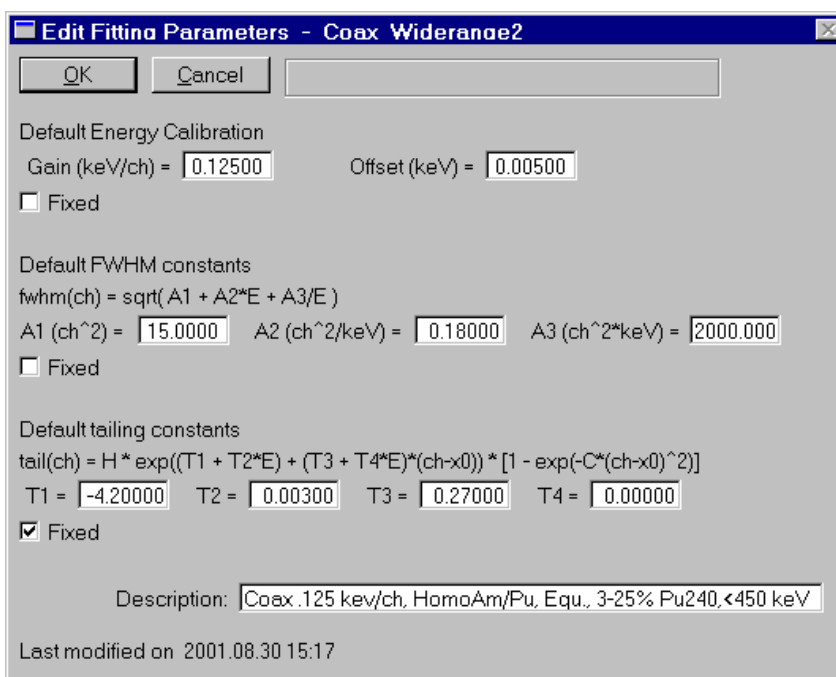


Fig. VI-4. The Edit Fitting Parameters screen in the Change Parameters Utility.

The **Default Energy Calibration** allows the user to match the analysis to the actual energy calibration of the spectrum under study. Most other isotopic analysis codes require a single fixed energy calibration that the spectrum must match. FRAM has no limitations in this respect except the global requirement that the number of channels in the peak must not be so small (keV/ch so large) that peak fitting fails. Peak fitting becomes difficult for energies below 200 keV for coaxial HPGe detectors when the gain is above 0.5 keV/ch and above 0.25 keV/ch for planar HPGe because the photopeak contains too few data points. The FRAM code uses the **Default Energy Calibration** to find the position of the internal energy calibration peaks. It must be accurate enough to predict the actual peak position to within  $\pm 10$  channels. This is seldom a problem because one can always view the spectrum before setting this parameter. The internal energy calibration is bypassed if the **Fixed** box is checked, although we have not encountered a measurement situation where this has been necessary.

While FRAM can successfully operate using a wide range of energy calibration values, we have the most experience operating with standard **Default Energy Calibration** values delivered with each parameter set. Table VI-1 displays these standard values.

## VI. PARAMETER FILES, THE KEY TO FRAM'S VERSATILITY

Table VI-1. Customary/Recommended Default Energy Calibration Values for FRAM.

Detector	Gain (keV/ch)	Zero (keV at ch 0)	No. Channels
Coaxial	0.125	0.0	8192
Planar	0.100	10.0	4096
Planar	0.105	0.0	4096

The wide analysis range and gain range capability of FRAM can be seen in Table VI-2.

Table VI-2. Data Acquisition/Analysis Conditions Successfully Used with FRAM.

Isotope	Detector	Analysis Range	Gain (keV/ch)	Comment
Plutonium	Planar	120–420 keV	0.100	
		120–420 keV	0.105	
		120–307 keV	0.075	
		90–208 keV	0.075	
		38–208 keV	0.075	
		38–130 keV	0.075	
	Coaxial	120–460 keV	0.125	
		120–460 keV	0.115	
		120–460 keV	0.250	
		120–460 keV	0.500	Not recommended <sup>1</sup>
		120–800 keV	0.125	
		200–800 keV	0.125	
Uranium	Coaxial	120–1024 keV	0.125	
		120–1024 keV	0.130	
		120–1300 keV	0.156	
		120–1024 keV	0.250	
	Planar	120–1024 keV	0.250	Not recommended <sup>1</sup>

<sup>1</sup> Combination of energy range and keV/ch not recommended. Peaks are too narrow at low energies for reliable shape calibration.

One example of the utility of the **Default Energy Calibration** selection occurs in the analysis of uranium with a coaxial detector. Our standard parameter files for uranium are set up to analyze data from 120–1024 keV collected in 8192 channels at a gain of 0.125 keV/ch. Under these conditions, the important 1001-keV uranium daughter peak is located at channel 8008. However, some successive approximations-type analog-to-digital converters (ADC) cut off their data storage at the high end of the range resulting in incorrect storage of count information right around the 8008 channel location of the 1001-keV peak. FRAM easily handles this problem if the user adjusts the gain of the electronics to 0.130 keV/ch and then changes the **Default Energy Calibration** gain to 0.130 keV/ch to match. The 100-keV peak now occurs at

## VI. PARAMETER FILES, THE KEY TO FRAM'S VERSATILITY

---

channel 7700, well away from the ADC's spectral distortion area. With this one change in the appropriate FRAM parameter file, the analysis at the new gain proceeds without a hitch.

The **Default FWHM constants** govern the energy variation of the FWHM in the absence of the internal FWHM calibration (V.B.1.c), that is, when the **Fixed** box is checked. Each parameter file for FRAM is loaded with **Default FWHM constants** appropriate for a high-quality detector of the type characteristic of the parameter file values. These default constants may be obtained from a medium length printout of an analysis using the parameter file of interest with the FWHM constants free. We have little, if any, experience using fixed values of the **Default FWHM constants** as essentially all analyses provide enough internal peaks to carry out the internal FWHM calibration.

The **Default tailing constants** govern the default values of the slope and amplitude of the exponential tail on the low-energy side of the peak. The four constants T1 through T4 allow both the slope and amplitude to be parameterized as a linear function of energy. In practice we set T4 to zero, leaving the slope independent of energy and the amplitude with linear energy dependence. These parameters are determined during the internal calibrations by fitting the residuals on the low energy side of the peak after subtracting the central Gaussian component.

Most new detectors are of such high quality that the low-energy tail is essentially invisible. This will occasionally cause the internal shape calibration to fail and default to the Default tailing constants. The **Default tailing constants** with LANL-delivered parameter sets are characteristic of high-quality detectors that do not exhibit any neutron damage or enhanced tailing characteristics.

The best results for spectra with good statistics should be obtained by leaving the **Default tailing constants** "free." In this manner the tailing will adapt to the slow increase in tails that appear with age and neutron exposure in most HPGe detectors.

Spectra with poor counting statistics may not have strong enough internal shape-calibration peaks to enable FRAM to extract good values for the tailing constants if the Default tailing constants are "free." The danger is not that the shape calibration will fail completely (the Default tailing constants will be used in that case) but that it will actually calculate tail parameters with very poor data, yielding bad peak shapes. For this reason we recommend that analysis of spectra with poor statistics proceed with the **Default tailing constants** "Fixed" in the **Edit Fitting Parameters** window.

In a general measurement situation where both good and poor statistics spectra may be encountered, we recommend "Fixing" the Default tailing constants for all analyses.

We have also observed over many years the different factors that can affect the tailing parameters. The shaping electronics, analog or digital, have a subtle effect, even when properly adjusted. Detectors from different manufacturers also exhibit different tail characteristics, even when new. For any new system (electronics or detector) we recommend that the user characterize the Default tailing constants and replace those delivered with the parameter set with new constants most characteristic of the specific system in use. Analyzing several spectra with good statistics and the tailing parameters "Free" easily performs this characterization. The new tailing parameters are listed in the medium length printout. Averaged results from several measurements should be used as these parameters vary from run to run. This is a suggestion, not a requirement. The differences observed between optimum and nonoptimum tailing parameters are small and generally within the overall uncertainty of FRAM.

### 2. Gamma-Ray Peak Data

Selecting **Edit | Peaks** in the Change Parameter Utility brings up a window (see Fig. VI-5) allowing the user to specify information about the peaks to be used in the analysis. This window allows the user to customize the analysis for nearly any conceivable application.

## VI. PARAMETER FILES, THE KEY TO FRAM'S VERSATILITY

	isotope	peak energy	line width	branching ratio	fix area to	sum area with	used for eff	used for act	used for ecal	used for fcal	used for scal
24	Pu239	171.372	0.00	1.13000e-006	0	0	<input type="checkbox"/>	<input checked="" type="checkbox"/>	<input type="checkbox"/>	<input type="checkbox"/>	<input type="checkbox"/>
25	U235	185.718	0.00	5.73000e-001	0	0	<input type="checkbox"/>	<input checked="" type="checkbox"/>	<input type="checkbox"/>	<input type="checkbox"/>	<input type="checkbox"/>
26	U235	202.130	0.00	1.08000e-002	25	0	<input type="checkbox"/>				
27	Pu239	203.545	0.00	5.72700e-006	0	0	<input checked="" type="checkbox"/>	<input checked="" type="checkbox"/>	<input type="checkbox"/>	<input type="checkbox"/>	<input type="checkbox"/>
28	U235	205.311	0.00	5.05000e-002	25	0	<input type="checkbox"/>				
29	Pu241	208.000	0.00	5.39200e-006	0	0	<input checked="" type="checkbox"/>				
30	Am241	208.000	0.00	7.95400e-006	3	0	<input type="checkbox"/>				
31	Am243	209.750	0.00	3.42000e-002	34	0	<input type="checkbox"/>				

Fig. VI-5. The Edit Peak information screen in the Change Parameter Utility allows the user to customize the analysis.

### a. Isotope

The first column is the peak index number. The second column lists the isotope assigned to the peak. The isotope name must be listed in the Isotopes list if it is to be used for activity, efficiency, or for “stripping” outside its region of definition.

### b. Peak Energy

The second column lists the peak energy in keV.

### c. Line Width

The third column lists the line width in eV of any x-ray peak used in the analysis. This is used only for x-ray fitting in the 100 keV region.

### d. Branching Ratio

The branching intensity or branching ratio (photons/disintegration) is listed in the fifth column. Primary sources for this information are the Table of Isotopes (Firestone 96) and the 1976 publication by Gunnink (Gunnink 76a) that is reproduced in Appendix D. Some of the branching ratio values used in a FRAM parameter file are fine tuned from their published values.

### e. Uses in Analysis

The last seven columns detail how each peak is to be used in the analysis.

**fix area to** This column contains the number of the free peak that will be used to determine the peak area by use of the known activity, relative efficiency, and branching ratio of the two peaks in question. The ratio of the area  $A_i$  of peak  $i$  to the area  $A_j$  of peak  $j$  is given by

$$\frac{A_i}{A_j} = \frac{BR_i}{BR_j} \times \frac{RE_i}{RE_j} \times \frac{RA_i}{RA_j} \quad (\text{VI-1})$$

where BR = branching ratio, RE = relative efficiency, and RA = relative activity.

## VI. PARAMETER FILES, THE KEY TO FRAM'S VERSATILITY

**sum area with** This column contains the number of the free peak that the listed peak area will be summed with before the least-squares fitting is used to resolve the activities. Summing can be used to unravel very close or even coenergetic peaks that are too close together to be accurately resolved with the response function fitting.

**used for eff** A check placed in this column denotes that the peak will be used for the relative-efficiency determination.

**used for act** A check placed in this column denotes that the peak will be used for the activity determination.

**used for ecal** A check placed in this column denotes that the peak will be used in the internal energy calibration.

**used for fcal** A check placed in this column denotes that the peak will be used in the internal calibration of full width at half maximum.

**used for scal** A check placed in this column denotes that the peak will be used in the internal calibration of the peak shape tailing parameters.

### 3. Analysis Region Definition

Selecting **Edit | Regions by energy** or **Edit | Regions by channel** in the **Change Parameter Utility** brings up the window allowing the user to edit the regions of interest selected for analysis (see Fig. VI-6). The windows allow editing either by energy (illustrated below) or channel. The actual setup in the software is in energy units (keV). The default energy calibration is used for the energy/channel conversion. The code works in energy units, therefore the region information is independent of the energy calibration of the spectral data.

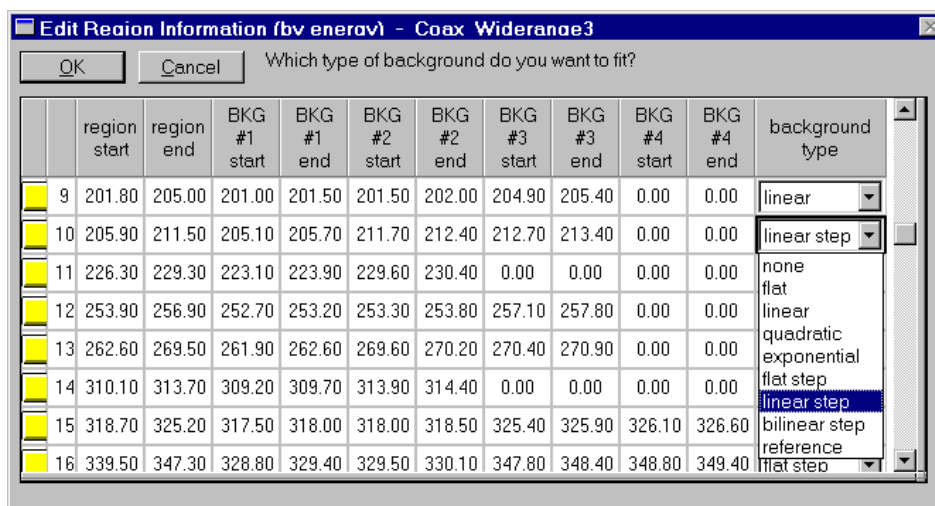


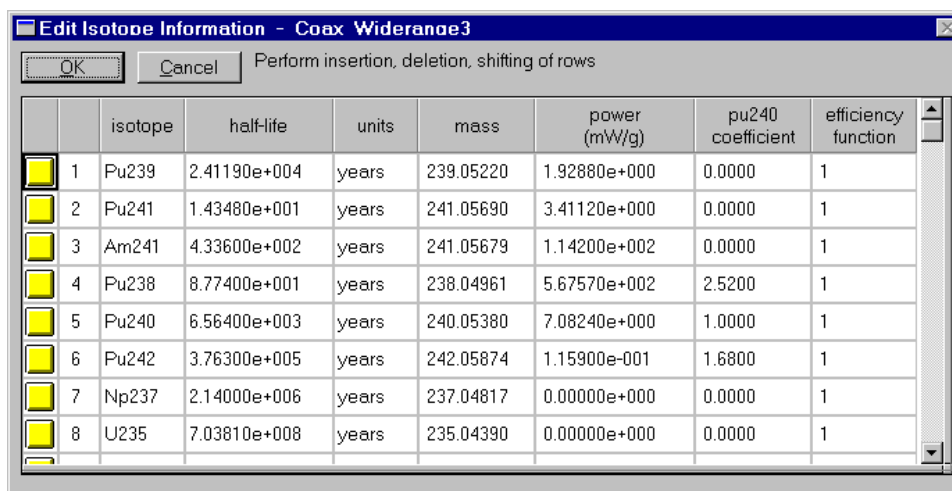
Fig. VI-6. The Edit Region Information window in the change Parameter Utility allows the user to set up or change analysis regions.

## VI. PARAMETER FILES, THE KEY TO FRAM'S VERSATILITY

The **Edit Region Information** window allows the user to specify the boundaries of a peak region and the boundaries of up to four background regions used to define the background continuum underneath the peak region. There are no limitations on the size and location of the background regions. Also, the peak region may contain multiple peaks. The user selects a **background type** from a choice of seven shapes from the drop down menu as shown above. The regions are analyzed in the order listed in the worksheet.

### 4. Isotope Information

Selecting **Edit | Isotopes** in the **Change Parameter Utility** brings up the window allowing the user to edit the names and data for the isotopes quantified in the analysis (see Fig. VI-7).



	isotope	half-life	units	mass	power (mW/g)	pu240 coefficient	efficiency function
1	Pu239	2.41190e+004	years	239.05220	1.92880e+000	0.0000	1
2	Pu241	1.43480e+001	years	241.05690	3.41120e+000	0.0000	1
3	Am241	4.33600e+002	years	241.05679	1.14200e+002	0.0000	1
4	Pu238	8.77400e+001	years	238.04961	5.67570e+002	2.5200	1
5	Pu240	6.56400e+003	years	240.05380	7.08240e+000	1.0000	1
6	Pu242	3.76300e+005	years	242.05874	1.15900e-001	1.6800	1
7	Np237	2.14000e+006	years	237.04817	0.00000e+000	0.0000	1
8	U235	7.03810e+008	years	235.04390	0.00000e+000	0.0000	1

Fig. VI-7. The *Edit Isotope Information* screen in the *Change Parameter Utility* allows the user to specify the parameters of the isotopes to be analyzed.

The first isotope in the list has special significance. All other isotopes are ratioed to the first isotope in the list. The first isotope in the list is usually the isotope that principally defines the relative-efficiency curve although it does not have to be. After the first isotope, the order of the remaining isotopes is not important.

The efficiency function is defined to be “1” for the first isotope in the isotope list. All isotopes that have the same spatial distribution as the first isotope will also have an efficiency function of “1.” Any isotope that is known to have a different spatial distribution should be assigned an efficiency function of 2 or higher. Any isotope with a different efficiency function must have enough gamma rays to fully define its efficiency function.

In principle, FRAM can have an unlimited number of efficiency functions. In practice, we only have experience using two functions. This experience is primarily with pyrochemical residues with the plutonium being present as metal fines or metal shot dispersed in a low-Z chloride matrix containing the americium. We define two efficiency curves for this case: number 1 for all the plutonium isotopes and number 2 for <sup>241</sup>Am (see sections II.D.2.a and II.F.6).

### 5. Application Constants

Selecting **Edit | Application constants** in the **Change Parameter Utility** brings up the window allowing the user to assign and edit the values for the Application Constants in the program (see Fig. VI-8).

## VI. PARAMETER FILES, THE KEY TO FRAM'S VERSATILITY

Grouping a wide variety of user-editable constants into this single option has proved to be of great advantage in allowing the user to adapt FRAM to specific facility/user needs. The **Edit Application constants** window contains a two column listing in the form of *Variable Name* | *Variable Value*. These variable-constant pairs control many options in the FRAM program, and the presence/absence of any given pair turns that option on/off. The use of these constants is discussed in detail in the FRAM Software User Manual (Kelley 97, Sampson 99a, Kelley 02). A short discussion of the classes of constants, their uses, and illustration of the user interface follows.

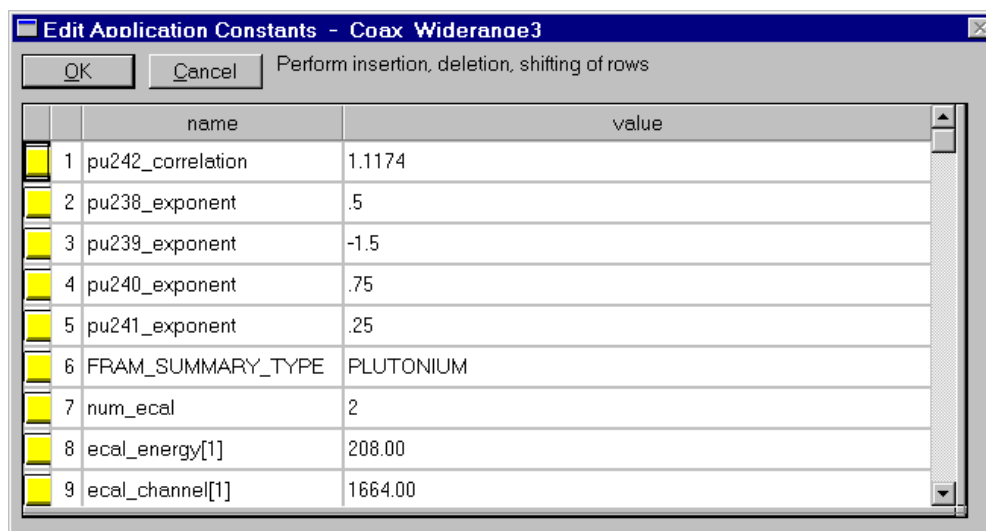


Fig. VI-8. Example of the Edit Application Constants window.

The Application Constants can appear in any order, even within a group of constants for the same application. Many of the tests, where appropriate, can be performed on as many peaks as the user desires.

The first grouping of constants 1–5 above, govern the calculation of the correlation to predict  $^{242}\text{Pu}$ .

$$^{242}\text{Pu} = A \times \left[ \left( ^{238}\text{Pu} \right)^B \times \left( ^{239}\text{Pu} \right)^C \times \left( ^{240}\text{Pu} \right)^D \times \left( ^{241}\text{Pu} + ^{241}\text{Am} \right)^E \right] \quad (\text{VI-2})$$

The first five application constants correspond to the constants A through E in Eq. VI-2.

The constant FRAM\_SUMMARY\_TYPE governs whether the output is formatted for uranium or plutonium.

The application constants govern customized diagnostic tests on detector performance. FRAM can test the peak position against a centroid  $\pm$  a channel limit, peak FWHM against an upper limit in eV, and peak tailing against a peak area percentage underneath the tail, all on a user-selectable number of peaks tested against user-established limits. Rows 7–9 above and 11–19 below (see Figs. VI-8 and VI-9) and show the interface for these tests.

As an example, row 7 defines that an energy calibration test is to be performed on 2 peaks. The second of these two peaks (line 11) has an energy of 662.456 keV. The 662.456-keV peak is expected to fall in channel 5299.40 (line 12) within a limit of  $\pm 4$  channels (line 13). Line 14 defines a FWHM test on a single peak with an energy (line 15) of 413.714 keV. The FWHM of the peak at 413.714 keV should be less than 1500 eV (line 16) for the test to pass.

## VI. PARAMETER FILES, THE KEY TO FRAM'S VERSATILITY

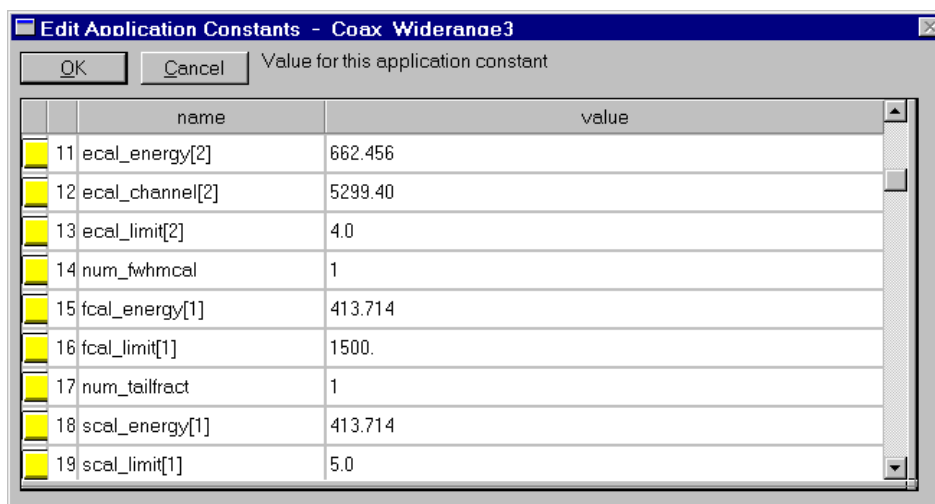


Fig. VI-9. Example of the Edit Application Constants window.

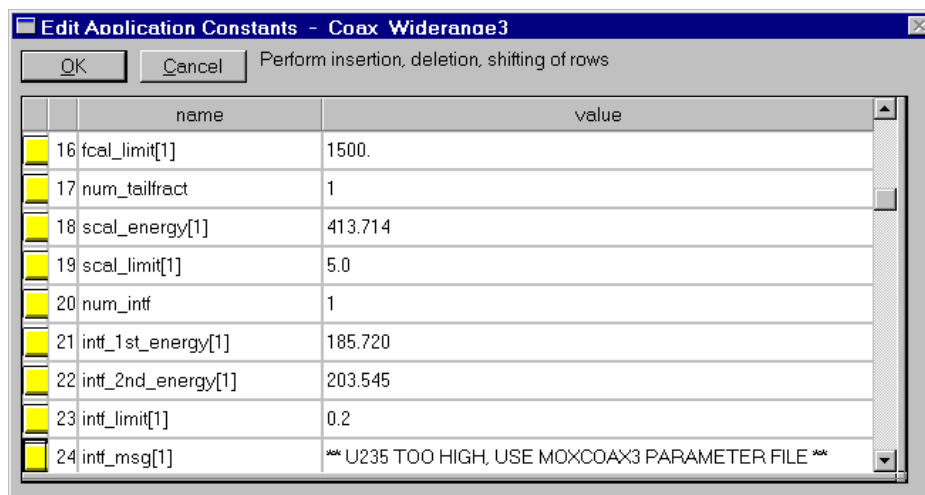


Fig. VI-10. Example of the Edit Application Constants window.

The user can test for the presence of any number of interference peaks that may appear rarely in the spectrum and are unaccounted for in the analysis. The presence of an interference peak above a certain magnitude may disrupt the analysis. The magnitude of an interference peak is determined by a ratio of the interference peak area to the area of a peak from a major isotope in the sample. A user editable message can direct the user to another analysis path. This test is illustrated in lines 20–24 above where the interference peak is at 185.72 keV and the denominator of the ratio is the area of the peak at 203.545 keV.

## VI. PARAMETER FILES, THE KEY TO FRAM'S VERSATILITY

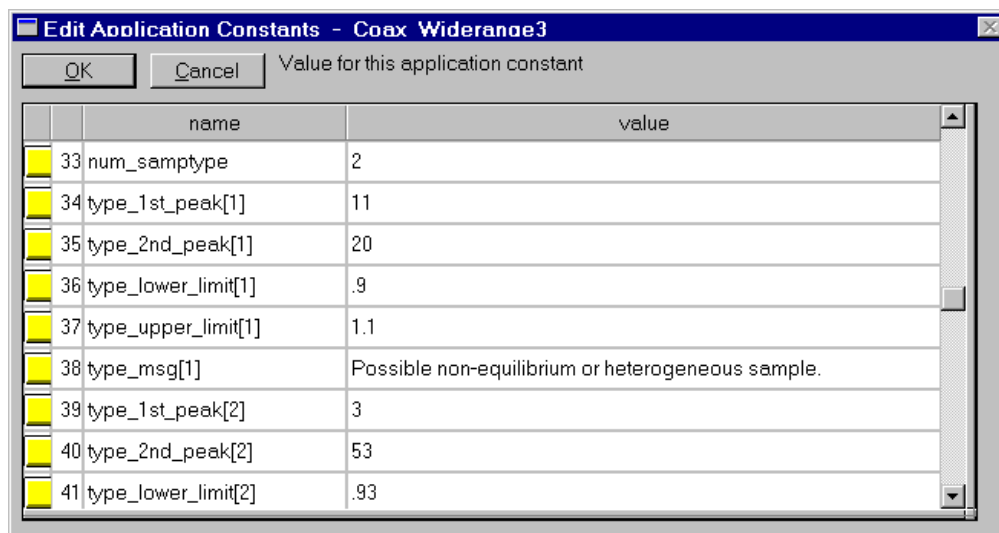


Fig. VI-11. Example of the Edit Application Constants window.

Tests called "sample type" tests check for Am/Pu heterogeneity and  $^{241}\text{Pu}$ - $^{237}\text{U}$  nonequilibrium. This test is illustrated in lines 33–38 (Fig. VI-11). The "sample type" tests compare the ratio of two peak areas against upper and lower limits. A message is printed when the test ratio falls outside the designated limits. This test uses the peak index numbers in the Peaks list (section VI.C.2).

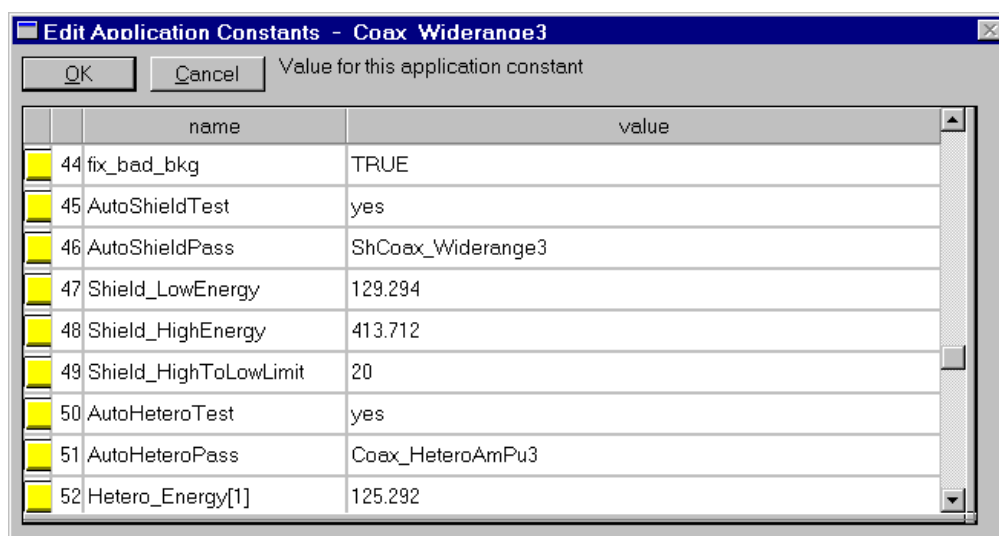


Fig. VI-12. Example of the Edit Application Constants window.

The fix\_bad\_bkg test (line 44, shown in Fig. VI-12) allows the code to default the selected region background type (VI.C.3) to a more simple shape if the code senses a poor background fit.

There are a number of Application Constants that direct the "Intelligent Isotopic Analysis" that is implemented in version 4.2. These constants direct tests to detect conditions that could affect the optimum choice of the parameter set. If these conditions are present, the Application Constants automatically direct FRAM to reanalyze the spectrum with a different parameter set. The conditions that FRAM looks for are 1) shielding that removes gamma-ray peaks below approximately 200 keV, 2)

## VI. PARAMETER FILES, THE KEY TO FRAM'S VERSATILITY

---

heterogeneous Am/Pu, and 3) very high  $^{241}\text{Am}/\text{Pu}$ . These tests are described further in section XIV.A.1. and in the manual for version 4 of FRAM (Kelly 02). Some of the constants governing these tests are shown starting in row 45.

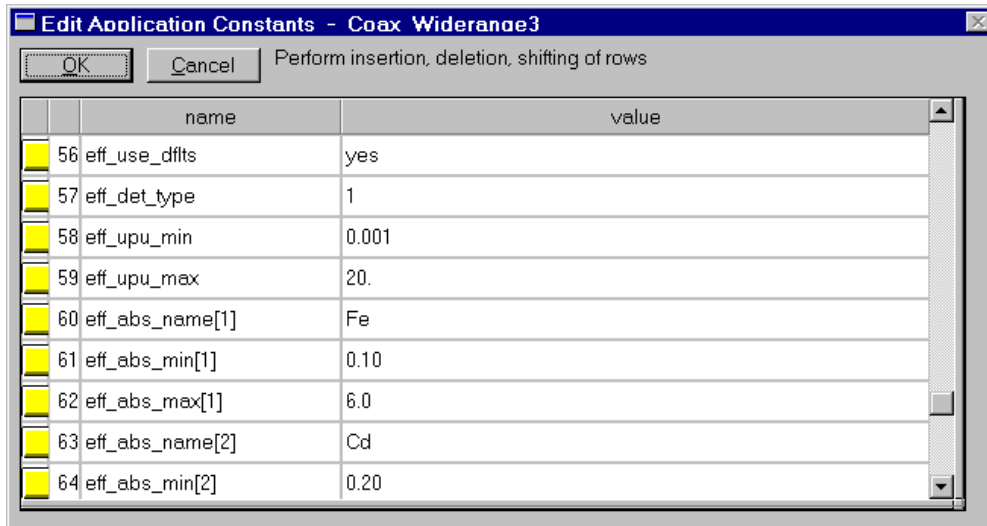


Fig. VI-13. Example of the Edit Application Constants window.

The final set of Application Constants, new in version 4.2, sets up default values for the parameters used in the fitting of the physical relative-efficiency curve (section II.F.5) (see Fig. VI-13). These include default ranges for the thickness of the plutonium (uranium) and thickness ranges for the chosen absorbers.

The entire category of Application Constants can appear quite formidable to a new user. However, the specific parameters and values have been carefully chosen and tested for appropriateness for each parameter file. The use of this option is usually completely transparent to the user.

### VII. FRAM USER INTERFACE

#### A. FRAM Main Menu

The main menu of FRAM (see Fig. VII-1) appears with four major options, File, Edit, Measure, and Options.

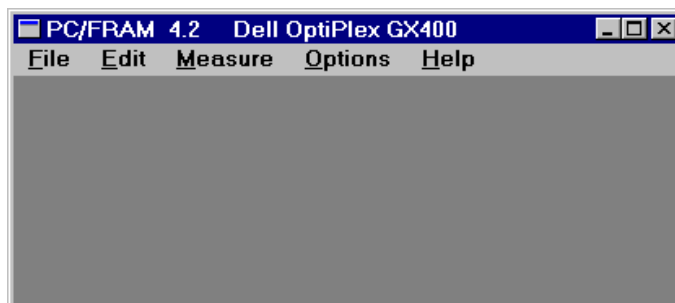


Fig. VII-1. The main menu of FRAM.

#### B. Main Menu Options

##### 1. File

The File option (see Fig. VII-2) allows the user to open a spectral data file and view it under Options. The file can also be saved in any of the supported data formats (section V.A). Saving the file in the ASCII text format makes it easy to plot the data in many graphical applications.

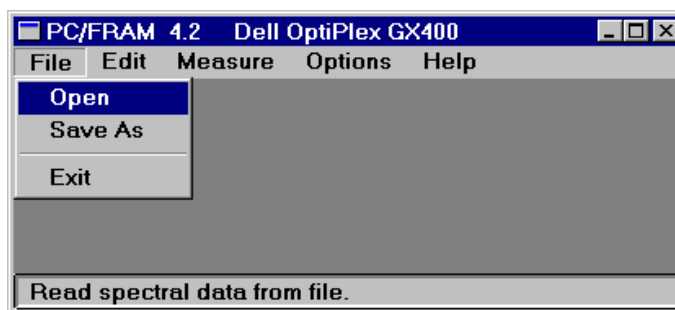


Fig. VII-2. Options under the File menu.

##### 2. Edit

The Edit menu (see Fig. VII-3) has three groups of options. Parameters have been discussed in chapter VI. General Defaults, shown below in Fig. VII-4, allows the user to set up global parameters that govern the data handling in the system, such as default paths for accessing FRAM, storing the spectral data and results files, and access to supported MCAs.

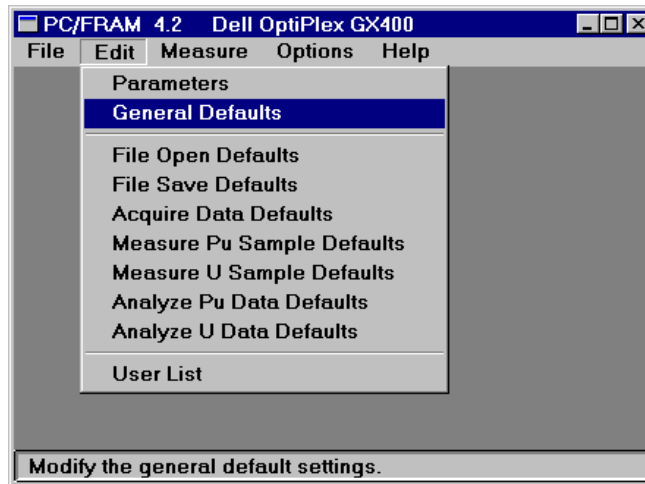


Fig. VII-3. Options under the Edit menu.

The second group of parameters under the **Edit** menu allows the user to set up default entries in many of the application windows. Some of these will be illustrated later in the discussion of those windows.

The third group is the password-protected **User List**. The User List controls access at three levels of password protection to all of the password-protected options.

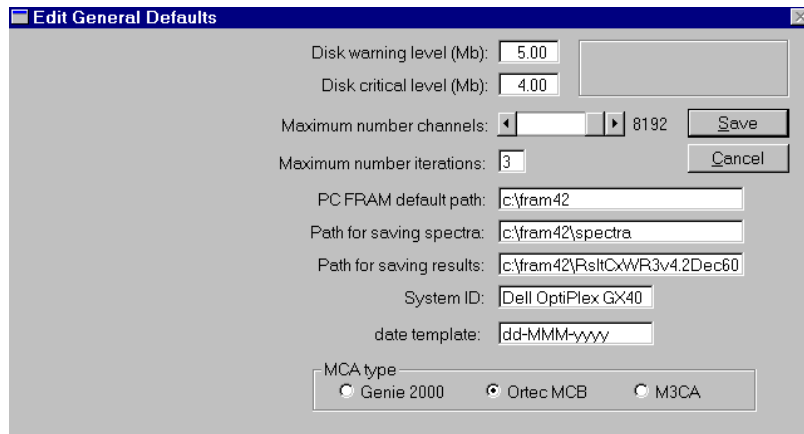


Fig. VII-4. The screen for setting General Default values.

### 3. Measure

The **Measure** menu (see Fig. VII-5) governs the acquisition and analysis of data from both "live" MCA sources and disk files.

## VII. FRAM USER INTERFACE

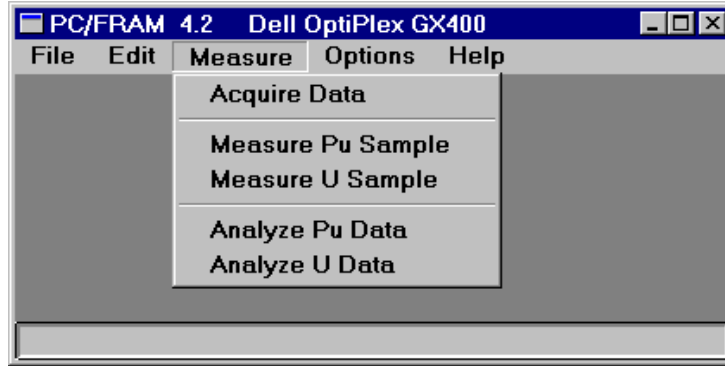


Fig. VII-5. Options under the Measure menu.

The **Acquire Data** option controls acquisition of data from a supported MCA and the storage of the data (without analysis) in a disk file. The **Measure Pu (U) Sample** options follow the data acquisition with an immediate analysis of the acquired spectrum, producing the measurement result seconds after completion of the data acquisition. **Analyze Pu (U) Data** analyzes the spectral data from an existing disk file. We show the **Measure Pu Sample** window below as an example.

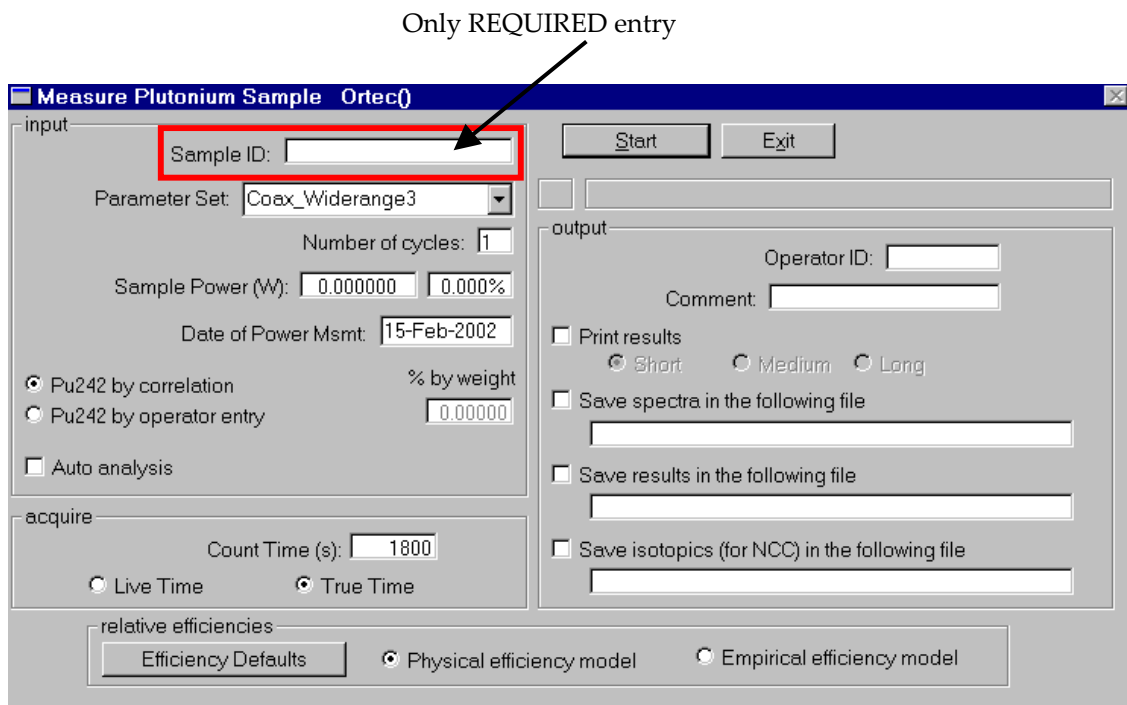


Fig. VII-6. The Measure Plutonium Sample window.

The **Measure Plutonium Sample** window (Fig. VII-6 above) is shown with some of the entries defaulted from the **Edit | Measure Pu Sample Defaults** option. At this point the only entry *required* to start the measurement and complete the analysis displaying results on the terminal is the entry of the Sample ID. With the use of defaults successive measurements may be completed with only identification of the sample and clicking the **Start** button. In many cases the user will also want to utilize some of the optional

## VII. FRAM USER INTERFACE

output options. To further make this easier, the entered **Sample ID** is defaulted as the filename for data storage purposes.

### 4. Options

The **Options** menu allows the user several ways to display and view the spectral data and the results of the analysis. The entire spectrum can be displayed and manipulated from the **Plot Spectrum** option with versatility similar to that of a commercial MCA emulator. The user can also display the peak fits and view the relative-efficiency curve. These options are invaluable when troubleshooting a suspect analysis. The results of selecting **Plot Efficiencies** and **Display Fits** are shown in Fig. VII-9 below with fits being displayed showing only the fit envelope (left) or with the individual components (right).

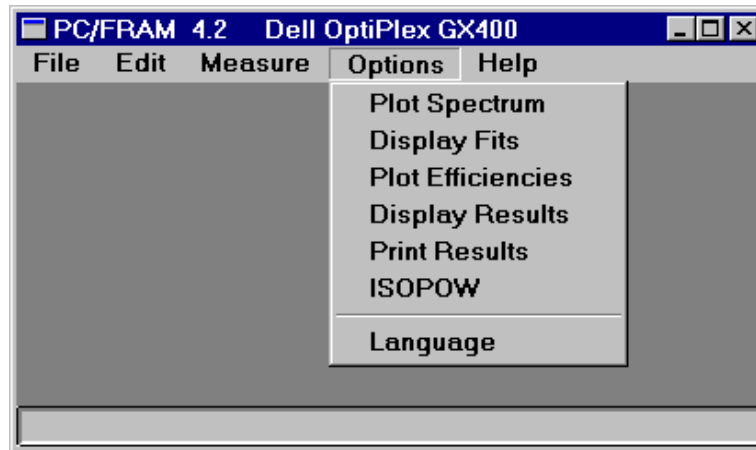


Fig. VII-7. Options under the Options menu.

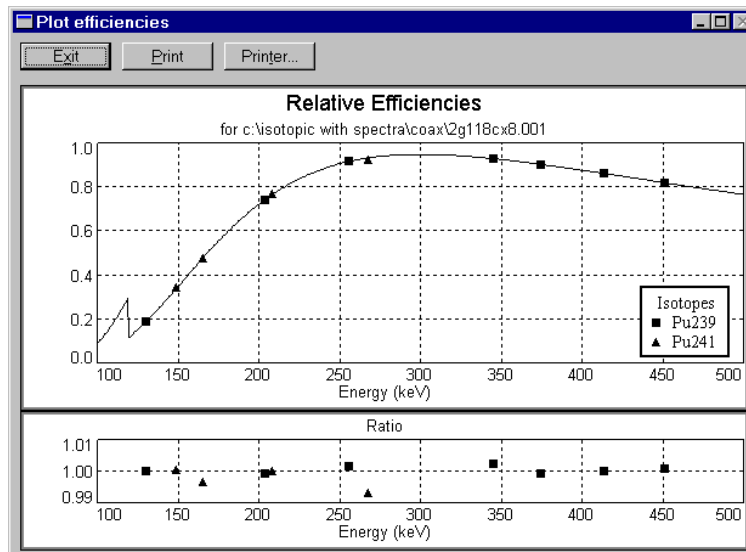


Fig. VII-8. Screen displaying fitting of relative-efficiency curve.

## VII. FRAM USER INTERFACE

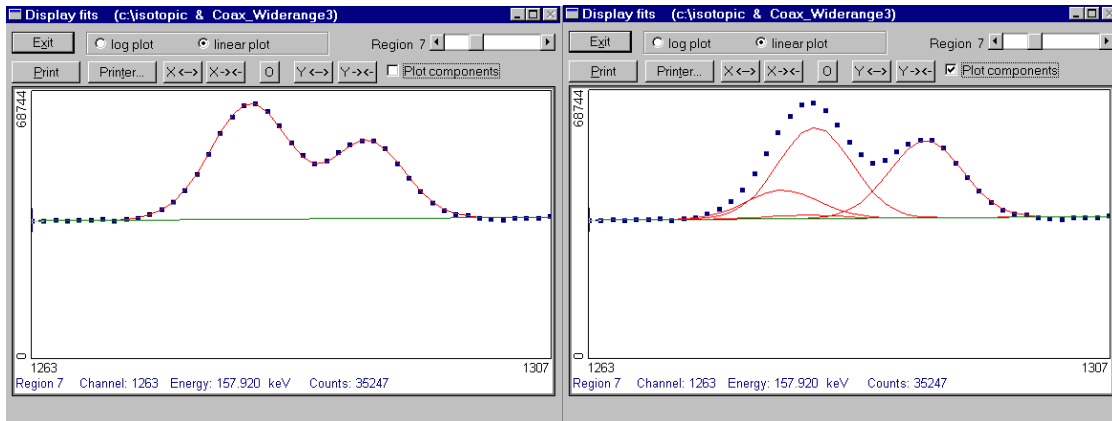


Fig. VII-9. Screens displaying peak fitting; fit envelope on left and individual components on right.

The ISOPOW option gives access to a plutonium and americium decay correction program (Sampson 86). The input values are defaulted to the results of the most recent analysis or the program can be used “off line” with arbitrary operator control of the input parameters.

### 5. Help

The Help option on the main menu lists copyright and contact information.

### C. Password Protection

Several options are password protected. The **Edit | Parameters**, **Edit | General Defaults**, and **Edit | User List** all require the entry of a valid user name and a valid password. Passwords are established at three levels for operator, supervisor, and manager, with manager being the highest level. Only the manager has access to the User List and only the manager can change the access levels of other users. A person with supervisor level privileges can edit the parameters and general defaults.

## VII. FRAM USER INTERFACE

---

### D. Dual Language Capability

The option **Language** under the **Options** menu allows the user to display the operator interface, FRAM program messages, and results in a language other than English. The language strings are kept in a text file allowing any European language to be used as the second language merely by editing the second language text file. The current second language used with FRAM is Russian. The main menu in Russian with "Options" pulled down is shown in Fig. VII-10. The user can switch between the two languages at will by clicking on the **Language** option.

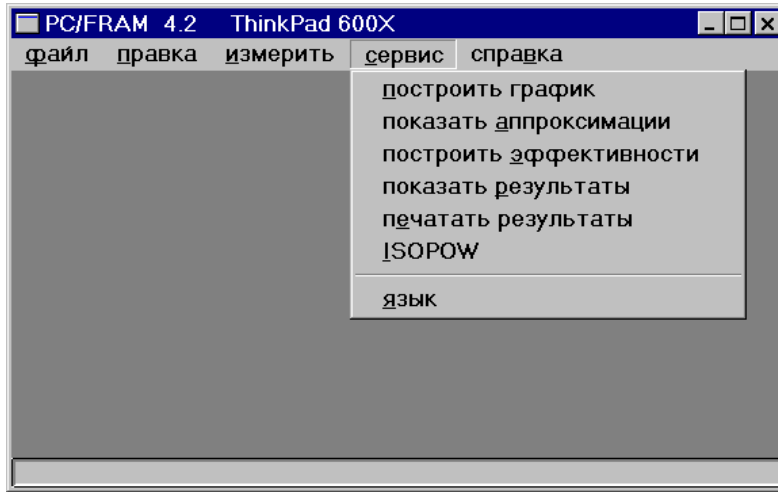


Fig. VII-10. The menu screen appearance when Russian is selected under Options/Language.

## VIII. FRAM COMPUTER REQUIREMENTS

---

### VIII. FRAM COMPUTER REQUIREMENTS

Current FRAM software, versions 3 and 4, should be run on PCs with Pentium III or Pentium 4 processors. Processor speed should be at least 200 MHz. When the physical relative-efficiency option is selected, version 4 runs slowly on a 200-MHz machine (approximately 1 minute analysis time).

Memory should be at least 128 MB. Both version 3 and version 4 have run under Windows 95, Windows 98, Windows NT, and Windows 2000. The choice of operating system does affect the ease with which the code can be set up to use Russian as the second language. Windows 2000 is particularly difficult to “Russify.”

Analysis time is almost never an issue with modern PCs but nevertheless is of interest. As FRAM has developed the code has gotten more complex, leading to longer analysis times, which have then been reduced by corresponding advances in computing power. As a benchmark, the first FRAM software running on a DEC MicroVAX (chapter IV.B) performed the analysis of a plutonium spectrum in the 120–420 keV range in about 30 s. Current analysis times tabulated in Table VIII-1 vary as much as a factor of 10, depending upon the specifics of the parameter file. The number of peaks analyzed may vary from 30 for a typical uranium parameter file to over 80 for a plutonium parameter file. In version 4 of FRAM the analysis time using the physical model relative-efficiency curve may be 4–5 times greater than using the empirical relative-efficiency curve because of the iterative analysis involved in the physical model calculation.

Table VIII-1 shows the analysis times for some typical conditions for two versions of FRAM.

Table VIII-1. Typical FRAM Analysis Times for Plutonium on a Dell Optiplex 400, Pentium 4, 1.4 Ghz.

FRAM Version	Analysis Range (keV)	Efficiency Model	Analysis Time (s) for 10 Spectra
3.2	120-420	Empirical	5
3.2	200-800	Empirical	7
4.2	120-420	Physical	22
4.2	200-800	Physical	48
4.2	120-420	Empirical	6
4.2	200-800	Empirical	10

**IX. FRAM PERFORMANCE**

**A. Measurement Precision or Repeatability**

**1. Definitions**

In this section we will describe the many interrelated factors that govern the statistical precision of an isotopic measurement. In this context the terms precision or repeatability refer to counting statistics and are usually denoted by the relative standard deviation (RSD) expressed as a percentage.

$$\%RSD = 100 \times \frac{\text{sigma}}{\text{measured value}} \quad . \quad (IX-1)$$

Here *sigma* is the absolute standard deviation, arising from counting statistics, of the *measured value*.

*Sigma* can be determined in at least two ways. First, the sigma from counting statistics is estimated within FRAM using standard error propagation techniques. This process is difficult given the amount of mathematical analysis involved, the presence of correlated variables, and the wide range of the magnitude of the measured values. However, this method gives an estimate or prediction of sigma for every measurement and is invaluable when one has only a single measurement. The second method of determining sigma is by repeated measurements. From *n*, repeated measurements of the variable *x*, we determine *s*, the standard deviation of the sample and use it as an estimate of the standard deviation of the population.

$$(s^2) = \frac{1}{n-1} \sum_1^n (x_i - \bar{x})^2 \quad (IX-2)$$

Sigma estimated in this fashion is also a random variable. That is, if the series of *n* measurements of *x* is repeated, *s* will be different. The mean value of *s* will be the population sigma. The relative standard deviation of *s* values is given by the formula

$$RSD(s) = \frac{1}{\sqrt{2(n-1)}} \quad . \quad (IX-3)$$

This expression is useful when comparing the standard deviation estimated in FRAM with the standard deviation (Eq. IX-2) observed from repeated measurements. One has to perform many repeated measurements to verify propagated error estimates accurately, as Table IX-1 illustrates.

Table IX-1. The RSD of Sigma (Error of the Error).

Number of Measurements	RSD of Sigma
10	0.235
15	0.189
25	0.144
50	0.101

This table should be kept in mind later on when we compare the sigmas from repeated measurements with FRAM's estimated sigmas.

One caveat should be mentioned before we proceed to the detailed discussion of measurement precision. For isotopic measurements of plutonium we usually express results in terms of weight percent (wt %) relative to total plutonium. The uncertainties are usually expressed as % RSD. Both the measured value and its error can be expressed as percentages. When the measured value and its uncertainty are both expressed as percentages, the reader may not know the units of the "% error." Is the % error an absolute error in units of wt % or is the % error a relative error being expressed as a % RSD? In FRAM outputs we try to be very clear about the units of the uncertainties. Uncertainties labeled as *sigma* are absolute uncertainties in the same units as the measured value. Uncertainties labeled as % are % RSD and have no units. One way we write this in FRAM output is

(Measured value  $\pm$  sigma) (% RSD)

where % RSD is as defined in Eq. IX-1.

### 2. Influencing Factors

In this section we will discuss some of the many factors that influence the precision or repeatability of the isotopic measurement. These factors are often interrelated and result in a general inability to estimate a priori the precision of a given measurement system unless all variables affecting this parameter are specified.

#### a. Count Rate and Throughput

The net counts in the photopeaks of the analyzed spectrum are the primary factors determining the measurement precision. The counting rate directly influences the net photopeak counts. While the counting rate in the detector is the parameter that is often observed, it is the actual data storage rate in the MCA that is of direct importance. The data storage rate depends upon the settings of the electronics, including shaping times and the use of pulse pileup rejection. Measurement systems are usually optimized by measuring a throughput vs incoming count rate curve along with system resolution vs incoming count rate and choosing the compromise settings best for the application at hand. An excellent discussion of these compromises may be found in Parker (Parker 91a).

These throughput curves show that higher counting rates do not always produce better measurement precision. Indeed, there is a maximum throughput rate beyond which throughput decreases and counting precision worsens. The best compromise for throughput and resolution is usually chosen to be at a counting rate significantly below the throughput maximum. Operating at input counting rates that are 50%–60% of the count rate at the throughput maximum usually yields throughput values that are 80%–90% of maximum while simultaneously preserving detector resolution.

Figure IX-1 shows the throughput and resolution measured with a 25% relative-efficiency coaxial HPGe detector coupled with first generation digital signal processing electronics (an ORTEC DSpec) operated with a rise time of 4  $\mu$ s (equivalent to a 2- $\mu$ s shaping time in an analog amplifier). The sample is 965 g PuO<sub>2</sub> with 16.85-wt % <sup>240</sup>Pu.

## IX. FRAM PERFORMANCE

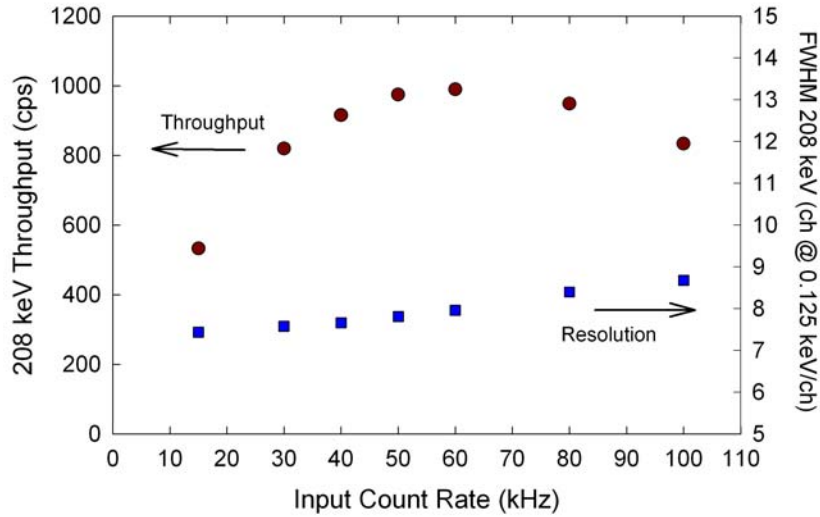


Fig. IX-1. Throughput and resolution for the 208-keV peak of  $^{241}\text{Pu}$ - $^{237}\text{U}$  with 965 g  $\text{PuO}_2$  with 16.85%  $^{240}\text{Pu}$ , a 25% relative-efficiency HPGe detector, and an ORTEC DSPEC operated at 4- $\mu\text{s}$  rise time.

Here the throughput maximum occurs at an input count rate of 60 kHz, but we usually choose to operate at a maximum input rate of around 40 kHz, where the resolution is better.

Optimizations performed in this manner affect the primary results of a FRAM isotopic analysis measurement. Figure IX-2 shows how the precision of the FRAM result for  $^{240}\text{Pu}$  and  $P_{\text{eff}}$  varies for the same data set presented in Fig. IX-1. Collection of spectral data at an input rate of 40 kHz gives essentially the same precision as operating at the 60-kHz peak of the throughput curve. The precision does not change very rapidly in a broad range about the throughput maximum, but it does change significantly above that at low count rates. In the range where the throughput curve is linear at rates below 15 kHz, the precision varies with the square root of the counting rate.

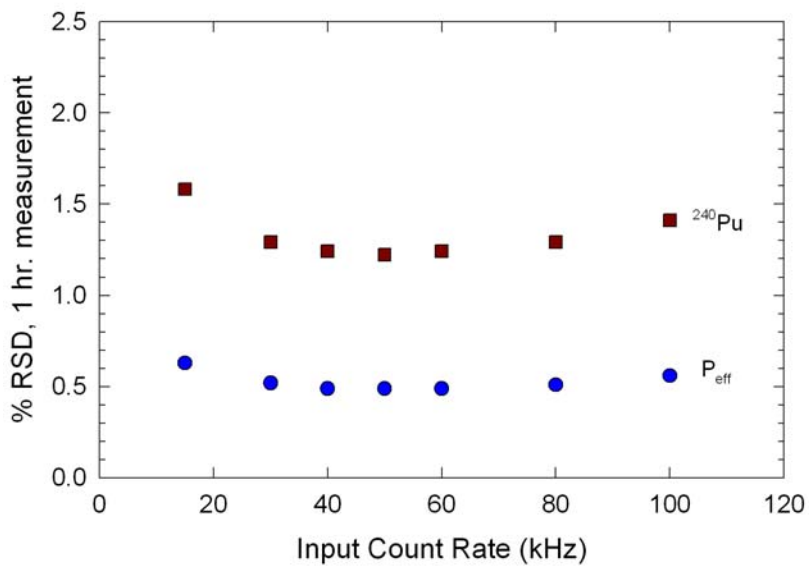


Fig. IX-2. % RSD of FRAM measurement of  $^{240}\text{Pu}$  and  $P_{\text{eff}}$  for 965 g  $\text{PuO}_2$  with 16.85%  $^{240}\text{Pu}$ , a 25% relative-efficiency HPGe detector, and an ORTEC DSPEC operated at 4- $\mu\text{s}$  rise time with analysis in the 120–450 keV region.

### b. Electronic Settings

The amplifier shaping time is the single most influential electronic setting affecting system performance. The shaping time-resolution tradeoff is well known and is discussed in detail by Parker (Parker 91a). The term “rise time” is usually used in characterizing digital spectroscopy systems with the rise time being about twice the customary analog shaping time. Throughput generally varies inversely with the shaping time. A shorter or lower shaping time improves throughput.

Longer shaping times usually correspond to better resolution and lower throughput although for any specific system the user will find that the resolution-shaping time curve goes through a broad minimum that is dependent upon the type of detector being characterized. One always operates on the low or shorter shaping time side of this minimum. We most often find that it is best to give up a little resolution in order to improve throughput. Fortunately the minimum is broad and resolution does not have to suffer too much.

For the relatively small coaxial detectors (25%–30% relative efficiency) often used with FRAM, we obtain good results with analog systems using 2- $\mu$ s Gaussian or triangular shaping. This corresponds to a rise time setting of 4  $\mu$ s for digital systems. With these settings good resolution is obtained at maximum counting rates of approximately 30 kHz (analog) and 40 kHz (digital).

For the planar detectors most often used with FRAM (16–25 mm diam. by 13–15 mm deep) we currently recommend a 1- $\mu$ s triangular shaping with an analog system or a 2- $\mu$ s rise time with digital system. The historical evolution of this setting for planar detectors parallels the development of improved amplifiers and pulse-processing methods. The first Los Alamos isotopic systems in the early 1980s (Chapter III) used 16-mm by 13-mm planar detectors, analog electronics, 100-MHz Wilkinson ADCs, and an analog amplifier shaping time of 3  $\mu$ s. Amplifier and ADC improvements in the late 1980s led to approximately 500-MHz Wilkinson ADCs and analog amplifiers with improved triangular shaping. With these systems we operated with an analog amplifier shaping time of 2  $\mu$ s and later changed to 1- $\mu$ s triangular shaping. These changes, coupled with the increase in counting rate allowed by the shorter time constants, gave a total improvement of about a factor of 3 in the precision for  $^{240}\text{Pu}$  or  $P_{\text{eff}}$ .

Pileup rejection is the other principal electronic setting that the user usually controls. Pileup rejection should always be used, if available, for isotopic measurements. Pileup rejection will prevent most of the distorted, time-overlapping events from being stored in the MCA. Pileup events, if stored, will distort the spectrum, especially the spectrum continuum, making it more difficult to extract accurate peak areas. Note, however, that pileup rejection will not prevent the storage of true coincidence events nor will it prevent the storage of random events separated in time by less than the typical pulse-pair resolution of the pileup rejector (0.5–1.0  $\mu$ s).

### c. Count Time

Poisson counting statistics are an appropriate model to represent the influence of counting time on the precision of FRAM isotopic analysis measurements. That is, the % RSD of the measurement of an isotopic fraction varies inversely with the square root of the counting time,  $T$ .

$$\%RSD \approx \frac{1}{\sqrt{T}} \quad (\text{IX-4})$$

Increasing the counting time by a factor of 2 improves (decreases) the % RSD by a factor of 1.4.

### d. Energy Range

The energy range used in the analysis is often the single largest factor in determining the precision or repeatability of a FRAM isotopic measurement. Several factors contribute to precision differences among the different energy ranges.

## IX. FRAM PERFORMANCE

The foremost factor contributing to the precision of the isotopic measurement is the intrinsic intensity of the gamma rays used in the analysis. Table IX-2 displays these intensities for the principal gamma rays from each of the four energy regions that have been historically used for isotopic analysis. It is of interest to note the intensity variation of the even isotopes  $^{238}\text{Pu}$  and  $^{240}\text{Pu}$  as one moves from lower energies to higher energies. The intensities drop by roughly an order of magnitude as one moves to each successively higher energy region. This leads to the conclusion that the best precision measurements, at least for the important  $^{240}\text{Pu}$  and  $^{238}\text{Pu}$  isotopes, come from the regions of lowest energy.

The 40–60 keV energy region is used only in the special case of freshly reprocessed ( $^{241}\text{Am}$  and  $^{237}\text{U}$  removed) plutonium-bearing solutions, mainly in reprocessing plants. This region is not used widely, if at all, in mainstream isotopic analysis applications for two reasons. First, the Compton continuum from the 59.5-keV  $^{241}\text{Am}$  peak swamps the other plutonium peaks in the 40-keV region for materials more than 45 days from a chemical separation, and second, these low-energy gamma rays are easily absorbed precluding their easy escape from many types of containers. For example, the mean free path of the 45-keV  $^{240}\text{Pu}$  gamma ray is about 0.5 mm in steel.

In contrast, the 90–105 keV region has widely been used for isotopic analysis and offers, in many cases, the best available precision for the measurement of  $^{240}\text{Pu}$ . Strong attenuation of these low-energy gamma rays does preclude the use of this region for samples in thick-walled or shielded containers. An absorber of 10 mm of steel is usually enough to defeat plutonium isotopic analysis measurements in this region.

Table IX-2. Intrinsic Gamma-Ray Intensities of Major Gamma Rays in Principal Energy Regions.

Region (keV)	$^{238}\text{Pu}$		$^{239}\text{Pu}$		$^{240}\text{Pu}$		$^{241}\text{Pu}$ - $^{237}\text{U}$ (*)		$^{241}\text{Am}$			
	(keV)	$\gamma/\text{s/g}$	(keV)	$\gamma/\text{s/g}$	(keV)	$\gamma/\text{s/g}$	(keV)	$\gamma/\text{s/g}$	(keV)	$\gamma/\text{s/g}$		
40–60	43.5	2.5 e8	51.6	6.2 e5	45.2	3.8 e6			59.5	4.5 e10		
90–105	99.9	4.6 e7	98.8	2.8 e4	104.2	5.9 e5	103.7	3.9 e6	98.9	2.6 e7		
									103.0	2.5 e7		
120–450	152.7	6.1 e6	129.3	1.4 e5	160.3	3.4 e4	148.6	7.2 e6	125.3	5.2 e6		
			375.0	3.6 e4					*208.0	2.0 e7	335.4	6.3 e5
			413.7	3.4 e4					*332.4	1.1 e6		
450–800	766.4	1.4 e5	646.0	3.4 e2	642.5	1.0 e3			662.4	4.6 e5		
									722.0	2.5 e5		

The 120–450 keV region is the most versatile single region for plutonium isotopic analysis measurements and has historically been the region addressed by isotopic measurements at Los Alamos. Measurements in this region can easily be performed through as much as 12 mm of steel and have also been carried out through 0.3 mm of lead shielding (Sampson 97). This small amount of lead shielding precludes any analysis in the 100-keV region.

FRAM was the first isotopic analysis code to carry out a complete plutonium isotopic analysis using gamma rays in the 200–800 keV region (Kelley 95, Sampson 95). This capability allows measurements in heavy-walled containers or containers whose internal shielding prevents gamma rays with energies below 200 keV from reaching the detector. Variants of this analysis allow a complete plutonium isotopic analysis through shielding of up to 25 mm of lead (Hypes 00). Figure IX-3 shows the low energy region of the gamma-ray spectrum from a plutonium oxide sample, with and without 1.6 mm of lead shielding.

## IX. FRAM PERFORMANCE

The ability to analyze the energy region from 200-800 keV for the complete plutonium isotopic distribution gives the FRAM user several more options for the analysis of large samples. The inherent advantage of the 100-keV energy region for  $^{240}\text{Pu}$  and  $^{238}\text{Pu}$  analysis is reduced for large samples analyzed at high energy because of the increased penetrability of the higher-energy gamma rays in the 600–800 keV range relative to the penetrability of 100-keV gamma rays. In effect, the higher-energy gamma rays sample a larger volume of the measured item because they can escape from deeper into the measured item. This effect of increased penetrability is apparent principally for items with larger areal plutonium densities. Table IX-3 shows the parameters that affect penetrability for the three  $^{240}\text{Pu}$  gamma rays at 104, 160, and 642 keV. This is the effect causing the relative-efficiency curves for large items to increase in magnitude as one moves to higher energies (see Fig. II-1).

Table IX-3 shows the somewhat unexpected result that the self-absorption at 160 keV is actually greater than at 104 keV. This arises because the plutonium K edge falls at 121.8 keV, between the two energies. The mean free path (mfp) at 642 keV is about 15 times greater than at 160 keV. Samples with a thickness greater than three mfp at 642 keV will have an emission rate increase at 642 keV over that at 160 keV that nearly compensates for the intrinsic intensity ( $\gamma/s/g$ ) difference (Table IX-2) at the two energies. When this is coupled with the lower background continuum present at higher energies, one often obtains better precision for measurement of  $^{240}\text{Pu}$  at 642 keV than at 160 keV.

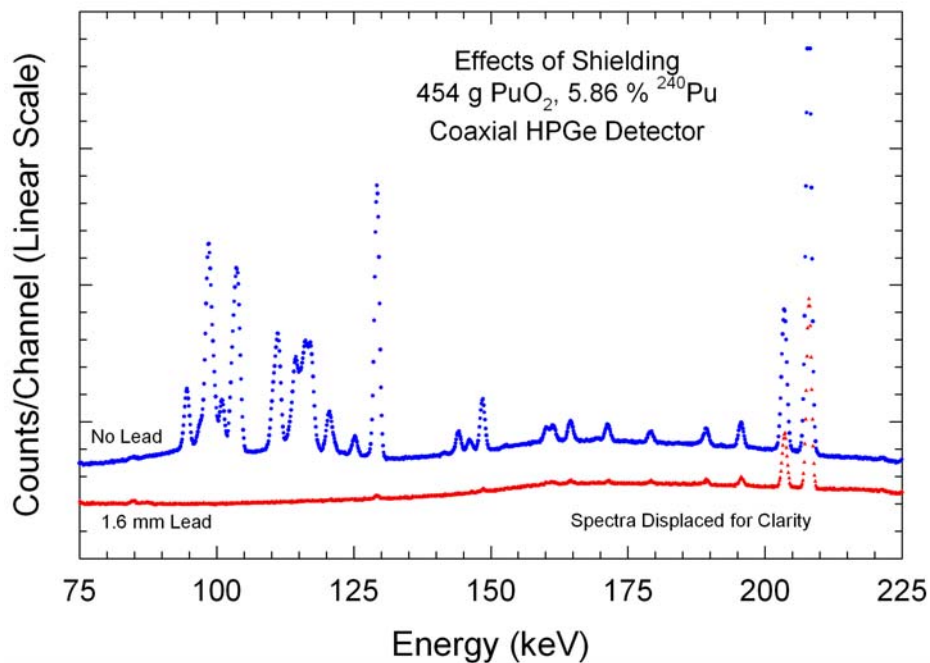


Fig. IX-3. Effect of sample shielding on the gamma-ray spectrum of 454 g  $\text{PuO}_2$  with 5.86%  $^{240}\text{Pu}$  taken with a 25% relative-efficiency HPGe detector. The sample is bare in the spectrum on top and shielded with 1.6 mm of lead in the bottom graph.

Table IX-3. Absorption Properties for  $\text{PuO}_2$  at  $\rho = 3\text{g/cm}^3$  for Gamma Rays from  $^{240}\text{Pu}$ .

Energy (keV)	$\mu/\rho$ ( $\text{cm}^2/\text{g}$ )	$\mu$ ( $\text{cm}^{-1}$ )	Mean Free Path (cm)
104	1.62	4.9	0.21
160	2.01	6.0	0.17
642	0.131	0.39	2.5

## IX. FRAM PERFORMANCE

Another consideration for the use of the 200–800 keV analysis range for larger samples is that one is often able to improve the precision still further by filtering the detector with additional lead. While this may seem strange, what happens is the additional lead filter removes the gamma rays below 200 keV that do not contribute to the 200–800 keV analysis. The sample counts at a constant input counting rate are shifted preferentially to higher energies and a greater fraction of the incoming count rate will fall into the 600-keV region compared to an unfiltered sample.

Table IX-4 summarizes the precision for all isotopes for a variety of samples with masses greater than 60 g plutonium. For nearly all measurements the counting rate is constant at 30 kHz and the precisions are given for a 1-hour count time. The precisions are those estimated by the FRAM software so the dependence on analysis range and filtering is not masked by the variability inherent in using the precision from repeated measurements. The table lists the precision from the bare sample analyzed in the 120–450 keV range, the precision from the same bare sample spectra analyzed in the 200–800 keV range, and also the precision from a lead-filtered spectrum. The lead filter thickness, with one exception, is 1.6 mm or 3 mm.

Table IX-4. Coaxial Detector Analysis With and Without Lead Filters, at 120–450 keV and 200–800 keV Analysis. Count rate = 30 kHz, Count time = 1 hour

Sample	Shielding	Analysis Range (keV)	238 % rsd	239 % rsd	240 % rsd	241 % rsd	Am % rsd	Peff % rsd	Pu Mass (g)	wt% Pu240	Ct. Rate kHz
CALEX	Bare	120–450	12.40	0.16	2.54	0.24	0.49	0.52	398	5.86	30
CALEX	Bare	200–800	5.15	0.11	1.69	0.23	0.31	0.32	398	5.86	30
CALEX	1.6 mm Pb	200–800	4.24	0.09	1.41	0.30	0.28	0.26	398	5.86	30
PUEU7	Bare	120–450	6.98	0.14	2.30	0.22	0.92	0.48	2000	5.86	30
PUEU7	Bare	200–800	3.49	0.10	1.62	0.21	0.43	0.32	2000	5.86	30
PUEU7	1.6 mm Pb	200–800	2.79	0.08	1.31	0.28	0.36	0.26	2000	5.86	30
JOO1325	Bare	120–450	11.40	0.17	2.62	0.28	0.57	0.55	500	5.90	30
JOO1325	Bare	200–800	3.90	0.10	1.61	0.26	0.32	0.31	500	5.90	30
JOO1325	0.8 mm Pb	200–800	3.43	0.09	1.37	0.31	0.29	0.26	500	5.90	30
JOO1325	2.4 mm Pb	200–800	3.15	0.08	1.25	0.53	0.29	0.24	500	5.90	30
STD8	Bare	120–450	7.62	0.11	1.66	0.22	0.51	0.36	239	6.30	30
STD8	Bare	200–800	6.66	0.14	2.06	0.27	0.38	0.42	239	6.30	30
STD8	1.6 mm Pb	200–800	5.31	0.11	1.65	0.36	0.34	0.33	239	6.30	30
SD4030	Bare	120–450	1.89	0.18	1.31	0.22	0.27	0.39	869	11.79	30
SD4030	Bare	200–800	1.48	0.16	1.23	0.22	0.25	0.35	869	11.79	30
SD4030	1.6 mm Pb	200–800	1.13	0.13	0.94	0.20	0.21	0.27	869	11.79	30
LAO225	Bare	120–450	1.83	0.16	0.82	0.19	0.24	0.33	869	16.53	30
LAO225	Bare	200–800	1.28	0.16	0.79	0.20	0.22	0.30	869	16.53	30
LAO225	1.6 mm Pb	200–800	1.00	0.13	0.65	0.18	0.19	0.25	869	16.53	30
LAO250	Bare	120–450	2.51	0.19	0.97	0.23	0.27	0.39	60	16.27	28
LAO250	Bare	200–800	1.89	0.20	1.05	0.25	0.27	0.40	60	16.27	28
LAO250	3 mm Pb	200–800	1.64	0.20	1.00	0.32	0.31	0.38	60	16.27	11

## IX. FRAM PERFORMANCE

Table IX-4 (Continued)

Sample	Shielding	Analysis Range (keV)	238	239	240	241	Am	Peff	Pu Mass (g)	wt% Pu240	Ct. Rate kHz
			% rsd								
LAO251	Bare	120–450	3.21	0.24	1.20	0.27	0.31	0.49	172	16.45	30
LAO251	Bare	200–800	1.73	0.20	0.99	0.24	0.27	0.37	172	16.45	30
LAO251	3 mm Pb	200–800	1.26	0.16	0.80	0.34	0.29	0.30	172	16.45	25
LAO252	Bare	120–450	3.43	0.26	1.33	0.30	0.34	0.54	322	16.31	32
LAO252	Bare	200–800	1.62	0.19	0.96	0.24	0.26	0.36	322	16.31	32
LAO252	3 mm Pb	200–800	1.23	0.16	0.81	0.27	0.24	0.30	322	16.31	32
LAO253	Bare	120–450	3.28	0.25	1.27	0.29	0.33	0.51	613	16.47	34
LAO253	Bare	200–800	1.54	0.18	0.90	0.23	0.25	0.34	613	16.47	34
LAO253	3 mm Pb	200–800	1.12	0.14	0.72	0.32	0.26	0.27	613	16.47	34
LAO255	Bare	120–450	3.21	0.25	1.25	0.28	0.32	0.50	544	16.35	30
LAO255	Bare	200–800	1.61	0.18	0.93	0.24	0.26	0.35	544	16.35	30
LAO255	3 mm Pb	200–800	1.13	0.14	0.71	0.26	0.23	0.27	544	16.35	30
LAO256	Bare	120–450	3.63	0.27	1.37	0.31	0.35	0.56	385	16.35	30
LAO256	Bare	200–800	1.65	0.19	0.94	0.24	0.26	0.36	385	16.35	30
LAO256	3 mm Pb	200–800	1.12	0.14	0.69	0.27	0.22	0.26	385	16.35	30
LAO261	Bare	120–450	3.56	0.26	1.31	0.30	0.34	0.54	849	16.45	30
LAO261	Bare	200–800	1.58	0.18	0.91	0.24	0.26	0.35	849	16.45	30
LAO261	3 mm Pb	200–800	1.15	0.14	0.70	0.27	0.23	0.27	849	16.45	30
PEO381	Bare	120–450	4.97	0.18	1.55	0.23	0.25	0.43	614	10.36	30
PEO381	Bare	200–800	2.06	0.12	1.07	0.19	0.19	0.27	614	10.36	30
PEO381	3 mm Pb	200–800	1.86	0.12	1.05	0.35	0.23	0.27	614	10.36	30
PEO382D	Bare	120–450	7.07	0.23	2.07	0.29	0.33	0.56	300	9.70	30
PEO382D	Bare	200–800	3.06	0.16	1.47	0.26	0.26	0.37	300	9.70	30
PEO382D	3 mm Pb	200–800	2.12	0.12	1.08	0.37	0.23	0.27	300	9.70	30
PEO385	Bare	120–450	7.24	0.21	2.05	0.28	0.34	0.56	459	9.28	30
PEO385	Bare	200–800	3.07	0.14	1.38	0.25	0.25	0.34	459	9.28	30
PEO385	3 mm Pb	200–800	2.21	0.11	1.05	0.41	0.23	0.26	459	9.28	30
PEO447	Bare	120–450	5.15	0.24	2.07	0.30	0.33	0.57	778	10.16	30
PEO447	Bare	200–800	2.14	0.15	1.35	0.24	0.24	0.34	778	10.16	30
PEO447	3 mm Pb	200–800	1.56	0.12	1.04	0.36	0.23	0.26	778	10.16	30
SRP12-1	Bare	120–450	3.58	0.27	1.94	0.31	0.38	0.62	875	11.85	30
SRP12-1	Bare	200–800	1.52	0.16	1.16	0.23	0.26	0.35	875	11.85	30
SRP12-1	3 mm Pb	200–800	1.07	0.12	0.88	0.29	0.23	0.26	875	11.85	30

The trend is very clear for these larger samples. Measurement precision improves as the analysis moves into the 200–800 keV range and improves further when the spectrum is filtered. Plutonium-241 does not improve in every case because its analysis is carried out at the lowest energies (200–340 keV) of the analysis range.

### e. Detector Type

The influence of the detector type is directly related to the energy range used in the analysis. Two principle types of HPGe detectors have been most often used for isotopic analysis with the FRAM code.

Planar Detectors Planar detectors of dimensions 16 mm diam. by 13 mm thick and 25 mm diam. by 15 mm thick are commonly used for FRAM measurements. These detectors have historically been used in the 120–420 keV energy range and with the advent of version 4 of FRAM, can now be used in the 100-keV region. For most measurements on samples in thin containers, analysis of the spectrum in the 100-keV region will provide better precision for all of the isotopes than the analysis of the spectrum in the 120–420 keV region. For samples in containers with steel wall thicknesses in the range of 5–10 mm, the optimum analysis region for a planar detector becomes less clear. Above a wall thickness of approximately 10 mm of steel, the 100-keV region analysis may fail leaving analysis in the 120–420 keV region as the only viable option.

Coaxial Detectors Coaxial detectors of approximately 25%–30% relative efficiency (relative to a 3-in.-diam. by 3-in.-thick NaI(Tl) detector for  $^{60}\text{Co}$  at a distance of 25 cm) have been most often used with FRAM. The precision of a coaxial detector's measurements depends upon the energy range and shielding, as discussed previously. It is not always possible to predetermine which detector, planar or coaxial, will have the better precision in the 120–420 keV region. Suffice to say that the measurement precision in this energy range is often similar for the two detector types, and the choice is often made empirically with measurements under realistic conditions. When samples are shielded, planar detectors will not be viable and the coaxial detector choice often comes down to whether or not to use additional filters.

CdTe Detectors Although version 4 of FRAM can also analyze spectra from CdTe detectors, the precision of CdTe detector results is not as good as with HPGe detectors. This is because of the small size of the CdTe detectors (dimensions of a few millimeters) giving volumes over a thousand times smaller than a coaxial HPGe detector (Vo 02). detectors are discussed further in Chapter XIII.

### f. Sample Characteristics

Characteristics of the measured item, such as mass, density, and shape, affect measurement precision in conjunction with other variables. While we have seen the effect of larger mass samples on the analysis energy range (Table IX-4) the effect of the combination of density and shape at a constant mass is less apparent.

Compare a sample with a large area presented to the detector, but with a low areal density ( $\text{g}/\text{cm}^2$ ) of plutonium, to a sample of the same mass with less surface area and higher areal density. In the large-area, low areal density case, the lower-energy gamma rays will be enhanced relative to those at higher energy and analysis in the 120–450 keV region may produce the best precision. Conversely, the sample with the greater areal density will have an enhanced high-energy region relative to the low areal density sample. These characteristics can often be observed in the shape of the relative-efficiency curve (see Fig. II-1). The relative-efficiency curve tends to fall off with increasing energy more rapidly for low areal density samples while samples with a greater areal density tend to have a higher relative efficiency continuing to higher energies.

### 3. Prediction of Precision in the FRAM Code

The output of every FRAM measurement includes a predicted value for  $\sigma$ , the absolute error in the measured mass %, where  $\sigma$  is obtained from the propagation of counting statistics uncertainties in the photopeak areas used in the analysis. These fundamental values are seen in the “boxed” portion of the FRAM output displayed in Fig. IX-4. This predicted counting statistics error is also reported as a % RSD where % RSD has been defined in Eq. IX-1. These fundamental errors are further propagated to produce the absolute and relative errors in the other parameters in the output.

We purposely do not include any systematic error components (such as errors in branching ratios, half lives, or fitting errors described by a reduced Chi squared value) in the  $\sigma$  or % RSD values so we may check our purely statistical error prediction with repeated measurements.

## IX. FRAM PERFORMANCE

```

*****
PC FRAM (4.2) Isotopic Analysis 17-Jun-2002 16:01:19
(Fixed energy Response function Analysis with Multiple efficiencies)
System ID: Demonstration

spectrum source: c:\fram42\testspect.chn\70coax8k.chn
spectrum date: 11-Oct-1993 15:08:14
live time: 5778 s
true time: 7200 s
num channels: 8192

parameter set: Coax_Wlidebarange3 (2002.06.10 18:25)
Coax .125 kev/ch, HomoAm/Pu, Equ., 3-25% Pu240,<450 keV
*****
*****
diagnostics passed.

                                                                    (By Corr)      (ug/gPu)
Pu238      Pu239      Pu240      Pu241      Pu242      Am241
mass% 0.8303    74.7812    18.1917    3.9603    2.2366    28036.9
sigma 0.0032    0.1914    0.2081    0.0107    0.0238    80.4
%RSD  0.39%     0.26%     1.14%     0.27%     1.06%     0.29%
%TotPwr 43.70    13.38     11.95     1.25     0.02     29.69

Specific Power (W/gPu): ( 10.7827 +/- 0.0229)e-003 ( 0.21%)

Effective Pu240 fraction: ( 24.0414 +/- 0.2121)e-002 ( 0.88%)

Time since chemical separation: 4077.7 +/- 4.3 days ( 0.11%)

Relative mass (Np237 / Pu): 2.949e-004 ( 0.52%)
Relative mass ( U235 / Pu): 1.713e-003 ( 65.74%)
Relative mass (Am243 / Pu): 3.524e-008 ( 69.67%)
*****

```

Fig. IX-4. FRAM output showing the absolute statistical error (*sigma*) and the relative error (% RSD) propagated from counting statistics.

We confirm the correctness of the error propagation within the FRAM code by analyzing many sets of repeated measurements on many different types of samples. We compare the *sigma* predicted by the FRAM software with the *sigma* calculated from the distribution of the repeated measurements (see section IX.A.1). The ratio of the propagated *sigma* to the *sigma* observed from repeated measurements should be near unity within the uncertainty of the observed *sigma* (Eq. IX-3).

These comparisons are made with a database containing over 40 repeat measurement data sets, with each data set containing from 10 to 25 repeat measurements. Table IX-4 displays the average ratio over many data sets of the FRAM-propagated *sigma* to the estimate of *sigma* observed from repeated measurements on plutonium samples. Table IX-5 displays the same information for repeated measurements on uranium.

## IX. FRAM PERFORMANCE

Table IX-4. Comparison of Predicted and Observed Statistical Uncertainties for Plutonium Analysis Using FRAM version 4.

Detector	Region (keV)	No. Data Sets	No. Meas.	Average Ratio: Predicted/Observed					
				<sup>238</sup> Pu	<sup>239</sup> Pu	<sup>240</sup> Pu	<sup>241</sup> Pu	<sup>241</sup> Am	P <sub>eff</sub>
Coaxial	120–450	46	751	0.97	0.97	0.98	0.65	0.74	1.28
Coaxial	200–800	53	828	0.73	0.94	0.94	0.59	0.82	1.18

Table IX-5. Comparison of Predicted and Observed Statistical Uncertainties for Uranium Analysis Using FRAM version 4.

Detector	Region (keV)	No. Data Sets	No. Meas.	Average Ratio: Predicted/Observed		
				<sup>234</sup> U	<sup>235</sup> U	<sup>238</sup> U
Coaxial	120–1001	33	415	1.35	0.84	0.80

We predict the statistical uncertainty very well for <sup>238</sup>Pu, <sup>239</sup>Pu, and <sup>240</sup>Pu. FRAM underestimates the statistical error by about 25% (relative) for <sup>241</sup>Pu and <sup>241</sup>Am. This likely arises from the difficulty in correctly apportioning the uncertainties for the coenergetic peaks that contain contributions from both <sup>241</sup>Pu (and daughter <sup>237</sup>U) and <sup>241</sup>Am. The statistical error in P<sub>eff</sub> is overestimated in FRAM, probably because of the correlations resulting from the normalization condition that all isotopic fractions must sum to unity.

On the average, the statistical predictions for uranium are reasonably good. When displayed as a function of <sup>235</sup>U enrichment (Fig. IX-5), we do see some <sup>235</sup>U dependence. The error bars in Fig. IX-5 show the uncertainty from the finite number of measurements (Eq. IX-3) for the observed uncertainty in each data set.

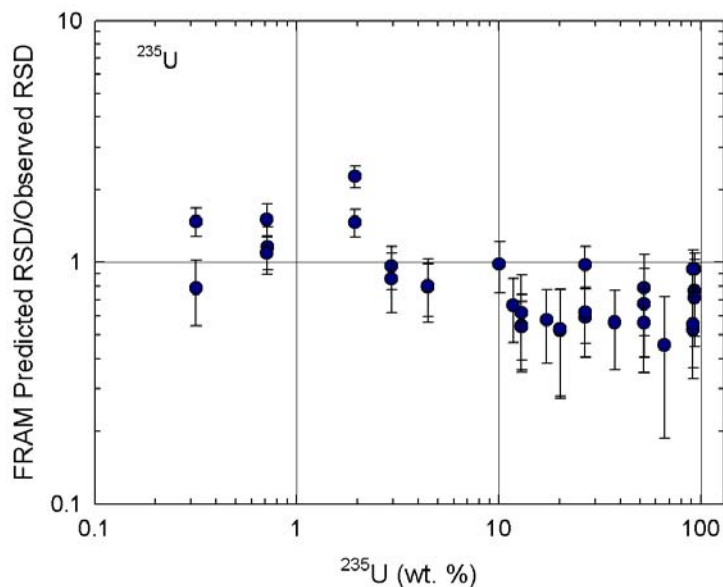


Fig. IX-5. Uranium-235 dependence of FRAM estimate of <sup>235</sup>U statistical uncertainty.

#### 4. Examples of FRAM's Statistical Precision

In this section we present examples of FRAM's statistical precision taken from the precision observed from archival data sets of repeated measurements. In Fig. IX-6 we display the precision for plutonium observed from repeated measurements plotted vs sample mass for  $P_{\text{eff}}$ . Figure IX-7 displays the same data plotted for  $^{240}\text{Pu}$  percentage.

These data represent not only different samples, different sample masses, and different isotopic compositions, but also different detectors, counting times, counting rates, and data acquisition electronics. Counting times for most data sets are 1 hour, but some data sets have 30-minute or 2-hour count times. As such, the data display the wide range of precisions that one might expect to obtain under the many different measurement conditions applicable to FRAM analysis.

One should also note that these are laboratory measurements, in most cases, where one was able to attain an optimum counting rate from the sample. In many field applications detector-to-sample distance constraints prevent this and lead to poorer measurement precision.

The coax and planar data in the 120–450 (420) keV region show similar results, at least at lower masses. We do see a definite trend [precision becomes poorer (larger) as mass decreases] in the precision vs mass for the 200–800 keV analysis region. This precision is worse than that in the 120–450 (420) keV region for small masses but can be, in many cases, the best choice for large mass samples.

Figures IX-8 and IX-9 display the same data plotted as a function of  $^{240}\text{Pu}$  percentage.

Figure IX-10 extracts data for a single-analysis-method-coaxial-detector data analyzed in the 120–450 keV region. Each sample's data set is analyzed for precision of  $^{240}\text{Pu}$  and  $P_{\text{eff}}$ . The  $P_{\text{eff}}$  precision is better in every case as shown by the ratio [% RSD  $^{240}\text{Pu}$ /% RSD  $P_{\text{eff}}$ ] being greater than 1 for all samples.

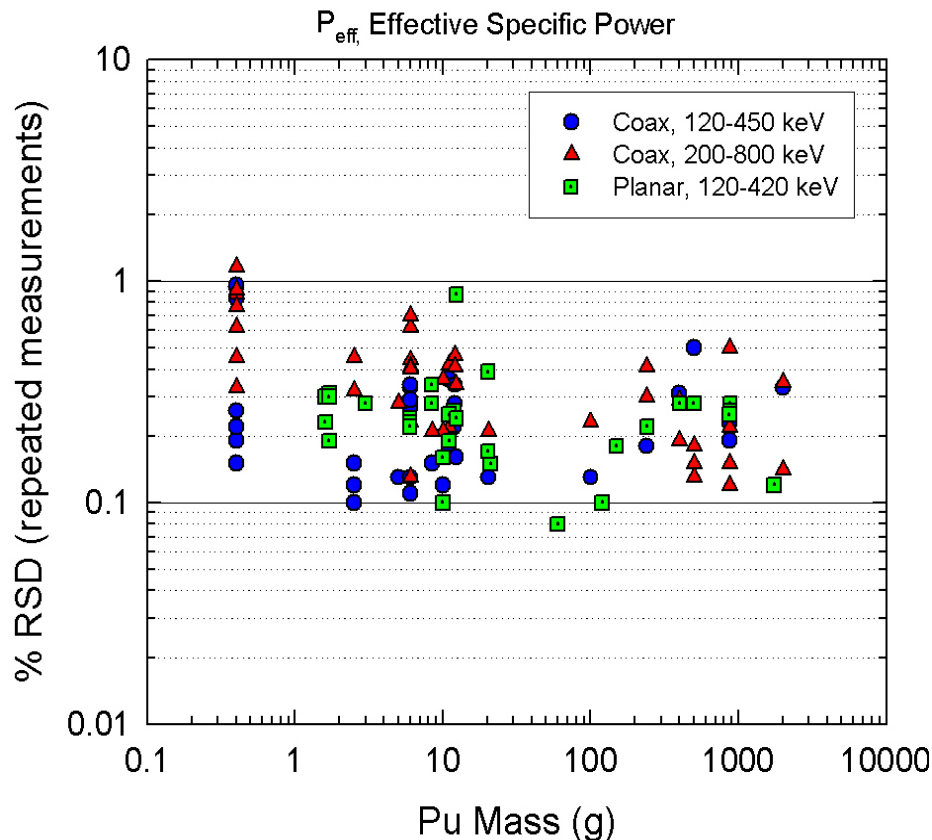


Fig. IX-6. Observed precision for  $P_{\text{eff}}$  for different detectors, different isotopic compositions, different count times, and different analysis regions as a function of plutonium mass.

IX. FRAM PERFORMANCE

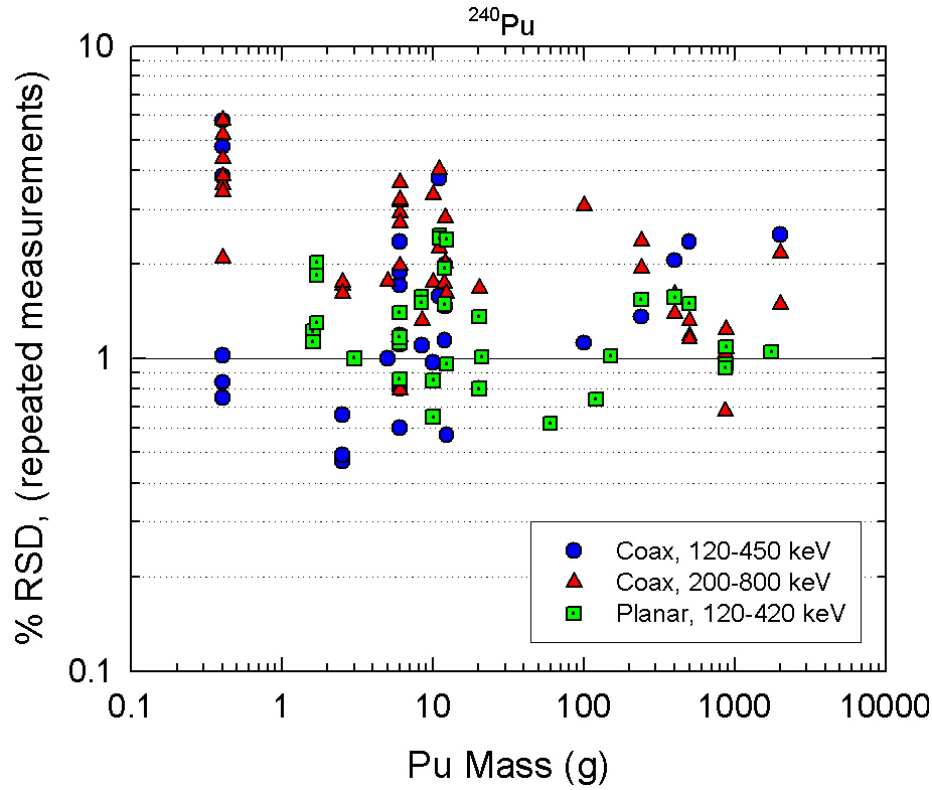


Fig.IX-7. Observed precision for  $^{240}\text{Pu}$  for different detectors, different isotopic compositions, different count times, and different analysis regions as a function of plutonium mass.

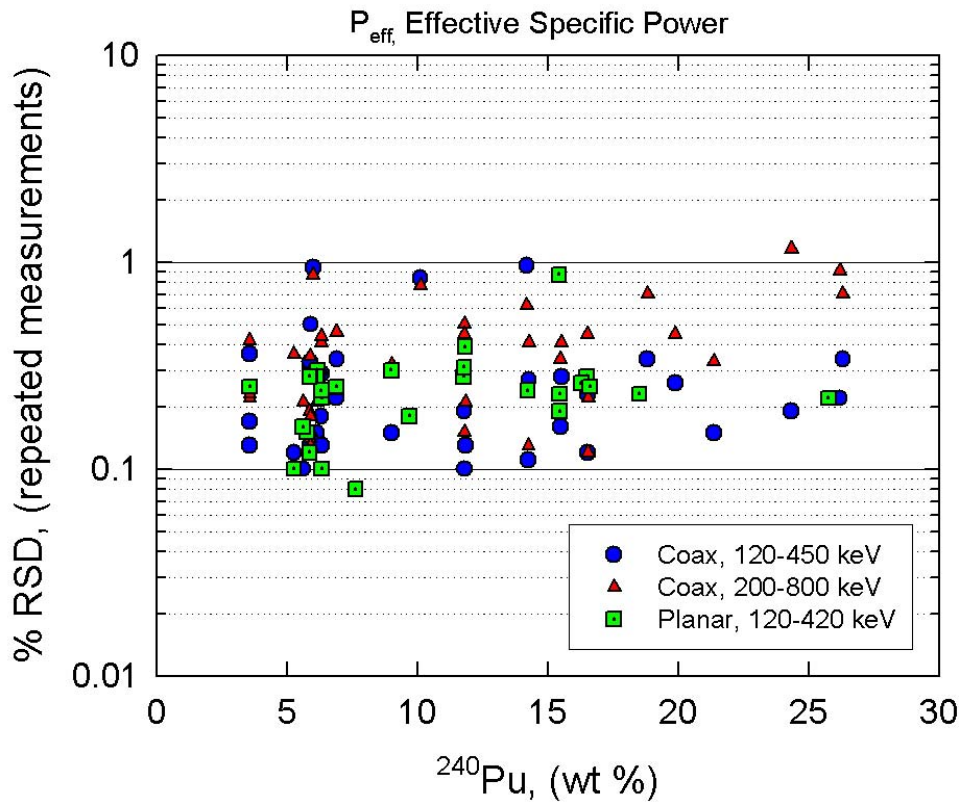


Fig.IX-8. Observed precision for  $P_{\text{eff}}$  for different detectors, different isotopic compositions, different count times, and different analysis regions as a function of  $^{240}\text{Pu}$  percentage.

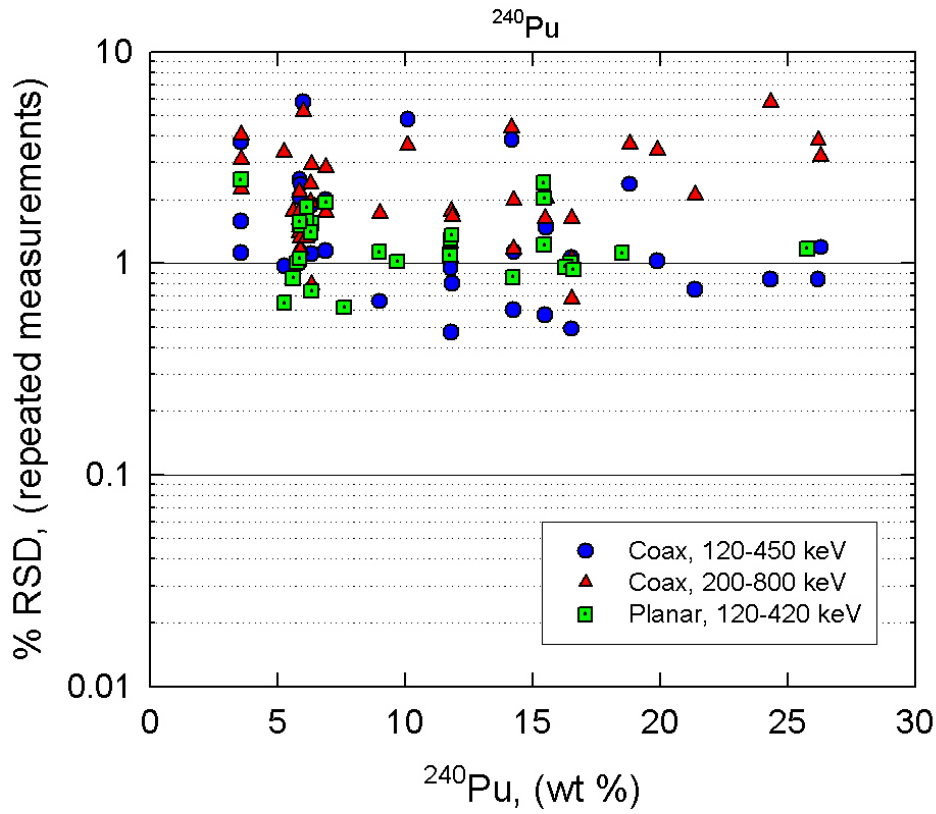


Fig.IX-9. Observed precision for  $^{240}\text{Pu}$  for different detectors, different isotopic compositions, different count times, and different analysis regions as a function of  $^{240}\text{Pu}$  percentage.

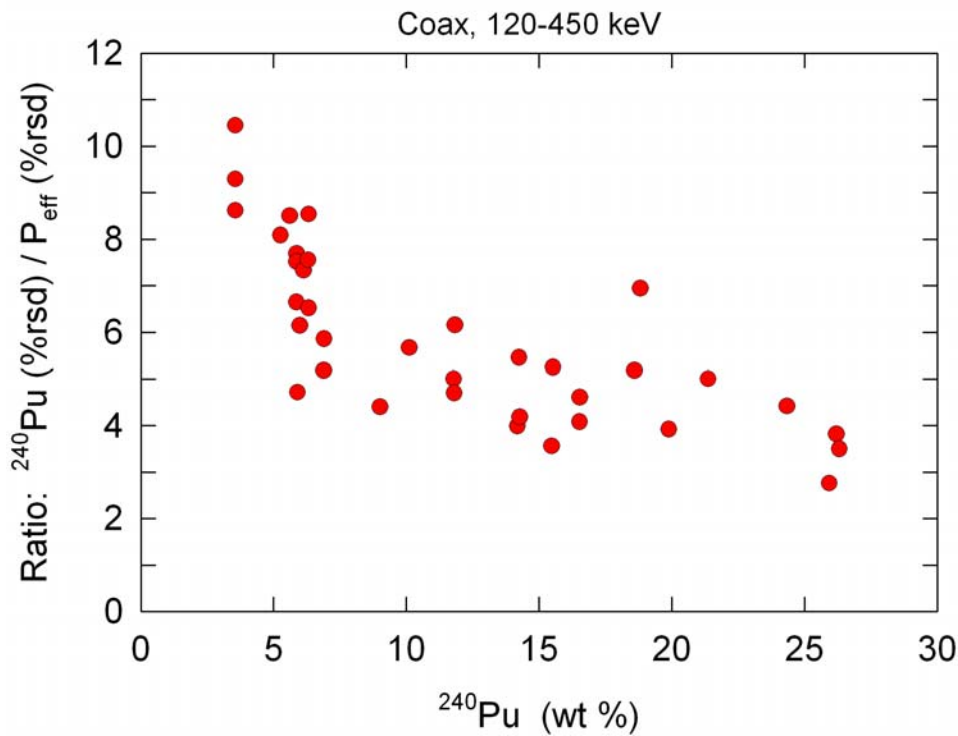


Fig. IX-10. The ratio of the observed precision for  $^{240}\text{Pu}$  to that for  $P_{\text{eff}}$  for a coaxial detector with analysis in the 120-450 keV region is plotted vs the percentage of  $^{240}\text{Pu}$  in the sample. Every sample shows better precision for  $P_{\text{eff}}$  than for  $^{240}\text{Pu}$  (ratio > 1) for the same data.

## IX. FRAM PERFORMANCE

We also document the performance of FRAM for analysis in the 100-keV region, as this is one of the newest features of version 4 of FRAM. The available data are less extensive than those shown for the analyses above 120 keV. It does demonstrate, however, that FRAM analyses in this energy region can be more precise than other analyses for unshielded samples in thin-walled containers.

Table IX-6 compares the 100-keV region precision from planar detector data to planar detector analyses in the 120–420 keV region and also to a coaxial detector analysis in the 120–450 keV

Table IX-6. 100 keV Region Planar Detector Precision Compared With 120-420(450) keV Analysis. Thirty-Minute Count Time at Indicated Counting Rate.

Sample Name	Detector Energy Range	Pu-240 % RSD	Spec Pow % RSD	Pu Mass (g)	Ct. Rate (kHz)	Pu-240 wt %
CBNM93	Planar 100 keV	1.74	0.30	6.0	26	6.314
	Planar 120–420	2.11	0.31	6.0	10	6.314
	Coax 120–450	1.93	0.30	6.0	40	6.314
CBNM84	Planar 100 keV	0.53	0.21	6.0	31	14.270
	Planar 120–420	1.24	0.35	6.0	10	14.234
	Coax 120–450	1.02	0.25	6.0	40	14.269
CBNM70	Planar 100 keV	0.96	0.37	6.0	38	18.828
	Planar 120–420	1.57	0.31	6.0	25	18.509
	Coax 120–450	2.25	0.34	6.0	40	18.819
CBNM61	Planar 100 keV	0.78	0.37	6.0	38	26.330
	Planar 120–420	1.63	0.31	6.0	25	25.776
	Coax 120–450	1.20	0.38	6.0	40	26.314
STDEUPU7	Planar 100 keV	0.61	0.14	5.0	24	5.864
	Coax 120–450	1.25	0.19	5.0	30	5.864
STDISO3	Planar 100 keV	2.06	0.17	11.0	27	3.560
	Planar 120–420	4.47	0.45	11.0	8	3.562
	Coax 120–450	2.17	0.18	11.0	40	3.560
STDISO6	Planar 100 keV	0.92	0.15	8.4	26	6.131
	Planar 120–420	2.15	0.33	8.4	7	6.130
	Coax 120–450	1.40	0.25	8.4	40	6.131
STDISO9	Planar 100 keV	1.15	0.20	11.9	30	6.896
	Planar 120–420	2.79	0.33	11.9	9	6.891
	Coax 120–450	1.44	0.29	11.9	40	6.896
STDISO12	Planar 100 keV	0.55	0.19	20.2	38	11.854
	Planar 120–420	1.97	0.52	20.2	11	11.821
	Coax 120–450	1.42	0.33	20.2	40	11.854
STDISO15	Planar 100 keV	0.40	0.22	12.3	38	15.523
	Planar 120–420	3.34	1.17	12.3	11	15.437
	Coax 120–450	1.25	0.24	12.3	40	15.523
PIDIE6-1	Planar 100 keV	2.05	0.30	0.4	5	5.990
	Coax 120–450	1.43	0.21	0.4	12	5.990
PIDIE6-3	Planar 100 keV	0.70	0.31	0.4	8	14.200
	Coax 120–450	1.04	0.20	0.4	17	14.200
PIDIE6-5	Planar 100 keV	0.53	0.20	0.4	12	21.415
	Coax 120–450	0.84	0.19	0.4	26	21.415
PIDIE6-7	Planar 100 keV	0.53	0.19	0.4	28	26.433
	Coax 120–450	0.99	0.29	0.4	40	26.433

## IX. FRAM PERFORMANCE

region. Note that the measurements are not at a constant counting rate. The precisions are those observed from repeated measurements with most data sets having  $n > 20$ . Also, the 100-keV region data are not optimum as they were acquired with more cadmium filtering than necessary. Even so, Table IX-6 shows that measurements in the 100-keV region are more precise than measurements at higher energies, especially for small samples. This is, of course, as expected from the branching ratio values discussed earlier and has been well demonstrated in other isotopic analysis codes (Gunnink 90).

Figure IX-11 displays the precision of the measurement of the  $^{235}\text{U}$  isotopic fraction in pure uranium samples. The precisions are those from repeated measurements and the data sets represent both 30-minute and 1-hour data. The detectors used are 25%–30% relative-efficiency coaxial detectors. The measurement precision (counting statistics) is pretty much constant for  $^{235}\text{U}$  enrichments below approximately 10%. In this case the measurement precision is driven by the intensity of the 258-keV  $^{238}\text{U}$  daughter peak that effectively controls the normalization of the relative-efficiency curve. The intensity of this peak does not change very much for enrichments below 10 wt %.

The precision of the measurement of  $^{234}\text{U}$  is also of interest for higher enrichment samples as this isotope provides the overwhelming majority of the heat produced for calorimetry measurements. Figure IX-12 displays the  $^{234}\text{U}$  precision for all  $^{235}\text{U}$  enrichments for which you can measure  $^{234}\text{U}$ . Only the enrichments above approximately 90%  $^{235}\text{U}$  coupled with kilogram-sized samples can currently be measured by calorimetry. For these samples, measurement precision can be in the 1%–2% range for  $^{234}\text{U}$ .

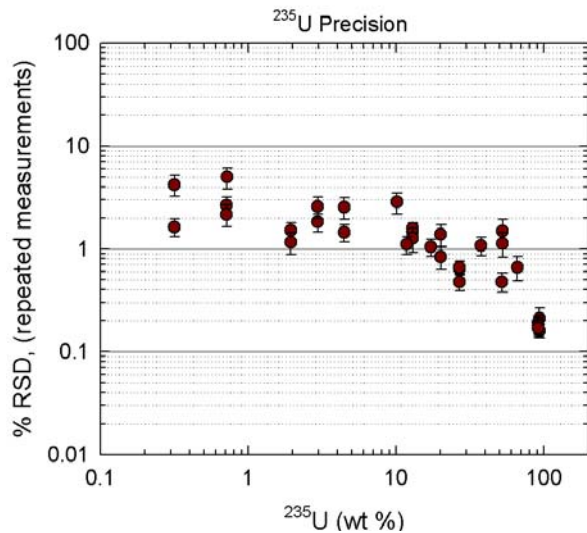


Fig. IX-11. Uranium-235 measurement precision.

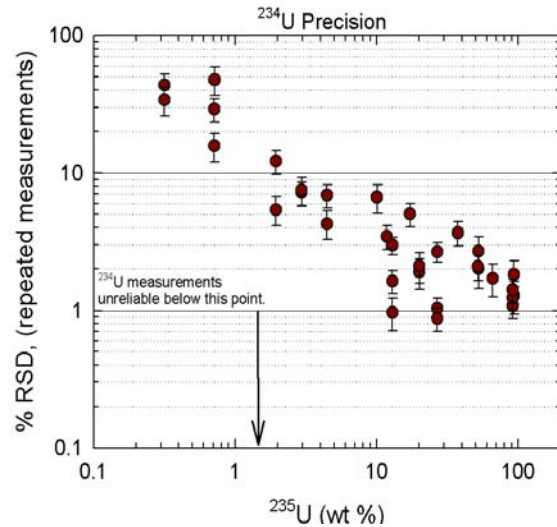


Fig. IX-12. Uranium-234 measurement precision.

### B. Measurement Bias

#### 1. Introduction

Bias is defined as the difference between the measured value and the true value. For all examples we estimate the true value by using the best available value for the isotopic composition and  $^{241}\text{Am}$  content of the measured item. The best available values almost always are derived from mass spectrometry measurements, sometimes supplemented with alpha counting for  $^{238}\text{Pu}$  and/or  $^{241}\text{Am}$ . In this document bias is expressed as a ratio of the measured value divided by the best available or “accepted value.”

NDA practitioners at Los Alamos have access to a large number of well-characterized plutonium, uranium, and MOX-bearing items having well-known isotopic distributions and  $^{241}\text{Am}$  content. Several

of the items are certified reference materials (CRM) traceable to the national measurement system and are national and international standards. Most of the remaining items have well-documented mass spectrometry values from routine analytical characterizations. Still others have mass spectrometry values determined by several different laboratories or with extensive measurements at a single laboratory. We find that routine mass spectrometer measurements on modern instruments are nearly always adequate for characterization of the bias of a gamma-ray isotopic composition measurement. Nevertheless, we always examine the mass spectrometer and gamma-ray measurements closely. We especially look for problems with  $^{238}\text{Pu}$ ,  $^{241}\text{Pu}$ , and  $^{241}\text{Am}$ .

Plutonium-238 This isotope is one of the most difficult to measure by mass spectrometry. First of all, its low concentration, in the range of 0.01% for weapons grade plutonium, approaches the sensitivity limit for mass spectrometry. Second, it has the same mass as  $^{238}\text{U}$ . The most careful procedures are necessary to keep the plutonium sample (typically nanograms of plutonium) from being contaminated with environmental uranium. Any such contamination will result in too large a value for the  $^{238}\text{Pu}$  isotopic fraction from the mass spectrometer. We have observed these biases from old (20–30 years) mass spectrometer measurements of plutonium. Alpha counting can obviate these problems. Typical analytical uncertainties for  $^{238}\text{Pu}$  fall in the 1%–3% (relative) range and can be the limiting factor in characterizing the  $^{238}\text{Pu}$  bias for gamma-ray isotopic composition measurements.

Plutonium-241 The measurement of  $^{241}\text{Pu}$  by mass spectrometry requires a chemical separation of the mass spectrometry sample to remove isobaric  $^{241}\text{Am}$ . If this chemical separation is not complete, the mass spectrometer measurement of the  $^{241}\text{Pu}$  isotopic fraction may be biased high.

Americium-241 There are no CRMs for characterizing the concentration of  $^{241}\text{Am}$  in plutonium. This limits the ability of the analytical chemists to make traceable  $^{241}\text{Am}$  measurements. Typical characterizations may be biased by several percent.

We discover these problems by comparing gamma-ray measurements of the sample in question with gamma-ray measurements on another sample of similar isotopic composition that is known to have a bias-free analytical characterization. We have not observed any problems with mass spectrometry measurements on uranium.

### 2. Plutonium Measurement Bias

Los Alamos has a large archive of spectral data from plutonium going back to 1988. These data encompass many different detectors and varying electronic configurations including NIM, portable MCA, and digital spectroscopy systems. Some of the samples have been measured on different dates, separated in some cases by eight or more years. This has proven invaluable for verifying the proper analysis for  $^{241}\text{Am}/^{241}\text{Pu}$ .

One such archival data set of over 800 measurements for plutonium using coaxial HPGe detectors is shown in Table F-1 in Appendix F. Similar, though less extensive, data sets exist for plutonium measurements with planar HPGe detectors as well as coaxial and planar detector measurements on uranium. Analysis consists of averaging results for the multiple runs for each sample and then averaging the averages for all samples to obtain an overall bias for the entire data set. The results of this analysis for the data set of Table F-3 (analysis of all data sets in Table F-3 in the 200–800 keV region) are displayed in Table IX-7. We manually enter the accepted value for  $^{242}\text{Pu}$  so the correlation does not affect the results. We have omitted the averages for  $^{238}\text{Pu}$  for samples known to have incorrect accepted values or have measurements so statistically poor as to be unreliable. In these cases we also omitted the value for  $P_{\text{eff}}$  that can depend strongly on  $^{238}\text{Pu}$ .

**IX. FRAM PERFORMANCE**

Table IX-7. Bias Analysis of Archival Coaxial Data, 200–800 keV Analysis

File Name	Ratio: [Average Measured/Accepted]								Pu Mass (g)	No. runs	Ct. Rate (kHz)	Ct time (h)	Data Date
	238	239	240	241	242	241 Am	Spec Pow	Pu240 Eff					
ISO03CX-2001	1.0629	1.0010	0.9721	1.0147	1.0001	0.9991	0.9986	0.9727	10.97	20	40	0.5	10-Aug-2001
stdiso03_01	0.9894	1.0005	0.9863	1.0137	1.0001	0.9979	0.9986	0.9864	11	20	40	0.5	23-Mar-2001
ISO3CX8K	1.0384	1.0007	0.9820	1.0093	1.0000	1.0101	0.9994	0.9824	10.97	10	30	2	10-May-1994
SGCOAX8K	1.0632	1.0003	0.9923	1.0071	1.0000	1.0169	1.0008	0.9927	100	10	30	2	21-Oct-1993
92COAX8K		1.0006	0.9889	0.9987	1.0000	0.9959		0.9891	10	10	30	2	18-Oct-1993
86COAX8K		1.0009	0.9849	0.9983	1.0000	1.0223		0.9847	10	10	30	2	20-Oct-1993
CALX30	0.9129	0.9998	1.0032	0.9995	1.0000	0.9948	0.9981	1.0028	398.2	10	30	1	2-Nov-1994
CALX30PB	0.8995	1.0003	0.9962	0.9916	1.0000	0.9930	0.9968	0.9959	398.2	11	30	1	6-Dec-1994
EUPU7CX8	1.0652	0.9988	1.0180	1.0081	1.0000	1.0115	1.0048	1.0180	5	10	30	2	22-Oct-1993
PUEU730	0.9639	0.9997	1.0050	0.9943	1.0000	1.0033	0.9996	1.0046	2000	11	30	1	3-Nov-1994
PUEU7PB	0.9136	1.0005	0.9930	0.9917	1.0000	1.0017	0.9964	0.9926	2000	11	30	1	8-Nov-1994
STDEUPU7-2001	0.9896	0.9992	1.0119	1.0139	0.9999	0.9983	1.0010	1.0116	5	30	30	0.5	18-Sep-2001
JOO1325	1.1419	0.9997	1.0047	0.9893	1.0000	1.0130	0.9994	1.0052	499.6	11	30	1	22-Dec-1994
J1325PB1	0.9341	1.0002	0.9977	0.9848	1.0000	0.9981	0.9980	0.9975	499.6	11	30	1	20-Dec-1994
J1325PB2	0.8667	1.0003	0.9957	0.9754	1.0000	1.0014	0.9963	0.9952	499.6	11	30	1	17-Dec-1994
PIDIE6-1-2001		1.0004	0.9943	1.0124	0.9999	0.9898		0.9934	0.4	21	40	0.5	8-Aug-2001
PID6_1		1.0027	0.9578	1.0041	1.0000	0.9891		0.9570	0.4	21	2.9	1	2-Oct-1996
ISO6CX8K	1.0618	0.9994	1.0089	1.0015	1.0000	1.0078	1.0035	1.0090	8.45	10	30	2	6-May-1994
ISO06CX-2001	1.0285	0.9991	1.0141	1.0111	1.0000	0.9984	1.0025	1.0140	8.4	21	40	0.5	8-Aug-2001
STD830	1.0084	0.9999	1.0011	0.9981	1.0000	0.9977	1.0001	1.0011	239.5	11	30	1	10-Jan-1995
STD8PB	0.9839	1.0006	0.9920	0.9863	1.0000	0.9942	0.9981	0.9920	239.5	11	30	1	23-Dec-1994
cbnm93_01	1.1285	0.9999	1.0011	1.0026	1.0000	0.9920	1.0023	1.0016	0.6	20	40	0.5	19-Mar-2001
93COAX8K	1.1781	1.0001	0.9983	0.9987	1.0000	0.9963	1.0039	0.9991	6	10	30	2	9-Oct-1993
ISO9CX8K	1.0269	0.9992	1.0109	0.9998	1.0000	1.0045	1.0030	1.0109	11.9	10	30	2	7-May-1994
stdiso09_01	1.0205	0.9985	1.0193	1.0049	1.0001	0.9930	1.0027	1.0190	12	20	40	0.5	26-Mar-2001
ISO09CX-2001	1.0347	0.9989	1.0143	1.0049	1.0000	0.9971	1.0030	1.0142	11.9	29	40	0.5	8-Aug-2001
2G118CX8	0.9192	0.9992	1.0078	0.9989	1.0000	1.0022	0.9977	1.0071	2.5		30	2	23-Oct-1993
PID6_2	0.8973	1.0008	0.9930	1.0025	1.0000	0.9743	0.9908	0.9926	0.4	21	3.2	1	4-Oct-1996
SD4030	1.0576	0.9987	1.0092	0.9992	1.0000	0.9995	1.0070	1.0096	869	11	30	1	9-Nov-1994
SD4030PB	0.9980	0.9989	1.0078	1.0000	1.0000	0.9938	0.9998	1.0075	869	11	30	1	21-Nov-1994
2G119CX8	0.9792	1.0008	0.9940	1.0020	1.0000	1.0035	0.9984	0.9940	2.5	10	30	2	24-Oct-1993
ISO12C8K	0.9910	0.9973	1.0196	0.9998	1.0000	1.0003	1.0028	1.0187	20.2	10	30	2	8-May-1994
ISO12CX-2001	1.0222	0.9975	1.0184	1.0021	1.0000	0.9979	1.0046	1.0179	20.2	20	40	0.5	9-Aug-2001
PID6_3	1.0044	1.0019	0.9883	1.0012	1.0000	0.9855	0.9942	0.9887	0.4	21	3.2	1	3-Oct-1996
PIDIE6-3-2001	0.9915	0.9995	1.0029	1.0090	1.0000	0.9855	0.9957	1.0027	0.4	26	17	0.5	6-Aug-2001
84COAX8K	1.0248	0.9983	1.0100	0.9971	1.0000	0.9977	1.0042	1.0098	6	10	30	2	10-Oct-1993
cbnm84_01	1.0163	0.9951	1.0291	0.9984	1.0000	0.9925	1.0054	1.0278	0.6	20	40	0.5	21-Mar-2001
ISO15C8K	1.0014	0.9964	1.0192	0.9964	1.0000	0.9992	1.0037	1.0175	12.3	10	30	2	9-May-1994
stdiso15_01	1.0043	0.9987	1.0069	1.0021	1.0000	0.9969	1.0013	1.0063	12	20	40	0.5	27-Mar-2001
ISO15CX-2001	1.0050	0.9955	1.0239	0.9994	1.0000	0.9971	1.0044	1.0218	12.3	26	40	0.5	9-Aug-2001
2G121CX8	0.9960	1.0001	0.9993	1.0042	1.0000	1.0104	1.0018	0.9993	2.5	10	30	2	3-Nov-1993
LAO225PB	1.0284	0.9970	1.0147	1.0027	1.0000	0.9951	1.0043	1.0143	868.8	11	30	1	15-Dec-1994
LAO22530	1.0315	0.9976	1.0119	1.0009	1.0000	0.9966	1.0043	1.0117	868.8	10	30	1	20-Dec-1994
70COAX8K	0.9887	1.0038	0.9849	1.0022	1.0000	0.9919	0.9914	0.9874	6	10	30	2	10-Oct-1989
cbnm70_01	0.9911	0.9952	1.0202	0.9952	1.0000	0.9861	0.9930	1.0149	0.6	20	40	0.5	22-Mar-2001
PID6_4	1.0188	1.0016	0.9937	1.0006	1.0000	0.9955	0.9988	0.9943	0.4	21	6.5	1	4-Dec-1996
PIDIE65	1.0125	0.9998	1.0007	0.9982	1.0000	0.9971	1.0002	1.0008	0.4	21	15	1	29-Nov-1996
PIDIE6-5-2001	1.0321	0.9976	1.0083	1.0044	1.0000	0.9962	1.0028	1.0082	0.4	21	26	0.5	7-Aug-2001
PIDIE66	0.9792	1.0107	0.9701	1.0074	1.0000	0.9984	0.9896	0.9763	0.4	21	28	1	30-Nov-1996
61COAX8K	0.9816	1.0052	0.9870	1.0054	1.0000	0.9984	0.9896	0.9892	6	10	30	2	11-Oct-1989
PIDIE67	0.9715	1.0169	0.9582	1.0121	1.0000	1.0026	0.9862	0.9683	0.4	21	29	1	1-Dec-1996
cbnm61_01	0.9941	0.9997	1.0012	0.9978	1.0000	0.9911	0.9944	1.0004	0.6	20	40	0.5	20-Mar-2001
PIDIE6-7-2001	0.9917	1.0116	0.9705	1.0123	1.0000	1.0015	0.9953	0.9786	0.4	26	40	0.5	7-Aug-2001
Average	1.0049	1.0003	0.9999	1.0013	1.0000	0.9982	0.9994	1.0002					
Std. Dev.	0.0586	0.0037	0.0158	0.0076	0.0000	0.0081	0.0047	0.0145					
% RSD	5.83	0.37	1.58	0.76	0.00	0.81	0.47	1.45					

## IX. FRAM PERFORMANCE

The standard deviation of the individual averages (second line from bottom in Table IX-7) is a parameter that captures the fluctuations in the measurements caused by different sample characteristics (size and isotopic composition), container characteristics, detector and data acquisition conditions, and errors in the accepted values. This becomes the minimum error or uncertainty that could be quoted a priori for an arbitrary measurement on an arbitrary sample and is the limiting uncertainty or minimum bias that should be assigned to an arbitrary measurement. This parameter is similar in interpretation to the between-sample variance from an analysis of variance calculation. The plutonium bias data for  $P_{eff}$  and  $^{240}\text{Pu}$  from Table IX-7 are plotted in Figs. IX-13 and IX-14.

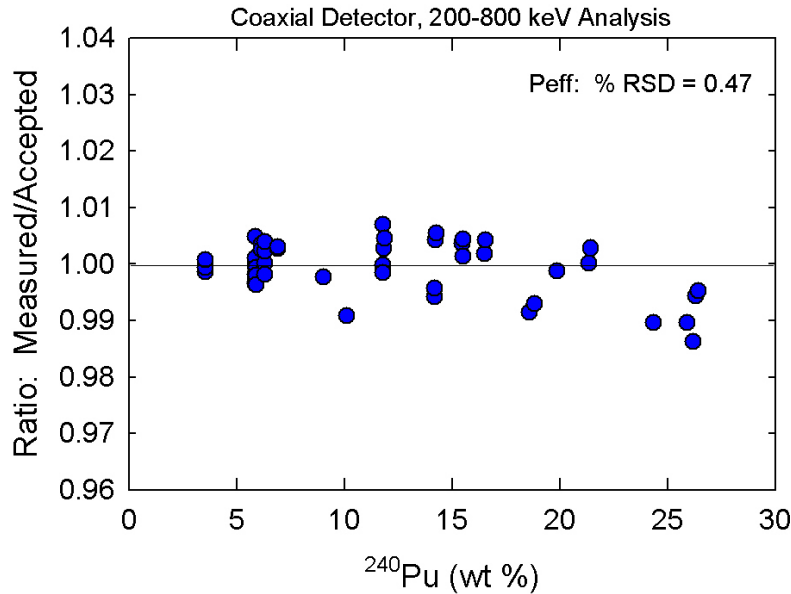


Fig.IX-13. Plutonium measurement bias for  $P_{eff}$ , 200–800 keV analysis on coaxial detectors.

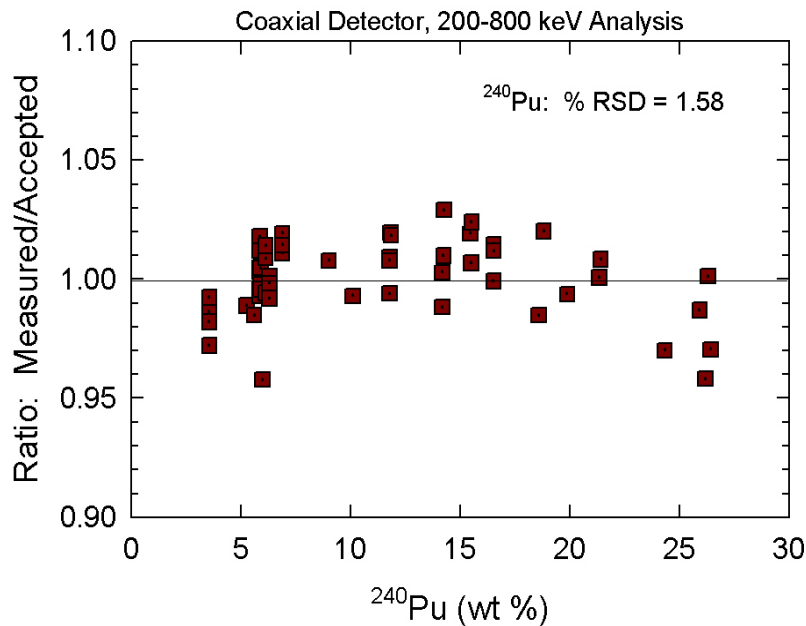


Fig.IX-14. Plutonium measurement bias for  $^{240}\text{Pu}$ , 200–800 keV analysis on coaxial detectors.

## IX. FRAM PERFORMANCE

This same type of data is available for the 120–450 keV analysis with coaxial detectors and also for planar detector analysis in the 120–420 keV region. The bias analysis for all three data sets is summarized in Table IX-8 for all isotopes.

Table IX-8. FRAM Version 4, Bias for Plutonium.

		<sup>238</sup> Pu	<sup>239</sup> Pu	<sup>240</sup> Pu	<sup>241</sup> Pu	<sup>241</sup> Am	P <sub>eff</sub>
Coax 200–800 keV	Bias	1.0049	1.0003	0.9999	1.0013	0.9982	0.9994
	% RSD	5.83	0.37	1.58	0.76	0.81	0.47
Coax 120–450 keV	Bias	0.9958	1.0001	1.0000	0.9999	0.9955	0.9993
	% RSD	1.81	0.12	0.82	0.59	0.93	0.21
Planar 120–420 keV	Bias	1.0002	1.0002	0.9995	0.9979	0.9965	0.9995
	% RSD	1.91	0.12	0.77	0.61	1.30	0.24

### 3. Uranium Measurement Bias

Just as for plutonium, NDA personnel at Los Alamos have a large number of well-characterized uranium-bearing items used routinely for standards. The extent of these standards and the quality of their characterization is unique in the DOE complex (Parker 88).

The isotopic characteristics of the uranium standards used in characterizing FRAM's performance are given in Table F-2 in Appendix F.

For comparison with standards, we use an operator-entered accepted value for <sup>236</sup>U since it does not have detectable gamma rays and is determined by isotopic correlation in FRAM. This is analogous to the method used to analyze plutonium standards for <sup>242</sup>Pu.

The bias for uranium measurements is displayed in Table IX-9. This table contains individual measurement data from many samples and multiple data sets for several samples. The data sets encompass data from different detectors, different data acquisition systems, and different measurement geometries. The latter is particularly important to note. It demonstrates that version 4 of FRAM does indeed correct properly for the coincidence summing effects that affected earlier uranium measurements (Vo 99a). The values for individual items come from the average of repeated measurements of typically 30-minute or 1-hour duration. One sees for the important <sup>235</sup>U isotope that the average bias for all samples, over the enrichment range from 0.3%–93% is 0.25%. The % RSD, in the same fashion as discussed for plutonium, is just under 1% for <sup>235</sup>U. Recall that the interpretation of this parameter is the a priori measurement uncertainty for an arbitrary sample attributed to sample specific and measurement specific conditions.

The measurement bias data of Table IX-9 is plotted in Fig. IX-15.

**IX. FRAM PERFORMANCE**

Table IX-9. Uranium Bias for Version 4 of FRAM.

Filename	Accepted Wt % <sup>235</sup> U	Measured/Accepted		
		<sup>234</sup> U	<sup>235</sup> U	<sup>238</sup> U
NBL93_03	93.1703	0.99495	0.99953	1.00875
NBL93_00	93.1703	1.00583	0.99777	1.03636
C2080001	93.1700		0.99901	
U91C2G20	91.3356	0.98896	0.99890	1.01493
U91C2T30	91.3356	0.97910	0.99823	1.02431
UIO91_N	91.3356	1.01151	0.99819	1.02087
U66C2G20	66.0405	1.00983	0.99437	1.01106
NBL53_10	52.4880	0.99612	1.00049	0.99948
NBL53_03	52.4880	1.01046	1.00351	0.99598
U52C2G20	52.1174	1.02696	0.99345	1.00704
U38C2G15	37.5518	1.01110	0.99733	1.00157
UIO_27	26.7519	1.02056	0.99782	1.00074
UIO27PS	26.7519	1.01997	0.99494	1.00180
UIO27	26.7519	0.99837	0.97735	1.00833
NBL20_01	20.1070	1.00905	0.99662	1.00084
NBL20_05	20.1070	0.99096	1.00318	0.99921
U17C2T10	17.2386	1.02646	0.99036	1.00197
UIO_13	12.9543	1.04940	1.02127	0.99678
UIO13_P	12.9543	1.04751	1.01551	0.99764
UIO13	12.9543	1.02076	1.00058	0.99989
UIO1212	11.7974	1.00117	1.00961	0.99871
A1324PS	10.0863	1.00801	0.99039	1.00107
NBS44612	4.4623	0.98043	0.99669	1.00016
NBS446PS	4.4623	1.00557	0.98285	1.00080
NBS29512	2.9491	0.96287	0.98473	1.00047
NBS295PS	2.9491	0.96205	0.98514	1.00046
NBS19412	1.9421	1.03156	1.00125	0.99997
NBS194PS	1.9421	0.97662	0.98849	1.00023
A11127PS	0.7167	1.29268	1.01235	0.99990
NBS07112	0.7119	1.07897	0.99649	1.00002
NBS071PS	0.7119	1.02303	0.99389	1.00004
NBS03112	0.3166	1.43220	0.99606	1.00000
NBS031PS	0.3166	1.03553	1.00190	0.99999
Average		1.0054 *	0.9975	1.0040
Std. Dev.		0.0221	0.0089	0.0088
% RSD		2.20	0.90	0.88

\*Uranium-234 Average and Std. Dev. exclude enrichments with <sup>235</sup>U < 1.9%. This enrichment value is at the sensitivity limit of FRAM for <sup>234</sup>U.

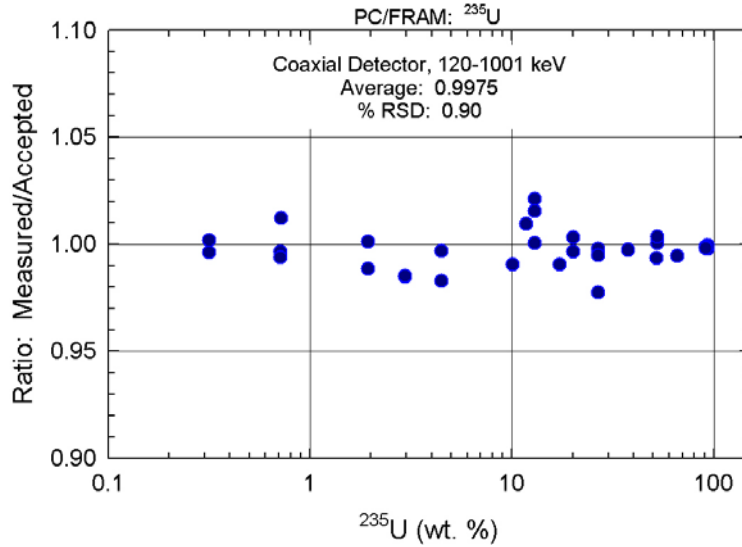


Fig. IX-15. FRAM Version 4 Measurement Bias for  $^{235}\text{U}$ .

**4. MOX Measurement Bias**

Version 4 of FRAM can analyze the gamma spectra from MOX samples giving results, in many cases, for the complete plutonium isotopic distribution, the  $^{235}\text{U}/\text{Pu}$  ratio, and the  $^{238}\text{U}/\text{Pu}$  ratio.

MOX samples can be measured in several ways by FRAM depending upon the energy region analyzed and the amount of shielding surrounding the sample. Uranium-235 is always analyzed at 185.7 keV. This gamma ray may not be present in a shielded sample and is not visible above the continuum for  $^{235}\text{U}/\text{Pu}$  ratios below approximately 0.005. If the sample is lightly shielded, FRAM can obtain both the  $^{235}\text{U}/\text{Pu}$  ratio at 185.7 keV and the  $^{238}\text{U}/\text{Pu}$  ratio at 1001 keV. For heavily shielded samples, the  $^{238}\text{U}/\text{Pu}$  ratio at 1001 keV may be the only uranium measurement available.

Los Alamos has a limited number of MOX samples. The “HUA” series is described in Table F-3 in Appendix F. Results from unshielded sample measurements analyzed in the 120–450 keV range with version 4 of FRAM are given in Table IX-10. In the 120–450 keV analysis range we only have access to  $^{235}\text{U}$  at 185.7 keV. The % RSD of the  $^{235}\text{U}/\text{Pu}$  ratio, calculated from the distribution of the individual bias values, is about 4%. Some of the variation in the bias may arise from a different distribution of particle sizes between the uranium and the plutonium in the different samples.

Table IX-10. Unshielded Measurements, 120–450 keV Analysis.

	Ratio: Measured/Accepted							
	$^{238}\text{Pu}$	$^{239}\text{Pu}$	$^{240}\text{Pu}$	$^{241}\text{Pu}$	$^{241}\text{Am}$	Spec. Pow	$^{240}\text{Pu}_{\text{eff}}$	$^{235}\text{U}/\text{Pu}$
HUA5062	0.97219	0.99813	1.01382	1.00258	1.01133	1.00411	1.01295	1.05023
HUA5065	0.98209	0.99661	1.02495	1.00382	1.00085	1.00226	1.02380	1.03559
HUA5069	0.98625	0.99680	1.02417	0.99727	0.99518	1.00058	1.02310	1.01876
HUA5301	0.96699	0.99754	1.01842	1.00526	0.96656	0.99228	1.01745	0.95162
HUA8971	0.97511	0.99410	1.04362	1.00208	0.99487	1.00339	1.04159	0.98511
Average	0.9765	0.9966	1.0250	1.0022	0.9938	1.0005	1.0238	1.0083
Std. Dev.	0.0077	0.0015	0.0114	0.0030	0.0166	0.0048	0.0109	0.0399
% RSD	0.79	0.15	1.11	0.30	1.67	0.48	1.06	3.96

## IX. FRAM PERFORMANCE

In Table IX-11 we show the results from the analysis of the unshielded samples using data in the 200–800 keV energy range. With this analysis we are still able to analyze for  $^{235}\text{U}$  at 185.7 keV as well as for  $^{238}\text{U}$  at 1001 keV. (Note: The designation of an energy range for analysis refers to the main plutonium analysis. Other gamma rays outside of that range may also be used for analysis, i.e., 185.7 and 1001 keV for uranium analysis, if they are present. The standard data collection range for coaxial detectors is 0–1024 keV.)

Table IX-11. Unshielded Measurements, 200–800 keV Analysis.

	Ratio: Measured/Accepted								
	$^{238}\text{Pu}$	$^{239}\text{Pu}$	$^{240}\text{Pu}$	$^{241}\text{Pu}$	$^{241}\text{Am}$	Spec. Pow	$^{240}\text{Pu}_{\text{eff}}$	$^{235}\text{U}/\text{Pu}$	$^{238}\text{U}/\text{Pu}$
HUA5062	0.99196	0.99831	1.01240	1.00265	1.01013	1.00493	1.01184	1.05627	1.00610
HUA5065	0.97503	0.99858	1.01038	1.00576	1.00053	0.99973	1.00967	1.03709	1.00829
HUA5069	1.10796	0.99836	1.01164	1.00273	0.99419	1.00717	1.01244	1.02364	1.02691
HUA5301	1.03498	0.99935	1.00448	1.00633	0.96630	0.99475	1.00466	0.96645	1.03412
HUA8971	1.05086	0.99836	1.01146	1.01007	0.99776	1.00521	1.01157	0.98461	1.00068
Average	1.0322	0.9986	1.0101	1.0055	0.9938	1.0024	1.0100	1.0136	1.0152
Std. Dev.	0.0524	0.0004	0.0032	0.0031	0.0165	0.0051	0.0032	0.0372	0.0145
% RSD	5.08	0.04	0.32	0.30	1.66	0.51	0.31	3.67	1.42

In Table IX-12 we show results from the third possible method of analyzing MOX data from coaxial detectors. Here the samples are shielded with 3 mm of lead, making the 185.7-keV  $^{235}\text{U}$  gamma ray undetectable. We can only analyze for  $^{238}\text{U}/\text{Pu}$ .

Table IX-12. Shielded Measurements, 3 mm Lead, 200–800 keV Analysis.

	Ratio: Measured/Accepted								
	$^{238}\text{Pu}$	$^{239}\text{Pu}$	$^{240}\text{Pu}$	$^{241}\text{Pu}$	$^{241}\text{Am}$	Spec. Pow	$^{240}\text{Pu}_{\text{eff}}$	$^{235}\text{U}/\text{Pu}$	$^{238}\text{U}/\text{Pu}$
HUA5062	0.96534	1.00071	0.99475	1.00478	1.00929	1.00034	0.99450		1.04017
HUA5065	0.97299	1.00159	0.98809	1.00759	1.00089	0.99685	0.98819		1.04377
HUA5069	1.07305	1.00051	0.99548	1.00881	0.99510	1.00281	0.99648		1.04978
HUA5301	0.99139	1.00048	0.99609	1.00940	0.96484	0.98996	0.99614		1.05726
HUA8971	1.00948	1.00059	0.99515	1.01022	0.99855	0.99961	0.99544		1.03340
Average	1.00245	1.00077	0.99391	1.00816	0.99373	0.99792	0.99415		1.04488
Stddev	0.04301	0.00046	0.00329	0.00212	0.01698	0.00493	0.00342		0.00912
% RSD	4.29	0.05	0.33	0.21	1.71	0.49	0.34		0.87

All of the MOX measurements tabulated in Tables IX-13–IX-15 were made for a 1-hour counting time at counting rates between 30 and 40 kHz. We typically made 12–15 repeated measurements. The % RSD is calculated from the distribution of the five individual averages of the repeated measurements.

The details of how MOX measurements are set up in FRAM have been described previously in some detail (Sampson 99b). The FRAM Technical Note, “Measurement of MOX with PC/FRAM” is reproduced in its entirety in Appendix A of this Application Guide. Appendix A describes the application of MOX

measurements in version 3.2 of FRAM, which does not include  $^{238}\text{U}$  analysis. The results above are from version 4.2 and include analysis for  $^{238}\text{U}$ .

### C. Intercomparison Exercises

#### 1. The PIDIE Exercise

The Plutonium Isotopic Determination Intercomparison Exercise (PIDIE) was the first exercise designed to characterize gamma-ray isotopic analysis measurements and analysis on a worldwide basis. This exercise was organized in Europe and was notable in that the organizers provided to each participant seven identical sets of nominal 0.4 g plutonium as  $\text{PuO}_2$  samples. The international shipment of the sample sets containing plutonium proved to be extraordinarily difficult because of shipping regulation and compliance issues.

These samples came to Los Alamos around 1980 at the time when we were developing our first isotopic analysis software (see section III). Los Alamos submitted measurement results with a “preproduction” version of our first RT-11 based analysis software. The Los Alamos measurement results were comparable to other measurements that were submitted, but at this writing are so obsolete that they will not be discussed. The results of the exercise have been reported by Morel (Morel 1991), nearly 15 years after the exercise was first planned.

The outcome of this pioneering exercise influenced how future exercises were handled. In the later exercises described below, the participants brought their equipment to a common location and made measurements for a fixed time period, thus negating the requirement for sample shipment across international borders. The samples used in the PIDIE exercise are a well-documented legacy of the PIDIE measurements and are still used today at Los Alamos and elsewhere to characterize gamma-ray plutonium isotopic composition measurements (see for example Tables F-3 and IX-7).

#### 2. Uranium Enrichment Measurement Exercise, IRMM 1996

The Uranium Enrichment Measurement Exercise, sponsored by the European Safeguards Research and Development Agency (ESARDA) was held at the Institute of Reference Materials and Measurements (IRMM) in Geel, Belgium in 1996. For this exercise the participants brought their own equipment to IRMM, where they were allotted one week for measurements on a set of well-characterized standards. The exercise took about a year to complete because there were so many participants. This year-long time span was much more rapid than the PIDIE exercise and the formal results were reported in less than two years (Morel 98, Morel 00).

Many participants made only “classical” infinite sample  $^{235}\text{U}$  enrichment measurements, reporting results only for  $^{235}\text{U}$ , as the exercise was organized primarily to test that method. Los Alamos participated with FRAM measurements giving results for  $^{234}\text{U}$ ,  $^{235}\text{U}$ , and  $^{238}\text{U}$ . The organizers only reported certified values for  $^{235}\text{U}$ . Table IX-13 displays the average of all FRAM measurements made during this exercise.

The biases displayed are very similar to those shown in Fig. IX-15. Samples X and Y in Table IX-13 are of interest because they are freshly separated and the daughter products  $^{234}\text{Pa}$  and  $^{234\text{m}}\text{Pa}$  used to characterize  $^{238}\text{U}$  in a FRAM measurement have been removed from the sample. They grow back in with the 24.1-day half-life of  $^{234}\text{Th}$ . For samples X and Y in Table IX-13 we made a correction using the known separation time. This correction reduced the error from approximately 20% to the approximately 4% errors shown. The residual error may arise from an incomplete separation.

This separation time correction has been incorporated into version 4 of FRAM. To our knowledge, FRAM is the only gamma-ray isotopic analysis code available with the capability to make this correction. The user enters the known separation date to make the correction.

## IX. FRAM PERFORMANCE

Table IX-13. FRAM Results for IRMM Uranium Enrichment Exercise.

Sample	Measured wt % <sup>235</sup> U mean ± sigma(mean)	Certified wt % <sup>235</sup> U	% Difference 100*(M - C)/C	Comment
1614	1.521 ± 0.011 (0.71%)	1.4972	1.59%	
1541	1.984 ± 0.018 (0.91%)	1.9952	-0.56%	
1542	2.826 ± 0.023 (0.80%)	2.8774	-1.79%	
1613	3.097 ± 0.061 (2.0%)	3.1094	-0.40%	
125VA	93.35 ± 0.048 (0.051%)	93.1556	0.21%	
X	3.316 ± 0.049 (1.48%)	3.4317	-3.37%	freshly separated
Y	2.547 ± 0.011 (0.43%)	2.6846	-5.13%	freshly separated
Average difference excluding freshly separated -0.19%				

### 3. The Pu-2000 Exercise

The most recent intercomparison exercise sponsored by the ESARDA NDA Working Group was conducted at IRMM during the calendar year 2000. This exercise was organized in a fashion similar to that of the Uranium Enrichment Measurement Exercise with participants using their own equipment in a one-week measurement window at IRMM. The principal purpose of this exercise, known as the Pu-2000 exercise, was to test the performance of recent isotopic analysis methods over a wide range of abundances and to investigate possible sources of error. Los Alamos was one of eight participating laboratories. Twenty unknown samples characterized by IRMM were available for measurement. Four additional certified samples were available as known references.

Seventeen of the twenty samples contained plutonium or MOX with <sup>240</sup>Pu ranging from 1.6 to 26.9 wt %. The remaining three samples were isotopically pure samples of <sup>239</sup>Pu, <sup>240</sup>Pu, and <sup>241</sup>Am.

Table IX-14 displays the average measured FRAM result and the IRMM certified result for the Los Alamos FRAM measurements. We did not measure all of the unknown samples because, in fact, samples E through K were known to us (the PIDIE samples) and we already had access to these in Los Alamos. In a few instances the IRMM certified value was known to have a large uncertainty and the average of all the results submitted by all participants is used instead. An asterisk denotes these cases.

Table IX-15 displays the results reported by FRAM for the three isotopically pure samples. The Los Alamos FRAM code was the only code to report results for all three samples. The versatility of the FRAM code allowed us to modify parameter files for these very special samples.

## IX. FRAM PERFORMANCE

Table IX-14. Los Alamos FRAM Results for the Pu-2000 Exercise, Unknown Samples (Results in wt % relative to total plutonium).

Sample	Type		<sup>238</sup> Pu (sigma)	<sup>239</sup> Pu (sigma)	<sup>240</sup> Pu (sigma)	<sup>241</sup> Pu (sigma)	<sup>241</sup> Am (sigma)
A	4.23g PuO <sub>2</sub>	FRAM	0.1085 (0.0008)	79.747 (0.17)	18.756 (0.17)	0.724 (0.001)	1.699 (0.002)
		Certified	0.1086*	79.506	18.990	0.724	1.689*
B	4.66g PuO <sub>2</sub>	FRAM	1.415 (0.010)	62.016 (0.46)	26.258 (0.50)	4.255 (0.032)	8.381 (0.065)
		Certified	1.44	61.327	26.887	4.290	8.25*
C	7.38g PuO <sub>2</sub>	FRAM	0.0098 (0.0004)	93.479 (0.13)	6.357 (0.13)	0.114 (0.0004)	1.154 (0.004)
		Certified	0.0110	93.522	6.314	0.113	1.188
D	7.38g PuO <sub>2</sub>	FRAM	0.0104 (0.001)	93.537 (0.09)	6.298 (0.09)	0.115 (0.0003)	1.147 (0.003)
		Certified	0.0110	93.522	6.314	0.113	1.173
F	0.45g PuO <sub>2</sub>	FRAM	0.0207 (0.0008)	89.623 (0.07)	10.017 (0.08)	0.246 (0.0002)	0.452 (0.005)
		Certified	0.0209	89.571	10.073	0.242	0.457
G	0.45g PuO <sub>2</sub>	FRAM	0.0433 (0.0005)	85.243 (0.09)	13.927 (0.09)	0.550 (0.002)	1.074 (0.003)
		Certified	0.0428	85.029	14.150	0.542	1.061
I	0.45g PuO <sub>2</sub>	FRAM	0.118 (0.0008)	76.958 (0.11)	21.094 (0.11)	1.134 (0.002)	2.701 (0.006)
		Certified	0.121	76.716	21.338	1.129	2.650
J	0.45g PuO <sub>2</sub>	FRAM	0.857 (0.0014)	68.612 (0.06)	24.115 (0.05)	2.932 (0.010)	6.308 (0.025)
		Certified	0.871	68.254	24.450	2.938	6.091
K	0.45g PuO <sub>2</sub>	FRAM	1.173 (0.005)	64.755 (0.16)	25.867 (0.18)	3.644 (0.013)	6.739 (0.024)
		Certified	1.182	64.229	26.385	3.639	6.556
L	3.5g PuO <sub>2</sub>	FRAM	0.0043 (0.0007)	98.232 (0.12)	1.692 (0.12)	0.0483 (0.0002)	1.198 (0.007)
		Certified	0.0039*	98.295	1.630	0.0469	1.200
M	5.04g PuO <sub>2</sub>	FRAM	0.0109 (0.0001)	93.525 (0.05)	6.311 (0.05)	0.114 (0.0001)	0.205 (0.002)
		Certified	0.0110	93.546	6.292	0.112	0.203
N	2.21g PuO <sub>2</sub>	FRAM	1.302 (0.004)	64.883 (0.22)	24.250 (0.24)	4.963 (0.015)	5.214 (0.043)
		Certified	1.300	65.073	24.051	4.929	5.074
O	8.67g metal	FRAM	0.0063 (0.0009)	95.377 (0.12)	4.548 (0.12)	0.0618 (0.0002)	0.155 (0.0027)
		Certified	0.0060	95.418	4.510	0.0586	0.165
P	MOX pellet	FRAM	1.106 (0.007)	64.596 (0.20)	26.486 (0.21)	3.477 (0.020)	1.480 (0.006)
		Certified	1.107	64.777	26.262	3.510	1.394
Q	MOX sol.	FRAM	1.106 (0.013)	65.202 (0.21)	25.869 (0.20)	3.488 (0.03)	1.502 (0.009)
		Certified	1.107	64.777	26.262	3.510	1.394

\* Average value from all participants

## IX. FRAM PERFORMANCE

Table IX-15. Los Alamos FRAM Results Reported for Isotopically Pure Samples. (Wt % Relative to Total Plutonium).

Sample	Type		<sup>238</sup> Pu	<sup>239</sup> Pu	<sup>240</sup> Pu	<sup>241</sup> Pu	<sup>241</sup> Am (μg/gPu)
R	Pu-239	FRAM	0.00031	99.964	0.0325	0.0029	75
		Certified	0.0000	99.979	0.0210	0.0001	3
S	Pu-240	FRAM	0.1027	0.0084	99.860	0.0001	13.6
		Certified	0.0119	0.023	99.935	0.00098	20.2
T	Am-241	FRAM					100.00
		Certified					100.00

### D. Factors Influencing Measurement Bias

This section describes the many factors that influence the bias of a gamma-ray isotopic measurement, biases that have been extensively characterized for FRAM in the preceding sections.

#### 1. Sample Composition Characteristics

The elemental makeup of the sample influences self-absorption in the sample and thereby influences the shape of the relative-efficiency curve. Version 4 of FRAM accounts for this effect by allowing up to three different elements or compounds to define the matrix. (Eq. II-11 and section II.F.5.) These elements or compounds may be chosen from a list of seven (aluminum, iron, cadmium, erbium, lead, water, and concrete). The available elements were chosen not only for their likelihood of being part of the sample, but also to sample the entire range of atomic number. If the matrix contains elements other than the three designated in the analysis parameter file, the FRAM software will use a linear combination of the three designated components to approximate the relative-efficiency curve. Differences from the true relative-efficiency curve are likely to be compensated for by the Hoerl function correction factor and the result is almost always a good fit to the relative-efficiency points, even if the three chosen components are not a good match for the actual sample matrix.

#### 2. Branching Ratios

The branching ratios (gamma rays per decay) of the gamma rays used in the analysis directly affect the bias in the measured isotopic ratios (Eq. II-5). Most of the branching ratios for the gamma rays used in the analysis have been directly measured by gamma-ray spectrometry techniques. Absolute measurements of this type are very difficult and the very best results usually have an associated uncertainty of no better than 1% (relative). Later on we will discuss in more detail the removal of biases associated with the fundamental branching ratio data.

#### 3. Coincidence Summing

Coincidence summing occurs when a gamma-ray decay includes cascades of two or more gamma rays that are emitted simultaneously in coincidence with each other. These two gamma rays may interact simultaneously in the detector and the single detected pulse will often not represent either gamma ray. This takes events away from the full energy peak in a manner that is dependent upon the measurement geometry.

Summing effects depend upon the square of the detector solid angle (Knoll 00) and can be reduced by increasing the sample-to-detector distance.

For coincidence summing to be a problem for a specific isotope, the two coincident gamma rays must be of high enough intensity to be useful in the analysis. They also must be of high enough energy to escape the sample and its containment. Coincidence summing of a high-energy gamma ray with a low-energy (less than approximately 70 keV) gamma ray occurs fairly often in the complex uranium and plutonium decay schemes. However, the low-energy gamma ray is usually absorbed before it reaches the detector, averting a summing problem.

### a. Uranium

Coincidence summing effects are present in low-enriched uranium measurements analyzed in the 120–1001 keV energy range. The 258-keV gamma ray from the  $^{238}\text{U}$  daughter  $^{234\text{m}}\text{Pa}$  is particularly affected. In general, measurements on highly enriched uranium are not affected because the 258-keV gamma ray is not used in the analysis. The  $^{235}\text{U}$  isotopic result can be biased by as much as 15%, without correction, depending upon the sample-to-detector distance. Because of the solid angle dependence, the effects are particularly pronounced for sample-to-detector distances less than 5 cm. The effects become small at distances greater than 15 cm.

FRAM version 4 incorporates a correction factor for coincidence summing (Vo 99a). The correction factor is derived by examining the intensities of several gamma rays affected by coincidence summing in different proportions while knowing their correct branching ratios. This allows a correction to be made by comparing intensity ratios of the affected peaks to the ratios expected without coincidence summing.

### b. Plutonium

Coincidence summing is not recognized to be a problem with plutonium measurements. Many of the possible opportunities do not occur because the filtering present for plutonium measurements removes the low energy coincident gamma rays.

## 4. Peak Area Determination

### a. Background Shape

When we set up a parameter file for FRAM we pay very careful attention to setting the best regions of interest (peak and background) and choosing the most appropriate background shape (see section VI. C. 3.) to characterize the continuum underneath the peak region. Recall that the user can choose from seven background types, denoted as 1) flat, 2) linear, 3) quadratic, 4) exponential, 5) flat step, 6) linear step, or 7) bilinear step.

A parameter file is set up for application to a wide range of measurement conditions such as isotopic composition (including  $^{241}\text{Am}$  content), sample mass, sample composition, sample container and shielding, detector resolution, and measurement geometry. Many of these measurement conditions affect the shape of the background continuum underneath the peak regions. The parameter file setup of the region data must allow for a background continuum shape (background type) that will adapt itself to many different conditions. A poor choice of background type can lead to a bias in the peak area determination and concomitant errors in the isotopic fractions. Some of the “tricky” regions are illustrated and discussed below.

Continuum at 160 keV The definition of the background type for the region around 160 keV is critical for  $^{240}\text{Pu}$  analysis in the 120–450 keV region as the peak at 160.3 keV is the only peak available for analysis of  $^{240}\text{Pu}$  in this region. We see in Fig. IX-16 that the background has an inflection point near this energy and has a generally concave upward shape. We customarily define a quadratic background for this region with background ROIs below 160 and above 165 keV. For coaxial detector parameter files we do

## IX. FRAM PERFORMANCE

not set a background ROI between 161.5 and 164 keV to allow for varying detector resolutions and the possible presence of  $^{235}\text{U}$  at 163.3 keV.

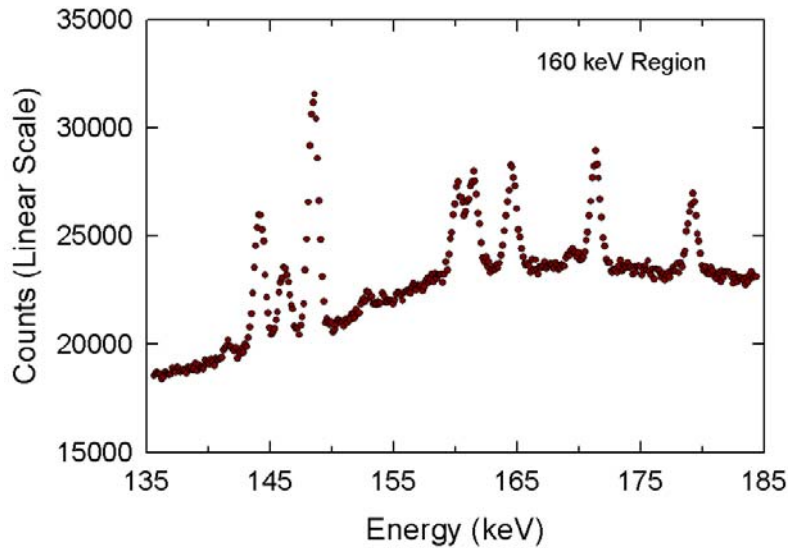


*Fig. IX-16. The background in the region around 160 keV shows curvature making definition of the background continuum difficult. Poor definition can bias the  $^{240}\text{Pu}$  peak area at 160.3 keV.*

Continuum at 148 keV The background continuum underneath the 148.6-keV peak from  $^{241}\text{Pu}$  is usually positively sloping as is shown in Fig. IX-17. One would like to use a linear background with a smoothed step function (linear step) to account for the increased Compton continuum below 148 keV, which arises from the 148-keV peak. However, since the background is higher above 148 keV than it is below, the “step” in the background goes the wrong way and becomes unphysical. FRAM can sense this condition and will automatically recalculate the background continuum with the simpler linear form that does not incorporate a step. The background ROIs are typically set below 140 keV, between 150 and 152 keV, and above 153 keV.

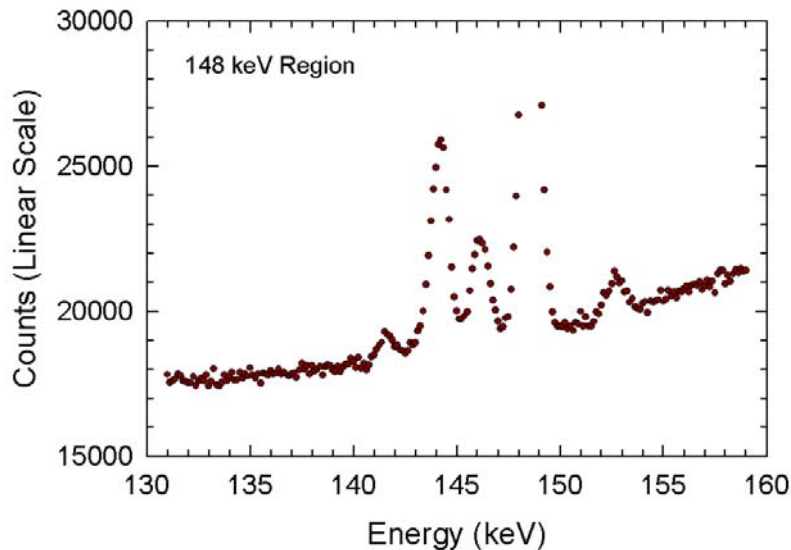


*Fig. IX-17. The positive sloping background at 148 keV makes it difficult to calculate an accurate background continuum for the 148.6 keV from  $^{241}\text{Pu}$*

## IX. FRAM PERFORMANCE

Continuum at 208 keV The  $^{241}\text{Pu}$ – $^{237}\text{U}$  peak at 208 keV can vary in intensity over a factor of 500 relative to neighboring peaks, depending upon the isotopic composition of the sample. This peak usually presents the classic case of the linear step function background type. We see in Figs. IX-18 and XI-19 that the underlying continuum can change slope above and below 208 keV. While a linear step-function works well in Fig. IX-18, the continuum in Fig. IX-19 is better characterized by what we call a bilinear step, which has a different slope above and below the 208-keV peak. FRAM will automatically switch a bilinear step background type to a linear step if it finds the bilinear step inappropriate.

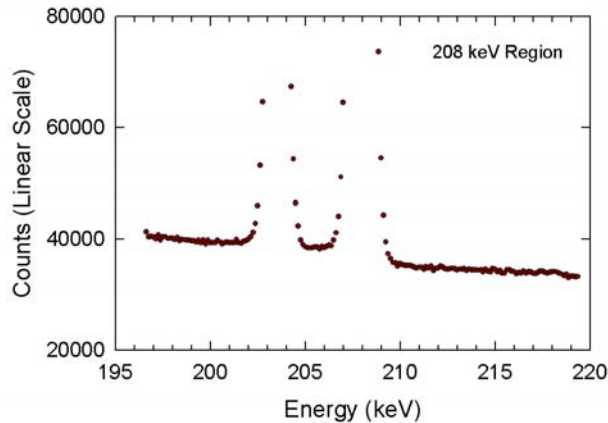


Fig. IX-18. The 208 keV region from a low burnup plutonium sample. The background continuum has the same slope above and below 208 keV.

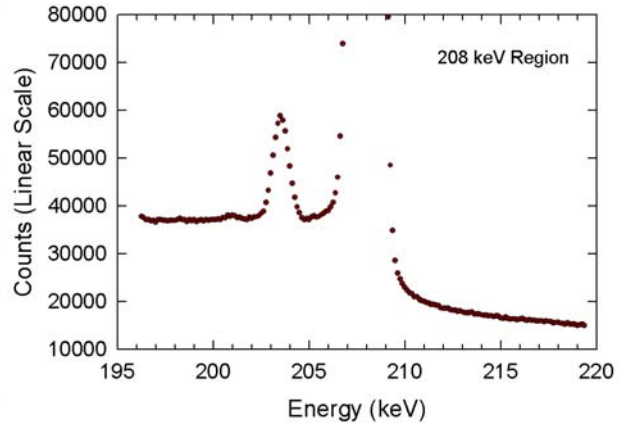


Fig. IX-19. The 208 keV region from a high burnup plutonium sample. The background continuum has different slopes above and below 208 keV.

### b. Interferences

FRAM can be characterized as a response function code. The peak shapes are determined in the internal calibration phase of the analysis, and the peaks for analysis are predetermined by the setup of the parameter file (section VI. C. II.). An unexpected peak (a peak not accounted for in the peak list in the parameter file) appearing in an analyzed region of the spectrum, may bias the analysis of the designated peaks in the region. This bias can arise by direct interference with the peak area determination, or the interference may appear in a region used to define the background continuum, thus biasing the peak area via an incorrect background subtraction. The good news with FRAM is, of course, that once an interference peak is recognized, one can easily modify the parameter file to include the interference peak and reanalyze the data.

The general-purpose plutonium parameter files delivered with version 4 of FRAM are set up to include common interferences from  $^{235}\text{U}$ ,  $^{243}\text{Am}$ – $^{239}\text{Np}$ , and  $^{237}\text{Np}$ . The general-purpose parameter files are usually adequate for low concentrations of these interferences but may require modification for very high concentrations.

The user has another tool in FRAM to discover unexpected interference peaks. The user should open the spectrum data file in question using the **File | Open** option and then display the spectral data using the **Options | Plot Spectrum** option. Click on the **display...** button in the plotting window and then click on the **regions** button in the **Display Choices** window. Choose the parameter file to be used in the analysis from the pull down **FRAM Parameter Sets** window.

The analysis regions for the selected parameter file appear highlighted in red, and the background regions appear highlighted in green. Examination of the highlighted spectrum will reveal if any unexpected interference peaks appear in a background region. Highlighting the analysis regions can be used to show if the energy calibration of the spectrum matches that set up in the parameter file. If the red-highlighted peak regions do not contain the peaks, the energy calibration in the parameter file may not be appropriate for the spectrum.

### E. Bias Correction

We have developed several procedures for identifying and correcting biases in the isotopic results. In general, the procedures rely on measurement of standards, identification of the source of the bias, and correction of the bias, usually by adjustment of branching ratios.

The first step is to carefully set up the parameter file for the analysis. This includes identifying the full range of measurement conditions, isotopic compositions,  $^{241}\text{Am}$  content, interferences, and any other parameters that might affect the gamma-ray spectrum. The user then very carefully establishes the peak and background ROIs based on representative spectra. This is perhaps the most important step in making bias corrections.

#### 1. Adjustment of Branching Ratios

If we still observe biases even after careful set up of the parameter file, we will generally make an adjustment in the branching ratios to reduce or eliminate the bias. There is good justification for this approach, although it is questioned by some as inappropriate because branching ratios are (imperfectly) known constants of nature. Our reasoning is that we are making corrections for imperfections in the analysis in addition to correcting for uncertainties in our knowledge of the branching ratio values.

One type of bias arises from peak area uncertainties caused by imperfect background subtraction. A second peak area uncertainty comes from imperfections in the response function fitting of closely lying, overlapping peaks. A third uncertainty arises from biases and random errors in the published branching intensities. We have also previously mentioned imperfections in the modeling of the relative-efficiency curve as a contributor to bias. Imperfections in the coincidence summing correction (uranium) and unrecognized coincidence summing problems with plutonium also contribute. Finally, the model (Gaussian plus an exponential tail on the low-energy side of the peak) that is used to fit the peak areas is itself imperfect.

#### 2. Branching Ratio Values

We have already noted (section IX. D. II.) that the branching ratio value directly affects the isotopic measurement result. There are two principle sources of branching ratio values for plutonium; the work of Gunnink and coworkers (Gunnink 76a) and the Table of the Isotopes (Firestone 96). Any adjustment of plutonium branching ratio values usually starts from the values in these sources.

#### 3. Observation of Peak Area Biases

We can use the medium output of a FRAM analysis to look for inconsistencies in the activities calculated for a series of gamma rays from a single isotope. The ratio of  $^{239}\text{Pu}/^{239}\text{Pu}$  from a medium printout are shown as an example in Table IX-16. The ratios are relatively consistent within the error (% RSD from counting statistics). When we look at the consistency we consider the counting statistics for analyses from many different samples. Any inconsistency that shows up regularly is examined in closer detail.

This analysis method only works for isotopes with several available analysis peaks. Usually we only have a single analysis peak for  $^{238}\text{Pu}$  and  $^{240}\text{Pu}$ .

## IX. FRAM PERFORMANCE

Table IX-16. FRAM Printout of Individual Isotopic Ratios (relative to  $^{239}\text{Pu}$ ) for Analysis Gamma Rays from  $^{239}\text{Pu}$ .

pk	isotope	energy	area	error	activity ratios	mass ratios
4	Pu239	129.294	563932	0.27%	1.00039e+000	1.00039e+000
17	Pu239	161.482	30354	2.38%	9.66128e-001	9.66128e-001
24	Pu239	171.372	35361	2.10%	9.83841e-001	9.83841e-001
27	Pu239	203.545	309449	0.32%	9.98056e-001	9.98056e-001
36	Pu239	255.380	71442	0.85%	9.83843e-001	9.83843e-001
58	Pu239	345.011	777047	0.17%	9.99775e-001	9.99775e-001
66	Pu239	375.042	2368514	0.11%	9.99400e-001	9.99400e-001
71	Pu239	413.712	2433540	0.11%	1.00172e+000	1.00172e+000
76	Pu239	451.474	330898	0.24%	9.92351e-001	9.92351e-001

The correction of bias for an isotope with only a single gamma ray ( $^{238}\text{Pu}$  and  $^{240}\text{Pu}$  are usually in this category) can be straightforward. We examine the bias as a function of the isotopic fraction, usually from data such as displayed in Table IX-7 above. A simple branching ratio adjustment is usually indicated when the data do not show a trend with changing isotopic composition. The situation is more complex, however, if there is a trend. This could indicate unresolved or imperfect subtraction of interferences or could indicate a background continuum subtraction that does not adapt well over the full range of data.

#### 4. Least-Squares Adjustment of Branching Ratios

A more general adjustment method utilizes high precision data from multiple measurements on samples with well-characterized isotopic compositions. A "Downhill Simplex Method" is incorporated into a special developer's version of FRAM and used to minimize the weighted chi-square of the chosen isotopic ratio(s). Multiple branching ratios are varied iteratively to find a minimum. The data sets span a wide range of isotopic compositions and ages. The large, varied data sets are especially important for the adjustment of branching ratios of  $^{241}\text{Am}$  and  $^{241}\text{Pu}$ – $^{237}\text{U}$  because much of the input data comes from coenergetic peaks—contributions from both  $^{241}\text{Am}$  and  $^{241}\text{Pu}$ – $^{237}\text{U}$ —that would otherwise not provide independent information for samples with nearly the same age.

With this method we can obtain accuracies of a percent (relative) or less for the individual isotopic ratios. This fine-tuning usually does not make large adjustments from the published values. Indeed, if the adjustment is large (say greater than 5%) then one should carefully examine the data in more detail to see if it is justified.

The proof of the appropriateness of this approach can be seen by examination of how well the adjusted branching ratios agree with the published values. Table IX-17 below lists several sources of branching ratios for the major analysis peaks of plutonium above 120 keV. Columns 3 and 4 are the references often used as starting points. These reference values are not independent as the Table of Isotopes is a compilation and uses much of the data published in UCRL-52139 (Gunnick 76a). The FRAM values arise from the two principal coaxial-detector parameter files used with version 4 of FRAM and have been determined in most part by the least-squares fitting method described above. The FRAM branching ratios agree with the fundamental published values validating the least-squares adjustment process.

**IX. FRAM PERFORMANCE**

Table IX-17. Plutonium and Americium Branching Ratios (gammas/decay) for Major Gamma Rays.

Isotope	keV	UCRL-52139	Eight Edition Table of Isotopes	FRAM 120-450 keV	FRAM 200-800 keV
<sup>241</sup> Am	125.3	4.08 E-05	4.08 E-05	4.136 E-05	
<sup>239</sup> Pu	129.3	6.26 E-05	6.31 E-06	6.29 E-06	
<sup>241</sup> Pu	148.6	1.87 E-06	1.85 E-06	1.894 E-06	
<sup>238</sup> Pu	152.7	9.56 E-06	9.37 E-06	9.37 E-06	
<sup>240</sup> Pu	160.3	4.02 E-06	4.02 E-06	4.035 E-06	
<sup>241</sup> Pu- <sup>237</sup> U	164.6	4.51 E-07	4.54 E-07	4.663 E-07	
<sup>241</sup> Am	164.6	6.67 E-07	6.67 E-07	6.879 E-07	
<sup>239</sup> Pu	203.5	5.60 E-06	5.69 E-06	5.727 E-06	5.727 E-06
<sup>241</sup> Pu- <sup>237</sup> U	208.0	5.32 E-06	5.18 E-06	5.392 E-06	5.392 E-06
<sup>241</sup> Am	208.0	7.91 E-06	7.91 E-06	7.954 E-06	7.954 E-06
<sup>241</sup> Pu- <sup>237</sup> U	267.5	1.81 E-07	1.74 E-07	1.786 E-07	1.786 E-07
<sup>241</sup> Am	267.5	2.63 E-07	2.63 E-07	2.635 E-07	2.635 E-07
<sup>241</sup> Pu- <sup>237</sup> U	332.4	2.97 E-07	2.928 E-07	2.974 E-07	2.974 E-07
<sup>241</sup> Am	332.4	1.490 E-06	1.49 E-06	1.476 E-06	1.476 E-06
<sup>241</sup> Pu- <sup>237</sup> U	335.4	2.380 E-08	2.33 E-08	2.392 E-08	2.392 E-08
<sup>241</sup> Am	335.4	4.960 E-06	4.96 E-06	4.872 E-06	4.872 E-06
<sup>239</sup> Pu	345.0	5.592 E-06	5.56 E-06	5.533 E-06	5.533 E-06
<sup>239</sup> Pu	375.0	1.570 E-05	1.554 E-05	1.554 E-05	1.554 E-05
<sup>239</sup> Pu	413.7	1.489 E-05	1.466 E-05	1.469 E-05	1.469 E-05
<sup>239</sup> Pu	451.5	1.89 E-06	1.894 E-06	1.898 E-06	1.898 E-06
<sup>240</sup> Pu	642.5	1.245 E-07	1.3 E-07		1.243 E-07
<sup>239</sup> Pu	645.9	1.489 E-07	1.52 E-07		1.491 E-07
<sup>241</sup> Am	662.4	3.64 E-06	3.64 E-06		3.619 E-06
<sup>241</sup> Am	722.0	1.96 E-06	1.96 E-06		1.889 E-06
<sup>238</sup> Pu	766.4	2.19 E-07	2.2 E-07		2.177 E-07

**5. Use of Standards**

All of the adjustment processes ultimately depend upon comparison of a measured value with a reference value. Thus while gamma-ray isotopic composition measurements do not directly depend upon standards (Eq. II-5), we do rely heavily on comparison with standards for ultimate validation of the technique as well as the “fine tuning” of the analysis process such as we have just described. We have discussed analytical characterization issues in section IX. B. 1. It is worth repeating here that analytical characterization problems are not recognized to affect <sup>239</sup>Pu and <sup>240</sup>Pu. Some characterization and traceability issues are still present with <sup>238</sup>Pu and <sup>241</sup>Am. Problems with characterization of the <sup>241</sup>Pu isotopic fraction are seldom seen in the modern analytical laboratory.

### X. MAKING MEASUREMENTS FOR FRAM ANALYSIS

The FRAM analysis of a gamma-ray spectrum can only be as good as the data will permit. Poor quality spectral data may limit the ability of FRAM to derive accurate results from the measurement, although the flexibility of FRAM's analysis gives one a better chance of a good analysis than any other analysis method. Still, it is good to keep in mind the computer saying, "garbage in, garbage out." This chapter will present information on choosing and setting up equipment for gamma-ray spectrum measurements to be used for FRAM analysis.

#### A. Choice of Detector

FRAM has been used with a wide variety of HPGe detectors, both planar and coaxial, as well as with CdTe detectors. One doesn't have to know the ultimate detector or application before acquiring FRAM because the single version of the code (as of late 2002) can make such a wide range of analyses. Usually, the detector procurement question will revolve around what size and type of HPGe detector to procure.

The first consideration is the mix of samples to be measured and their packaging. A coaxial detector is the appropriate choice for the user who makes a wide range of measurements on samples contained both in thin-walled and heavy-walled or shielded containers. Coaxial detectors can literally "do it all" with the exception of analysis in the 100-keV region. Planar detectors can be a very good choice for samples in thin-walled containers and are required if one wishes to make measurements in the 100-keV region.

When coaxial detector analysis with FRAM was first developed in the early 1990s, we carefully considered the question of a standard detector and standard data acquisition conditions. We worked with the detector manufacturers to specify the best quality coaxial detector of modest size (to minimize the cost and optimize resolution) that could be reliably produced. At the same time we carried over some standard specifications for high-quality planar HPGe detectors that already had a successful track record for isotopic analysis applications. These specifications formed the basis for the line of Safeguards Detectors marketed by ORTEC. The characteristics of these detectors are given in Table X-1.

Many other types of HPGe detectors have been used for FRAM applications. Waste measurement applications have used coaxial detectors of nearly 100% relative efficiency. The poorer resolution of these larger detectors may introduce some biases and require ROIs to be enlarged. We have used large semi-planar detectors (70 mm diam. by 30 mm thick) very successfully for both plutonium and uranium analysis. Measurements made through large thick-walled containers are usually improved if the coaxial detectors have higher efficiency than the "standard" 25% in Table X-1.

A 25% coaxial detector is usually adequate for almost any measurement if one can achieve a small sample-to-detector distance (say 5–10 cm). However, many real world applications require much larger sample-detector distances and profit from a larger-diameter, higher-efficiency detector.

## X. MAKING MEASUREMENTS FOR FRAM ANALYSIS

Table X-1. HPGe Detector Specifications for General-Purpose FRAM Usage.

<b>Coaxial Detector</b>	
Geometry	Coaxial, P-type germanium <sup>1</sup>
Crystal Size	Approximate "square" size (diameter $\geq$ length) commensurate with efficiency
Efficiency	At least 25% relative efficiency at 1.33 MeV in the usual definition
Low Rate (1000 cps)	$\leq 750$ eV at $\leq 6$ - $\mu$ s shaping time <sup>2</sup>
Resolution at 122 keV	$\leq 870$ eV at $\leq 2$ - $\mu$ s shaping time
Low Rate (1000 cps)	$\leq 1.75$ keV at $\leq 6$ - $\mu$ s shaping time
Resolution at 1.33 MeV	$\leq 1.95$ keV at $\leq 2$ - $\mu$ s shaping time
High Rate (30 kHz)	$\leq 880$ eV at $\leq 2$ - $\mu$ s shaping time
Resolution at 122 keV	
High Rate (30 kHz)	$\leq 2.00$ keV at $\leq 2$ - $\mu$ s shaping time
Resolution at 1.33 MeV	
Peak Shape	[FW1/50M]/FWHM $\leq 2.50$ at all count rates $\leq 30$ kHz and time constants from 2–6 $\mu$ s
Preamplifier/Energy Rate	Resistive feedback preamplifier with Energy Rate $\geq 50,000$ MeV/s
<b>Planar Detector</b>	
Geometry	Planar
Crystal Size	$\geq 25$ mm diameter, $\geq 13$ mm thick
Low Rate (1000 cps)	$\leq 520$ eV at $\leq 6$ - $\mu$ s shaping time
Resolution at 122 keV	
High Rate (50 kHz)	$\leq 580$ eV at $\leq 1$ - $\mu$ s shaping time
Resolution at 122 keV	
Peak Shape	[FW1/50M]/FWHM $\leq 2.50$ at all count rates $\leq 50$ kHz and time constants from 1–6 $\mu$ s
Preamplifier/Energy Rate	Resistive feedback preamplifier with Energy Rate $\geq 10,000$ MeV/s <sup>3</sup>

<sup>1</sup> We specify P-type germanium because the resolution is usually better than that of N-type for the same detector size. N-type detectors have also been used successfully with FRAM.

<sup>2</sup> Shaping times are specified for analog amplifiers.

<sup>3</sup> The preamplifier energy rate for a planar detector is a tradeoff with low-rate resolution. This specification assures that the preamplifier will allow a maximum counting rate above 50 kHz for a typical plutonium spectrum. A more stringent low-rate resolution specification may be achieved at the expense of the maximum preamplifier count rate.

### B. Choice of Energy Range

**Planar Detector** With a planar detector, one has the choice of 1) analyzing plutonium data above 120 keV (typically taken in 4096 channels at a gain of approximately 0.1 keV/ch to include 120–420 keV) or 2) analyzing the 100-keV region (typically taken in 4096 channels at a gain of approximately 0.075 keV/ch to include 0–300 keV). The 120–420 keV analysis provides more penetrability and will work through 12–15 mm of steel that will defeat analysis in the 100-keV region. The 100-keV region analysis provides better precision for plutonium in thin-walled containers at the same counting time or equivalent

## X. MAKING MEASUREMENTS FOR FRAM ANALYSIS

or better precision at shorter counting times, compared to the higher-energy analysis. Planar detectors are not usually used for uranium analysis in the 120–1001 keV region but can be used for this analysis (Sampson 01) if required.

**Coaxial Detector** A coaxial detector provides the most versatile detector choice if one is limited to choosing just a single detector. It can analyze all the samples that a planar detector can plus it can analyze samples contained in very substantially-shielded containers, up to and including approximately 25 mm of lead (Hypes 00). The amount of shielding governs the energy range used in the analysis. “Bare” samples are analyzed starting at approximately 120 keV. Samples shielded with approximately 6 mm lead or less are analyzed starting at approximately 200 keV. Analysis of samples with more than 12 mm of lead starts at about 300 keV, as all gamma rays below that energy are removed by the shielding.

We have chosen a recommended data acquisition range for use with coaxial detectors. We typically acquire data in 8192 channels at a gain of 0.125 keV/ch spanning the energy range of 0–1024 keV. This range is very convenient as it allows analysis of both uranium and plutonium spectra with the same electronic settings.

Table X-2 (similar to table VI-2) shows the analysis range and gain (keV/ch) combinations that have been used successfully with FRAM. The standard or recommended settings are shaded. Those entries that are not shaded also work but other choices may be more appropriate. Some choices are noted as “not recommended.” These choices have produced successful analyses but in general, the keV/ch value is too high (the peaks are too narrow at low energies) to produce a reliable internal peak-shape calibration (section V. B. 1. d.). When FRAM is used under these conditions we perform the shape calibrations offline and fix the shape parameters in the parameter file.

Table X-2. Successful Analysis Ranges for FRAM. (Recommended Choices are Shaded).

Detector	Element	Analysis Range (keV)	Gain (keV/ch)	Comment
Planar	Plutonium	120 – 420	0.10	Not recommended <sup>1</sup>
	Plutonium	120 – 420	0.105	
	Plutonium	120 – 307	0.075	
	Plutonium	30 – 210	0.075	
	Plutonium	60 – 210	0.075	
	Uranium	120 – 1001	0.25	
Coaxial	Plutonium	120 – 460	0.125	
	Plutonium	200 – 800	0.125	
	Plutonium	300 – 800	0.125	
	Plutonium	120 – 460	0.25	
	Plutonium	120 – 460	0.50	
	Uranium	120 – 1001	0.125	
	Uranium	120 – 1200	0.156	
Uranium	120 – 1001	0.25		

<sup>1</sup>Combination of energy range and keV/ch not recommended. Peaks are too narrow at low energies for reliable shape calibration.

The use of FRAM under “not recommended” conditions usually arises because of the requirement to perform an isotopic analysis on data that was originally acquired for other purposes (see Appendix B) or

## X. MAKING MEASUREMENTS FOR FRAM ANALYSIS

---

because the user is constrained to use data acquisition/MCA equipment that does not allow the recommended keV/ch (Sampson 01).

The theoretical peak width at low energies can be found from the quoted detector resolution at 122 keV and the keV/ch of the measurement setup. Dividing the detector resolution by the keV/ch gives an approximate peak width at 122 keV. The recommended analysis ranges for both planar and coaxial detectors all have peak widths at 122 keV of between 5 and 6 channels. The peak width values are on the order of 1.5 to 2 channels for the conditions that are “not recommended.” Values below about 3 channels are generally not recommended.

### C. Collection of Pulse Height Spectra

#### 1. Electronics

Data acquisition electronics used to collect spectral data for isotopic analysis span the range from simple analog systems to highly sophisticated modern digital data-acquisition systems. Both types of systems have been implemented in mains-powered and battery-powered versions. The MCAs that record the spectra have advanced over the years from dedicated standalone desktop units to modern units consisting solely of a computer and MCA emulator software.

The functions necessary for data acquisition are best illustrated by noting the specific modules present in an analog NIM data acquisition system.

High-Voltage Bias Supply This module provides low-noise, high-voltage bias to the HPGe detector. Planar detectors usually operate in the range from 1000V to 2500V. Coaxial detectors usually operate in the range from 3000V to 5000V.

Preamplifier The preamplifier processes the pulse directly from the detector and provides an output pulse compatible with the input of the spectroscopy amplifier. The preamplifier is almost always an integral part of the HPGe detector and does not have to be procured separately. The user may be offered the choice between resistive feedback and pulsed optical feedback. Isotopic analysis systems use resistive feedback preamplifiers because of their superior throughput characteristics.

Spectroscopy Amplifier The spectroscopy amplifier processes the pulse from the preamplifier and produces a shaped, low-noise pulse of 0–10 V amplitude suitable for amplitude analysis. Commercial spectroscopy amplifiers with pole zero cancellation, baseline restoration, Gaussian and triangular shaping, and a time constant range from 0.5 to 8  $\mu$ s are the standard for a high-quality NIM system. Planar detectors use analog shaping times of 1–2  $\mu$ s while coaxial detectors typically operate in the 2–4  $\mu$ s range. Very large coaxial detectors may require an even longer time constant. These larger systems will suffer throughput degradation as a result of the longer time constant.

Digital Stabilizer A digital stabilizer will correct for gain and baseline drifts in the modules preceding it. Digital stabilizers are recommended to reduce peak broadening from electronic drift and to assure that peaks fall at their expected location. FRAM can accommodate significant peak drift when it finds the peaks for the internal energy calibration (see section V.B. 1. a.).

ADC The analog-to-digital converter converts the linear output of the analog amplifier to a digital signal. The clock speed in a modern Wilkinson type ADC should be a minimum of 100 MHz with 400–500 MHz ADCs being more desirable. Successive approximations ADCs with analysis times of less than 10  $\mu$ s are recommended. Little is gained using successive approximations ADCs with analysis times less than approximately 2  $\mu$ s as the analog amplifier’s pulse length will control the dead time in these cases.

MCA The multichannel analyzer used with a FRAM system should have a memory of at least 8192 (8K) channels if it is to be used with all detector types. Memory of 4096 (4K) channels is adequate for a system used only below 500 keV with planar detectors.

## X. MAKING MEASUREMENTS FOR FRAM ANALYSIS

---

All of these functions are integrated into smaller, portable, battery-powered systems suitable for field use. The portable MCAs also operate from mains power, making them useful in both the laboratory and the field. The small size and low power requirements of portable, battery-powered analog systems usually extract a toll in system performance when compared to NIM module systems (Sampson 01a).

Digital data acquisitions systems have now reached the stage of full commercial application. These systems remove the analog amplifier and ADC by digitizing the signal directly out of the preamplifier. Digital data acquisition systems are available in both portable and mains-powered units. They offer an expanded selection of time constants and simultaneously improve performance of both resolution and throughput over that from corresponding analog systems (Vo 98, Sampson 01a). Digital systems, even in their portable, battery-powered form, demonstrate performance superior to even the best analog systems. We recommend that new procurement of a data acquisition system for isotopic analysis be a digital system.

Vo has performed extensive testing of the performance of many commercially available data acquisition systems. The first tests (Vo 98) reported a comparison between the first commercially available completely digital spectroscopy unit with a standard NIM-based analog system. Further testing (Vo 99b) evaluated 9 different digital and analog MCAs with both planar and coaxial (up to 92% relative efficiency) detectors. Other tests (Vo 99c) compared first- and second-generation digital spectroscopy systems (DSPEC and DSPEC Plus) from ORTEC. The most recent testing (Vo 02a) has evaluated portable, battery powered digital spectrometer systems, the Inspector 2000 and the DigiDART, in comparison with a mains-powered digital system (DSPEC Plus) and an analog NIM system.

The web sites of Canberra and ORTEC (Canberra 02, ORTEC 02), the two major manufacturers of nuclear instrumentation, can be accessed for additional information on availability and application of nuclear instrumentation. These manufacturers provide a large amount of very useful information of direct applicability to FRAM measurements. FRAM, under license from Los Alamos, can be purchased from both manufacturers. Additional information concerning data acquisition for gamma spectrometry can be found in the PANDA (Passive Nondestructive Assay of Nuclear Materials) manual (Parker 91a).

### 2. Electronics Interconnections and Settings

In the previous section we listed the functions necessary for a data acquisition system, broken down to commonly available NIM modules. Below we show how these modules might be interconnected in a typical NIM system. The example is just one of the myriad ways one can connect the many available NIM modules from different manufacturers. We show specific modules from two different manufacturers as an example of a system that was assembled at Los Alamos. We wish to emphasize that other modules from the same or different manufacturers may be used. While the ADC, MCA, and digital stabilizer are usually chosen from the same manufacturer, the example below in Fig.X-1 shows a configuration that is an exception. Figure X-1 also contains a timer/counter, a module not included in the functional list given earlier. While this module is not required, it is very useful for monitoring the absolute counting rate coming out of the amplifier and is strongly recommended for every NIM-based FRAM system.

Figure X-2 shows a system with the same functionality using a digital data acquisition system. The interconnections are greatly simplified. A separate timer/counter is usually not required with the digital systems because they can display the count rate on the computer display.

Some typical system settings for plutonium measurements for an 8192-channel, coaxial detector system are shown in Table X-3. We recommend a 30-kHz maximum count rate for the coaxial detector system with analog electronics. We recommend a maximum counting rate of about 40–50 kHz for a coaxial detector used with a digital data acquisition system.

## X. MAKING MEASUREMENTS FOR FRAM ANALYSIS

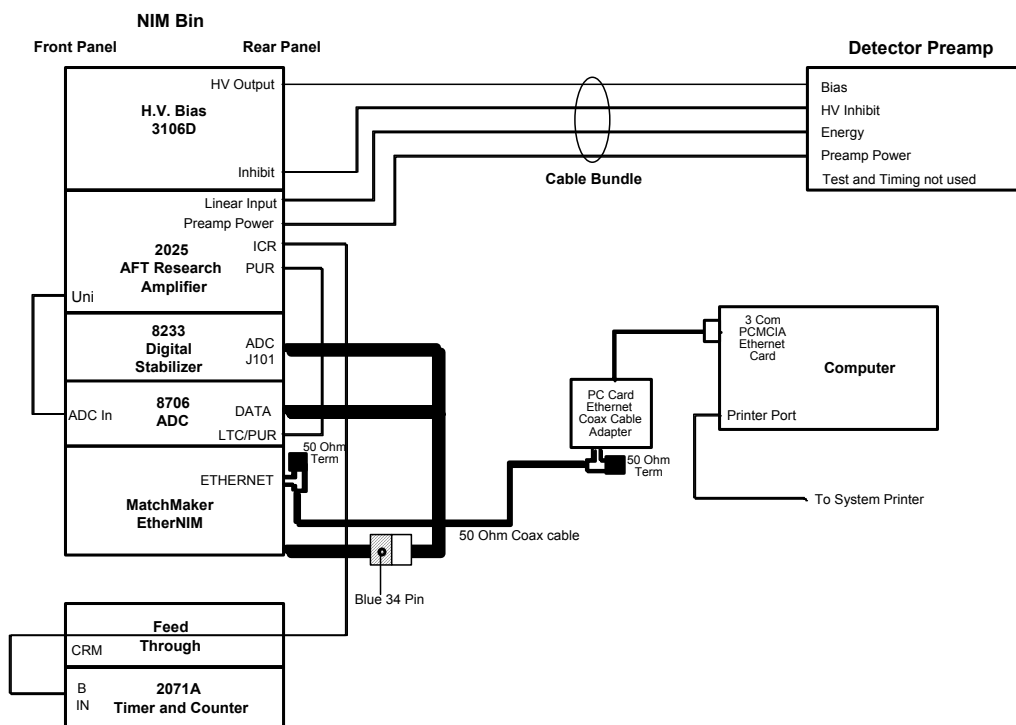
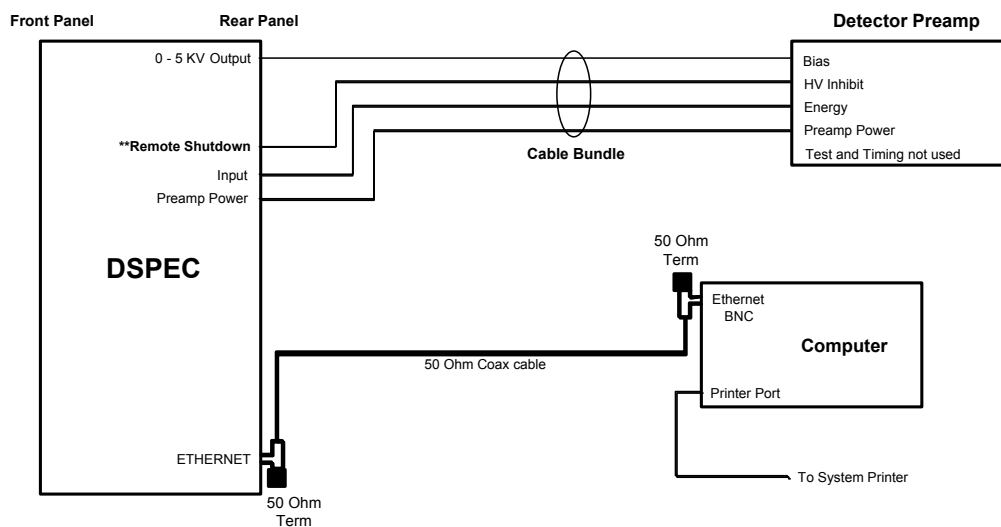


Fig. X-1. Interconnections of the electronics in an analog NIM system used for isotopic analysis with FRAM.



\*\* Remote Shutdown--Check DSPEC manual for use with an incompatible (non ORTEC) detector.

Fig. X-2. Interconnections with a typical digital data acquisition system used for isotopic analysis with FRAM.

The digital stabilizer settings for both uranium and plutonium are shown. The first settings at 208 and 662.4 keV are recommended for plutonium because you can measure most shielded as well as unshielded samples without making any changes. Optional settings for plutonium when measuring and analyzing

## X. MAKING MEASUREMENTS FOR FRAM ANALYSIS

---

data in the 120–450 keV region are also given. The only change that is made when you switch measurements between uranium and plutonium is the setting of the digital stabilizer.

The other widely used option, a planar-detector system, uses 4096 channels at 0.1 keV/ch with a 10-keV offset collecting data from 10–420 keV (0–420 keV) for plutonium measurements. This gain and offset is historical, allowing an easy conversion of channel number to energy, and is not required. Indeed, it cannot be used with a DSPec because of the lack of a zero adjustment on the DSPec. A slightly lower gain of about 0.105 keV/ch with no zero offset also works well. The planar detector system typically uses a 1- $\mu$ s, triangular shaping time (equivalent to a 2- to 2.4- $\mu$ s rise time on the DSPec), with zero stabilization at 129 keV and gain stabilization at 413.7 keV for plutonium. Its maximum count rate for an analog system is usually limited to less than 40 kHz.

Table X-3. Typical Analog System Settings (Coaxial detector, 8K ch, 0.125 keV/channel).

### H. V. Power Supply

Kilovolts	(as required by detector)
Polarity:	positive (for most coaxial detectors, check to be sure)
Voltage dial:	(as appropriate for chosen unit)

### Spectroscopy Amplifier

Coarse Gain:	as appropriate for detector
Fine Gain:	as appropriate for detector
Uni Shaping:	Triangle
PZ:	Auto
Shaping Time:	2 $\mu$ s
BLR Rate:	Auto
Input:	as appropriate for detector

### ADC

Gain:	8K
Range:	8K
Offset:	0

### Digital Stabilizer

Zero	Peak: ch 1664 (208 keV) plutonium
	Peak: ch 1034 (129 keV) plutonium (optional)
	Peak: ch 1486 (186 keV) uranium
Gain	Peak: ch 5299 (662.4 keV) plutonium
	Peak: ch 3310 (413.7 keV) plutonium (optional)
	Peak: ch 8008 (1001 keV) uranium

### 3. Counting Rate Considerations

The importance of the system's counting rate in the collection of high-quality spectra cannot be overestimated. Too high a counting rate may lead to degraded detector resolution, tailing caused by pulse pileup, and random sum peaks, all of which can lead to measurement biases. Conversely, very low counting rates yield spectra with fewer counts and poorer statistical precision. Increasing the counting time to compensate for low counting rates often leads to unacceptably low sample throughput rates. The

## X. MAKING MEASUREMENTS FOR FRAM ANALYSIS

counting rate–resolution–throughput tradeoff is one that needs to be evaluated for every measurement system and measurement situation. Many of the factors contributing to this question have been discussed in section IX.A.2 and have also been described by Parker (Parker 91a).

One of the first tests that a user can perform is the simultaneous measurement of throughput and resolution under realistic end-use measurement conditions. For these measurements the user selects a prominent peak in the spectrum and measures its net peak area and FWHM for a fixed counting time (true time or real time) while varying the input counting rate for a constant value of the time constant. The required peak areas and FWHMs can be obtained from the MCA or MCA emulator. The peak can be from a standard test source,  $^{57}\text{Co}$  at 122 keV,  $^{137}\text{Cs}$  at 661.6 keV, or more realistically from plutonium at 129.3 keV and 208.0 keV. The throughput and resolution can be plotted as shown in Fig. X-3 (shown previously as Fig. IX-1). The user then repeats the measurements for other time constants.

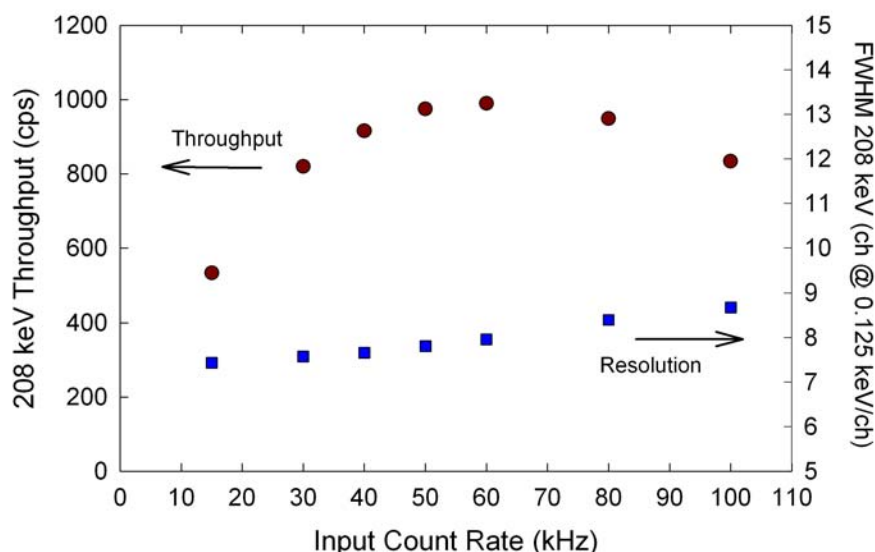


Fig.X-3. Throughput and resolution for 208-keV peak of  $^{241}\text{Pu}$ - $^{237}\text{U}$  with 965 g  $\text{PuO}_2$  with 16.85%  $^{240}\text{Pu}$ , a 25% relative-efficiency HPGc detector, and an ORTEC DSpec operated at 4  $\mu\text{s}$  rise time.

Shorter time constants will usually increase the throughput, move the throughput maximum to a higher input rate value, and make the resolution poorer (larger FWHM). For analog systems, the resolution may worsen very rapidly at higher counting rates. If possible you should choose to operate at an input rate about 50%–70% of the rate at peak throughput. This operating point captures over 80% of the maximum throughput while minimizing the resolution.

There are measurement situations where the sample-to-detector distance is constrained and fixed. A large sample may produce an unacceptably high counting rate leading to resolution that is too poor for a successful FRAM analysis. These cases benefit greatly from the use of a digital spectrometer system. FRAM has been successfully used with a digital spectroscopy system operating with input count rates up to 100 kHz and has made bias-free analyses for all of the conditions displayed in the curves in Fig. X-3 above (Kelley 99).

The type of detector and analysis region chosen for the system can influence whether one chooses to optimize resolution or throughput. We give some general suggestions below.

## X. MAKING MEASUREMENTS FOR FRAM ANALYSIS

---

100-keV region, planar detector Optimization for measurements in the 100-keV region should concentrate on obtaining the best resolution at the expense of throughput. The larger branching intensities in this region can make up for lowered throughput arising from increasing the time constant to 2  $\mu$ s or even 3  $\mu$ s from the usual 1- $\mu$ s time constant.

120–420 keV region, planar detector Optimization in this case usually concentrates on maximizing throughput by use of a 1- $\mu$ s time constant and perhaps increasing the area of the detector. Resolution is secondary because we routinely use coaxial detectors with great success in this same region. Coaxial detector resolution at 122 keV is typically 1.5 times larger than that of a planar detector.

120–450 keV region, coaxial detector We tend to optimize for throughput in this region because of the lower intrinsic intensity of the gamma rays. Digital spectrometer use can simultaneously improve resolution and throughput for this case. Analog time constants can be as low as 2  $\mu$ s for top quality 25%–30% relative-efficiency coaxial detectors. Higher-efficiency detectors usually require a longer time constant.

200–800 keV region, coaxial detector This region is difficult to optimize. The intrinsic plutonium gamma-ray intensities are low, which calls for larger, generally poorer-resolution detectors. The peak fitting in the 637–646 keV peak region, containing five peaks including the important  $^{240}\text{Pu}$  peak at 642.5 keV, demands the best possible resolution. Digital spectrometers improve the measurements in this region allowing FRAM to work at input rates as large as 100 kHz (Kelley 99).

120–1024 keV region, coaxial detector, uranium The uranium spectrum is not as complex as for plutonium and does not demand as good resolution. Systems for uranium can usually be optimized for throughput.

### 4. Pulse Pileup

#### a. Coincidence Summing

Coincidence summing occurs when two gamma rays are emitted in coincidence from cascade decay. It is possible for these two gamma rays with energies  $E_1$  and  $E_2$  to be detected simultaneously in the HPGe detector in a much shorter time than the resolving time of the pulse processing electronics. The result is a new, full-energy peak at the energy of the sum of the two gammas,  $E_{\text{sum}} = E_1 + E_2$ . More important for isotopic analysis measurements is the diminution of the individual peak areas at  $E_1$  and  $E_2$  from this summing. Coincidence summing is dependent on the isotope and decay scheme and does not cancel out in isotopic analysis measurements as random summing does. The effect is proportional to the solid angle of the detector as seen from the sample and can be reduced by increasing the sample-to-detector distance. Vo (Vo 99a) has studied this problem extensively. He finds that coincidence summing for uranium measurements can be important for small sample-to-detector distances (less than 5–10 cm). The effect becomes unimportant for distances exceeding approximately 15 cm but that sample-to-detector distance usually leads to very low counting rates for low-enriched uranium samples. This makes the correction for coincidence summing very important for good FRAM performance. We have briefly discussed, in section IX.D.3, the results of the coincidence summing corrections in version 4 of FRAM on uranium measurement bias.

### b. Random Summing

Random pulse pileup occurs when two pulses from independent decays arrive at the detector with a time separation shorter than the pulse-processing time of the analysis system. The output of the analysis system will be a single distorted pulse with a pulse height that is not related to either input pulse. When the pileup occurs from random events it can be minimized by a proper pole-zero cancellation adjustment on the analog amplifier, or the proper pulse shape optimization on a digital spectroscopy system. Pileup rejection circuitry in modern amplifier systems can reject the storage of these pileup pulses if they can be resolved by the timing circuitry of the pileup rejector, which is typically on the order of 0.5  $\mu$ s.

In addition to the electronic pileup reduction methods there are also two system setup conditions that affect random pulse pileup. Pulse pileup can be reduced by operating at a shorter time constant or by operating at a lower counting rate.

Pulse pileup can affect an isotopic analysis measurement. The principal effect of random pulse pileup is to add misshapen peaks and structure to the spectrum. If these additional peaks fall inside a peak or background region defined in the parameter file, the analysis of that region will likely result in a bias. An example of random summing or random pulse pileup is shown in Fig. X-4 and tabulated in Table X-4. This example shows the summing of the 59.54-keV  $^{241}\text{Am}$  peak with several peaks in the 100-keV region. The arrows show the location of the full energy of the sum peaks. The random sum peak that falls directly under the 160.3-keV  $^{240}\text{Pu}$  peak is especially important. Its presence will cause a bias in the 160.3-keV peak area and its presence may not be noticed if the other sum peaks are weak.

Random summing is assumed to result in peak losses that are equal throughout the entire spectrum. Thus, isotopic ratio methods should be unaffected by the peak losses. This assumption may not hold precisely because peak widths increase with energy, but it appears that the peak losses occurring from random summing do not materially affect isotopic ratio measurements.

### 5. Filtering

Spectroscopists place absorbing materials or “filters” in front of the detector when they want to preferentially absorb lower-energy radiation that is not useful for the measurement. Filters are typically chosen to have their K-absorption edge near to but below the energy of the radiation to be absorbed. This maximizes the absorption of the filter and minimizes its effect on higher-energy gamma rays. The removal of unwanted low-energy gamma rays eliminates them as a source of pulse pileup summing, both random and coincidence summing.

The 59.54-keV gamma ray of  $^{241}\text{Am}$  is most often targeted for filtering. The activity of this gamma ray is about 3–5 orders of magnitude greater than that of any other widely used plutonium gamma ray. This gamma ray will dominate the spectrum of any plutonium in a thin-walled container, often being many thousands of times more intense than any other gamma ray in the spectrum. Even when filtered, its presence can disturb the spectrum by random summing, as has been shown in Fig. X-4. If not filtered, the dead time produced by the analysis of this gamma ray will prevent any useful spectroscopic information from being recorded. The unfiltered counting rate from this gamma ray can be so intense as to paralyze the detector and counting electronics.

## X. MAKING MEASUREMENTS FOR FRAM ANALYSIS

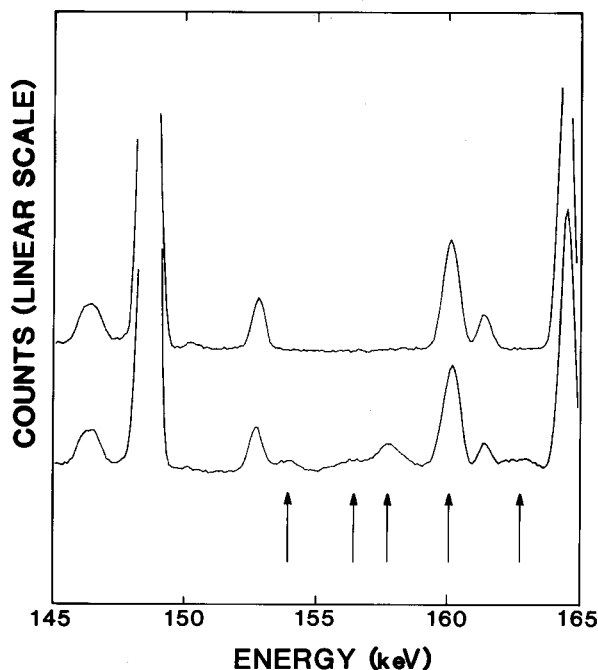


Fig. X-4. The effect of random pulse pileup on the 160 keV region of the plutonium spectrum from a planar HPGe detector can be dramatic. The top trace is a spectrum without pileup peaks. The bottom trace shows the effects of pileup of the 59.54 keV  $^{241}\text{Am}$  peak with other peaks in the 100 keV region. The arrows mark the location of the pileup peaks.

Table X-4. Strongest Sum Peaks from  $^{241}\text{Am}$  59.54 keV and 100-keV region Peaks.

100-keV region Peak Energy (keV)	Origin	Sum Peak Energy (keV)
94.66	UK $\alpha$ 2	154.20
97.07	NpK $\alpha$ 2	156.61
98.44	UK $\alpha$ 1	157.98
101.07	NpK $\alpha$ 1	160.61
102.97	$^{241}\text{Am}$	162.51
103.75	PuK $\alpha$ 1	163.29

Thin sheets of cadmium (Cd, Z = 48, K shell binding energy = 26.71 keV) are most widely used for filtering a plutonium spectrum. This material can be cut into disks and placed on the detector's end cap or can be wrapped around the sample. Tin (Sn, Z = 50, K shell binding energy = 29.20 keV) is used in situations where environmental concerns preclude the use of cadmium. Lead (Pb, Z = 82, K shell binding energy = 88.00 keV) is also used because of its wide availability.

A widely used "rule of thumb" is that the filter for a plutonium measurement should be thick enough to reduce the intensity of the 59.5-keV gamma ray of  $^{241}\text{Am}$  to the same magnitude as the intensity of the 100-keV complex of gamma rays and x-rays. When this condition is met one does not observe pileup in the 160-keV region (see top trace in Fig. X-4).

The FRAM systems used at the Los Alamos Plutonium Facility measure the isotopic composition of plutonium over a very wide range of  $^{241}\text{Am}$  content (from less than 100 ppm to more than 500,000 ppm) where ppm is parts per million with respect to total plutonium. This dynamic range of nearly 10,000 makes it difficult to optimize the amount of filtering for all measurements. At Los Alamos we have

## X. MAKING MEASUREMENTS FOR FRAM ANALYSIS

chosen to use a single filter for all measurements, a filter that is thick enough to filter the  $^{241}\text{Am}$  59.5-keV gamma ray at the highest concentrations. The choice of a single filter is made for operational purposes so the instrument operator does not have to make any filtering decisions.

The filter used at Los Alamos consists of approximately 0.080 in. of Cd backed by 0.010–0.020 in. of copper. This total cadmium thickness of approximately 2mm is the same thickness recommended by the IAEA for their plutonium inspection/verification measurements. The purpose of the copper (or like Z material) is to absorb any x-rays produced in the cadmium. We use this type of graded filter to keep the portion of the spectrum below 80 keV as free as possible from photopeaks. This minimizes pileup summing originating from strong, low-energy peaks. We adhere to the philosophy that any low-energy peak (below 100 keV) that is not used in the analysis is a “bad” peak. It cannot help in the measurement and may hurt the measurement by contributing to sum peaks.

The “one-size-fits-all” filter does degrade the intensity of useful photopeaks below 200 keV. Measurement precision for the  $^{241}\text{Am}$  peak at 125.3 keV and the  $^{240}\text{Pu}$  peak at 160.3 keV can be improved if one uses less filtering for samples with  $^{241}\text{Am}$  less than 10,000 ppm. The precision of measurements in the 100-keV region will usually be improved using filters that are less than 0.080 in. of cadmium because the sum peaks do not fall into an energy region that is used in the analysis. The user, for each specific measurement situation, can carry out the optimization of cadmium thickness. Table X-5 displays the transmission of common filter components at several important gamma ray energies. The results for tin will be approximately the same as for cadmium. The transmission of copper used to filter x-rays from cadmium is shown in Table X-6.

Table X-5. Transmission of Common Filter Components.

Energy (keV)	Cadmium			Lead	
	0.016 in	0.032 in	0.080 in	0.016 in	0.032 in
59.5	0.127	0.016	0.000032	0.118	0.014
104.2	0.638	0.407	0.105	0.109	0.012
125.3	0.756	0.571	0.247	0.251	0.063
160.3	0.856	0.733	0.461	0.474	0.224

Table X-6. Transmission of Copper Used to Suppress X-rays from Cadmium.

Energy (keV)	Copper	
	0.010 in	0.020 in
26	0.027	0.0007

### 6. Shielding

The shielding used around the HPGe detector for analysis of plutonium isotopic composition is usually tailored to the energy range of the analysis; the main purpose of the shielding is to reduce direct photopeak interferences from other plutonium stored in the vicinity of the measurement system. A system making high-energy measurements in the 600–800 keV range requires more shielding than a system used in the 100-keV region. If size, space, and weight constraints permit, the shielding around the

## X. MAKING MEASUREMENTS FOR FRAM ANALYSIS

lateral surface of the detector should provide an attenuation of at least a factor of 100 for the highest-energy gamma ray critical to the analysis. Back shielding or shielding behind the detector is certainly desirable if the detector's cryostat and dewar design permit. Most isotopic systems use minimal collimation in front of the detector and thus will benefit from shadow shielding behind the sample.

The shielding for direct photopeak interferences is of primary importance, as these interferences will directly bias the measurement. The shielding for continuum gamma rays is of secondary importance. Background gamma rays falling in the continuum will worsen measurement precision but usually will not bias the measurement.

Lead (Pb) and machinable tungsten (W) are commonly used for shields. Lead is an environmental hazard and is often canned into a steel container to alleviate that concern. Machinable tungsten is used where maximum shielding is required for minimum size and is usually used without the necessity for additional canning. Tungsten is, however, very expensive, precluding its use in many cases. Table X-7 below shows the thickness of lead and tungsten shields required to provide a factor of 100 attenuation at commonly used analysis energies.

Table X-7. Thickness in cm (in.) for Factor of 100 Attenuation.

Energy (keV)	Pb ( $\rho = 11.35$ )		W ( $\rho = 15$ )	
104	0.084	(0.033)	0.080	(0.032)
185	0.362	(0.143)	0.351	(0.138)
208	0.476	(0.187)	0.461	(0.181)
414	2.00	(0.787)	1.82	(0.715)
662	3.94	(1.55)	3.33	(1.31)
766	4.61	(1.82)	3.84	(1.51)
1001	5.97	(2.35)	4.83	(1.90)

The weight of the shield becomes an overriding consideration for portable measurement systems, which are often operated with inadequate shielding simply because of the weight. Sampson (Sampson 99c) describes uranium isotopic measurements with FRAM on UF<sub>6</sub> cylinders arranged in a stacked array, a commonly found condition. Because FRAM uses energies up to 1001 keV, he concluded that the measurements using a portable hand-held HPGe detector suffered from inadequate shielding (~ 0.5 in. Pb was used) even when using the thickest shield that was practical for mobile measurements.

We have used FRAM at the Los Alamos Plutonium Facility in a mobile, mains-powered system that can be easily transported to the measurement site. Figure X-5 shows this system as initially configured on a commercial thyroid scanner cart and Fig. X-6 shows the system in use measuring a 200-liter waste drum. This system uses approximately 0.75 in. of machinable tungsten shielding which Table X-7 shows provides about a factor of 100 attenuation at 414 keV.

Fixed station FRAM systems are usually configured with at least a 2-in.-thick lead shield around the lateral surface whether used with a coaxial or planar HPGe detector. This configuration will provide a factor of 160 attenuation at 766 keV, the highest-energy routinely analyzed in a shielded-sample measurement.

## X. MAKING MEASUREMENTS FOR FRAM ANALYSIS

---



*Fig. X-5. A mobile PC/FRAM system configured on a commercial thyroid scanner cart for use at the Los Alamos Plutonium Facility. The shielding around the detector is 0.75 in. of machinable tungsten.*



*Fig. X-6. A mobile FRAM system measuring the isotopic composition of the contents of a 200-liter waste drum.*

Table X-7 shows that for the same attenuation, a machinable tungsten shield will be thinner than a lead shield. This leads to tungsten shields that are more compact than lead shields. The actual design and dimensions of the shield will determine if the tungsten shield is lighter. For a cylindrical shield with a 3-in. inner diameter typically used for HPGe detectors, tungsten and lead with  $\times 100$  attenuation will have essentially the same mass per unit length.

### XI. MODIFYING PARAMETER FILES FOR SPECIAL CASES

#### A. Standard Parameter Files

The distribution of FRAM includes several standard, general-purpose parameter files for plutonium analysis in various energy ranges and also a parameter file for uranium analysis. These parameter files can be used for most routine analyses and can also be used as the basis for building a parameter file for special problems. Two parameter files are listed in Appendix C. The first is for plutonium analysis with a coaxial detector in the 120–450 keV region. The second is for uranium analysis with a coaxial detector in the 120–1001 keV energy range.

The standard parameter file for coaxial detector analysis of plutonium in the 120–450 keV region (Coax\_Widerange3) analyzes for  $^{238-241}\text{Pu}$  and  $^{241}\text{Am}$  and obtains  $^{242}\text{Pu}$  by either a correlation or operator entry. The results are presented as wt % relative to total plutonium with  $^{241}\text{Am}$  presented in units of  $\mu\text{g }^{241}\text{Am/gPu}$ . In addition, the analysis directed by this parameter file quantifies the ratio of several other isotopes ( $^{237}\text{Np}$ ,  $^{235}\text{U}$ , and  $^{239}\text{Np}$ - $^{243}\text{Am}$ ) with respect to total plutonium. Typical results for the plutonium isotopes and  $^{241}\text{Am}$  as well as limited results for  $^{235}\text{U}$  have been previously discussed. We are not able to present any comparisons for  $^{237}\text{Np}$  and  $^{239}\text{Np}$ - $^{243}\text{Am}$  because samples with certified values of these isotopes are not available.

The standard parameter file for coaxial detector analysis of uranium in the 120–1001 keV region (U121\_1001Coax) directly analyzes for  $^{234}\text{U}$ ,  $^{235}\text{U}$ , and  $^{238}\text{U}$ . Uranium-236 does not have any detectable gamma rays and is determined by an empirical correlation (or operator entry), much in the same manner as for  $^{242}\text{Pu}$ . The correlation calculation for  $^{236}\text{U}$  is unique to FRAM, version 4. This parameter file has been demonstrated to work over the enrichment range from 0.2% to more than 99%  $^{235}\text{U}$ . Results for the ratio of  $^{228}\text{Th/U}$  are presented for each analysis. The specific power in watts/gU is also calculated, as calorimetry is a practical measurement method for multi-kg quantities of highly enriched uranium.

#### B. General Approach to Parameter File Modification

The parameter files delivered with FRAM are suitable for almost every routine application. Nevertheless, it is desirable to be able to modify a parameter file for special analyses. The user has password-protected control over five groups of parameters, previously discussed in Chapter VI.

- Fitting parameters
- Peaks
- Regions
- Isotopes
- Application Constants

##### 1. Start With Existing Parameter File

It is almost always easiest to start with an existing parameter file and edit existing values rather than start from a completely new and empty parameter file. One accesses the parameter file by entering the Password-protected Change Parameter Utility **Edit | Parameters**. Then one selects the parameter file in **File | Open** and chooses the parameter file from the pull down menu that is presented.

##### 2. Set Energy Calibration Defaults and Isotopes for Analysis

The Default Energy Calibration can be accessed from the Change Parameter Utility after choosing **Edit | Fitting parameters**. These two parameters are changed to accommodate spectra with different energy calibrations. Set the **Gain (keV/ch)** and **Offset (keV)** to match the spectra being analyzed. We have already discussed acceptable values for these parameters in section X.B.

## XI. MODIFYING PARAMETER FILES FOR SPECIAL CASES

---

The other default values for the FWHM parameters and tailing parameters can usually remain at their default values as long as the new energy calibration is not significantly different from the old one. If the change is more than 50%, new values should be obtained from the medium printout of the analysis of a good quality spectrum where all fitting parameters are NOT Fixed.

Designate the isotopes to be used in the analysis by selecting **Edit | Isotopes** in the Change Parameter Utility. This window has been discussed in section VI.C.4.

### 3. Select Gamma-Ray Peaks for Analysis

Next the user enters the information on the peaks to be analyzed after selecting **Edit | Peaks** in the Change Parameter Utility. The parameters in this window have been discussed in section VI.C.2.

### 4. Select Regions for Analysis

The boundaries of the regions for analysis and the background regions are entered next as discussed in section VI.C.3. The selection of region boundaries is somewhat of an art. It is not difficult to do for a single specific spectrum and can be done in many equally acceptable ways in this case. It does become more difficult if one wants to make the new parameter file applicable to a wider range of samples. In this case one must be especially aware of the positioning of the background ROIs. An ROI that is satisfactory for one spectrum may not be applicable to another spectrum that has additional interference isotopes present. Changing  $^{241}\text{Am}$  concentrations can be troublesome in this regard and it is best to guide your region setup using a spectrum with the highest  $^{241}\text{Am}$  concentration available. A listing of gamma rays from the plutonium isotopes and  $^{241}\text{Am}$ , such as is found in Appendix D (Gunnink 76a), is useful for setting up both the region boundaries as well as the gamma-ray peaks.

### 5. Select Peaks for Internal Calibrations

The user now designates the peaks to be used in the internal calibrations, although this can also be done when the peaks were selected (sec. XI.B.3 above). This is a critical part of the parameter file setup because poor internal calibrations will quickly invalidate an analysis. Sometimes this is all that has to be done to modify a parameter file. Peaks chosen for internal calibration of energy, FWHM, and peak shape should be, to the greatest extent possible, clean single peaks. Peaks selected for the internal shape calibration should be completely free from interferences to at least  $1.5 \times \text{FWHM}$  below the peak centroid.

The piecewise linear internal energy calibration requires a minimum of two peaks. The FWHM calibration requires a minimum of three peaks, preferably sampling the extremes of the analysis range. The shape calibration should also come from peaks at high and low energies. Two peaks are sufficient but they should be intense peaks so that the tailing can be pulled out of the noise. The shape calibration requirements are often the most difficult to satisfy and lead to our recommendation of fixing the shape parameters for most analyses.

One can recalibrate the shape parameters offline if they seem to have changed. You observe this by examining the peak fits using **Options | Display Fits**. Poor fits in the tail region are a signal that the shape calibration should be updated. Acquire several spectra with good counting statistics and analyze them with the shape parameters set to be free (remove the check in the Fixed box for the Default tailing constants, Edit Fitting Parameters, Change Parameter Utility). Updating of shape parameters should be infrequent but will probably need to be done as the detector ages and absorbs neutron damage over its lifetime. Enter the new parameters obtained from a medium printout and continue analysis, fixing the new parameters.

### 6. Edit Application Constants

The user can edit the Application Constants last as most of these constants do not affect the analysis. To clean up the application constants the user should first make sure that the peak channels in the diagnostic tests agree with the default energy calibration, because the diagnostic test channels are not linked to the default energy calibration. One should check that the interference peaks are appropriate for the data to be analyzed. The user will usually not change the isotopic correlation constants for  $^{242}\text{Pu}$  or  $^{236}\text{U}$  or change the FRAM SUMMARY TYPE.

The penalty for not changing the application constants is often a large number of error messages. The messages usually do not signify that anything is wrong with the analysis but are very disconcerting to an auditor looking over formal measurement results. Be sure to clean up the application constants before any new parameter file is put into formal use.

### C. Discussion of Special Cases

In the following sections we will discuss examples of parameter file modifications made to analyze spectra not readily analyzed by the standard parameter files delivered with FRAM. The average user may not encounter very many, if any, of these cases. However, we believe the discussion will make the user more familiar with FRAM's versatility and guide the user to the modifications required to address their own special cases. The Los Alamos Safeguards Science and Technology staff is also available to help users with unusual analysis problems.\*

#### 1. Very Low Plutonium-240

This material type can be defined roughly as having a  $^{240}\text{Pu}$  content less than approximately 2%. Spectra from these materials usually have very little  $^{241}\text{Pu}$  so the  $^{241}\text{Pu}$ - $^{237}\text{U}$  peaks may not be strong enough to use for internal calibrations. Plutonium-239 lines are strong and suffer little interference because of the low  $^{241}\text{Pu}$  and  $^{238}\text{Pu}$  content in the sample. The gamma-ray lines from  $^{239}\text{Pu}$  at 129, 203, 345, 414, and 451 keV are ideal to use for the internal calibrations. Figure XI-1 displays the 120–210 keV portion of a gamma-ray spectrum from a plutonium sample with 2%  $^{240}\text{Pu}$ . At these low levels, the 208-keV gamma ray from  $^{241}\text{Pu}$ - $^{237}\text{U}$  is less intense than the  $^{239}\text{Pu}$  gamma ray at 203.5 keV. This is just the reverse of what is usually seen in plutonium spectra from higher burnup samples. This spectrum represents the approximate limit of the analysis range of the standard parameter files supplied with FRAM. The analysis can be improved by removing weak  $^{241}\text{Pu}$ - $^{237}\text{U}$  peaks from the internal calibrations. Note that the 152.7-keV  $^{238}\text{Pu}$  peak is essentially undetectable.

We have analyzed the isotopic composition of research grade samples of pure  $^{239}\text{Pu}$  with FRAM. One such analysis compared with the mass spectrometry certificate values is shown in Table XI-1. FRAM also obtained values for  $^{238}\text{Pu}$ ,  $^{241}\text{Pu}$ , and  $^{241}\text{Am}$  at extremely low levels but still much higher than the certified values. These FRAM values are thought to arise from interference and increased background from other plutonium samples in the vicinity of the measurement.

---

\* A Word Regarding Analysis of Isotopically Pure Samples: The results that are shown, for cases in which the major isotope comprises over 99% of the sample, can be somewhat misleading. FRAM is able to obtain results for these analyses in all cases whereas analysis with other codes fails completely. That is the good news. The absolute error and bias on the major isotope results is extremely small but the user may see very large relative errors for the minor constituents. Each analysis must be examined for the causes of the minor isotope errors. Many times the peaks from the minor isotopes are simply below the level at which FRAM or any gamma-ray analysis code can analyze. Other sources of error at these ultralow levels can arise from background from plutonium stored in the vicinity of the measurement or background from neighboring measurements. The normalization condition—all of the plutonium isotopic fractions must sum to unity—more or less guarantees that the 99+ % abundant major isotope will be measured accurately. The minor constituents are another story.

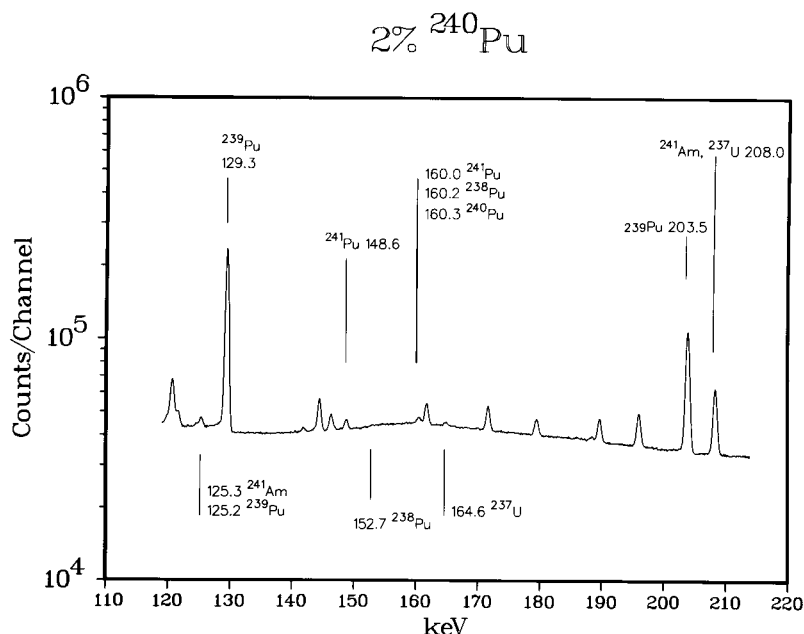


Fig. XI-1. A spectrum from a very low burnup plutonium sample containing 2% by weight of <sup>240</sup>Pu shows weak peaks from <sup>241</sup>Pu and its daughters. (Note: the peak at 160.2 keV should be labeled <sup>239</sup>Pu.)

Table XI-1. FRAM Analysis of a Sample with 99.9+ % <sup>239</sup>Pu.

	Pu-239	% RSD	Pu-240	% RSD
FRAM measured	99.964	0.05	0.032	> 99
Certified	99.979		0.021	

## 2. Very High Plutonium-240

Samples with more than 90% <sup>240</sup>Pu are used in physics research applications and in safeguards applications for calibration of neutron coincidence counters. FRAM's standard coaxial detector parameter file (Appendix C) with analysis in the 120–450 keV region does reasonably well with samples up to 95% <sup>240</sup>Pu.

Table XI-2 compares a FRAM measurement on a 0.69-g plutonium sample with 95% <sup>240</sup>Pu to mass spectrometry (MS) results. Operator entry of the MS value for <sup>242</sup>Pu was used in the analysis. FRAM's standard coaxial detector parameter file was used for the analysis showing that samples with the <sup>240</sup>Pu levels shown in Table XI-2 do not require special analysis.

Table XI-2. FRAM Analysis of a Sample with 95% <sup>240</sup>Pu.

	Pu-238	Pu-239	Pu-240	Pu-241
FRAM measured	0.010	1.123	94.08	0.197
Mass spectrometry	0.014	0.960	94.14	0.295

## XI. MODIFYING PARAMETER FILES FOR SPECIAL CASES

---

Research grade samples with 99+ %  $^{240}\text{Pu}$  do require parameter file modifications. Plutonium-239 lines are too weak for use in determining the relative-efficiency or performing the internal calibrations. The samples of this type that we have seen do have some strong lines from the small amounts of the minor isotopes such as  $^{238}\text{Pu}$ ,  $^{243}\text{Am}$ ,  $^{239}\text{Np}$ ,  $^{237}\text{Np}$ , and  $^{241}\text{Am}$ . We use gamma-ray lines from these isotopes for the internal calibrations and the relative-efficiency curve. Spectra from these very high purity samples also exhibit some of the weak gamma-ray lines from  $^{240}\text{Pu}$  that are not visible in normal spectra. These lines at 212 and 687 keV may be used in the analysis for activity and relative efficiency. We analyze the entire energy range from 120 keV to 800 keV.

Table XI-3. FRAM Analysis of a Sample with 99.9+%  $^{240}\text{Pu}$ .

	Pu-240
FRAM measured	99.860
Mass spectrometry	99.935

### 3. Very High Neptunium-237

In the United States we account for  $^{237}\text{Np}$  at the gram level just as for plutonium. This isotope is present in almost every plutonium sample as a direct decay product of  $^{241}\text{Am}$  and the  $^{237}\text{U}$  daughter of  $^{241}\text{Pu}$ . The levels vary as a function of the age of the sample, the burnup of the sample (initial  $^{241}\text{Pu}$  content), and the chemical processing history. The Los Alamos archival plutonium samples used to characterize FRAM performance (see Table F-1, for example) have  $^{237}\text{Np}/\text{Pu}$  ratios in the range from  $10^{-5}$  to  $10^{-3}$ . The standard plutonium parameter files for analysis in the 120–450 keV region and the 200–800 keV region delivered with version 4 of FRAM quantify the  $^{237}\text{Np}/\text{Pu}$  ratio on every measurement without the need for any operator intervention (see Fig. IX-4).

We characterize the concentration of  $^{237}\text{Np}$  in plutonium by analysis of the gamma rays from its  $^{233}\text{Pa}$  daughter ( $T_{1/2} = 27.0$  d). The gamma-ray activity from  $^{233}\text{Pa}$  will be in secular equilibrium with  $^{237}\text{Np}$  after about 150 days. This condition does not present a problem except for materials fresh from chemical processing. The decay of  $^{233}\text{Pa}$  produces intense gamma rays at 271.5, 300.1, 311.9, 340.5, 375.4, 398.5, and 415.8 keV that can be used for the quantification of the  $^{237}\text{Np}/\text{Pu}$  ratio and/or must be considered as interferences for the plutonium isotopic composition measurement. Table XI-4 tabulates the branching ratios for these gamma rays.

For “normal”  $^{237}\text{Np}/\text{Pu}$  ratios in the range from  $10^{-5}$  to  $10^{-3}$  we quantify  $^{237}\text{Np}/\text{Pu}$  using the 312.2-keV line. We also account for the 375.4 and 415.8 keV lines because of their interference with prominent  $^{239}\text{Pu}$  gamma rays.

Plutonium-bearing samples containing  $^{237}\text{Np}$  at levels above a  $^{237}\text{Np}/\text{Pu}$  ratio of approximately  $10^{-2}$  usually require additional analysis. (Figure XI-2 shows a spectrum with a concentration near this limit.) At this level the 312-keV gamma ray is the most intense gamma ray in the spectrum. The  $^{233}\text{Pa}$  gamma rays begin to contribute significantly to the dose from the sample. At Los Alamos, samples containing significant quantities of  $^{237}\text{Np}$  are usually packaged in lead- shielded containers to reduce the dose to those who handle the samples. The lead shielding eliminates all gamma rays below 200 keV, necessitating analysis in the 200–800 keV region. This analysis with a suitably modified parameter file works up to  $^{237}\text{Np}/\text{Pu}$  ratios of approximately 1 for samples shielded with 3 mm of lead. At a  $^{237}\text{Np}/\text{Pu}$  ratio of approximately 1 the  $^{233}\text{Pa}$  gamma rays dominate

## XI. MODIFYING PARAMETER FILES FOR SPECIAL CASES

Table XI-4. A Partial List of  $^{233}\text{Pa}$  Gamma Rays (Firestone 96).

Energy (keV)	Branching Ratio
271.5	0.00328
300.3	0.0662
312.2	0.386
340.8	0.0447
375.4	0.00679
398.5	0.0139
415.8	0.0175

the spectrum, making the analysis of the plutonium gamma rays very difficult (see Fig. XI-3). Sum peaks from the intense  $^{233}\text{Pa}$  gamma rays dominate the region around 640 keV. FRAM can analyze spectra from samples shielded with 3 mm of lead with  $^{237}\text{Np}/\text{Pu}$  ratios up to approximately 2. With suitably modified data acquisition conditions (addition of extra lead filtering) we would expect to be able to analyze spectra with  $^{237}\text{Np}/\text{Pu}$  ratios up to approximately 10.

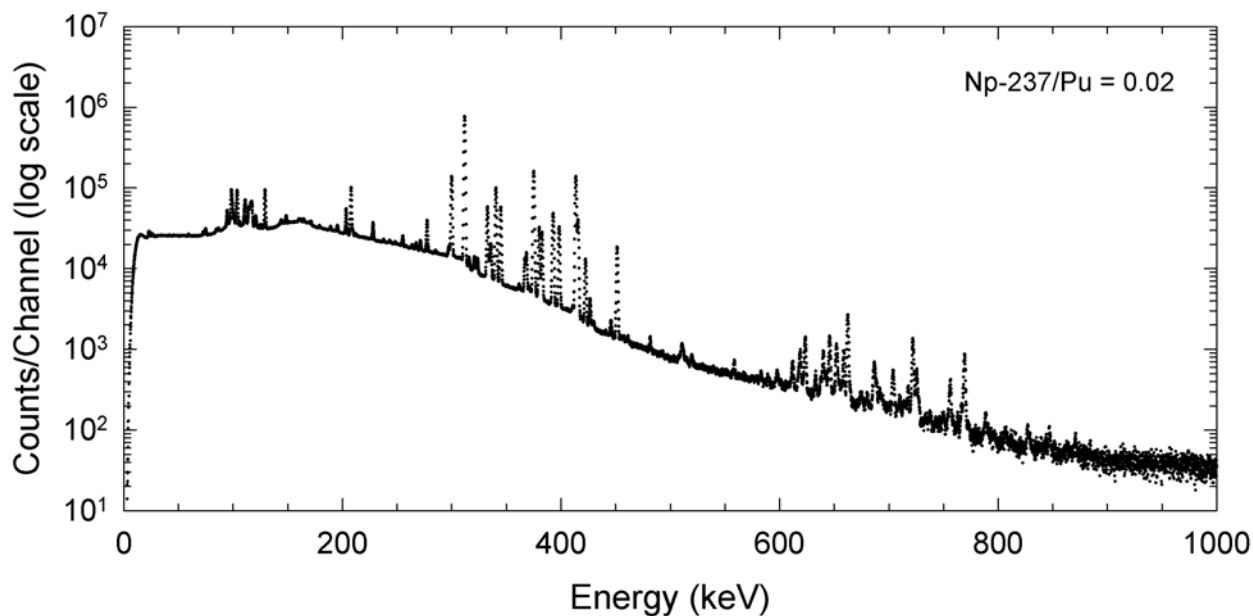


Fig. XI-2. A plutonium spectrum, measured with a coaxial detector, from an unshielded sample with a  $^{237}\text{Np}/\text{Pu}$  ratio of 0.02. This concentration is at the upper end of the range that can be analyzed with standard FRAM parameter files. The most intense peak in the spectrum is the 312-keV gamma ray from the  $^{233}\text{Pa}$  daughter of  $^{237}\text{Np}$ , but all the major plutonium gamma rays are visible. This spectrum can be analyzed in either the 120–450 keV region or in the 200–800 keV region.

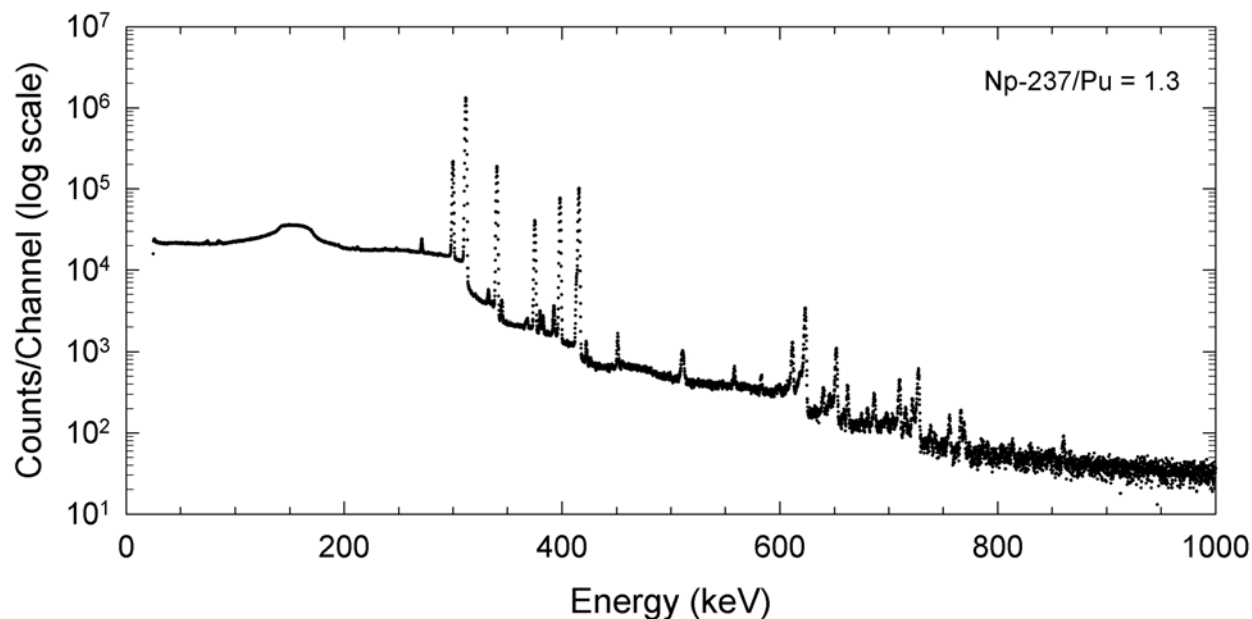


Fig. XI-3. A plutonium spectrum, measured with a coaxial detector, from a shielded sample with a  $^{237}\text{Np}/\text{Pu}$  ratio of 1.3. This concentration is at the upper limit for analysis with a specially modified parameter file for high neptunium. The six major peaks in the 300–400 keV region are all  $^{237}\text{Np}$  related. They overpower the plutonium peaks in this region. The three most intense peaks in the 600–650 keV region arise from sum peaks from  $^{233}\text{Pa}$  gamma ray and likewise overpower the plutonium gamma rays in this region.

#### 4. Very High Americium-241

There is naturally a continuum of  $^{241}\text{Am}/\text{Pu}$  concentrations that FRAM measures. The concentration that qualifies as “very high  $^{241}\text{Am}$ ” is ill defined, but falls in the range of  $^{241}\text{Am}/\text{Pu}$  greater than 0.1. This is a convenient dividing line because most plutonium samples containing  $^{241}\text{Am}$  solely from the decay of  $^{241}\text{Pu}$  will be at levels below this limit. Americium-241 concentrations above 10% relative to plutonium usually arise only in residues and wastes containing  $^{241}\text{Am}$  concentrated from purification processes.

The  $^{241}\text{Am}$  in a typical plutonium sample produces almost as many gamma rays as  $^{239}\text{Pu}$ . The  $^{239}\text{Pu}$  isotopic fraction may change by less than a factor of two over the entire range of plutonium samples encountered. In comparison, the  $^{241}\text{Am}/\text{Pu}$  ratio may change over a range of  $10^6$  considering all of the material streams in a plutonium processing facility. Ratios of  $^{241}\text{Am}$  to plutonium may approach 1:1 in residues from purification processes.

Problems arise in the analysis of the gamma-ray spectra from very high concentration americium samples in several areas:

1. Americium gamma-ray activity will dominate the spectrum. The peaks remaining from plutonium that haven’t been swamped by americium gamma rays will ride on top of a large continuum from the americium gamma rays. The resulting signal/background ratio will be poor and the plutonium gamma-ray peaks will have poor statistical precision.
2. Americium peaks normally too weak to be visible above the background continuum will suddenly appear in the spectrum. These “new” peaks interfere with peak and background ROIs established for analyses of samples with “normal” americium concentrations.

The second problem can be handled by using a spectrum with a very high  $^{241}\text{Am}$  concentration to guide the set up of the peak and background regions. The first problem is more or less intractable as it resides in the data. At Los Alamos, items containing  $^{241}\text{Am}/\text{Pu}$  greater than 0.1 are often packaged in lead-lined

containers, making it necessary to analyze the data in the 200–800 keV region and extracting  $^{240}\text{Pu}$  at 642 keV. The data in Fig. XI-4 show that the analysis for  $^{240}\text{Pu}$  in this region can be difficult to essentially impossible for samples with very high  $^{241}\text{Am}$  because the  $^{241}\text{Am}$  peak at 641.5 keV swamps the  $^{240}\text{Pu}$  peak at 642.6 keV.

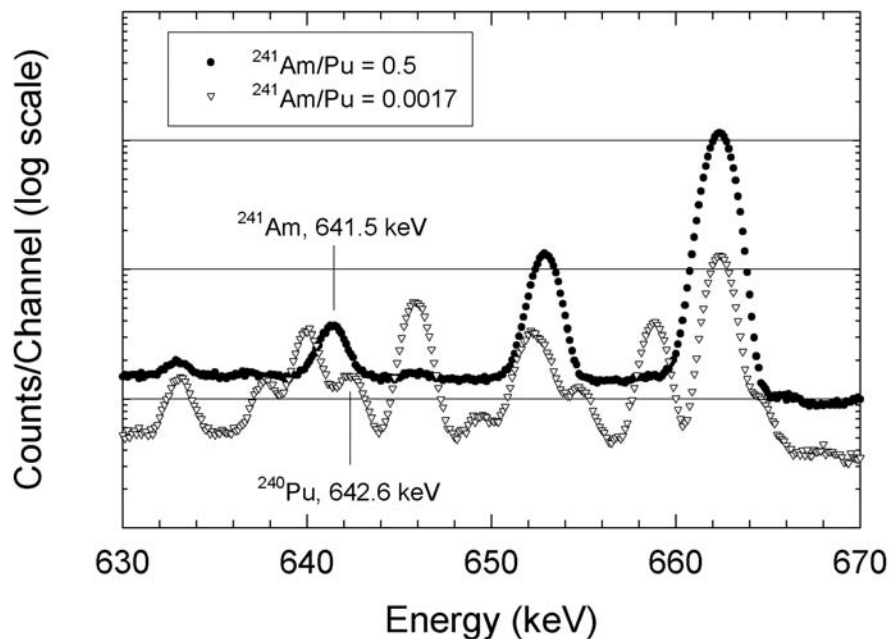


Fig. XI-4. The  $^{240}\text{Pu}$  peak in the 600-keV region is hidden in the spectra from samples with very high  $^{241}\text{Am}$ .

The FRAM analysis (200–800 keV region) of the spectrum ( $^{241}\text{Am}/\text{Pu} = 0.5$ ) in Fig. XI-4 produces a result for  $^{240}\text{Pu}$  that has a RSD of 30%. This is more or less at the limit of detectability. However, the analysis can still be used to interpret a calorimetry measurement because over 95% of the power arises from  $^{241}\text{Am}$ . The % RSD for  $P_{\text{eff}}$  is less than 1% for the same analysis.

### 5. Heterogeneous Am/Pu

Pyrochemical purification processes such as molten salt extraction and electrorefining produce residues where the americium and plutonium are in different matrices. The americium is concentrated in a low-Z matrix in the form of  $\text{AmCl}_3$ , whereas small amounts of plutonium metal are imbedded in the low-Z matrix. The relative-efficiency curve will be different for an americium gamma ray escaping from a chloride matrix from that for a plutonium gamma ray escaping from plutonium metal. The FRAM code calculates the different relative-efficiency curve shapes for americium and plutonium based on a model proposed by Fleissner (Fleissner 83), (see section II.F.6). The plutonium metal pieces found in a molten salt extraction residue are shown in Fig. XI-5. Most of the very high concentration americium samples contain these heterogeneous Am/Pu residues.



*Fig. XI-5. The dressing jar lid contains small plutonium metal pieces sieved from a molten salt extraction residue.*

The user sets up the heterogeneous analysis through the Change Parameter Utility in FRAM. First select **Edit | Parameters** to enter the Change Parameter Utility. Next open the desired parameter file with **File | Open**. Then select **Edit | Isotopes** and assign efficiency function = 2 for americium. FRAM can accommodate multiple relative-efficiency curves but Los Alamos only has experience using two.

The analysis results for the ratio of  $^{241}\text{Am}/^{239}\text{Pu}$  can be simply checked by visual examination of the pulse height spectrum. In Appendix E we have used the fundamental expression for isotopic ratios (Eq. II-5) to tabulate the  $^{241}\text{Am}/^{239}\text{Pu}$  ratio for closely spaced peaks under the condition of equal peak heights. (The authors are indebted to Jack Parker for first producing this table.)

### 6. Plutonium with Cs-137 Interference

Cesium-137 emits a well-known gamma ray at 661.66 keV. The cesium gamma ray interferes with the  $^{241}\text{Am}$  gamma ray at 662.40 keV that is usually used as an internal self-calibration peak for energy and FWHM.

#### a. Analysis in the 600-keV region

The energy calibration using the  $^{241}\text{Am}$  gamma ray at 662.4 keV will be incorrect for situations where the cesium gamma ray dominates the americium gamma ray and its presence is unrecognized. We handle this case easily by

1. adding  $^{137}\text{Cs}$  to the isotope list,
2. placing the 661.66 keV  $^{137}\text{Cs}$  gamma ray in the peak list,
3. using the cesium gamma ray for activity,
4. adjusting the ROI boundaries, if needed, to account for both  $^{241}\text{Am}$  and  $^{137}\text{Cs}$ , and
5. using the americium gamma ray only for activity. Delete any assignment for energy calibration, FWHM calibration, or shape. You may continue to use the  $^{241}\text{Am}$  peak at 722 keV for the energy calibration.

These changes allow the quantification of  $^{137}\text{Cs}/\text{Pu}$  while still allowing the 662.40-keV  $^{241}\text{Am}$  gamma ray to contribute to the analysis.

#### b. Analysis below 450 keV

Cesium-137 does not contribute any direct interference to the 120–450 keV region. Analysis for plutonium and americium can proceed normally in most cases. A problem could arise from a very high

cesium concentration. In this case the Compton continuum from the 661.6-keV cesium gamma ray could swamp the lower energy plutonium gamma rays making it difficult to obtain a plutonium isotopic analysis.

### 7. Uranium with Cs-137 Interference

FRAM has been applied to the analysis of the  $^{137}\text{Cs}/\text{U}$  ratio in critical assembly fuel plates to determine burnup or neutron exposure in the fuel. Cesium-137 does not contribute any direct interferences; one modifies the normal uranium parameter file by

1. adding  $^{137}\text{Cs}$  to the isotope list,
2. placing the 661.66 keV  $^{137}\text{Cs}$  gamma ray in the peak list,
3. using the cesium gamma ray for activity,
4. assigning a peak region for the 661.6 keV peak, and
5. using the cesium peak for energy, FWHM, and shape calibration as desired.

These changes produce the usual uranium isotopic composition plus the  $^{137}\text{Cs}/\text{U}$  ratio. We have seen the situation where the Compton continuum from the 661.6-keV cesium gamma ray swamps the lower-energy uranium gamma rays.

### 8. Heat Source Grade Pu-238

FRAM has analyzed the gamma-ray spectra from numerous items containing heat source grade  $^{238}\text{Pu}$ . The first waste shipments to the Waste Isolation Pilot Plant (WIPP) from Los Alamos contained items with heat source grade plutonium. FRAM successfully analyzed all of these items (Mercer 99).

Heat source grade plutonium typically contains approximately 80%  $^{238}\text{Pu}$ , and 2%–4%  $^{240}\text{Pu}$  with the remainder being mostly  $^{239}\text{Pu}$ . Plutonium-241 and  $^{241}\text{Am}$  are also present and can be analyzed. The  $^{236}\text{Pu}$  that is originally present in parts per million (ppm) amounts produces strong gamma-ray peaks from its thorium daughter decay products. We use the thorium daughter gamma-ray peaks to help define the relative-efficiency curve.

We analyze data in the energy range from 140 keV to 860 keV from a coaxial detector operating in 8192 channels at the standard gain of 0.125 keV/ch. The analysis includes the well-known  $^{238}\text{Pu}$  peaks at 152.7 and 766.4 keV and also includes weaker  $^{238}\text{Pu}$  peaks at 201.0, 742.8, and 786.3 keV. The analysis for  $^{239}\text{Pu}$  and  $^{241}\text{Pu}$  is straightforward using the major higher energy peaks. The usually strong 129.3 keV  $^{239}\text{Pu}$  peak is not visible and the 203.5 keV  $^{239}\text{Pu}$  peak is also not useful.

Plutonium-240 is the most difficult isotope to analyze, as its peaks at 160.3 and 642.5 keV are essentially undetectable. This results in very large % RSD values for  $^{240}\text{Pu}$  as shown in the output listing in Fig. XI-6. The user must use prior knowledge or stream average data for  $^{242}\text{Pu}$  as the standard FRAM isotopic correlation does not apply.

## XI. MODIFYING PARAMETER FILES FOR SPECIAL CASES

```

*****
PC FRAM (4.2) Isotopic Analysis 26-Nov-2002 18:32:18
(Fixed energy Response function Analysis with Multiple efficiencies)
System ID: T. Sampson, Carefree Office

spectrum source: c:\documents and settings\tsampson\desktop\fram isotopics\isotopic
                  spectra\isotopic spectra\pu238\std1493.s01
spectrum date:   17-Jun-1998 06:07:30
live time:      6252 s
true time:     7200 s
num channels:  8192

parameter set: Pu238_Coax (2002.11.26 18:03)
                Coax, .125 kev/ch, ~80% Pu238 125-780 keV
*****
diagnostics passed.

                                     (OpEntry)   (ug/gPu)

      Pu238      Pu239      Pu240      Pu241      Pu242      Am241
mass%  79.1196    15.9171    4.0773    0.3861    0.5000    2501.5
sigma  1.4407     0.3093     1.7420    0.0087    0.0000    61.6
%RSD   1.82%      1.94%      42.72%    2.27%    < .01%    2.46%

%TotPwr 99.80      0.07      0.06      < .01    < .01      0.06

Specific Power (W/gPu):  ( 449.9543 +/- 0.7242)e-003 ( 0.16%)
Effective Pu240 fraction: ( 204.2987 +/- 4.0269)e-002 ( 1.97%)
Time since chemical separation: 3803.7 +/- 64.4 days ( 1.69%)

Relative mass (Th228 / Pu):  1.285e-008 ( 1.83%)
Relative mass (Np237 / Pu):  4.464e-004 ( 2.65%)
*****

```

Fig. XI-6. Output from the analysis of a sample of heat source grade  $^{238}\text{Pu}$ .

### 9. Uranium-Plutonium Mixed Oxide (MOX)

We no longer consider MOX analysis to be a “special case” when using the current versions of FRAM, although historically there have not been many opportunities for MOX analysis in the United States. This may change in the future if current plutonium disposition plans are carried out.

The standard coaxial detector parameter files for plutonium (both shielded and unshielded) also analyze for uranium, if present. Some of these results have been presented previously in section IX.B.4, which discusses MOX measurement bias.

The standard plutonium parameter file for analysis in the 120–450 keV region also analyzes for  $^{235}\text{U}$  at 185.7 keV and includes  $^{235}\text{U}$  peaks at 143.8, 163.4, 202.1, and 205.3 keV as interference peaks.

The standard plutonium analysis in the 200–800 keV region analyzes for  $^{235}\text{U}$  at 185.7 keV (this peak may not be present if there is shielding around the sample) and analyzes for  $^{238}\text{U}$  at 1001.0 keV. The parameter file also has interference peaks from  $^{235}\text{U}$  at 202.1 and 205.3 keV as well as a  $^{238}\text{U}$  interference peak at 766.4 keV. Plutonium-238 and  $^{238}\text{U}$  both contribute to peaks at 766.4 and 1001.0 keV. All four of these peaks are included in the parameter file. In most MOX samples, the 766.4-keV peak arises mainly from  $^{238}\text{Pu}$ , and the 1001.0-keV peak arises mainly from  $^{238}\text{U}$ . We account for this by fixing the  $^{238}\text{U}$  component at 766 keV to the  $^{238}\text{U}$  component at 1001 keV and fixing the  $^{238}\text{Pu}$  component at 1001 keV to

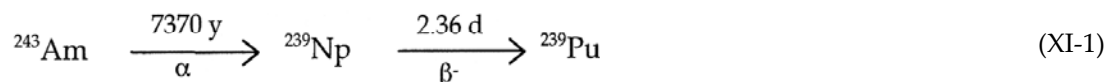
## XI. MODIFYING PARAMETER FILES FOR SPECIAL CASES

the larger  $^{238}\text{Pu}$  component at 766 keV. The iterative FRAM analysis then further refines this starting point.

The reader is referred to Appendix A for more details. In this appendix we have described in some detail the considerations that have gone into the setup of parameter files for MOX analysis.

### 10.Am-243–Np-239

Americium-243 may be present in plutonium samples. This isotope decays as shown in Eq. XI-1 below.



The short half live of  $^{239}\text{Np}$  means that it will be in equilibrium with  $^{243}\text{Am}$  and gamma rays from  $^{239}\text{Np}$  can be used to characterize  $^{243}\text{Am}$ . We do not see the gamma rays from the direct decay of  $^{243}\text{Am}$  but the gamma rays from the decay of  $^{239}\text{Np}$  are very strong and easily identified in a plutonium spectrum. We list the strongest gamma rays from  $^{239}\text{Np}$  in Table XI-4. These gamma rays, along with a few weaker neighboring gamma rays, are accounted for in analysis for  $^{243}\text{Am}$ .

Table XI-5. Prominent Gamma Rays from the Decay of  $^{239}\text{Np}$ .

Energy (keV)	Branching Fraction
209.75	0.0342
228.18	0.108
277.60	0.144
334.31	0.0207

We must account for these gamma rays in every plutonium spectrum, even if we are not directly interested in the  $^{243}\text{Am}$  concentration. The background region above the 208.00-keV  $^{241}\text{Pu}$ - $^{237}\text{U}$  peak usually must be adjusted to account for the possible presence of the 209.75-keV gamma ray from  $^{239}\text{Np}$ . The 334.31-keV peak of  $^{239}\text{Np}$  provides a direct interference in the 332–336 keV analysis region. The 228.18-keV peak is analyzed for the activity of  $^{243}\text{Am}$ . We do not use the 277.6-keV peak because of other weak interferences that are usually present in this region. However, its presence, along with the 228-keV peak, provide unambiguous visual identification of the presence of  $^{243}\text{Am}$ .

The standard FRAM parameter files easily analyze spectra from samples with “normal” concentrations of  $^{243}\text{Am}$ . Very high concentrations are characterized by the peak height of the 209-keV  $^{239}\text{Np}$  peak being an appreciable fraction of or greater than the peak height of the 208.00-keV  $^{241}\text{Pu}$ - $^{237}\text{U}$  peak. These cases should be examined more closely as it may be necessary to “tweak” the boundaries of some of the ROIs to obtain the best results.

### 11. Physically, Spatially, and Isotopically Heterogeneous Waste

Waste drums packaged for disposal are the principal representatives of this material category. Users often fill waste drums with many smaller containers of individually packaged waste. Even if the small containers have been segregated by  $^{240}\text{Pu}$  value, the small containers, taken all together, will likely be isotopically heterogeneous at some level. A waste drum specified to contain plutonium with a nominal  $^{240}\text{Pu}$  concentration of 6% might actually contain packages with  $^{240}\text{Pu}$  contents ranging from 4 to 7 percent. Similarly, the other isotopic components could easily vary over a range of a factor of two or more. The

## XI. MODIFYING PARAMETER FILES FOR SPECIAL CASES

---

isotopic heterogeneity may not simply be confined to different isotopic vectors in different containers. Some drums might contain packages that, in addition, exhibit an Am/Pu ratio heterogeneity as described in XI.C.5 above.

The individual packages almost always contain waste that is physically heterogeneous and their distribution in a waste drum adds an additional dimension of spatial heterogeneity.

These multiple factors, including, a spread of isotopic distributions, physical heterogeneities within a package, spatially heterogeneous distribution of packages in the drum, and Am/Pu heterogeneities within a package, combine to produce an extremely difficult problem for any isotopic analysis software.

There is no single FRAM parameter file designed for this situation. The best we can do is to give some guidelines that may help to mitigate the biases caused by these effects.

- Carry out the analysis at high energies using parameter files set up to analyze in the 200–800 keV region, assuming that the counting rate will permit. The increased penetrability of the higher-energy gamma rays allows better averaging, both spatially and isotopically.
- Use a parameter file set up for Am/Pu heterogeneity if you have knowledge that those waste streams may be represented in some of the packages.
- Use rotation and translation of the waste drum during the measurement.

## XII. DIFFICULT MEASUREMENT SITUATIONS

---

### XII. DIFFICULT MEASUREMENT SITUATIONS

#### A. Using FRAM With Rate-Loss Correction Sources

We have successfully analyzed data taken with a rate-loss correction source attached to the detector (a rate-loss correction source is used in systems such as an SGS or tomographic gamma scanner (TGS) performing transmission-corrected passive assay). A rate-loss correction source complicates the FRAM analysis in two ways. The rate-loss correction source may have gamma rays that interfere directly with plutonium gamma rays used in the FRAM analysis. In addition, the gamma or x-rays from the rate-loss source may randomly sum with plutonium gamma rays to produce unwanted interferences.

FRAM has analyzed data from both situations. We present a detailed discussion on using FRAM with rate-loss sources in Appendix B.

#### B. Simultaneous FRAM/AWCC Measurements

An AWCC user wished to perform passive coincidence counting measurements with the AWCC (no neutron sources and no nickel ring) while simultaneously making an isotopic measurement with an HPGe detector. The user suggested modifying the AWCC with a hole through the wall to bring out an unattenuated gamma-ray beam to the detector.

Thinking that the hole was unnecessary, we made direct measurements using a 25% relative-efficiency coaxial detector on plutonium inside an *unmodified* AWCC. The sample was a container holding 847 g PuO<sub>2</sub> with nominal 16% <sup>240</sup>Pu. Table XII-1 displays the isotopic composition of the sample on the measurement date.

The face of the detector was positioned about 1.5 in. from the cylindrical outer surface of the AWCC giving a gross counting rate of 40 kHz. The center line of the uncollimated detector was positioned vertically at 1.5 in. above the bottom of the container. The total sample-to-detector distance was about 12 in. We made 10 measurements of 30 minutes each.

Table XII-1. Isotopic Composition (wt %) on Measurement Date.

Pu-238	Pu-239	Pu-240	Pu-241	Pu-242	Am-241
0.053	82.554	16.449	0.601	0.343	0.796

We were able to analyze each spectrum in the 120–450 keV region and also in the 200–800 keV region. That is to say, the attenuation provided by the body of the AWCC did not completely attenuate the gamma rays below 200 keV. There were even visible peaks in the 100-keV region. Table XII-2 below gives the results of the two analyses of the 10 measurements.

The measurement results are clearly more precise using the 200–800 keV analysis. Both sets of results show that spectra suitable for FRAM analysis can be obtained by collecting the spectra data through the body of the neutron counter.

## XII. DIFFICULT MEASUREMENT SITUATIONS

Table XII-2. FRAM Analysis Results through AWCC Wall (Pu-242 operator entered).

Analysis	Pu-238	Pu-239	Pu-240	Pu-241	Am-241
<u>120–450 keV Analysis</u>					
Avg: Measured/Accepted	0.9745	0.9999	1.0010	0.9842	1.0127
% RSD distribution	13.0	1.3	6.4	1.4	2.5
<u>200–800 keV Analysis</u>					
Avg: Measured/Accepted	1.0163	1.0049	0.9747	1.0163	0.9868
% RSD distribution	3.5	0.26	1.4	0.90	0.91

### C. Measurements Through Thick Shielding

FRAM's ability to make measurements through very thick shielding is, perhaps, its most important, useful, and well-known characteristic. While we cannot document all possible measurement scenarios, we will give some examples of the extreme measurement conditions encountered for shielded samples.

#### 1. Steel Shielding

A thickness range of 10–12 mm of steel is the limit for reliable measurements using gamma rays and x-rays in the 100-keV region.

##### a. Plutonium

Very early in the application of FRAM we showed that FRAM could easily analyze plutonium isotopic data collected in the 120–450 keV region taken through 12.5 mm (0.5 in.) of steel. This is a routine capability of FRAM using the standard parameter file for analysis in the 120–450 keV region.

Somewhat later (Sampson 99c) we demonstrated the analysis of a plutonium spectrum taken through 25 mm of steel. In this case the analysis was performed using the standard parameter file for analysis in the 200–800 keV region. It is clear that FRAM can perform plutonium isotopic measurements through steel much thicker than 25 mm but we have not yet performed the experiments to define a higher limit.

##### b. Uranium

A common uranium measurement problem is that of the measurement of the enrichment or isotopic composition of low-enriched uranium in UF<sub>6</sub> cylinders. Cylinders containing UF<sub>6</sub> with enrichments in the 1%–5% range typically have a wall thickness of 13 mm. The wall material may be nickel or a nickel alloy possessing approximately the same absorption properties as steel. Depleted or natural UF<sub>6</sub> is often found in cylinders with 16-mm-thick walls.

FRAM does not have any problem analyzing coaxial detector data from uranium samples shielded with 16 mm of steel (Sampson 01). We have made numerous measurements with a 28% relative-efficiency coaxial detector on enrichment standards in a geometry that simulates the measurement of a UF<sub>6</sub> cylinder. Figure XII-1 displays this geometry.

## XII. DIFFICULT MEASUREMENT SITUATIONS

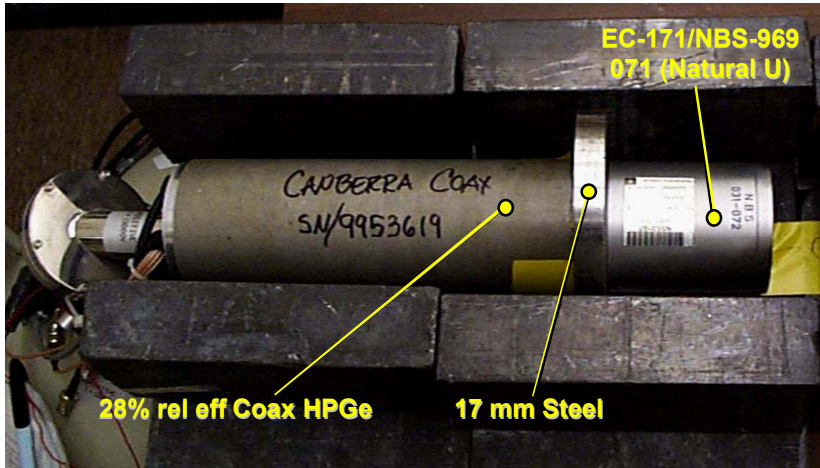


Fig. XII-1. Measurement geometry, with detector, steel absorber, and sample, that simulates the measurement of a UF<sub>6</sub> cylinder.

In Fig. XII-2 we display, as a function of enrichment and counting time, the relative standard deviation of a single measurement obtained from the distribution of 15 replicates of these mockup measurements.

We repeated these measurements using a 70-mm-diam. by 30-mm-thick semiplanar detector to see if the larger detector diameter would improve the peak-to-background ratio at 258 keV. We obtained the same results as for the coaxial detector. This is thought to occur because much of the continuum underneath the 258-keV peak arises from bremsstrahlung, not Compton scattering.

Los Alamos personnel have used FRAM to analyze spectra that were acquired from type 30B UF<sub>6</sub> cylinders at the ABB Atom fuel fabrication facility in Vasteras, Sweden (Sampson 99c). A type 30B UF<sub>6</sub> cylinder has 13-mm-thick steel walls. These measurements were made with a 26% relative-efficiency coaxial detector in 8192 channels. The measurements on 30B cylinders showed a measurement precision or repeatability of 6%–8% (1 RSD) for 20–30 minute measurements covering enrichments from natural to 4.7%. This is consistent with the results in Fig. XII-2 and even better than the results shown in Fig. XII-2 for natural uranium.

In the report describing the measurements at ABB Atom we made several observations comparing FRAM isotopic analysis measurements with the classical enrichment meter method (Smith 91).

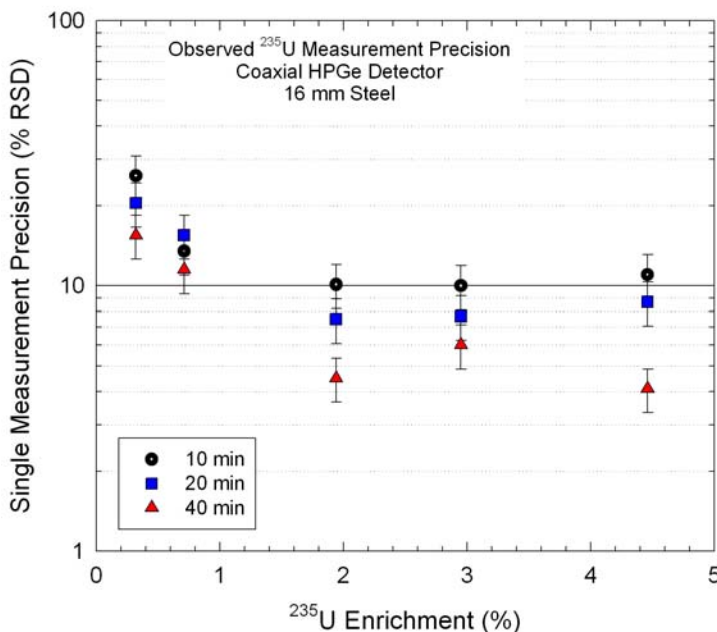


Fig. XII-2. Single measurement precision of the <sup>235</sup>U fraction calculated from 15 replicates. The five standards were measured in 8192 channels with a 28% relative-efficiency coaxial HPGe detector and analyzed with the FRAM software. The measurements were made in the mockup geometry of Fig. XII-1.

## XII. DIFFICULT MEASUREMENT SITUATIONS

---

One should consider the following when choosing between FRAM or the classical enrichment method for UF<sub>6</sub> cylinder measurements. Note that we do not compare measurements in the 100-keV region because they are unreliable for the 13–16-mm-thick cylinder walls.

The advantages of using FRAM include the following:

- Because FRAM does not require calibration, it is faster for a limited number of measurements than the classical enrichment method.
- The classical enrichment method requires an auxiliary measurement of the wall thickness of the cylinder. This ultrasonic measurement adds time and uncertainty to the measurement process as well as requires additional equipment.
- The FRAM measurement has no geometric reproducibility requirements. The classical enrichment method requires that the measurement geometry for the unknown be the same as for the calibration.
- FRAM can measure other materials in the facility such as scrap, waste, oxide powder, and anything else that might be encountered. The classical enrichment method is not able to do most of the other measurements without a new calibration and the assurance of a geometry that possesses “infinite thickness.”

There are situations in which it is advantageous to use classical enrichment methods:

- The classical enrichment method has a shorter measurement time after calibration is complete.
- FRAM requires decay equilibrium (approximately 100 days from separation of daughter products) in the <sup>238</sup>U decay. The classical enrichment method does not because it measures <sup>235</sup>U directly.
- Shielding requirements are more stringent with FRAM because FRAM measures gamma rays up to 1 MeV. The system must provide shielding against background at this energy. The classical enrichment method measures at 185 keV.

The discussion of gamma-ray isotopic analysis measurements on UF<sub>6</sub> cylinders would not be complete without noting the capability of planar HPGe detectors for this application. Planar HPGe detectors have long been considered to be too small and not efficient enough for the FRAM type measurements that measure up to 1 MeV.

The IAEA has many planar HPGe detectors (25 mm diam. by 15 mm thick) that are routinely used for isotopic measurements on plutonium with analysis in the 100-keV region. Because of the availability of these detectors they wished to use these same detectors for uranium measurements on UF<sub>6</sub> cylinders. The experience of IAEA personnel showed that uranium isotopic analysis methods using the 100-keV region with the Multi Group Analysis Uranium software (MGAU) failed because of the attenuation in the thick steel walls of the UF<sub>6</sub> cylinders. IAEA personnel also knew that FRAM could successfully analyze data from measurements of UF<sub>6</sub> cylinders taken with coaxial HPGe detectors.

Los Alamos was asked to put the two together to see if FRAM could analyze data from planar HPGe detector measurements on UF<sub>6</sub> cylinders. An additional requirement was that the data was to be acquired in 4096 channels to match the IAEA’s standard MCAs. We set up the measurement geometry as pictured in Fig. XII-1 using a 25-mm-diam. by 16-mm-thick planar detector in place of the coaxial detector pictured.

These measurements on uranium using a planar HPGe detector operating at 0.25 keV/ch (4096 channels spanning 0–1024 keV) were very difficult for FRAM to analyze. The spectra were weak because of the small detector. Even more important was the low number of channels/keV resulting in very narrow

## XII. DIFFICULT MEASUREMENT SITUATIONS

peaks at low channel numbers for the high-resolution planar detector. The full width at half maximum for the 185-keV  $^{235}\text{U}$  peak was less than 3 channels. We made measurements on samples with enrichments of 0.31, 0.71, 1.94, 4.46, and 10.09 wt % using steel thicknesses of 13 and 16 mm and count times of 15, 30, and 60 minutes. Each combination was measured 24 times for a total of 720 measurements.

The results (Sampson 01) from the most difficult measurements (0.31 wt %  $^{235}\text{U}$  for a 15-minute count time) are shown in Table XII-3. The % RSD is that for a single measurement determined from the distribution of the 24 repeated measurements.

The measurements displayed in Table XII-3 demonstrate that FRAM can perform these measurements successfully in a count time as short as 15 minutes, albeit with quite large statistical uncertainties. Coaxial detector measurements are still the measurement of choice as the precision is about a factor of two better, (see Fig. XII-2), than that of the planar detector.

Table XII-3. Twenty-Four 15-Minute Measurements, Planar HPGe detector (25 mm by 16 mm).

Sample	Accepted wt % $^{235}\text{U}$	16 mm Steel Absorber			13 mm Steel Absorber		
		Measured wt % $^{235}\text{U}$	Meas./Accept.	% RSD	Measured wt % $^{235}\text{U}$	Meas./Accept.	% RSD
EC-171-031	0.3166	0.3131	0.9889	37.4	0.3556	1.1232	27.9
A1-408-1	0.7135	0.7231	1.0135	16.9	0.7100	0.9951	14.1
EC-171-194	1.9420	1.9495	1.0039	18.6	1.9968	1.0282	15.7
EC-171-446	4.4623	4.5950	1.0297	20.9	4.3954	0.9850	11.9
A1-324-1	10.086	10.093	1.0007	14.9	10.453	1.0364	8.0
		Average	1.0073		Average	1.0336	

### 2. Lead Shielding

The ability of FRAM to analyze data acquired through lead shielding was one of the first “difficult applications” demonstrated for FRAM. Numerous examples of FRAM measurement performance on relatively lightly lead-shielded samples have been given in chapter IX. Hypes (Hypes 00) has demonstrated that FRAM can obtain a complete isotopic analysis from measurements made through as much as 25 mm of lead. Figure XII-3 displays spectra for lead thicknesses of 0, 12, and 25 mm.

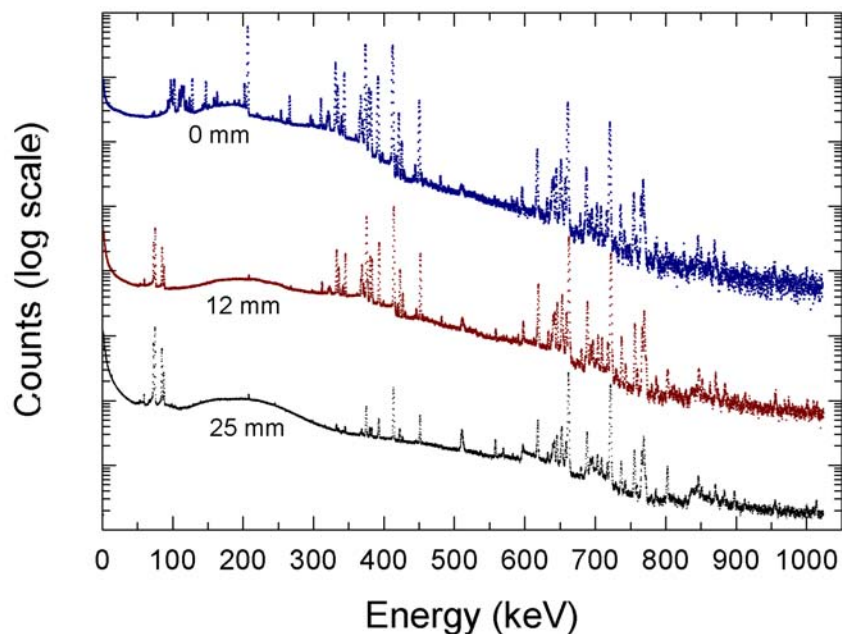


Fig. XII-3. HPGe detector gamma ray spectra from a sample shielded with 0, 12, and 25 mm of lead. The peaks around 75 keV are Pb x-rays from the lead shielding in front of the detector.

These extreme thicknesses require some parameter file modification because lower-energy gamma rays “disappear” as the lead thickness increases. The 203-keV and 208-keV peaks of  $^{239}\text{Pu}$  and  $^{241}\text{Pu}$ - $^{237}\text{U}$  respectively are present and can be analyzed for most samples for lead shielding thicknesses up to about 6 mm. At double this thickness, 12 mm of lead, we see gamma-ray peaks only above approximately 300 keV. This still allows analysis for  $^{241}\text{Pu}$  using the 330-keV region and the 370-keV region. With shielding of 25 mm of lead the 330-keV region becomes very weak and one is forced to measure  $^{241}\text{Pu}$  using gamma rays in the 370-keV region. If the attenuation becomes still greater and the 370-keV region is not available one will not be able to measure the  $^{241}\text{Pu}$  isotopic fraction as 370.94 keV is the highest-energy gamma ray emitted by  $^{241}\text{Pu}$  or its  $^{237}\text{U}$  daughter. It is also of interest to note the differential attenuation of the 375- and 414-keV gamma rays from  $^{239}\text{Pu}$ . These gamma rays are the most intense peaks in the 375-425 keV region in the above plot. Visually the peaks are of approximately equal height with no shielding, as expected because their branching intensities differ by only about 6% (see Appendix D). The differential attenuation becomes visually apparent for 12 mm of lead shielding and is approximately a factor of two for the 25-mm lead thickness.

We also note that 148.6 keV is the highest measurable gamma ray directly from  $^{241}\text{Pu}$ . All the higher energy gamma rays come from the  $^{237}\text{U}$  daughter of  $^{241}\text{Pu}$ . This means that  $^{241}\text{Pu}$ - $^{237}\text{U}$  decay equilibrium (more than 45 days from chemical separation) must be present for measurement of  $^{241}\text{Pu}$  for any samples shielded with enough lead to remove the 148-keV gamma ray (approximately 1 mm of lead).

### 3. 9975 Shipping Container

The 9975 shipping container provides a real-world example of a container that is difficult to measure. This shipping drum is used by DOE facilities to ship and store plutonium-bearing materials slated for disposition or long-term storage. This shipping drum will hold the nominal 5-in.-diameter DOE 3013 plutonium storage container. A view of the interior of a 9975 is shown in Fig. XII-4.

## XII. DIFFICULT MEASUREMENT SITUATIONS



*Fig. XII-4. A view of the interior of a 9975 shipping drum showing four different layers of materials surrounding the central cavity. These layers consist of approximately 0.75 in. steel, 0.5 in. lead, and 5 in. of Cellutex.*

A coaxial detector gamma-ray spectrum from a sample of approximately 4 kg of weapons plutonium contained in a 9975 (Hypes 01) is presented in Fig. XII-5 below. It is not very much different from the spectrum seen through 25 mm of lead, shown in Fig. XII-3.

Data from samples contained in a 9975 shipping container are analyzed with a FRAM parameter set that uses gamma rays above 300 keV. The sawtooth structure in the spectrum at energies of 600 keV and above arises from neutron inelastic scattering from the germanium in the detector crystal.

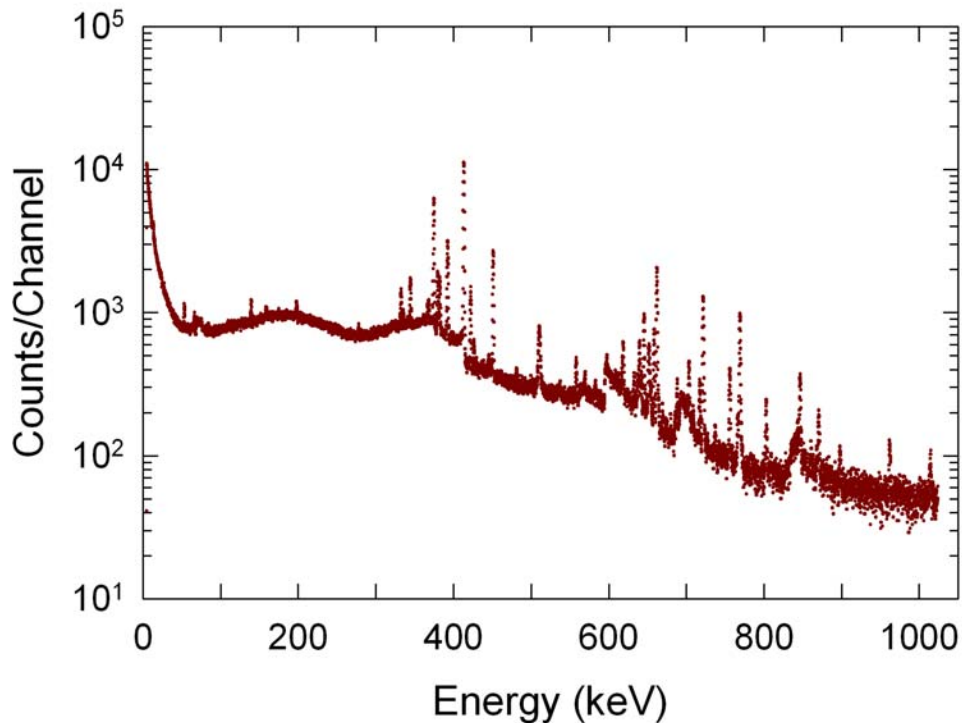


*Fig. XII-5. A spectrum taken with a coaxial detector from 4 kg of weapons plutonium inside a 9975 shipping container*

## XII. DIFFICULT MEASUREMENT SITUATIONS

---

### D. Measurements on Am-Be Neutron Sources

Hypes (Hypes 02) used FRAM to analyze data from americium-beryllium (AmBe) neutron sources to quantify other heat-producing isotopes in addition to  $^{241}\text{Am}$ . These measurements were performed to support calorimetry measurements of the sources prior to disposal. He analyzed for  $^{239}\text{Pu}$ ,  $^{243}\text{Am}$ ,  $^{237}\text{Np}$ , and  $^{239}\text{Np}$  relative to the principal heat-producing isotope of  $^{241}\text{Am}$ .

Data acquisition can be a problem for measurements on neutron sources, in the long term, because of the potential for neutron damage to the HPGe crystal. These measurements did not result in any noticeable neutron damage and successfully demonstrated the ability of FRAM to analyze spectra containing neither plutonium nor uranium.

XIII. FRAM APPLICATION WITH CADMIUM TELLURIDE (CDTE) DETECTORS

The successful application of an unmodified version 4 of FRAM to data taken from a 10-mm by 10-mm by 1.5-mm Peltier-cooled CdTe detector is another demonstration of the extreme versatility of the FRAM isotopic analysis software (Vo 02). This is the first successful application of an unmodified general-purpose isotopic analysis code to any room temperature semiconductor detector.

Several characteristics of the spectra from CdTe detectors provide an extreme challenge for FRAM. The energy calibration is not linear, unlike the highly linear energy calibration from HPGe detectors. This is easily handled by the piecewise linear energy calibration built into FRAM. The very large tails on the photopeaks are discussed in detail in (Vo 02) and are the greatest limitation for the use of the unmodified version 4 of FRAM for analysis of CdTe.

The spectra from NaI, CdZnTe, and HPGe detectors are overlaid with a CdTe spectrum for two different plutonium isotopic compositions in Figs. XIII-1,2.

Note the region around 203–208 keV. The two gamma-ray peaks at 203.5 keV ( $^{239}\text{Pu}$ ) and 208.0 keV ( $^{241}\text{Pu}$ - $^{237}\text{U}$ ) are completely resolved in the HPGe spectra of both samples. The peaks are partially resolved in the CdTe spectrum from the 94%  $^{239}\text{Pu}$  sample but the 203.5-keV peak is completely hidden under the tail of the 208-keV peak in the spectrum from the 64%  $^{239}\text{Pu}$  sample. This difficult analysis situation contributes to the significantly larger errors seen in the CdTe analysis when compared to the HPGe analysis. Nevertheless, FRAM successfully analyzes the complete isotopic distribution for samples with  $^{240}\text{Pu}$  ranging from 3% to 26%.

Table XIII-1 displays the bias for a group of measurements from a CdTe detector used to measure standards at LANL. The description of the standards is included in Table F-1 in Appendix F.

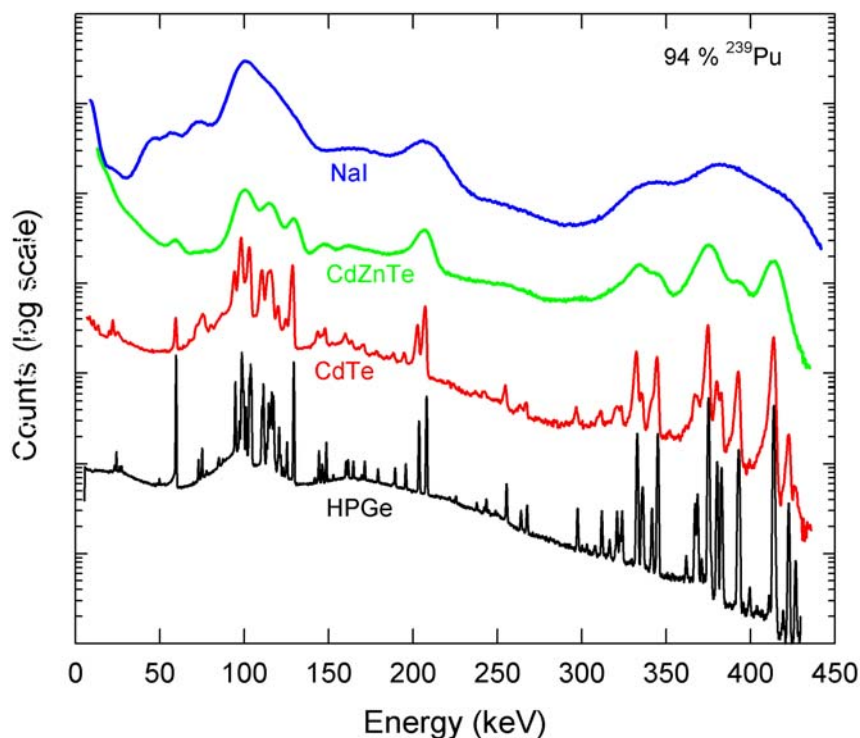


Fig. XIII-1. Comparison of the gamma ray spectra from a sample containing 94%  $^{239}\text{Pu}$ , 6%  $^{240}\text{Pu}$  for four different detectors. Version 4 of FRAM can obtain the complete isotopic distribution from the HPGe detector and from the CdTe detector.

### XIII. FRAM APPLICATION WITH CADMIUM TELLURIDE (CDTE) DETECTORS

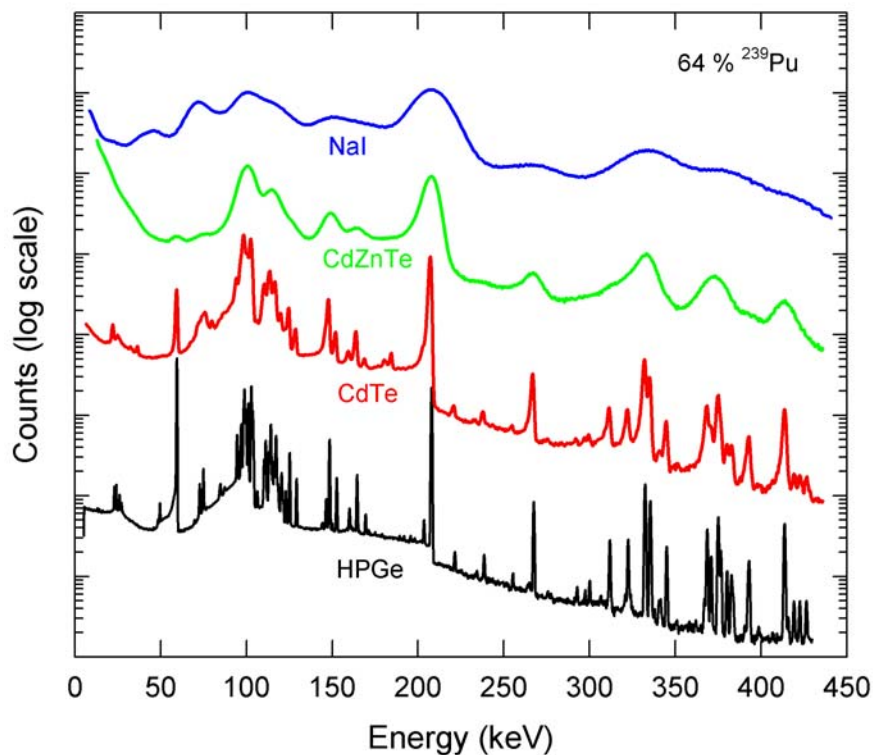


Fig. XIII-2. Comparison of the gamma-ray spectra from a sample containing 64%  $^{239}\text{Pu}$  and 26%  $^{240}\text{Pu}$  for four different detectors. Version 4 of FRAM can obtain the complete isotopic distribution from the HPGe detector and from the CdTe detector.

Table XIII-1. Percent Bias in the FRAM Analysis of CdTe Detector Spectra from Reference Standards.

Sample	$^{240}\text{Pu}$ mass %	Percent Bias = $100 * (\text{Measured} - \text{Accepted})/\text{Accepted}$					
		$^{238}\text{Pu}$	$^{239}\text{Pu}$	$^{240}\text{Pu}$	$^{241}\text{Pu}$	$^{241}\text{Am}$	$P_{\text{eff}}$
STDISO03	3.56	-30.23	-0.33	8.98	-1.00	-3.06	0.19
PIDIE6_1	5.99	-76.71	-0.06	0.97	3.00	-9.33	-2.77
STDISO06	6.13	6.32	-0.67	10.24	-1.04	9.25	2.18
CBNM93	6.31	8.69	-0.45	6.67	0.68	-24.23	-1.25
STDISO09	6.90	-0.53	1.41	-18.93	-2.74	-0.83	-2.65
STDISO12	11.85	-6.31	0.81	-5.79	-3.13	3.25	-0.91
PIDIE6_3	14.20	-17.7	-0.37	2.31	-1.32	2.26	0.03
CBNM84	14.27	-10.67	-0.14	1.06	-5.40	-4.95	-1.86
STDISO15	15.52	-6.56	0.33	-1.61	-1.08	2.12	-1.07
CBNM70	18.81	-6.99	-3.75	16.38	-6.98	-6.21	-3.65
PIDIE6_5	21.41	-15.82	1.99	-6.80	-4.43	-6.59	-5.68
CBNM61	26.29	-4.08	-0.37	1.50	-3.19	-3.66	-2.92
PIDIE6_7	26.39	-4.44	1.16	-2.39	-1.64	-0.32	-2.01
	Avg Bias	-12.69	-0.03	0.97	-2.17	-3.25	-1.72
	% RSD	21.73	1.39	8.86	2.59	8.02	1.96

### **XIII. FRAM APPLICATION WITH CADMIUM TELLURIDE (CDTE) DETECTORS**

---

The larger bias of the CdTe measurements, compared to the bias seen in HPGe detector measurements, arises from two sources. First, the counting statistics are poorer because of the small size of the crystal—over 500 times smaller in volume than a typical 25% relative-efficiency coaxial HPGe detector used by FRAM. The second source arises from the imperfect fit of the HPGe detector peak-shape model to the severely tailed peaks from CdTe.

The CdTe results can be significantly improved by modifying the analysis to include peak shape models that are more applicable to CdTe and applying this new analysis to the 100-keV region.

We note that the FRAM analysis was successfully applied to spectra from a CdTe detector, not CdZnTe. While CdZnTe is in more common use, its resolution is too poor (see Figs. XIII-1 and XIII-2) to allow analysis of its spectra by an unmodified version of FRAM.

### XIV. FRAM APPLICATIONS IN AUTOMATED SYSTEMS

#### A. ROBOCAL

FRAM is now being applied in robotic, automated systems designed to operate continuously and unattended, 24 hours a day. This places an additional burden on the FRAM software because FRAM may not know anything about the type of material being measured.

ROBOCAL (robotic calorimetry) is a robotic system for remote calorimetric and gamma-ray isotopic analysis of special nuclear materials that has been operating at the Plutonium Facility of the Los Alamos National Laboratory since 1990 (Hurd 89, Harp 91). ROBOCAL has recently been upgraded (Bonner 01) with new robotics, new computers and software, and a FRAM isotopic analysis system called the Intelligent Isotopic Unit (IIU).

##### 1. Intelligent Isotopic Unit Autoanalysis

Because ROBOCAL runs unattended and without the opportunity for operators to input information on the items to be analyzed, the IIU is designed to assay an extended range of samples, consisting of normal samples or pyrochemical residues in shielded or unshielded containers, all without operator intervention. Normally, when a varied range of sample types is presented to FRAM in a manual mode, the operator must choose an appropriate parameter set for each sample, based on existing knowledge of the sample. This knowledge may be imperfect and the analysis may have to be repeated if the initial choice was bad.

In the FRAM software for the IIU, we have incorporated some additional logic and diagnostic tests, based on the actual spectrum under analysis, to choose the best parameter set for the analysis. The automated logic or intelligence in the modified version 4 of FRAM for the IIU automatically chooses from six different parameter sets that accommodate all combinations of unshielded, shielded, homogeneous or heterogeneous Am/Pu, and very high  $^{241}\text{Am}$ .

The automatic selection process starts with acquisition of data with an Autoanalysis flag set. The IIU acquires this data using a 25%–30% efficient coaxial HPGe detector. The spectral data is first analyzed in the 120–450 keV region, assuming the sample is unshielded. The data is reanalyzed, if necessary, with other members of the six parameter sets based on the results of three diagnostic tests described next.

- Test for Shielded Sample This test forms the ratio of the relative efficiency of a peak at high energy relative to one at low energy. The ratio is tested against an empirical limit. If the ratio is less than the limit, the sample is not shielded; if it is greater than the limit, the sample is shielded. This test is based on the fact that absorbers attenuate low-energy peaks (and hence decrease the relative efficiency) more than at high energies.
- Test for Am/Pu Heterogeneity This test forms the ratio of Am/Pu from a low-energy peak to Am/Pu from a high-energy peak. If americium and plutonium are in the same matrix, this ratio should be unity. If americium is in a different matrix (heterogeneous Am/Pu) than the plutonium, the ratio will differ from unity because of the different attenuation suffered by americium and plutonium gamma rays at the same gamma-ray energy. The test also accounts for the statistical uncertainties in the two Am/Pu ratios. When Am/Pu heterogeneity is detected, the spectrum is reanalyzed with a second relative efficiency curve assigned to americium.
- Test for High Americium Concentration This test compares the measured Am/Pu fraction against a user-defined limit. A different parameter file is used for high americium because of the

## XIV. FRAM APPLICATIONS IN AUTOMATED SYSTEMS

additional americium peaks appearing in the spectrum that are not visible for lower concentrations. A typical user-defined limit for High Americium is  $\text{Am/Pu} > 0.1$ .

### 2. Intelligent Isotopic Unit Hardware

The IIU hardware provides for motion with three degrees of freedom. The sample is rotated and translated vertically in front of the detector. In addition, the detector is mounted on a platform that moves in the horizontal plane to vary the sample to detector distance. The sample rotation and vertical translation evens out the response from heterogeneous samples. The horizontal motion of the detector allows the system to position the detector to optimize the system counting rate.

The hardware for the FRAM system in the upgraded ROBOCAL environment is shown in Fig. XIV-1. Figure XIV-2 shows the system inside the ROBOCAL work envelope with a sample about to be placed on the sample table.



Fig. XIV-1. The hardware for the IIU at the Los Alamos Plutonium Facility is shown before its installation.

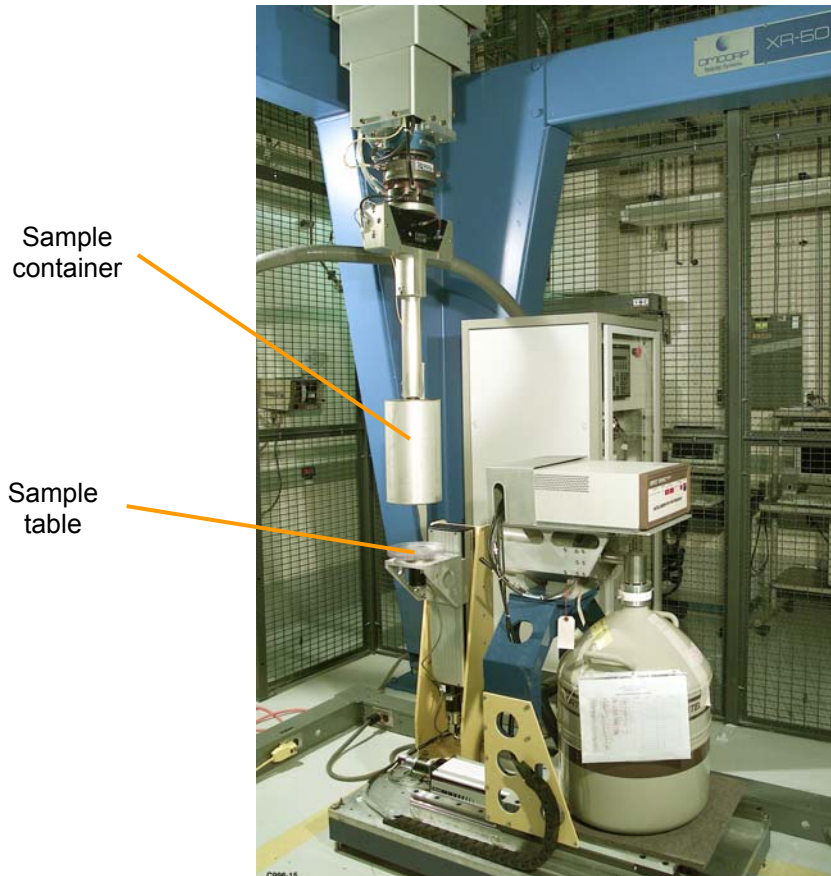


*Fig. XIV-2. The ROBOCAL robot is about to place a container on the sample table of the IIU at the Los Alamos Plutonium Facility.*

#### **B. ARIES NDA System**

ARIES (Advanced Retirement and Integrated Extraction System) is a series of processes designed to extract plutonium metal from retired weapons components, convert it to plutonium oxide, and package it for long-term storage, disposition, or feed for MOX fuel fabrication. The ARIES NDA system consists of three NDA instruments and a robot, under central host-computer control, that nondestructively quantify the plutonium mass in the containers of oxide produced by the ARIES processes. The three NDA instruments are a heat flow calorimeter, an active-passive neutron multiplicity counter, and a FRAM gamma-ray isotopic analysis system.

The FRAM gamma-ray isotopic analysis system is similar in concept and execution to the ROBOCAL system previously described. The experience from ROBOCAL in the area of robotics and host computer-instrument-robot communications has been invaluable in the development of the ARIES NDA system. One major departure from ROBOCAL is that the overall ARIES NDA system was designed for glove box operations. While this requirement is no longer applicable, the original design requirement is responsible for the glove box size and configuration of the NDA system pictured in Fig. XIV-3. A close-up of the FRAM detector is seen in Fig. XIV-4.

#### XIV. FRAM APPLICATIONS IN AUTOMATED SYSTEMS

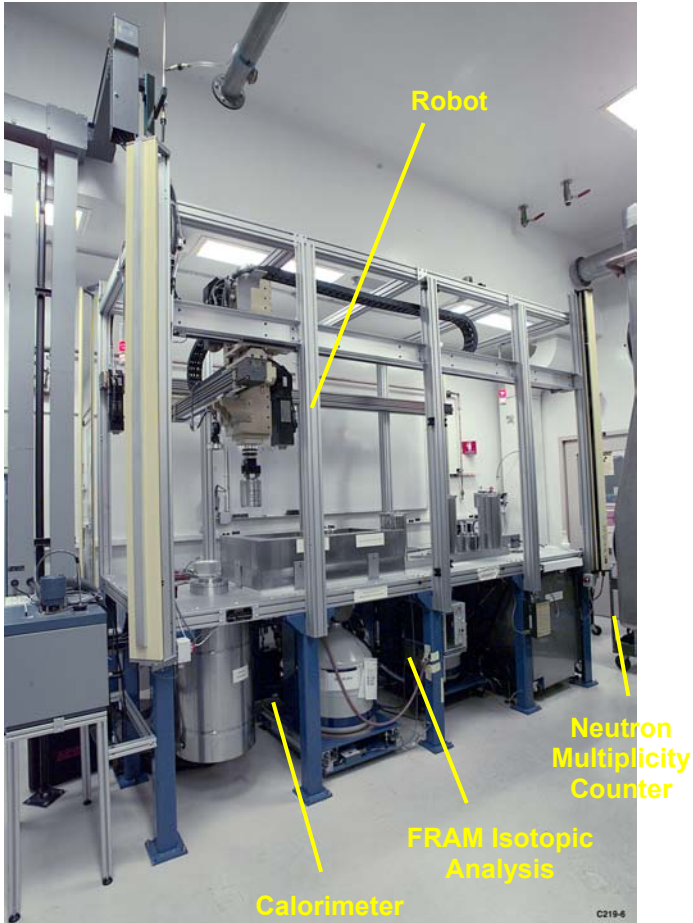


Fig. XIV-3. The ARIES NDA system installed at the Los Alamos Plutonium Facility.

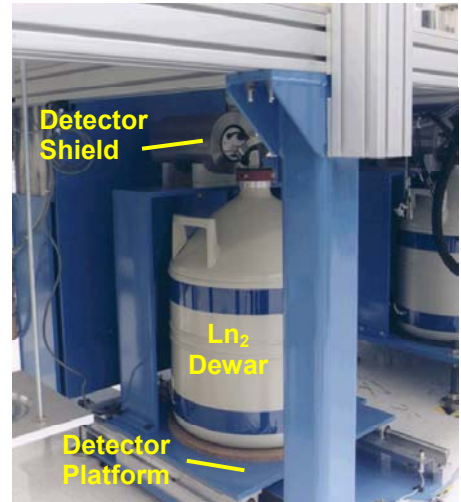


Fig. XIV-4. A closeup of the FRAM isotopic analysis station in the ARIES NDA system.

The FRAM system in ARIES uses a 25-mm-diam. by 16-mm-thick planar HPGe detector and collects and analyzes data in the 120–420 keV region. Several standards have been fabricated for use in the calibration and measurement control for the instruments in the ARIES NDA system. The characteristics of the ARIES NDA standards are displayed in Table F-4 in Appendix F. Some measurement results for FRAM analysis of data from these standards are shown in Table XIV-1.

Table XIV-1 displays the results of several sets of repeated measurements on the standards characterized in Table XIV-1. Each entry (row) shows the unweighted average (over the No. Meas.) of the Measured/Accepted value for the displayed parameter. The obs % RSD is obtained from the distribution of individual repeated measurements and is an estimate of the standard deviation of a single measurement arising from counting statistics. All measurements were for one hour.

Personnel at Los Alamos are continuing to refine this system, and they plan to test other measurement regimes using different detector types and different energy regions for analysis. The data displayed and discussed in chapter IX indicate that other detector-energy region combinations may offer improved precision over the results in Table XIV-1.

**XIV. FRAM APPLICATIONS IN AUTOMATED SYSTEMS**

Table XIV-1. Results from FRAM Analysis of Spectra from ARIES NDA Standards.

Ratio = Average Measured/Accepted (<sup>242</sup>Pu by Operator Entry)

Sample	No. Meas	Pu238		Pu239		Pu240		Pu241		Am241		Peff		eff Pu240	obs %rsd
		obs %rsd	obs %rsd												
Calex	15	1.0106	11.1	0.9997	0.11	1.0041	1.83	1.0110	0.36	1.0193	0.77	1.0028	0.30	1.0041	1.81
Calex	15	0.9691	13.2	0.9999	0.17	0.9969	2.71	1.0048	0.38	0.9985	0.46	0.9987	0.45	1.0039	2.67
Calex	5	1.0288	8.5	0.9999	0.09	1.0023	1.37	1.0044	0.33	0.9935	0.62	1.0001	0.18	1.0023	1.34
<b>Avg Calex</b>		<b>1.0028</b>		<b>0.9998</b>		<b>1.0011</b>		<b>1.0067</b>		<b>1.0037</b>		<b>1.0005</b>		<b>1.0034</b>	
MC005	15	0.9691	7.76	1.0005	0.14	0.9917	2.26	0.9943	0.32	1.0230	1.47	0.9994	0.30	0.9917	2.20
MC005	5	1.0072	6.50	0.9994	0.16	1.0092	2.50	0.9895	0.48	0.9903	1.14	1.0008	0.36	1.0091	2.44
MC005	5	1.0199	3.51	1.0000	0.12	0.9997	1.96	0.9899	0.32	0.9920	1.11	1.0001	0.22	0.9999	1.91
MC005	5	1.0627	5.60	0.9998	0.10	1.0029	1.55	0.9916	0.14	0.9921	1.35	1.0018	0.29	1.0033	1.51
MC004	13	1.0064	7.20	0.9996	0.13	1.0057	2.07	0.9882	0.30	0.9841	1.20	1.0000	0.32	1.0059	2.02
MC004	20	1.0424	10.40	1.0000	0.10	0.9997	1.64	0.9893	0.32	0.9897	1.54	1.0006	0.33	1.0000	1.59
MC003	14	1.0167	7.79	0.9999	0.17	1.0022	2.67	0.9874	0.43	0.9845	1.15	0.9998	0.49	1.0023	2.64
MC003	14	0.9921	7.50	0.9995	0.11	1.0076	1.67	0.9905	0.38	0.9865	1.20	0.9999	0.29	1.0075	1.63
<b>Avg all MC</b>		<b>1.0146</b>		<b>0.9999</b>		<b>1.0023</b>		<b>0.9901</b>		<b>0.9928</b>		<b>1.0003</b>		<b>1.0025</b>	

## REFERENCES

- ASTM 00 "Standard Test Method for Nondestructive Assay of Plutonium, Tritium and  $^{241}\text{Am}$  by Calorimetric Assay," ASTM C 1458-00 (American Society of Testing and Materials, West Conshohocken, PA, 2000).
- Banham 83 Banham, M. F. and Jones R., *Int. J. Appl. Radiat. Isot.* **34**, 1225 (1983).
- Bignan 95 Bignan, G., H. Recroix, B. Mitterrand, W. Ruhter, "Recommendations for the  $^{242}\text{Pu}$  Content Evaluation Using a New Algorithm," *Fifth International Conference on Facility Operation Safeguards Interface* (American Nuclear Society, LaGrange Park, Illinois, 1995), p. 225.
- Bonner 01 Bonner, Charles A., James M. Pecos, and Brian Kast, "RoboCal—An Automated NDA System," Los Alamos National Laboratory report LA-UR-01-6552 (2001). *Eight Environmental Management Nondestructive Assay Characterization Conference* (Denver, Colorado, December 11-13, 2001).
- Bracken 02 Bracken, D. S., R. S. Biddle, L. Carrillo, P. Hypes, C. R. Rudy, C. M. Schneider, and M. K. Smith, "Application Guide to Safeguards Calorimetry," Los Alamos National Laboratory report LA-13867-MS (January 2002).
- Canberra 02 <http://www.canberra.com>
- Ensslin 91a Ensslin, N., Chapter 11, "The Origin of Neutron Radiation," in *Passive Nondestructive Assay of Nuclear Materials*, Doug Reilly, Norbert Ensslin, and Hastings Smith, Jr., Eds. US Nuclear Regulatory Commission report NUREG/CR-5550 (March 1991).
- Ensslin 98 Ensslin, N., W. C. Harker, M. S. Krick, D. G. Langner, M. M. Pickrell, J. E. Stewart, "Application Guide to Neutron Multiplicity Counting," Los Alamos National Laboratory manual LA-13422-M (November 1998).
- Firestone 96 Firestone, R. B. , *Table of Isotopes, Eighth Edition* (John Wiley & Sons, Inc., New York, 1996.)
- Fleissner 81 Fleissner, J. G., "GRPAUT: A Computer Code for Automated Isotopic Analysis of Plutonium Spectra," *Journal of the Institute of Nuclear Materials Management*, **10**, 461–466 (1981).
- Fleissner 81a Fleissner, J. G., "GRPAUT: A Program for Pu Isotopic Analysis (A User's Guide)," Mound Facility report MLM-2799/ISPO-128 (1981).
- Fleissner 83 Fleissner, J. G., "Nondestructive Assay of Plutonium Isotopically Heterogeneous Salt Residues," in *Proceedings of the Conference on Safeguards Technology: The Process-Safeguards Interface* (Hilton Head Island, South Carolina, Nov. 28–Dec. 2, 1983) CONF-831106, pp. 275-285.
- Gunnink 71 Gunnink, R. and J. B. Niday, "Computerized Quantitative Analysis by Gamma-Ray Spectrometry," Lawrence Livermore Laboratory report UCRL-51061, Vol. 1 (1971).

- Gunnink 74 Gunnink, R., J. B. Niday, and P. D. Siemens, "A System for Plutonium Analysis by Gamma Ray Spectrometry, Part 1: Techniques for Analysis of Solutions," Lawrence Livermore Laboratory report UCRL-51577 Vol. 1 (April 1974).
- Gunnink 76 Gunnink, R., "An Algorithm for Fitting Lorentzian-Broadened, K-Series X-Ray Peaks of the Heavy Elements," Lawrence Livermore Laboratory report UCRL-78707 (1976).
- Gunnink 76a Gunnink, R., J. E. Evans, and A. L. Prindle, "A Reevaluation of the Gamma-Ray Energies and Absolute Branching Intensities of  $^{237}\text{U}$ ,  $^{238}$ ,  $^{239}$ ,  $^{240}$ ,  $^{241}\text{Pu}$ , and  $^{241}\text{Am}$ ," Lawrence Livermore Laboratory report UCRL-52139 (October 1976).
- Gunnink 80 Gunnink, R., "Use of Isotope Correlation Techniques to Determine  $^{242}\text{Pu}$  Abundance," *Nuclear Materials Management* **9** (2) (Summer 1980).
- Gunnink 81 Gunnink, R., A. L. Prindle, Y. Asakura, J. Masui, N. Ishiguro, A. Kawasaki, and S. Kataoka, "Evaluation of TASTEX Task H: Measurement of Plutonium Isotopic Abundances by Gamma-ray Spectrometry," Lawrence Livermore Laboratory report UCRL-52950/ISPO-111 (October 1981).
- Gunnink 81a Gunnink, R., "Plutonium Isotopic Analysis of Nondescript Samples by Gamma-Ray Spectrometry," *Conference on Analytical Chemistry in Energy Technology* (Gatlinburg, Tennessee, October 6–8, 1981) UCRL-86737.
- Gunnink 90 Gunnink, R., "MGA: A Gamma-Ray Spectrum Analysis Code for Determining Plutonium Isotopic Abundances, Volume I, Methods and Algorithms," Lawrence Livermore National Laboratory report UCRL-LR-103220, Vol. I/ISPO No. 317, Task No. A.161 (April 1990).
- Haas 74 Haas, F. X., "Plutonium Isotopic Measurements by Gamma-Ray Spectroscopy," in *Mound Laboratory Activities for the Division of Safeguards and Security: January-June 1974*, Mound Laboratory report MLM-2186 (December 1974).
- Harp 91 Harp, Faith J., "ROBOCAL: An Automated Assay System," Los Alamos National Laboratory report LALP-91-14, (1991).
- Hsue 80 Hsue, S.-T., T. E. Sampson, J. L. Parker, S. S. Johnson, and D. F. Bowersox, "Plutonium Isotopic Composition by Gamma-Ray Spectroscopy," Los Alamos Scientific Laboratory report LA-8603-MS (November 1980).
- Hurd 89 Hurd, J. R., C. A. Bonner, C. A. Ostenak, P. F. Phelan, W. D. Powell, N. L. Scheer, D. N. Schneider, and H. C. Staley, "ROBOCAL: An Automated NDA Calorimetry and Gamma Isotopic System," Los Alamos National Laboratory report LA-UR-89-3837 (1989).
- Hypes 00 Hypes, Philip A., "Plutonium Source Isotopic Analysis With Up To 25 mm Pb Shielding Using the FRAM Isotopic Analysis Code," in *Proceedings of the Institute of Nuclear Material Management, 41st Annual Meeting* (New Orleans, Louisiana, July 16-20, 2000). Los Alamos National Laboratory report LA-UR-00-2511 (June 2000).
- Hypes 01 Hypes, Phillip, David J. Mercer, and Derek R. Dinwiddie, "Gamma Ray Isotopic Analysis of Plutonium Within Highly Attenuating Shipping Containers," in *Proceedings of the Institute of Nuclear Materials Management, 42nd INMM Annual Meeting* (July 16–18, 2001). (CD ROM)

- Hypes 02 Hypes, Philip A., "Analysis of Americium-Beryllium Neutron Source Composition Using the FRAM Code," in *Proceedings of the Institute of Nuclear Materials Management*, 43rd Annual Meeting (Orlando, Florida, June 23–27, 2002). Los Alamos National Laboratory report LA-UR-02-2529 (June 2002).
- Kelley 95 Kelley, T. A., T. E. Sampson, and D. DeLapp, "PC/FRAM: Algorithms for the Gamma-ray Spectrometry Measurement of Plutonium Isotopic Composition," *Fifth International Conference on Facility Operation Safeguards Interface* (American Nuclear Society, LaGrange Park, Illinois, 1995), p. 264.
- Kelley 97 Kelley, Thomas A., and Thomas E. Sampson, "Software User Manual, PC/FRAM, Version 2.2," Los Alamos National Laboratory report LA-UR-98-1657 (1998).
- Kelley 99 Kelley, Thomas A., Thomas E. Sampson, Ronald M. Keyser, and Timothy R. Twomey, "Recent Developments of LANL PC/FRAM Code," in *Proceedings of the Symposium on Safeguards and Nuclear Material Management*, 21st Annual Meeting (ESARDA, Seville, Spain, May 4-6, 1999).
- Kelley 02 Kelley, T. A., and T. E. Sampson, "Software User Manual, PC/FRAM, Version 4," Los Alamos National Laboratory report LA-UR-02-5268 (2002).
- Knoll 00 Knoll, Glenn F., *Radiation Detection and Measurement*, (John Wiley & Sons, New York, 2000).
- Likes 91a Likes, R., Chapter 21, "Principles of Calorimetric Assay," in "Passive Nondestructive Assay of Nuclear Materials," D. Reilly, N. Ensslin, and H. Smith, Jr., Eds., US Nuclear Regulatory Commission report NUREG/CR-5550 (March 1991a).
- Likes 91b Likes, R., Chapter 22, "Principles of Calorimetric Assay," in "Passive Nondestructive Assay of Nuclear Materials," D. Reilly, N. Ensslin, and H. Smith, Jr., Eds., US Nuclear Regulatory Commission report NUREG/CR-5550 (March 1991b).
- Longmire 90 Longmire, Victoria L., T. Cremers, W. Sedlacek, S. Long, A. Scarborough, and J. Hurd, "Isotopic Ratios and Effective Power Determined by Gamma-Ray Spectroscopy vs. Mass Spectroscopy for Molten Salt Extraction Residues," in *Proceedings of the 31st Annual Meeting of the Institute of Nuclear Materials Management* (Los Angeles, California, July 15-18, 1990) *Nuclear Materials Management* **19**, 378.
- Mercer 99 Mercer, D. J., G. R. Allen, M. C. Baker, S. E. Betts, R. J. Estep, D. K. Miko, H. Poths, T. H. Prettyman, C. D. Rael, T. E. Sampson, D. P. Taggart, and D. T. Vo, "PAN, TGS, and FRAM Measurements for the First Shipments to WIPP," *Nucl. Mater. Manage.* **28**, (1999). (CD-ROM)
- Mercer 02 Mercer, David, John Lestone, and Steve Hansen, *Application Note: Tomographic Gamma Scanner*, Los Alamos National Laboratory report LALP-02-217 (September 2002).
- Morel 91 Morel, J., C. Chauvenet, and ESARDA Working Group on Techniques and Standards for Non-Destructive Analysis, "Intercomparison of Plutonium Isotopic Composition Measurements by X- and Gamma-Ray Spectrometry, Results from the PIDIE Exercise," DAMRI Technical Note L.P.R.I. 91/278 – MARS (1991).

- Morel 98 Morel, J., C. Hill, M. Bickel, A. Alonso-Munoz, S. Napier, B. Thaurel, and ESARDS NDA-WG Members, report LPRI/98/23, DAMRI, Departement des Applications et de la Metrologie des Rayonnements Ionisants, Laboratoire Primaire des Rayonnements Ionisants, France, 1998.
- Morel 00 Morel, J., C. Hill, M. Bickel, A. Alonso-Munoz, S. Napier, B. Thaurel, and ESARDA NDA – WG Members, "Results From the International Evaluation Exercise for Uranium Enrichment Measurements," *Appl. Radiat. Isot.* **52**, 509–522 (2000).
- ORTEC 02 <http://www.ortec-online.com>
- Parker 74 Parker, J. L., and T. D. Reilly, "Plutonium Isotopic Determination by Gamma-Ray Spectroscopy," in "Nuclear Analysis Research and Development Program Status Report, January-April 1974," G. Robert Keepin, Ed. Los Alamos Scientific Laboratory report LA-5675-PR (August 1974).
- Parker 88 Parker, J. L., and M. Brooks, "Accurate, Wide-Range Uranium Enrichment Measurements by Gamma-Ray Spectroscopy. I. Characterization of Enrichment Standards, II. Demonstration of Enrichment Measurement Capability," Los Alamos National Laboratory report LA-11277-MS (September 1988).
- Parker 91 Parker, Jack L., Chapter 6, "Attenuation Correction Procedures," in *Passive Nondestructive Assay of Nuclear Materials*, Doug Reilly, Norbert Ensslin, and Hastings Smith, Jr., Eds. US Nuclear Regulatory Commission report NUREG/CR-5550 (March 1991).
- Parker 91a Parker, J. L., "General Topics in Passive Gamma-Ray Assay," in "Passive Nondestructive Assay of Nuclear Materials," D. Reilly, N. Ensslin, and H. Smith, Jr., Eds., US Nuclear Regulatory Commission report NUREG/CR-5550 (March 1991).
- Prettyman 93 Prettyman, T.H., R.J. Estep, and G.A. Sheppard, "Development of a Tomographic Instrument for Nondestructive Assay," *Transactions of the American Nuclear Society* **69**, 183–184 (1993).
- Reilly 91 *Passive Nondestructive Assay of Nuclear Materials*, D. Reilly, N. Ensslin, and H. Smith, Jr., Eds. US Nuclear Regulatory Commission report NUREG/CR-5550 (March 1991), Chapters 11–17.
- Reilly 91a *Passive Nondestructive Assay of Nuclear Materials*, Doug Reilly, Norbert Ensslin, and Hastings Smith, Jr., Eds. US Nuclear Regulatory Commission report NUREG/CR-5550, (March 1991), pp. 120-130.
- Ruhter 84 Ruhter, W. D., "A Portable Microcomputer for the Analysis of Plutonium Gamma-Ray Spectra, Vol. I. Data Analysis Methodology and Hardware Description," Lawrence Livermore National Laboratory report UCRL-53506, Vol.-I/ISPO-209 (1984).
- Sampson 72 Sampson, T. E., "Precision Measurement of Gamma Ray Energies from 238U Daughters," *Nucl. Instr. Meth.* **98**, 37 (1972).
- Sampson 80 Sampson, T. E., S. Johnson, and K. Kroncke, "242Pu Isotopic Verification," Los Alamos Scientific Laboratory report LA-8372-MS (May 1980).

- Sampson 80a Sampson, T. E., S. Johnson, and K. Kroncke, "242Pu Isotopic Verification," Los Alamos Scientific Laboratory report LA-8603-MS (November 1980).
- Sampson 82 Sampson, Thomas E., Sin-Tao Hsue, Jack L. Parker, Sue S. Johnson, and D. F. Bowersox, "The Determination of Plutonium Isotopic Composition by Gamma-Ray Spectroscopy," *Nucl. Instrum. Methods* **193**, 177 (1982).
- Sampson 83 Sampson, T. E., S.-T. Hsue, E. L. Sandford, J. L. Parker, D. F. Bowersox, K. Kroncke, S. S. Johnson, and G. Walton, "In Plant Experience with Automated Gamma-Ray Spectroscopy Systems for Plutonium Isotopic Composition Measurements," Los Alamos National Laboratory report LA-9789-MS (August 1983).
- Sampson 86 Sampson, T. E., J. L. Parker, "Equations for Plutonium and Americium-241 Decay Corrections," Los Alamos National Laboratory report LA-10733 (June 1986).
- Sampson 89 Sampson, Thomas E., George W. Nelson, and Thomas A. Kelley, "FRAM: A Versatile Code for Analyzing the Isotopic Composition of Plutonium from Gamma-Ray Pulse Height Spectra," Los Alamos National Laboratory report LA-11720-MS (December 1989).
- Sampson 90 Sampson, Thomas E., George W. Nelson, and Thomas A. Kelley, "FRAM: A New, Versatile Gamma-Ray Spectrometry Code for Measuring the Isotopic Composition of Plutonium," *Nucl. Matl. Mgt.* **19**, 402 (1990).
- Sampson 95 Sampson, T. E., T. A. Kelley, T. L. Cremers, T. R. Konkel, and R. J. Friar, "PC/FRAM: New Capabilities for the Gamma-Ray Spectrometry Measurement of Plutonium Isotopic Composition," *Fifth International Conference on Facility Operation Safeguards Interface* (American Nuclear Society, LaGrange Park, Illinois, 1995), p. 256.
- Sampson 97 Sampson, T. E., T. A. Kelley, K. E. Kroncke, H. O. Menlove, J. Baca, T. Asano, S. Terakado, Y. Goto, N. Kogawa, "Delivery and Installation of PC/FRAM at the PNC Tokai Works," Los Alamos National Laboratory report LA-13360-MS (November 1997).
- Sampson 99 Sampson, T. E., T. A. Kelley, and D. T. Vo, "Improvements in the PC/FRAM Isotopic Analysis Software," *Sixth International Conference on Facility Operations Safeguards Interface* (American Nuclear Society, LaGrange Park, Illinois, 1999) pp. 206–211.
- Sampson 99a Sampson, Thomas E., and Thomas A. Kelley, "Software User Manual, PC/FRAM Version 3.2," Los Alamos National Laboratory report LA-UR-99-998 (1999).
- Sampson 99b Sampson, T. E., "PC/FRAM Technical Note: Measurement of MOX With PC/FRAM," Los Alamos National Laboratory report LA-UR-99-2377 (1999).
- Sampson 99c Sampson, T. E., G. P. D. Verrecchia, M. T. Swinhoe, P. Schwalbach, J. Gustafsson, A. M. Anderson, J. Myatt, and B. Metcalfe, "Test and Evaluation of the FRAM Isotopic Analysis Code for EURATOM Applications," in *Proceedings of the 40th Annual Meeting of the Institute of Nuclear Materials Management* (Phoenix, AZ, July 25–29, 1999). *Nucl. Mater. Manage.* **28** (1999). (CD-ROM)
- Sampson 01 Sampson, Thomas E., Philip A. Hypes, and Duc T. Vo, "FRAM Isotopic Analysis of Uranium in Thick-Walled Containers Using High Energy Gamma Rays and

- Planar HPGe Detectors," Los Alamos National Laboratory report LA-13832/ISPO-463 (September 2001).
- Sampson 01a Sampson, T. E., D. T. Vo, T. L. Cremers, P. A. Hypes, Y. P. Seldiakov, A. B. Dorin, M. V. Kondrashov, and V. I. Timoshin, "LANL/Green Star Tests of the Green Star SBS-60 Spectrometer," Los Alamos National Laboratory report LA-13778-MS (April 2001).
- Smith 91 Smith, Jr., Hastings A., Chapter 7, *The Measurement of Uranium Enrichment*," in *Passive Nondestructive Assay of Nuclear Materials*, Doug Reilly, Norbert Ensslin, and Hastings Smith, Jr., Eds. (US Nuclear Regulatory Commission NUREG/CR-5550, March 1991).
- Vo 98 Vo, D. T., P. A. Russo, and T. E. Sampson, "Comparisons Between Digital Gamma-Ray Spectrometer (DSPec) and Standard Nuclear Instrumentation Methods (NIM) Systems," Los Alamos National Laboratory report LA-13393-MS (March 1998).
- Vo 99 Vo, D. T., J. S. Hansen, and T. K. Li, "Plutonium Isotopic Analysis Using Low-Energy Gamma-Ray Spectroscopy," in *Proceedings of the Sixth International Conference on Facility Operations—Safeguards Interface* (American Nuclear Society, Jackson Hole, Wyoming, September 20-24, 1999), pp. 173-178. Los Alamos National Laboratory report LA-UR-99-4890.
- Vo 99a Vo, D. T., and T. E. Sampson, "Uranium Isotopic Analysis with the FRAM Isotopic Analysis Code," Los Alamos National Laboratory report LA-13580 (May 1999).
- Vo 99b Vo, D. T., "Extended Evaluations of the Commercial Spectrometer Systems for Safeguards Applications," Los Alamos National Laboratory report LA-13604-MS (August 1999).
- Vo 99c Vo, D. T., P. A. Russo, and T. E. Sampson, "Comparisons of the DSPEC and DSPEC Plus Spectrometer systems," Los Alamos National Laboratory report LA-13671-MS (November 1999).
- Vo 01 Vo, D. T., and T. K. Li, "Plutonium Isotopic Analysis with FRAM v4 in the Los Energy Region," in *Proceedings of the Institute of Nuclear Materials Management, 42nd Annual Meeting*, (Indian Wells, California, July 15-19, 2001). Los Alamos National Laboratory report LA-UR-01-3538.
- Vo 01a Vo, D. T., and T. K. Li, "Plutonium Isotopic Analysis in the 30 keV to 210 keV Range," *23rd Annual Meeting, Symposium on Safeguards and Nuclear Material Management* (Bruges, Belgium, May 8–10, 2001). Los Alamos National Laboratory report LA-UR-01-2264.
- Vo 02 Vo, D. T., and P. A. Russo, "PC/FRAM Plutonium Isotopic Analysis of CdTe Gamma-Ray Spectra," *Nucl. Instr. Meth. A* **486**, 813–824 (2002).
- Vo 02a Vo, D. T., and P. A. Russo, "Comparisons of the Portable Digital Spectrometer Systems," Los Alamos National Laboratory report LA-13895-MS (February 2002).

## **APPENDIX A**

### **PC/FRAM Technical Note**

#### **Measurement Of Mox With PC/FRAM**

### **INTRODUCTION**

The measurement of the ratio of  $^{235}\text{U}/\text{Pu}$  in mixed uranium–plutonium oxides is an important problem for gamma-ray spectrometry measurements of the isotopic composition of plutonium. This problem is generally straightforward, as the most prominent gamma ray from  $^{235}\text{U}$  at 185.7 keV is usually easy to detect in the gamma-ray spectrum of MOX. This technical note will describe how this measurement is carried out in the PC/FRAM isotopic analysis software and will also describe some of the pitfalls and problems that can arise with the measurement. We will illustrate the performance of FRAM on several types of MOX samples and will describe how the user can “fine tune” FRAM for the particular type of MOX being measured. The note will illustrate the limits of this measurement with respect to the  $^{235}\text{U}/\text{Pu}$  ratio.

### **MEASUREMENT ASSUMPTIONS**

The principal assumption that is made when measuring MOX is one of homogeneity. The uranium and plutonium powders are assumed to be uniformly mixed and also assumed to have the same particle size.. Deviations from these assumptions will produce biases. Biases from these effects are not discussed in this note.

### **GAMMA-RAY MEASUREMENT CHARACTERISTICS OF $^{235}\text{U}$**

The PC/FRAM software can account for the major gamma rays from  $^{235}\text{U}$  when it is needed for isotopic ratio measurements or to account for interferences with plutonium gamma rays. The principal gamma rays from  $^{235}\text{U}$  and their use in PC/FRAM are tabulated in Table A-1.

The branching ratios are taken from Banham and Jones (Banham 83). Fixed to/Free refers to the condition that all of the  $^{235}\text{U}$  gamma-ray peak areas are determined by a ratio to the 185-keV peak, which accounts for branching fractions and relative-efficiency differences. We determine the  $^{235}\text{U}$  activity solely from the 185.7-keV peak. The interference regions refer to regions of the spectrum containing other gamma rays used in the MOX analysis.

Table A-1. U-235 Gamma Rays Used in PC/FRAM MOX Parameter File.

<b>Branching (keV)</b>	<b>Branching Fraction</b>	<b>Fixed to/Free</b>	<b>Purpose</b>
143.78	1.07 e-1	Fix to 185	Interference 141-148 keV
163.36	4.97 e-2	Fix to 185	Interference 160-164 keV
182.72	3.39 e-3	Fix to 185	Interference 185 keV
185.715	5.73 e-1	Free	U-235 activity
194.94	6.26 e-3	Fix to 185	Interference 195 keV
202.13	1.08 e-2	Fix to 185	Interference 203-208 keV
205.31	5.05 e-2	Fix to 185	Interference 203-208 keV

**FRAM MOX MEASUREMENTS**

FRAM has demonstrated the ability to analyze MOX measurements over a <sup>235</sup>U/Pu range from 0.005 to 35—a dynamic range of 7000. The measurement of the plutonium isotopic composition is very difficult at the high end of this range (above a ratio of approximately 10) because the <sup>235</sup>U gamma rays tend to overwhelm the plutonium gamma rays. Test spectra, taken with HPGe detectors, are included with the standard FRAM software distribution and give spectra with ratios from 0.01 to 35. Two parameter files are available for planar detector measurements over this wide range.

We have developed and tested a parameter file for coaxial detectors for analysis over the <sup>235</sup>U/Pu range from 0.005 to 8. An additional set of test spectra for coaxial detector MOX measurements has been developed for distribution with FRAM. The characteristics of these samples are shown in Table A-2.

Measurement results for a subset of these samples are presented in Table A-3. These measurements were made with a 28% relative-efficiency coaxial HPGe detector under the conditions given in Table A-2. The values in the table are the average of 12–15 one-hour measurements. The apparent bias in <sup>238</sup>Pu likely arises from contamination of the mass spectrometry measurement. Biases in the <sup>235</sup>U/Pu ratio can arise from several sources. A bias can arise from particle size differences between the uranium and plutonium powders. There is little the user can do about this. A bias can also arise in the <sup>235</sup>U/Pu ratio from the definition of the background regions around the 185.7-keV <sup>235</sup>U gamma-ray peak. The current parameter file for MOX measurements with a coaxial detector (MOXCoax3.pst) is set up as a compromise to measure over as wide a dynamic range of <sup>235</sup>U/Pu ratios as possible. For very low <sup>235</sup>U/Pu ratios one wants to set the background ROIs tightly around the 185-keV peak with the background ROI on the high side being between the 185-keV peak and the 188.2–189.3 keV <sup>239</sup>Pu peaks. For higher ratios it is probably better to move this background above the 189.3-keV peaks. Some portion of the biases from the analysis of the MOX test spectra arises from this compromise.

**APPENDIX A Measurement Of MOX With PC/FRAM**

Table A-2. PC/FRAM MOX Test Spectra.

File	Pu Declared Values (wt %)					ppm Am241	mW/gPu	wt % Pu240eff
	Pu238	Pu239	Pu240	Pu241	Pu242			
HUA 5062	0.0614	87.397	11.831	0.533	0.178	15864	4.7020	12.284
HUA5065	0.0613	87.399	11.831	0.531	0.178	16062	4.7244	12.284
HUA5069	0.0558	87.554	11.693	0.510	0.187	13960	4.4452	12.147
HUA 5301	0.0464	87.629	11.668	0.472	0.185	8180	3.7306	12.095
HUA 8971	0.0549	87.377	11.826	0.533	0.21	9431	3.9297	12.316
PUEU6	0.0137	93.852	5.864	0.204	0.0659	947	2.4186	6.009
PUEU5	0.0137	93.852	5.864	0.204	0.0659	947	2.4186	6.009
PUEU4	0.0137	93.852	5.864	0.204	0.0659	947	2.4186	6.009
9116	0.0209	91.934	7.766	0.226	0.053	10 000	3.5916	7.908
D051	1.029	65.972	24.34	4.753	3.906	49 460	14.652	33.495

File	Pu Mass	U Mass	U235	Ct. Rate	Ct. Time	Date	Note
	(g)	(g)	(%)				
HUA 5062	241.6	393.8	0.727	0.0118	30	1	8-Apr-99
HUA5065	304.9	438.8	0.769	0.0111	30	1	30-Apr-99
HUA5069	113.6	679.4	1.073	0.0642	30	1	28-Apr-99
HUA 5301	367.8	805.8	0.225	0.00495	30	1	5-May-99
HUA 8971	234.8	626	1.022	0.0272	31.5	1	20-Mar-99
PUEU6	1308	422	93.084	0.301	na	2	3-May-95 1
PUEU5	348	1352	93.084	3.61	na	2	4-May-95 1
PUEU4	174.5	1523	93.084	8.12	na	2	18-May-95 1
9116	54	445	29	2.39	na	0.5	na
D051	531	1864	48.5	1.70	na	0.38	na

<sup>1</sup>Strong low-energy attenuation from shipping container.

Table A-3 FRAM MOX Measurement Results

Sample	Ratio: Measured/Declared							
	Pu238	Pu239	Pu240	Pu241	Am241	mW/gPu	Pu240eff	U235/Pu
HUA 5301	0.957	1.0004	0.997	0.990	0.968	0.9886	0.9971	0.869
HUA 5062	0.971	1.0048	0.965	0.992	1.021	1.0012	0.9657	1.026
HUA 5065	0.979	1.0023	0.983	0.989	1.015	1.0019	0.9838	0.993
HUA 5069	0.983	0.9998	1.002	0.985	1.003	1.0001	1.002	0.970
HUA 8971	0.965	1.0000	1.000	0.983	1.014	1.0013	1.000	0.927

Analysis of the  $^{235}\text{U}/\text{Pu}$  ratio from HUA 5301 ( $^{235}\text{U}/\text{Pu} = 0.0049$ ) shows that the  $^{235}\text{U}$  is at the limit of detectability at this level for this sample. The statistical precision on the  $^{235}\text{U}/\text{Pu}$  ratio for a one-hour measurement is about 25% (1 relative standard deviation). The 185-keV region for three different  $^{235}\text{U}/\text{Pu}$  ratios is shown in Fig. A-1. You can infer the detectability limit from this figure as well as noting the possible problems in setting the optimum background ROIs. We suggest that the user tailor the 185 keV peak background ROIs specifically for the MOX material types being measured.

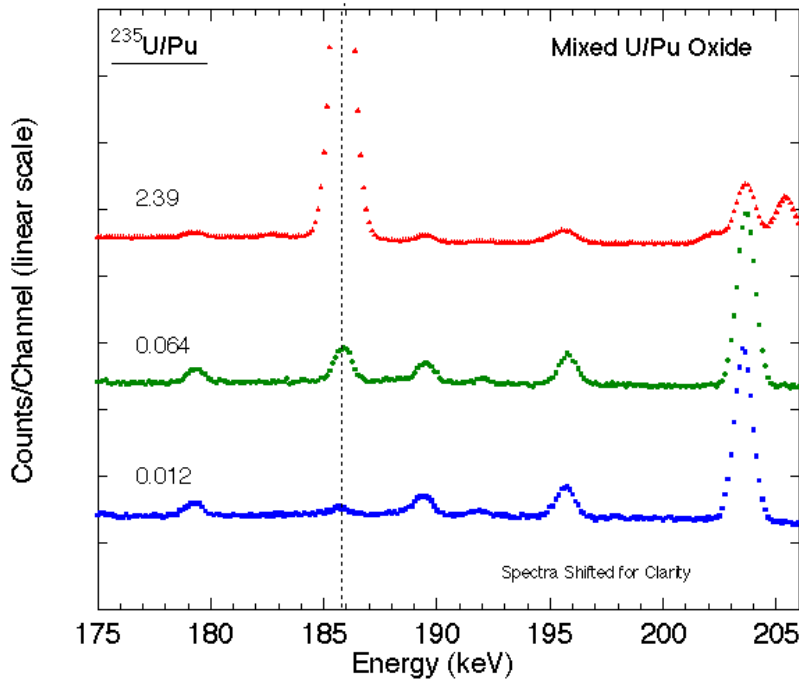


Fig.A-1. Spectra in the 185-keV region from MOX samples with varying  $^{235}\text{U}/\text{Pu}$  ratios.

## APPENDIX B

### PC/FRAM Technical Note

#### Considerations For The Use Of FRAM With Rate-Loss Correction Sources

#### INTRODUCTION

We describe the complications that can arise in a FRAM plutonium analysis when the spectrum is contaminated with gamma-ray peaks from an external rate-loss correction source. We describe two situations where FRAM has been asked to analyze spectra originally acquired for transmission-corrected passive assay [Segmented Gamma Scanner (SGS) or Tomographic Gamma Scanner (TGS)] purposes. We describe the methods used and compromises necessary to accommodate these measurements and also make some general recommendations and observations on this approach.

#### USE OF A <sup>109</sup>CD RATE-LOSS CORRECTION SOURCE

FRAM has been used to analyze plutonium gamma-ray spectra taken originally for TGS applications. The TGS used a <sup>109</sup>Cd source for rate-loss corrections required for that technique, with the <sup>109</sup>Cd source fixed to the end cap of the HPGe detector. The system also uses a cadmium metal filter between the detector and the measured sample to reduce the intensity of the 59.54-keV <sup>241</sup>Am peak present from plutonium-bearing samples. For the case at hand, the 1.5-mm-thick cadmium did not completely attenuate the 59.54-keV <sup>241</sup>Am gamma ray, so there was still a 59.54-keV americium photopeak in the spectrum.

Random summing between the 59.54-keV <sup>241</sup>Am peak and the 88.034-keV <sup>109</sup>Cd photopeak produces a sum peak around 147.6 keV. This sum peak interferes with the important 148.6-keV gamma ray from <sup>241</sup>Pu. The 148.6-keV gamma ray is the strongest and only measurable gamma ray arising directly from <sup>241</sup>Pu (not from a daughter) in the energy range above 120 keV and, as such, plays an important role in the plutonium isotopic analysis. If uncorrected, this sum peak interference would bias the 148.6-keV peak area.

#### SUM PEAK CORRECTION METHODS

##### Add Additional Filtering

The simplest way to solve this problem is to add more cadmium filtering to the detector to completely absorb the 59.54-keV <sup>241</sup>Am gamma ray. A filter of about 2 mm of cadmium will completely absorb the americium gamma ray for most samples. This solves the problem because there is no longer any gamma ray in the spectrum that can sum with 88 keV to produce an interference at 148 keV. At Los Alamos, we routinely use 2 mm of cadmium as a filter for all FRAM measurements.

##### Have FRAM Fit the Sum Peak

A less desirable method to make a first-order correction for this effect is to add a peak corresponding to the 147.6-keV sum peak to the Peak List in FRAM. Figure B-1 shows the region around 148 keV for a

sample of plutonium with 6%  $^{240}\text{Pu}$  and about 2000 ppm  $^{241}\text{Am}$ . An arrow marks the position of the random sum peak (not present in this picture) from  $^{241}\text{Am}$  and  $^{109}\text{Cd}$ .

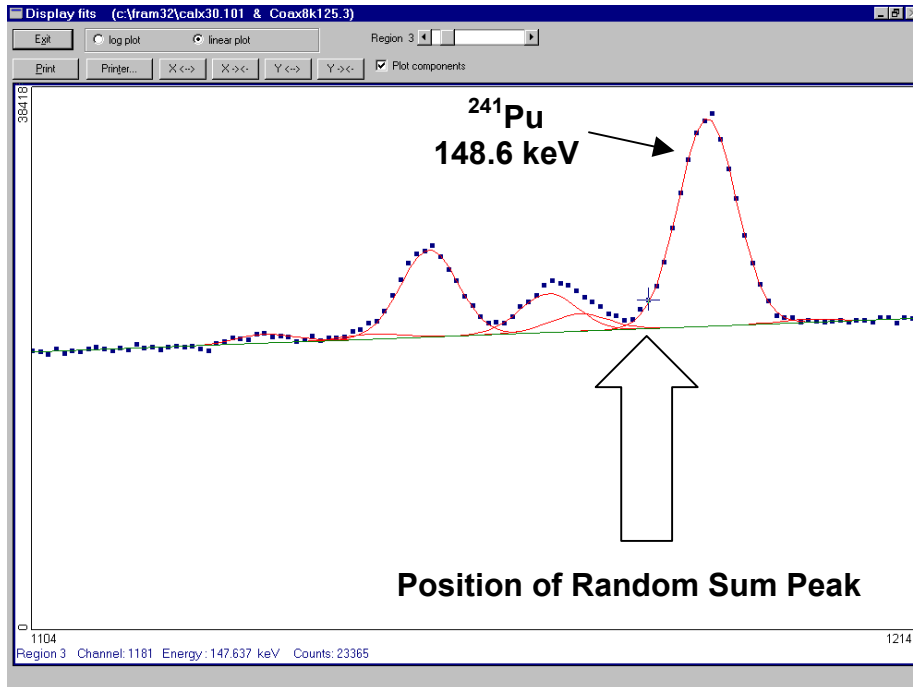


Fig.B-1. The 14- keV region from a low burnup sample of plutonium. The arrow indicates where the random summing peak should appear. No peak is present in this spectrum.

This is termed a first-order correction because sum peaks typically do not have a nice Gaussian shape. They usually tail off slowly on the low energy side of the sum peak because of the finite resolving time of the pileup rejector. This means that the fits may not be as good as they would be with a normal gamma-ray peak. This “fix” is, however, expected to make a reasonably good correction to the  $^{241}\text{Pu}$  peak area at 148.6 keV that is the principal peak of interest in the analysis.

### PROCEDURE TO ADD SUM PEAK TO PEAK LIST

Select **Edit** from the main menu. Then select **Parameters** from the drop down menu. Complete the User Validation screen according to the passwords on the system. Now you are in the Change Parameter Utility.

Select **File** from the Change Parameter Utility main menu. Then select **Open** from the drop down menu. Choose the parameter file to be modified. Select **Edit** from the Change Parameter Utility main menu. Then select **Peaks** from the drop down menu. Click the box at the left of the row for the 148.567-keV peak of  $^{241}\text{Pu}$ . Select **Insert a new row** from the window that will appear. An empty new row will be put into the peak list above the row for the 148-keV peak.

1. Leave the isotope name blank.
2. Fill in the peak energy as 147.57.
3. Fill in 0.00 for the branching ratio.
4. Set fix area to = 0.
5. Set sum area with = 0.
6. The remainder of the boxes are unchanged.

This section of the peak list should now look similar to that shown below in Fig. B-2.

	isotope	peak energy	line width	branching ratio	fix area to	sum area with	used for eff	used for act	used for ecal	used for fcal	used for scal
7	Pu239	141.657	0.00	3.20000e-007	9	0	<input type="checkbox"/>	<input type="checkbox"/>	<input type="checkbox"/>	<input type="checkbox"/>	<input type="checkbox"/>
8	Pu239	143.350	0.00	1.73000e-007	9	0	<input type="checkbox"/>	<input type="checkbox"/>	<input type="checkbox"/>	<input type="checkbox"/>	<input type="checkbox"/>
9	Pu239	144.211	0.00	2.84000e-006	0	0	<input type="checkbox"/>	<input checked="" type="checkbox"/>	<input type="checkbox"/>	<input type="checkbox"/>	<input type="checkbox"/>
10	Pu239	146.077	0.00	1.19000e-006	9	0	<input type="checkbox"/>	<input type="checkbox"/>	<input type="checkbox"/>	<input type="checkbox"/>	<input type="checkbox"/>
11	Am241	146.557	0.00	4.61000e-006	0	0	<input type="checkbox"/>	<input type="checkbox"/>	<input type="checkbox"/>	<input type="checkbox"/>	<input type="checkbox"/>
12		147.570	0.00	0.00000e+000	0	0	<input type="checkbox"/>	<input type="checkbox"/>	<input type="checkbox"/>	<input type="checkbox"/>	<input type="checkbox"/>
13	Pu241	148.567	0.00	1.83200e-006	0	0	<input checked="" type="checkbox"/>	<input checked="" type="checkbox"/>	<input checked="" type="checkbox"/>	<input checked="" type="checkbox"/>	<input type="checkbox"/>
14	Am241	150.110	0.00	7.20000e-007	11	0	<input type="checkbox"/>	<input type="checkbox"/>	<input type="checkbox"/>	<input type="checkbox"/>	<input type="checkbox"/>
15	Pu238	152.720	0.00	9.05000e-006	0	0	<input type="checkbox"/>	<input checked="" type="checkbox"/>	<input type="checkbox"/>	<input type="checkbox"/>	<input type="checkbox"/>

Fig. B-2. Row 12 has been added to account for the random sum peak. The peak is free in the fitting and no isotope has been assigned for the peak.

This process has allowed us to fit the random sum peak, if present, and remove its effect, to a first-order, from the fitting of the 148.6-keV <sup>241</sup>Pu peak area.

**USE OF A <sup>133</sup>BA RATE-LOSS CORRECTION SOURCE**

We have also been asked to perform a FRAM isotopic analysis on data from an SGS that used a <sup>133</sup>Ba source for its rate-loss correction source. Barium-133 has prominent gamma rays at 276.4, 302.9, 356.0, and 383.9 keV. A weaker, but still very visible, gamma-ray peak also occurs at 160.6 keV. This peak causes a direct interference (as opposed to a sum peak) in an already difficult area, the 160-keV region that contains contributions from three isotopes, including the only gamma ray (160.3 keV) from <sup>240</sup>Pu between the 100-keV region and the 640-keV region. This additional interference makes it very difficult to independently determine the <sup>240</sup>Pu contribution in this region. This region is shown in Fig. B-3 from a spectrum of a sample with 6% <sup>240</sup>Pu.

This specific problem posed a much greater difficulty than the illustration of Fig. B-3 would indicate because the data to be analyzed were taken at a conversion gain of 0.5 keV/ch, a factor of four higher than the 0.125 keV/ch illustrated above. The peaks were thus defined with one-fourth as many channels as in Fig. B-3. This was too coarse a spectrum to analyze accurately in this region. The <sup>133</sup>Ba interference peak was comparable in magnitude to the <sup>240</sup>Pu peak, causing even more difficulties.

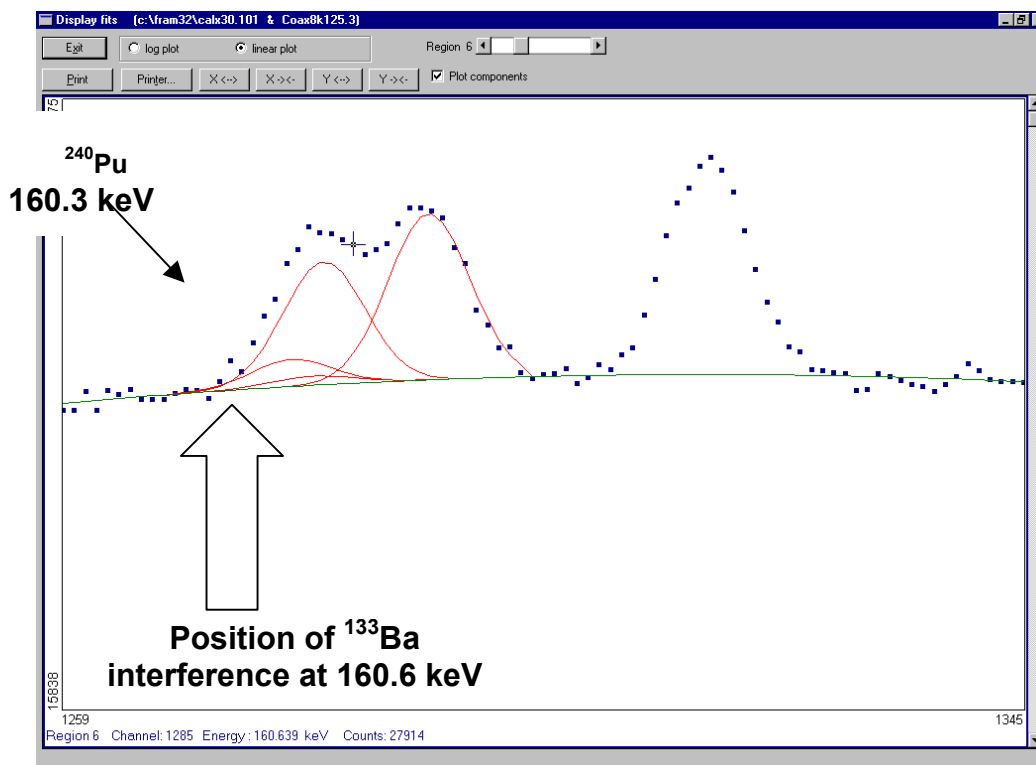


Fig. B-3. 160-keV region for a sample with 6%  $^{240}\text{Pu}$ . The large arrow shows where the  $^{133}\text{Ba}$  interference would fall. The component of the  $^{240}\text{Pu}$  peak at 160.3 keV is identified.

### Analysis Approach

The spectra were analyzed in the normal manner, including the  $^{133}\text{Ba}$  peak, as described above. We realized that the result for the  $^{240}\text{Pu}$  fraction reported by FRAM would not be accurate. However, the other isotopic ratios,  $\text{Pu}238/\text{Pu}239$ ,  $\text{Pu}241/\text{Pu}239$ , and  $\text{Am}241/\text{Pu}239$ , would not suffer this bias and their values were extracted from the results for these fundamental ratios displayed in the Medium Output. These ratios were combined with “acceptable knowledge” of the stream average values for  $^{240}\text{Pu}$  to extract a reasonable estimate of the entire isotopic distribution, within the limitations of the very coarse nature of the 0.5 keV/ch data.

### OBSERVATIONS AND RECOMMENDATIONS

A user will usually obtain inferior isotopic measurements from data taken with an instrument optimized for transmission-corrected passive assay (TCPA), i.e., SGS or TGS. The counting statistics are usually degraded compared to a dedicated isotopic system because of the collimation required for a TCPA. Counting statistics are also degraded, given the total TCPA measurement time, because isotopic data cannot be acquired during the transmission portion of the TCPA measurement. FRAM measurements are most always made without any collimation except for very hot samples measured in restricted geometries.

Detector resolution requirements are more demanding for isotopic analysis than they are for TCPA. Typical TCPA data resolution is usually poorer than that recommended for isotopic analysis, again producing an inferior isotopic result, although it is very difficult to quantify the degree of degradation of the isotopic results arising from poor detector resolution.

The advantages of this method are savings in hardware costs associated with the detector, data acquisition electronics (in some cases), and shielding and sample presentation fixtures. Reduced floor space requirements are often an additional important advantage. Reduced sample handling has the important benefit of lowering radiation exposure to the material handlers.

However, there are seldom throughput advantages to the combination measurement when samples are measured on a continuing basis. Exceptions to this can arise when instrument location gives rise to additional material movement and handling costs. Indeed, there are great flexibility advantages to be derived from separate, dedicated, isotopic analysis systems, as not all samples require both TCPA and isotopic analysis.

Much of the performance degradation could be recovered in a TCPA system designed with a second, additional detector dedicated to the isotopic measurement. This would enable the detector and collimation to be optimized for isotopic analysis while still minimizing material handling and movement costs, thereby reducing total hardware costs and minimizing facility floor space requirements. This type of system has not yet been built, to our knowledge.

Finally, we recommend a gain of less than 0.15 keV/ch for best plutonium isotopic analysis with a coaxial detector in the 120–450 keV energy range. The normal operating gain for FRAM in this energy range is 0.125 keV/ch, although we have used other gains as described above.

APPENDIX C

Parameter File Listings

Standard Parameter File for Plutonium Analysis, 120-450 keV

Below is the parameter file listing for Coax\_Widerange3, the standard parameter file for plutonium analysis in the 120–450 keV region using data from a coaxial detector and version 4 of FRAM. The parameter file is fully explained in the software user guide for version 4 of FRAM (Kelley 02). The text has been edited slightly for readability.

```
// fit information
name: Coax_Widerange3
desc: "Coax .125 kev/ch, HomoAm/Pu, Equ., 3-25% Pu240,<450 keV "
date: "2002.06.10 18:25"
ecal: 1.250000e-001 5.000000e-003
fix-ecal: N
fcgal: 1.500000e+001 1.800000e-001 2.000000e+003
fix-fcgal: N
scal: -4.200000e+000 3.000000e-003 2.700000e-001 0.000000e+000
fix-scal: Y

// peak information
num_peaks: 77
1 "Pu239" 124.490 0.000 6.000000e-007 0.000000e+000 0 0 N N N N N 2
2 "Pu239" 125.200 0.000 6.560000e-007 0.000000e+000 4 0 N N N N N 2
3 "Am241" 125.292 0.000 4.136000e-005 0.000000e+000 0 0 N Y N N N 2
4 "Pu239" 129.294 0.000 6.290000e-005 0.000000e+000 0 0 Y Y Y Y Y 1
5 "Pu239" 141.657 0.000 3.341000e-007 0.000000e+000 8 0 N N N N N 0
6 "Pu239" 143.350 0.000 1.806000e-007 0.000000e+000 8 0 N N N N N 4
7 "U235" 143.780 0.000 1.070000e-001 0.000000e+000 25 0 N N N N N 4
8 "Pu239" 144.211 0.000 2.888000e-006 0.000000e+000 0 0 N N N N N 4
9 "Pu239" 146.077 0.000 1.224000e-006 0.000000e+000 8 0 N N N N N 4
10 "Am241" 146.557 0.000 5.150000e-006 0.000000e+000 0 0 N N N N N 4
11 "Pu241" 148.567 0.000 1.894000e-006 0.000000e+000 0 0 Y Y Y Y N 4
12 "Am241" 150.113 0.000 7.570000e-007 0.000000e+000 0 0 N N N N N 4
13 "Pu238" 152.720 0.000 9.370000e-006 0.000000e+000 0 0 N Y N N N 5
14 "Pu241" 159.970 0.000 6.700000e-008 0.000000e+000 11 0 N N N N N 7
15 "Pu239" 160.180 0.000 5.768000e-008 0.000000e+000 17 0 N N N N N 7
16 "Pu240" 160.308 0.000 4.035000e-006 0.000000e+000 0 0 N Y N N N 7
17 "Pu239" 161.482 0.000 1.229000e-006 0.000000e+000 0 0 N Y N N N 7
18 "Am241" 161.540 0.000 1.900000e-008 0.000000e+000 3 0 N N N N N 7
19 "U235" 163.363 0.000 4.970000e-002 0.000000e+000 25 0 N N N N N 6
20 "Pu241" 164.597 0.000 4.663000e-007 0.000000e+000 0 0 Y Y Y Y Y 6
21 "Am241" 164.597 0.000 6.879000e-007 0.000000e+000 3 0 N N N N N 6
22 "Am241" 165.930 0.000 2.300000e-007 0.000000e+000 0 0 N N N N N 6
23 "Am241" 169.567 0.000 1.739000e-006 0.000000e+000 0 0 N Y N N N 8
24 "Pu239" 171.372 0.000 1.130000e-006 0.000000e+000 0 0 N Y N N N 8
25 "U235" 185.718 0.000 5.730000e-001 0.000000e+000 0 0 N Y N N N 3
26 "U235" 202.130 0.000 1.080000e-002 0.000000e+000 25 0 N N N N N 9
27 "Pu239" 203.545 0.000 5.727000e-006 0.000000e+000 0 0 Y Y N N N 9
28 "U235" 205.311 0.000 5.050000e-002 0.000000e+000 25 0 N N N N N 0
29 "Pu241" 208.000 0.000 5.392000e-006 0.000000e+000 0 0 Y Y Y Y Y 10
30 "Am241" 208.000 0.000 7.954000e-006 0.000000e+000 3 0 N N N N N 10
```

## APPENDIX C Parameter File Listings

```

31 "Am243" 209.750 0.000 3.420000e-002 0.000000e+000 34 0 N N N N N 10
32 "Am243" 226.360 0.000 2.800000e-003 0.000000e+000 34 0 N N N N N 11
33 "Am243" 227.810 0.000 5.100000e-003 0.000000e+000 34 0 N N N N N 11
34 "Am243" 228.160 0.000 1.076000e-001 0.000000e+000 0 0 N Y N N N 11
35 "Am243" 254.400 0.000 1.100000e-003 0.000000e+000 34 0 N N N N N 12
36 "Pu239" 255.380 0.000 7.987000e-007 0.000000e+000 0 0 Y Y N N N 12
37 "Pu239" 263.930 0.000 2.498000e-007 0.000000e+000 0 0 N N N N N 13
38 " " 264.850 0.000 0.000000e+000 0.000000e+000 0 0 N N N N N 13
39 "Pu239" 265.700 0.000 1.507000e-008 0.000000e+000 37 0 N N N N N 13
40 "Pu241" 267.540 0.000 1.786000e-007 0.000000e+000 0 0 Y Y Y N N 13
41 "Am241" 267.540 0.000 2.635000e-007 0.000000e+000 3 0 N N N N N 13
42 "Pu239" 311.700 0.000 2.617000e-007 0.000000e+000 58 0 N N N N N 14
43 "Np237" 311.900 0.000 3.860000e-001 0.000000e+000 0 0 N Y N N N 14
44 "Pu239" 319.828 0.000 4.545000e-008 0.000000e+000 0 0 N N N N N 15
45 "Pu239" 320.868 0.000 5.026000e-007 0.000000e+000 0 0 N N N N N 15
46 "Am241" 322.526 0.000 1.498000e-006 0.000000e+000 0 0 N Y N N N 15
47 "Pu239" 323.828 0.000 5.377000e-007 0.000000e+000 0 0 N N N N N 15
48 "Pu241" 332.387 0.000 2.974000e-007 0.000000e+000 0 0 N Y N N N 17
49 "Am241" 332.387 0.000 1.476000e-006 0.000000e+000 53 0 N N N N N 17
50 "Pu239" 332.850 0.000 4.940000e-006 0.000000e+000 58 0 N N N N N 17
51 "Am243" 334.310 0.000 2.070000e-002 0.000000e+000 34 0 N N N N N 17
52 "Pu241" 335.432 0.000 2.392000e-008 0.000000e+000 29 0 N N N N N 17
53 "Am241" 335.432 0.000 4.872000e-006 0.000000e+000 0 0 N Y N N N 17
54 "Pu239" 336.112 0.000 1.144000e-006 0.000000e+000 58 0 N N N N N 17
55 " " 337.720 0.000 0.000000e+000 0.000000e+000 0 0 N N N N N 17
56 " " 340.450 0.000 0.000000e+000 0.000000e+000 0 0 N N N N N 16
57 "Pu239" 341.495 0.000 6.603000e-007 0.000000e+000 58 0 N N N N N 16
58 "Pu239" 345.011 0.000 5.533000e-006 0.000000e+000 0 0 Y Y Y Y Y 16
59 "Pu239" 367.054 0.000 8.590000e-007 0.000000e+000 0 0 N N N N N 19
60 "Pu239" 368.534 0.000 8.992000e-007 0.000000e+000 66 0 N N N N N 19
61 "Pu241" 368.605 0.000 1.039000e-008 0.000000e+000 29 0 N N N N N 19
62 "Am241" 368.605 0.000 2.115000e-006 0.000000e+000 0 0 N Y N N N 19
63 "Pu241" 370.934 0.000 2.747000e-008 0.000000e+000 0 0 N N N N N 19
64 "Am241" 370.934 0.000 5.119000e-007 0.000000e+000 53 0 N N N N N 19
65 " " 372.450 0.000 0.000000e+000 0.000000e+000 0 0 N N N N N 19
66 "Pu239" 375.042 0.000 1.554000e-005 0.000000e+000 0 0 Y Y Y N N 18
67 "Np237" 375.300 0.000 6.790000e-003 0.000000e+000 43 0 N N N N N 18
68 "Am241" 376.610 0.000 1.520000e-006 0.000000e+000 0 0 N N N N N 18
69 "Pu239" 410.900 0.000 3.933000e-008 0.000000e+000 0 0 N N N N N 20
70 " " 412.000 0.000 0.000000e+000 0.000000e+000 0 0 N N N N N 20
71 "Pu239" 413.712 0.000 1.469000e-005 0.000000e+000 0 0 Y Y Y Y N 20
72 " " 414.800 0.000 0.000000e+000 0.000000e+000 0 0 N N N N N 20
73 "Np237" 415.731 0.000 1.745000e-002 0.000000e+000 43 0 N N N N N 20
74 " " 415.800 0.000 0.000000e+000 0.000000e+000 0 0 N N N N N 20
75 "Am241" 419.270 0.000 2.874000e-007 0.000000e+000 0 0 N N N N N 0
76 "Pu239" 451.474 0.000 1.898000e-006 0.000000e+000 0 0 Y Y Y Y Y 21
77 "Am241" 452.450 0.000 2.400000e-008 0.000000e+000 53 0 N N N N N 21

```

// region information

num regions: 21

```

1 127.600 131.000 127.100 127.700 131.000 131.600 131.800 132.400 0.000 0.000 6 "linear step"
2 124.200 126.500 126.600 127.100 127.100 127.700 0.000 0.000 0.000 0.000 2 "linear"
3 184.100 186.800 183.400 184.100 186.700 187.200 0.000 0.000 0.000 0.000 2 "linear"
4 142.700 150.900 138.100 139.200 151.000 151.400 0.000 0.000 0.000 0.000 2 "linear"
5 151.600 153.900 151.000 151.400 154.100 154.900 0.000 0.000 0.000 0.000 2 "linear"
6 162.800 166.700 162.500 163.100 166.900 167.800 0.000 0.000 0.000 0.000 2 "linear"
7 158.900 163.400 157.900 158.600 162.300 163.100 0.000 0.000 0.000 0.000 2 "linear"
8 168.500 172.700 167.700 168.300 173.000 173.600 0.000 0.000 0.000 0.000 2 "linear"
9 201.800 205.000 201.000 201.500 201.500 202.000 204.900 205.400 0.000 0.000 2 "linear"
10 205.900 211.500 205.100 205.700 211.700 212.400 212.700 213.400 0.000 0.000 6 "linear step"
11 226.300 229.300 223.100 223.900 229.600 230.400 0.000 0.000 0.000 0.000 2 "linear"
12 253.900 256.900 252.700 253.200 253.300 253.800 257.100 257.800 0.000 0.000 2 "linear"
13 262.600 269.500 261.900 262.600 269.600 270.200 270.400 270.900 0.000 0.000 6 "linear step"
14 310.100 313.700 309.200 309.700 313.900 314.400 0.000 0.000 0.000 0.000 2 "linear"
15 318.700 325.200 317.500 318.000 318.000 318.500 325.400 325.900 326.100 326.600 5 "flat step"
16 339.500 347.300 328.800 329.400 329.500 330.100 347.800 348.400 348.800 349.400 5 "flat step"
17 330.000 339.000 328.800 329.400 329.500 330.100 347.800 348.400 348.800 349.400 5 "flat step"

```

## APPENDIX C Parameter File Listings

---

```
18 373.000 378.000 363.800 364.400 364.500 365.100 385.500 386.100 386.200 386.800 5 "flat step"
19 365.300 372.900 363.800 364.400 364.500 365.100 385.500 386.100 386.200 386.800 5 "flat step"
20 409.200 417.200 404.000 404.600 404.900 405.500 432.200 432.800 433.000 433.600 5 "flat step"
21 449.000 453.500 448.200 448.800 455.900 456.500 0.000 0.000 0.000 0.000 5 "flat step"
```

```
// isotope information
```

```
num_isotopes: 9
```

```
1 "Pu239" 2.411900e+004 years 239.05220 1.92880 0.0000 1
2 "Pu241" 1.434800e+001 years 241.05690 3.41120 0.0000 1
3 "Am241" 4.336000e+002 years 241.05679 114.20000 0.0000 1
4 "Pu238" 8.774000e+001 years 238.04961 567.57000 2.5200 1
5 "Pu240" 6.564000e+003 years 240.05380 7.08240 1.0000 1
6 "Pu242" 3.763000e+005 years 242.05874 0.11590 1.6800 1
7 "Np237" 2.140000e+006 years 237.04817 0.00000 0.0000 1
8 "U235" 7.038100e+008 years 235.04390 0.00000 0.0000 1
9 "Am243" 7.370000e+003 years 243.06140 0.00000 0.0000 1
```

```
// appcon information
```

```
num_appcons: 65
```

```
1 "pu242_correlation" "1.1174"
2 "pu238_exponent" ".5"
3 "pu239_exponent" "-1.5"
4 "pu240_exponent" ".75"
5 "pu241_exponent" ".25"
6 "FRAM_SUMMARY_TYPE" "PLUTONIUM"
7 "num_ecal" "2"
8 "ecal_energy[1]" "208.00"
9 "ecal_channel[1]" "1664.00"
10 "ecal_limit[1]" "3.0"
11 "ecal_energy[2]" "662.456"
12 "ecal_channel[2]" "5299.40"
13 "ecal_limit[2]" "4.0"
14 "num_fwhmcal" "1"
15 "fcal_energy[1]" "413.714"
16 "fcal_limit[1]" "1500."
17 "num_tailfract" "1"
18 "scal_energy[1]" "413.714"
19 "scal_limit[1]" "5.0"
20 "num_intf" "1"
21 "intf_1st_energy[1]" "185.720"
22 "intf_2nd_energy[1]" "203.545"
23 "intf_limit[1]" "0.2"
24 "intf_msg[1]" "*** U235 TOO HIGH, USE MOXCOAX3 PARAMETER FILE ***"
25 "intf_1st_energy[2]" "228.140"
26 "intf_2nd_energy[2]" "203.545"
27 "intf_limit[2]" ".025"
28 "intf_msg[2]" "*** possible presence of Np239 ***"
29 "intf_1st_energy[3]" "311.887"
30 "intf_2nd_energy[3]" "345.011"
31 "intf_limit[3]" "2."
32 "intf_msg[3]" "*** possible presence of Np237 ***"
33 "num_samptype" "2"
34 "type_1st_peak[1]" "11"
35 "type_2nd_peak[1]" "20"
36 "type_lower_limit[1]" ".9"
37 "type_upper_limit[1]" "1.1"
38 "type_msg[1]" "Possible non-equilibrium or heterogeneous sample."
39 "type_1st_peak[2]" "3"
40 "type_2nd_peak[2]" "53"
```

## APPENDIX C Parameter File Listings

---

```
41 "type_lower_limit[2]" ".93"
42 "type_upper_limit[2]" "1.07"
43 "type_msg[2]" "Possible heterogeneous (Am/Pu) sample."
44 "fix_bad_bkg" "TRUE"
45 "AutoShieldTest" "yes"
46 "AutoShieldPass" "ShCoax_Widerange3"
47 "Shield_LowEnergy" "129.294"
48 "Shield_HighEnergy" "413.712"
49 "Shield_HighToLowLimit" "20"
50 "AutoHeteroTest" "yes"
51 "AutoHeteroPass" "Coax_HeteroAmPu3"
52 "Hetero_Energy[1]" "125.292"
53 "Hetero_Energy[2]" "335.422"
54 "Hetero_LowerLimit" ".9"
55 "Hetero_UpperLimit" "1.05"
56 "eff_use_dflts" "yes"
57 "eff_det_type" "1"
58 "eff_upu_min" "0.001"
59 "eff_upu_max" "20."
60 "eff_abs_name[1]" "Fe"
61 "eff_abs_min[1]" "0.10"
62 "eff_abs_max[1]" "6.0"
63 "eff_abs_name[2]" "Cd"
64 "eff_abs_min[2]" "0.20"
65 "eff_abs_max[2]" "3.0"
// end
```

**Standard Parameter File for Uranium Analysis**

Below is the parameter file listing for U121\_1001Coax, the standard parameter file for uranium analysis in the 120–1001 keV region using data from a coaxial detector and version 4 of FRAM. The parameter file is fully explained in the software user guide for version 4 of FRAM (Kelley 02). The text has been edited slightly for readability.

```
// fit information
name: U121_1001Coax
desc: " U Only, All Enrichments, 0.125 keV/ch, Coax Detector"
date: "2002.06.10 18:27"
ecal: 1.250000e-001 0.000000e+000
fix-ecal: N
fcal: 1.920000e+001 1.760000e-001 1.550000e+003
fix-fcal: N
scal: -4.870000e+000 3.840000e-003 1.530000e-001 0.000000e+000
fix-scal: Y
// peak information
num_peaks: 27
1 "U234" 120.905 0.000 3.390000e-004 0.000000e+000 0 0 N Y N N N 1
2 "U235" 140.760 0.000 2.620000e-003 0.000000e+000 0 0 N N N N N 2
3 "U235" 143.760 0.000 1.095000e-001 0.000000e+000 0 0 Y N Y Y Y 2
4 " " 145.940 0.000 0.000000e+000 0.000000e+000 0 0 N N N N N 2
5 "U235" 163.330 0.000 5.089000e-002 0.000000e+000 0 0 Y N Y Y Y 3
6 "U235" 182.610 0.000 4.024000e-003 0.000000e+000 0 0 N N N N N 4
7 "U235" 185.715 0.000 5.739000e-001 0.000000e+000 0 0 Y Y Y Y Y 4
8 "U235" 202.110 0.000 1.100000e-002 0.000000e+000 0 0 N N N N N 5
9 "U235" 205.311 0.000 4.993000e-002 0.000000e+000 0 0 Y N N N N 5
10 "Th228" 238.630 0.000 4.494000e-001 0.000000e+000 0 0 Y Y N N N 6
11 "U235" 240.870 0.000 6.984000e-004 0.000000e+000 0 0 N N N N N 6
12 "U238" 258.260 0.000 7.330000e-004 0.000000e+000 0 0 Y N N N N 7
13 "Th228" 583.190 0.000 2.944000e-001 0.000000e+000 0 0 Y Y N N N 8
14 "Th228" 727.300 0.000 6.577000e-002 0.000000e+000 0 0 Y Y N N N 9
15 "U238" 738.000 0.000 2.091000e-005 0.000000e+000 0 0 N N N N N 10
16 "U238" 739.950 0.000 1.165000e-004 0.000000e+000 0 0 N N N N N 10
17 "U238" 742.810 0.000 8.982000e-004 0.000000e+000 0 0 Y N N N N 10
18 "Th228" 763.300 0.000 6.380000e-003 0.000000e+000 0 0 N N N N N 11
19 "U238" 766.360 0.000 3.074000e-003 0.000000e+000 0 0 Y N Y Y Y 11
20 "Th228" 860.500 0.000 4.596000e-002 0.000000e+000 0 0 Y Y N N N 12
21 "U238" 880.450 0.000 2.119000e-004 0.000000e+000 0 0 Y N N N N 13
22 "U238" 883.220 0.000 2.121000e-004 0.000000e+000 0 0 Y N N N N 13
23 "U238" 941.940 0.000 2.851000e-005 0.000000e+000 0 0 N N N N N 14
24 "U238" 945.950 0.000 3.462000e-004 0.000000e+000 0 0 Y N N N N 14
25 "U238" 947.700 0.000 2.215000e-005 0.000000e+000 0 0 N N N N N 14
26 "U238" 994.940 0.000 5.656000e-005 0.000000e+000 0 0 N N N N N 15
27 "U238" 1001.030 0.000 8.371000e-003 0.000000e+000 0 0 Y Y Y Y Y 15

// region information
num_regions: 15
1 119.700 122.100 118.700 119.500 122.400 123.400 0.000 0.000 0.000 0.000 2 "linear"
2 139.200 147.000 136.800 137.700 137.900 139.000 147.100 148.200 148.500 149.600 6 "linear step"
3 160.800 165.000 158.400 159.700 159.800 161.000 166.300 167.400 167.800 169.000 6 "linear step"
4 181.200 187.500 177.000 178.500 180.000 181.000 189.100 190.500 190.800 192.000 7 "bilinear step"
5 198.100 207.000 197.500 198.000 200.000 200.500 207.000 208.000 211.000 212.000 6 "linear step"
6 237.500 242.000 231.000 232.000 243.000 244.000 0.000 0.000 0.000 0.000 2 "linear"
7 256.700 260.000 252.500 254.500 260.500 262.500 0.000 0.000 0.000 0.000 2 "linear"
8 581.000 585.000 579.000 580.000 586.000 587.000 0.000 0.000 0.000 0.000 2 "linear"
9 725.000 729.800 718.100 719.600 734.800 735.800 745.700 746.800 749.300 750.700 6 "linear step"
10 736.400 745.400 718.100 719.600 734.800 735.800 745.700 746.800 749.300 750.700 6 "linear step"
11 762.000 768.600 752.700 754.200 758.600 760.200 770.200 771.600 772.000 773.500 6 "linear step"
12 857.750 862.500 855.750 857.000 862.750 864.000 0.000 0.000 0.000 0.000 2 "linear"
```

## APPENDIX C Parameter File Listings

---

```
13 874.000 889.000 871.000 872.500 890.000 892.000 0.000 0.000 0.000 0.000 2 "linear"
14 940.000 949.000 938.000 939.500 954.000 956.000 0.000 0.000 0.000 0.000 2 "linear"
15 992.500 1006.000 987.000 988.500 990.000 991.500 1008.000 1010.000 1011.000 1013.000 6 "linear step"
```

```
// isotope information
num_isotopes: 5
1 "U238" 4.468300e+009 years 238.05078 0.00001 0.0000 1
2 "U235" 7.038100e+008 years 235.04393 0.00006 0.0000 1
3 "U234" 2.446000e+005 years 234.04090 0.18023 0.0000 1
4 "U236" 2.341500e+007 years 236.04556 0.00175 0.0000 1
5 "Th228" 1.913100e+000 years 228.02873 0.00000 0.0000 1
```

```
// appcon information
num_appcons: 31
1 "u236_correlation" "0.00472"
2 "u235_exponent" "0.925"
3 "u238_exponent" "0.075"
4 "FRAM_SUMMARY_TYPE" "URANIUM"
5 "num_ecal" "2"
6 "ecal_energy[1] (keV)" "185.718"
7 "ecal_channel[1]" "1486."
8 "ecal_limit[1] (channels)" "3.0"
9 "ecal_energy[2] (keV)" "1001.025"
10 "ecal_channel[2]" "8008."
11 "ecal_limit[2] (channels)" "5.0"
12 "num_fwhmcal" "2"
13 "fcal_energy[1] (keV)" "185.718"
14 "fcal_limit[1] (eV)" "1200.0"
15 "fcal_energy[2] (keV)" "1001.025"
16 "fcal_limit[2] (eV)" "2000.0"
17 "num_tailfract" "2"
18 "scal_energy[1] (keV)" "185.718"
19 "scal_limit[1] (percent)" "10.0"
20 "scal_energy[2] (keV)" "1001.025"
21 "scal_limit[2] (percent)" "20.0"
22 "eff_use_dflts" "yes"
23 "eff_det_type" "1"
24 "eff_upu_min" "0.01"
25 "eff_upu_max" "30."
26 "eff_abs_name[1]" "Fe"
27 "eff_abs_min[1]" "0.1"
28 "eff_abs_max[1]" "6.0"
29 "eff_abs_name[2]" "Cd"
30 "eff_abs_min[2]" "0.2"
31 "eff_abs_max[2]" "3.0"
// end
```

APPENDIX D

Plutonium and Americium Branching Ratios and Gamma-Ray Energies  
(Gunnink 76a)

Table D-1. Plutonium and Americium Branching Ratios and Gamma-Ray Energies.

Isotope	Energy (keV)	Branching Ratio (photons/dis)	Error (%)	Activity (photons/s/g)
237U	26.34	2.43E-02	0.5	2.28E+06
241Am	26.344	2.45E-02	0.1	3.10E+09
239Pu	30.040	2.170E-06	3	4.978E+03
241Am	32.183	1.74E-04	1	2.20E+07
237U	33.19	1.30E-03	1.6	1.22E+05
241Am	33.197	1.26E-03	0.3	1.59E+08
239Pu	38.664	1.050E-04	1.0	2.409E+05
239Pu	40.410	1.620E-06	10	3.717E+03
239Pu	42.060	1.650E-06	3	3.785E+03
237U	43.43	2.40E-04	7	2.25E+04
238Pu	43.477	3.930E-04	0.3	2.489E+08
241Pu	44.20	4.18E-08		1.60E+05
241Pu	44.86	8.36E-09		3.20E+04
240Pu	45.232	4.53E-04	0.2	3.80E+06
239Pu	46.210	7.370E-06	10	1.691E+04
239Pu	46.690	5.800E-07	6	1.331E+03
237U	51.005	3.40E-03	2	3.19E+05
239Pu	51.629	2.700E-04	0.2	6.194E+05
239Pu	54.040	2.000E-06	1.4	4.588E+03
241Pu	56.32	2.50E-08		9.56E+04
241Pu	56.76	9.75E-09		3.73E+04
239Pu	56.838	1.130E-05	1.0	2.592E+04
237U	59.536	3.45E-01	0.2	3.23E+07
241Am	59.536	3.59E-01		4.54E+10
237U	64.832	1.30E-02	0.5	1.22E+06
239Pu	65.741	4.530E-07	4	1.039E+03
239Pu	67.670	1.610E-06	2.0	3.694E+03
239Pu	68.720	5.100E-06	1	1.170E+04

**APPENDIX D Plutonium, Americium Branching Ratios and Gamma Ray Energies**

<b>Isotope</b>	<b>Energy (keV)</b>	<b>Branching Ratio (photons/dis)</b>	<b>Error (%)</b>	<b>Activity (photons/s/g)</b>
241Pu	71.6	2.86E-08	10	1.09E+05
241Pu	77.10	2.22E-07	3	8.49E+05
239Pu	77.607	3.900E-06	0.7	8.947E+03
239Pu	78.420	1.520E-06	1.4	3.487E+03
238Pu	94.658	1.050E-06	1.4	6.650E+05
240Pu	94.658	6.36E-07	5	5.34E+03
241Pu	94.658	3.03E-06	0.5	1.16E+07
239Pu	94.660	4.220E-05	0.25	9.681E+04
239Pu	96.130	2.230E-07	20	5.116E+02
237U	97.071	1.58E-01	0.4	1.48E+07
241Am	97.071	1.18E-05	2	1.49E+06
240Pu	98.442	1.02E-06	5	8.56E+03
239Pu	98.442	6.760E-05	0.3	1.551E+05
238Pu	98.442	1.690E-06	1.0	1.070E+06
241Pu	98.442	4.85E-06	0.5	1.85E+07
239Pu	98.780	1.220E-05	3	2.799E+04
241Am	98.951	2.03E-04	0.5	2.57E+07
238Pu	99.864	7.240E-05	0.2	4.585E+07
237U	101.066	2.52E-01	0.3	2.36E+07
241Am	101.066	1.90E-05	1.4	2.40E+06
241Am	102.966	1.95E-04	0.5	2.47E+07
239Pu	103.020	2.170E-06	1.6	4.978E+03
241Pu	103.680	1.01E-06	0.6	3.86E+06
240Pu	104.244	6.98E-05	0.4	5.86E+05
238Pu	110.421	2.000E-07		1.267E+05
239Pu	110.421	7.950E-06	0.8	1.824E+04
240Pu	110.421	1.18E-07		9.91E+02
241Pu	110.421	5.90E-07	1.5	2.26E+06
238Pu	111.300	3.900E-07		2.470E+05
239Pu	111.300	1.550E-05	0.6	3.556E+04
240Pu	111.300	2.30E-07		1.93E+03
241Pu	111.300	1.09E-06	1	4.17E+06
239Pu	111.890	3.070E-07	10	

**APPENDIX D Plutonium, Americium Branching Ratios and Gamma Ray Energies**

<b>Isotope</b>	<b>Energy (keV)</b>	<b>Branching Ratio (photons/dis)</b>	<b>Error (%)</b>	<b>Activity (photons/s/g)</b>
241Pu	111.89	3.31E-08		1.27E+05
237U	113.300	3.04E-02	0.5	2.85E+06
241Am	113.300	2.37E-06		3.00E+05
237U	114.230	5.85E-02	0.3	5.48E+06
241Am	114.230	4.72E-06		5.97E+05
238Pu	114.333			
239Pu	114.333	6.280E-06	2	1.441E+04
240Pu	114.333	9.32E-08		7.82E+02
241Pu	114.34	1.60E-07		6.12E+05
241Pu	114.56	3.64E-07		1.39E+06
238Pu	114.561	1.580E-07		1.001E+05
239Pu	114.561			
240Pu	114.561			
237U	114.950	3.35E-03	10	3.14E+05
241Am	114.950	2.30E-06		
239Pu	115.380	6.490E-06	1.5	1.489E+04
238Pu	115.400			
240Pu	115.40			
241Pu	115.40	1.34E-07		5.12E+05
239Pu	116.260	5.970E-06	1.5	1.370E+04
237U	117.340	7.90E-03		7.40E+05
241Am	117.340			
237U	117.580	1.56E-02		1.46E+06
241Am	117.580			
237U	118.43	8.23E-03		7.71E+05
241Am	118.43			
239Pu	119.708	3.000E-07	2	6.883E+02
241Pu	121.2	6.85E-09		2.62E+04
241Am	122.994	1.00E-05	0.8	1.27E+06
239Pu	123.620	1.970E-07	6	4.520E+02
239Pu	124.510	6.130E-07	3	1.406E+03
239Pu	125.210	7.110E-07	2	1.631E+03
241Am	125.292	4.08E-05	0.5	5.16E+06

**APPENDIX D Plutonium, Americium Branching Ratios and Gamma Ray Energies**

<b>Isotope</b>	<b>Energy (keV)</b>	<b>Branching Ratio (photons/dis)</b>	<b>Error (%)</b>	<b>Activity (photons/s/g)</b>
239Pu	129.294	6.260E-05	0.2	
241Am	139.53	5.34E-08	20	6.76E+03
239Pu	141.657	3.200E-07	2	7.341E+02
239Pu	143.350	1.730E-07	4	3.969E+02
239Pu	144.211	2.830E-06	0.6	6.493E+03
239Pu	146.077	1.190E-06	0.6	2.730E+03
241Am	146.557	4.61E-06	1	5.83E+05
241Pu	148.567	1.87E-06	0.3	7.15E+06
241Am	150.11	7.40E-07	2	9.36E+04
238Pu	152.680	9.560E-06	0.5	6.054E+06
239Pu	158.100		10	2.294E+01
241Pu	159.955	6.74E-08		2.58E+05
239Pu	160.190	6.200E-08	20	1.422E+02
240Pu	160.280	4.02E-06	0.7	3.37E+04
239Pu	161.450	1.200E-06	0.4	2.753E+03
237U	164.580	1.84E-02	0.5	1.72E+06
241Am	164.580	6.67E-07	3	8.44E+04
241Am	165.93	2.32E-07	4	2.94E+04
239Pu	167.810	2.930E-08	25	6.722E+01
241Am	169.557	1.73E-06	1	2.19E+05
239Pu	171.344	1.105E-06	0.8	2.535E+03
239Pu	173.700	3.050E-08	25	6.997E+01
241Am	175.09	1.82E-07	5	2.30E+04
239Pu	179.190	6.580E-07	1	1.510E+03
239Pu	184.550	2.120E-08	30	4.864E+01
239Pu	188.230	1.090E-07	10	2.501E+02
239Pu	189.320	8.300E-07	2	
241Am	190.40	2.19E-08	20	2.77E+03
241Am	191.90	2.16E-07	4	2.73E+04
239Pu	193.000	8.870E-08	10	2.035E+02
239Pu	195.660	1.064E-06	0.5	2.441E+03
239Pu	196.870	3.700E-08	12	8.489E+01
238Pu	200.980	4.080E-08	2	2.584E+04

**APPENDIX D Plutonium, Americium Branching Ratios and Gamma Ray Energies**

<b>Isotope</b>	<b>Energy (keV)</b>	<b>Branching Ratio (photons/dis)</b>	<b>Error (%)</b>	<b>Activity (photons/s/g)</b>
239Pu	203.537	5.600E-06	0.2	1.285E+04
241Am	203.87	2.90E-08	6	3.67E+03
237U	208.000	2.17E-01	0.2	2.03E+07
241Am	208.000	7.91E-06	0.5	1.00E+06
237U	221.73	2.12E-04	2	1.99E+04
241Am	221.73	4.24E-07	1	5.37E+04
239Pu	225.370		4	3.579E+02
241Am	233.87	4.64E-08	6	5.87E+03
237U	234.24	2.05E-04	2	1.92E+04
241Am	234.33	6.57E-09	40	8.31E+02
239Pu	237.380	1.440E-07	4	3.304E+02
239Pu	242.080	7.310E-08	7	1.677E+02
239Pu		2.530E-07	2	5.804E+02
239Pu	244.920	5.100E-08	10	1.170E+02
241Am	246.70	2.42E-08	10	3.06E+03
239Pu	248.950	7.240E-08	10	1.661E+02
239Pu	255.380	8.050E-07	2	1.847E+03
241Am	260.90	1.21E-08	15	1.53E+03
239Pu	263.930	2.610E-07	3	5.988E+02
241Am	264.85	9.04E-08	4	1.14E+04
239Pu	265.700	1.580E-08	25	3.625E+01
237U	267.54	7.40E-03	0.5	6.93E+05
241Am	267.54	2.63E-07	2	3.33E+04
241Am	271.58	6.37E-09	30	8.06E+02
241Am	275.68	6.57E-08	5	8.31E+03
239Pu	281.200	2.150E-08	15	4.933E+01
239Pu	285.300	1.910E-08		4.382E+01
241Am	291.21	3.08E-08	10	3.90E+03
241Am	292.78	1.42E-07	3	1.80E+04
239Pu	297.490	5.020E-07	2	1.152E+03
239Pu	302.870	5.130E-08	8	1.177E+02
241Am	304.23	1.01E-08	20	1.28E+03
239Pu	307.850	5.470E-08	7	1.255E+02

**APPENDIX D Plutonium, Americium Branching Ratios and Gamma Ray Energies**

<b>Isotope</b>	<b>Energy (keV)</b>	<b>Branching Ratio (photons/dis)</b>	<b>Error (%)</b>	<b>Activity (photons/s/g)</b>
239Pu	311.740	2.580E-07	2	5.919E+02
239Pu	316.410	1.360E-07	3	3.120E+02
239Pu	319.680	4.800E-08	10	1.101E+02
239Pu	320.880	5.360E-07	1	1.230E+03
241Am	322.503	1.518E-06	0.6	1.92E+05
239Pu	323.810	5.420E-07	1	1.243E+03
237U	332.354	1.21E-02	0.3	1.13E+06
241Am	332.354	1.490E-06	0.3	1.89E+05
239Pu	332.838	5.060E-06	0.2	1.161E+04
237U	335.405	9.70E-04	1.0	9.09E+04
241Am	335.405	4.960E-06	0.3	6.28E+05
239Pu	336.107	1.134E-06	0.3	2.602E+03
241Am	337.72	4.29E-08	5	5.43E+03
237U	337.75	8.90E-05	5	8.34E+03
237U	340.45	1.65E-05	20	1.55E+03
239Pu	341.510	6.620E-07	0.4	1.519E+03
239Pu	345.014	5.592E-06	0.2	1.283E+04
241Am	350.56	1.19E-08	20	1.51E+03
239Pu	350.800	1.750E-08	20	4.015E+01
239Pu	354.000	7.310E-09	40	1.677E+01
241Am	358.36	1.20E-08	20	
239Pu	361.890	1.220E-07	5	2.799E+02
239Pu	367.050	8.650E-07	0.3	1.984E+03
239Pu	368.550	9.030E-07	0.3	2.072E+03
237U	368.605	4.29E-04	2	
241Am	368.605	2.17E-06	0.3	2.75E+05
237U	370.934	1.103E-03	1.4	1.03E+05
241Am	370.934	5.23E-07	0.8	6.62E+04
239Pu	375.042	1.570E-05	0.1	3.602E+04
241Am	376.595	1.383E-06	0.7	1.75E+05
239Pu	380.166		0.2	7.000E+03
239Pu	382.751	2.587E-06	0.2	5.935E+03
241Am	383.74	2.82E-07		3.57E+04

**APPENDIX D Plutonium, Americium Branching Ratios and Gamma Ray Energies**

<b>Isotope</b>	<b>Energy (keV)</b>	<b>Branching Ratio (photons/dis)</b>	<b>Error (%)</b>	<b>Activity (photons/s/g)</b>
241Am	390.54	5.90E-08	4	7.47E+03
239Pu	392.530	5.527E-06	0.2	1.268E+04
239Pu	393.140			0.000E+00
239Pu	399.510	6.100E-08	4	1.399E+02
241Am	406.37	1.45E-08	15	1.84E+03
239Pu	406.900	6.350E-09	40	1.457E+01
239Pu	411.150		50	1.560E+02
239Pu	413.712	1.489E-05	0.1	3.416E+04
241Am	419.24	2.87E-07	2	3.63E+04
239Pu	422.586	1.193E-06	0.4	2.737E+03
241Am	426.39	2.46E-07	2	3.11E+04
239Pu	426.680	2.328E-07	1.5	5.341E+02
239Pu	428.400	1.000E-08	10	2.294E+01
241Am	429.84	1.15E-08	20	1.46E+03
239Pu	430.080	4.300E-08	3	
241Am	442.75	3.52E-08	7	4.45E+03
239Pu	445.720	8.700E-08	2	1.996E+02
239Pu	446.820	8.450E-09	15	1.939E+01
239Pu	451.474	1.890E-06	0.3	4.336E+03
241Am	452.21	2.40E-08	10	3.04E+03
241Am	454.62	9.70E-08	3	1.23E+04
239Pu	457.610	1.490E-08	1	3.418E+01
241Am	459.59	3.63E-08	7	4.59E+03
239Pu	461.250	2.270E-08	1	5.208E+01
239Pu	463.900	2.780E-09	10	
241Am	467.98	2.88E-08	7	3.64E+03
239Pu	473.900	5.360E-10	50	1.230E+00
239Pu	481.540	4.600E-08	0.6	1.055E+02
241Am	486.3	1.00E-08	30	1.27E+03
239Pu	487.060	2.650E-09	8.0	6.080E+00
239Pu	493.080	8.680E-09	3.0	1.991E+01
239Pu	497.000	4.610E-10	50	1.058E+00
241Am	514.2	2.58E-08	10	3.27E+03

**APPENDIX D Plutonium, Americium Branching Ratios and Gamma Ray Energies**

<b>Isotope</b>	<b>Energy (keV)</b>	<b>Branching Ratio (photons/dis)</b>	<b>Error (%)</b>	<b>Activity (photons/s/g)</b>
241Am	522.0	9.46E-09	30	1.20E+03
239Pu	526.400	5.720E-10	30	1.312E+00
239Pu	538.800	3.050E-09	6	6.997E+00
239Pu	550.500	4.220E-09	6	9.681E+00
239Pu	557.300	3.820E-10	50	8.764E-01
241Am	574.0	1.25E-08	15	1.58E+03
239Pu	579.400		20	1.968E+00
239Pu	582.890	6.150E-09	3	1.411E+01
239Pu	586.300	1.530E-09	10	3.510E+00
241Am	586.52	1.31E-08	15	1.66E+03
241Am	590.28	2.86E-08	7	3.62E+03
239Pu	596.000	3.900E-10	50	8.947E-01
241Am	597.42	7.41E-08	4	9.38E+03
239Pu	597.990	1.670E-08	3	3.831E+01
239Pu	599.600	1.990E-09	12	4.565E+00
239Pu	606.900	1.200E-09	10	2.753E+00
239Pu	608.900		10	2.661E+00
239Pu	612.830	9.460E-09	5	2.170E+01
239Pu	617.100	1.340E-08	5	3.074E+01
239Pu	618.280	2.040E-08	3	4.680E+01
241Am	619.00	5.94E-07	1	7.52E+04
239Pu	619.210	1.210E-08	6	2.776E+01
239Pu	624.780	4.570E-09	4	1.048E+01
241Am	627.2	5.64E-09	30	7.14E+02
241Am	633.0	1.26E-08	15	
239Pu	633.150	2.530E-08	1.2	5.804E+01
239Pu	637.837		1.2	5.873E+01
239Pu	640.075	8.200E-08	0.6	1.881E+02
241Am	641.42	7.10E-08	4	8.99E+03
240Pu	642.48	1.245E-07	1	1.05E+03
239Pu	645.969	1.489E-07	0.4	3.416E+02
239Pu	649.321	7.120E-09	7	1.633E+01
239Pu	650.529	2.700E-09	15	6.194E+00

**APPENDIX D Plutonium, Americium Branching Ratios and Gamma Ray Energies**

<b>Isotope</b>	<b>Energy (keV)</b>	<b>Branching Ratio (photons/dis)</b>	<b>Error (%)</b>	<b>Activity (photons/s/g)</b>
239Pu	652.074	6.550E-08	0.6	1.503E+02
241Am	652.96	3.77E-07	2	4.77E+04
239Pu	654.880	2.250E-08	1.2	5.162E+01
239Pu	658.929	9.690E-08	0.7	2.223E+02
241Am	662.420	3.64E-06	0.3	4.61E+05
239Pu	664.587	1.657E-08	1.6	3.801E+01
239Pu	668.200	3.930E-10	30	9.016E-01
241Am	669.9	3.80E-09	30	4.81E+02
239Pu	670.800	8.600E-11	50	1.973E-01
239Pu	674.050	5.150E-09	3	1.182E+01
241Am	675.8	6.40E-09	20	8.10E+02
241Am	680.06	3.13E-08	5	3.96E+03
239Pu	685.970	8.730E-09	3	2.003E+01
240Pu	687.7	3.55E-08	1.5	2.98E+02
239Pu	688.100	1.110E-09	10	
241Am	688.77	3.25E-07	1.5	4.11E+04
239Pu	690.810		5	1.278E+01
239Pu	693.200	5.000E-10	30	1.147E+00
241Am	693.49	3.68E-08	4	4.66E+03
241Am	696.44	5.34E-08	3	6.76E+03
239Pu	697.800	7.350E-10	20	1.686E+00
239Pu	699.600	7.910E-10	20	1.815E+00
239Pu	701.100	5.120E-09	3	1.175E+01
239Pu	703.730	3.950E-08	0.4	9.062E+01
238Pu	705.600	5.030E-10	40	
238Pu	708.400	5.000E-09	10	3.167E+03
241Am	709.41	6.41E-08	2	8.11E+03
239Pu	712.960	5.160E-10	12	1.184E+00
239Pu	714.710	7.850E-10	10	1.801E+00
239Pu	717.720	2.740E-08	0.4	6.286E+01
239Pu	720.300	4.850E-10	10	1.113E+00
241Am	721.990	1.96E-06	0.4	2.48E+05
239Pu	727.900	1.240E-09	5	2.845E+00

**APPENDIX D Plutonium, Americium Branching Ratios and Gamma Ray Energies**

<b>Isotope</b>	<b>Energy (keV)</b>	<b>Branching Ratio (photons/dis)</b>	<b>Error (%)</b>	<b>Activity (photons/s/g)</b>
241Am	729.52	1.33E-08	10	1.68E+03
241Am	731.5	4.70E-09	30	5.95E+02
239Pu	736.500		30	6.883E-01
241Am	737.29	8.00E-08	3	1.01E+04
239Pu	742.700	3.750E-10	30	8.603E-01
238Pu	742.820	5.170E-08	1	3.274E+04
239Pu	747.400	8.070E-10	20	1.851E+00
241Am	755.91	7.60E-08	3	9.62E+03
239Pu	756.400	3.470E-08	0.4	7.961E+01
241Am	759.46	1.67E-08	5	2.11E+03
241Am	763.4	1.96E-09	30	2.48E+02
239Pu	763.700	3.240E-10	50	7.433E-01
238Pu	766.410	2.190E-07	0.6	1.387E+05
239Pu	766.600	2.750E-09	5	6.309E+00
241Am	766.92	5.00E-08	3	6.33E+03
239Pu	769.370	1.120E-07	0.3	2.569E+02
241Am	770.58	4.74E-08	4	6.00E+03
241Am	772.13	2.66E-08	5	3.37E+03
239Pu	777.100	2.780E-10	25	6.378E-01
241Am	777.2	6.10E-10	50	7.72E+01
239Pu	779.610	1.360E-09	6	3.120E+00
241Am	780.5	2.50E-09	20	3.16E+02
238Pu	786.300	3.280E-08	1.0	2.077E+04
239Pu	786.900	8.610E-10	10	1.975E+00
239Pu	788.500	3.520E-10	20	8.076E-01
241Am	788.8	3.88E-09	15	4.91E+02
239Pu	792.900	2.000E-10	20	4.588E-01
239Pu	796.900	1.490E-10	20	3.418E-01
241Am	801.9	1.36E-08	10	1.72E+03
239Pu	803.200	6.370E-10	7	1.461E+00
238Pu	805.400	1.290E-09	15	8.170E+02
239Pu	805.900	2.760E-10	15	6.332E-01
238Pu	808.200	8.000E-09	3	5.066E+03

**APPENDIX D Plutonium, Americium Branching Ratios and Gamma Ray Energies**

<b>Isotope</b>	<b>Energy (keV)</b>	<b>Branching Ratio (photons/dis)</b>	<b>Error (%)</b>	<b>Activity (photons/s/g)</b>
239Pu	808.400	1.210E-09	5	2.776E+00
241Am	811.8	6.05E-09	12	7.66E+02
239Pu	813.700	4.510E-10	10	1.035E+00
239Pu	816.000	2.410E-10	15	5.529E-01
241Am	819.3	4.00E-09	15	5.06E+02
239Pu	821.300	5.520E-10	10	1.266E+00
241Am	822.6	2.18E-09	25	2.76E+02
239Pu	826.800	1.800E-10	30	4.130E-01
241Am	828.5	2.43E-09	25	3.08E+02
239Pu	828.900	1.330E-09	6	3.051E+00
239Pu	832.500	2.960E-10	12	6.791E-01
239Pu	837.300	1.910E-10	20	4.382E-01
239Pu	840.400	4.810E-10	10	1.104E+00
239Pu	844.000	1.340E-09	5	3.074E+00
241Am	851.5	3.77E-09	15	4.77E+02
238Pu	851.700	1.290E-08	2	8.170E+03
241Am	854.7	2.00E-09	20	2.53E+02
241Am	859.2	8.16E-10	30	1.03E+02
241Am	862.6	5.34E-09	10	6.76E+02
239Pu	879.200	3.160E-10	10	7.250E-01
241Am	887.5	2.22E-09	20	2.81E+02
239Pu	891.000	7.930E-10	10	1.819E+00
239Pu	895.400	7.490E-11	30	1.718E-01
239Pu	898.100	1.750E-10	20	4.015E-01
241Am	898.4	7.22E-10	40	9.14E+01
241Am	902.5	3.00E-09	15	3.80E+02
239Pu	905.500	7.510E-11	30	1.723E-01
239Pu	911.700	1.370E-10	25	3.143E-01
241Am	912.4	2.50E-09	20	3.16E+02
239Pu	918.700	8.440E-11	35	1.936E-01
241Am	922.2	1.91E-09	20	2.42E+02
241Am	928.8	5.52E-10	50	6.99E+01
239Pu	931.900	1.270E-10	35	2.914E-01

**APPENDIX D Plutonium, Americium Branching Ratios and Gamma Ray Energies**

<b>Isotope</b>	<b>Energy (keV)</b>	<b>Branching Ratio (photons/dis)</b>	<b>Error (%)</b>	<b>Activity (photons/s/g)</b>
239Pu	940.300	4.960E-10	10	1.138E+00
241Am	945.7	5.60E-10	50	7.09E+01
239Pu	955.600	3.090E-10		7.089E-01
241Am	955.7	5.78E-09	10	7.31E+02
239Pu	957.600	3.200E-10	10	7.341E-01
239Pu	979.700	2.760E-10	15	6.332E-01
239Pu	982.700	1.080E-10	25	2.478E-01
239Pu	986.900	2.090E-10	20	4.795E-01
239Pu	992.700	2.660E-10	15	6.103E-01
239Pu	1005.700	1.780E-10	15	4.084E-01
239Pu	1009.400	1.400E-10	20	3.212E-01

R. Gunnink, J. E. Evans, and A. L. Prindle, A Reevaluation of the Gamma-Ray Energies and Absolute Branching Intensities of <sup>237</sup>U, <sup>238</sup>, <sup>239</sup>, <sup>240</sup>, <sup>241</sup>Pu, and <sup>241</sup>Am, Lawrence Livermore Laboratory report UCRL-52139, October 1976.

Table D-2. Constants.

<b>Isotope</b>	<b>Atomic Mass</b>	<b>Half Life (yr)</b>	<b>Dis/s/g</b>
<sup>238</sup> Pu	238.049554	87.74	6.33310 E+11
<sup>239</sup> Pu	239.052157	24119	2.29419 E+09
<sup>240</sup> Pu	240.053808	6564	8.39468 E+09
<sup>241</sup> Pu	241.056845	14.348	3.82446 E+12
<sup>242</sup> Pu	242.058737	376300	1.45220 E+08
<sup>241</sup> Am	241.056823	433.6	1.26553 E+11
1 year	365.24220	days	
N <sub>0</sub>	6.0221367E+23	mol-1	
<sup>241</sup> Pu- <sup>237</sup> U	2.45E-05	branching fraction	

APPENDIX E

Americium-241/Plutonium-239 Peak Pairs

INTRODUCTION

Table E-1 below displays the  $^{241}\text{Am}/^{239}\text{Pu}$  concentration ratio for closely spaced (in energy) peak pairs when the two peaks have the same intensity. The calculation neglects differences in relative efficiency between the two peaks. Note, also, that the ratio is taken with respect to  $^{239}\text{Pu}$ , not total plutonium. This table can be used in conjunction with simple visual examination of the pulse height spectrum or can be applied to extracted peak area data.

We present ratios only for peak pairs that can be visually separated in the spectrum.

Table E-1. Useful Americium-241/Plutonium-239 Peak Pairs.

Am-241 (keV)	Pu-239 (keV)	$^{241}\text{Am}/^{239}\text{Pu}$ Concentration Ratio for Equal Peak Intensities	Comment
59.54	51.63	1.36 E-05	Can only be used for freshly separated materials.
125.29	129.29	0.0278	Best above 5000 ppm $^{241}\text{Am}$ . Pu-239 interferences to $^{241}\text{Am}$ neglected in ratio.
169.56	171.34	0.0116	
376.59	375.04	0.206	
419.24	413.71	0.942	Best for very high $^{241}\text{Am}$
662.42	645.97	0.00074	Best for very low $^{241}\text{Am}$

## **APPENDIX F**

### **Characteristics of Isotopic Standards**

This appendix tabulates the characteristics of the isotopic standards used to characterize the performance of the FRAM software.

Table F-1. Archival Data Set for Coaxial Detector Analysis.

File Name	Accepted Values								Pu Mass (g)	No. runs	Ct. Rate (kHz)	Ct time (h)	Data Date
	wt %					ppm 241 Am	mW/gPu Spec Pow	Pu240 Eff					
	238	239	240	241	242								
ISO03CX-2001	0.006	96.36	3.56	0.054	0.018	736	2.229	3.61	10.97	20	40	0.5	10-Aug-2001
stdiso03_01	0.006	96.36	3.56	0.055	0.018	726	2.228	3.61	11	20	40	0.5	23-Mar-2001
ISO3CX8K	0.006	96.34	3.56	0.076	0.018	518	2.207	3.61	10.97	10	30	2	10-May-1994
SGCOAX8K	0.006	96.34	3.56	0.078	0.018	499	2.205	3.61	100	10	30	2	21-Oct-1993
92COAX8K	0.008	94.63	5.26	0.084	0.014	2004	2.477	5.31	10	10	30	2	18-Oct-1993
86COAX8K	0.010	94.26	5.60	0.106	0.018	2192	2.526	5.66	10	10	30	2	20-Oct-1993
CALX30	0.009	93.92	5.86	0.176	0.029	1987	2.511	5.93	398.2	10	30	1	2-Nov-1994
CALX30PB	0.009	93.93	5.86	0.176	0.029	1995	2.512	5.93	398.2	11	30	1	6-Dec-1994
EUPU7CX8	0.014	93.84	5.86	0.220	0.066	793	2.402	6.01	5	10	30	2	22-Oct-1993
PUEU730	0.014	93.85	5.86	0.209	0.066	898	2.413	6.01	2000	11	30	1	3-Nov-1994
PUEU7PB	0.014	93.85	5.86	0.209	0.066	900	2.413	6.01	2000	11	30	1	8-Nov-1994
STDEUPU7-2001	0.013	93.91	5.86	0.150	0.066	1478	2.475	6.01	5	30	30	0.5	18-Sep-2001
JOO1325	0.011	93.93	5.90	0.132	0.028	1694	2.488	5.98	499.6	11	30	1	22-Dec-1994
J1325PB1	0.011	93.93	5.90	0.132	0.028	1693	2.488	5.98	499.6	11	30	1	20-Dec-1994
J1325PB2	0.011	93.93	5.90	0.132	0.028	1693	2.488	5.98	499.6	11	30	1	17-Dec-1994
PIDIE6-1-2001	0.010	93.86	5.99	0.103	0.035	3178	2.657	6.07	0.4	21	40	0.5	8-Aug-2001
PID6_1	0.010	93.83	5.99	0.131	0.035	2928	2.631	6.07	0.4	21	2.9	1	2-Oct-1996
ISO6CX8K	0.013	93.59	6.13	0.206	0.057	1163	2.455	6.26	8.45	10	30	2	6-May-1994
ISO06CX-2001	0.013	93.65	6.13	0.145	0.057	1755	2.517	6.26	8.4	21	40	0.5	8-Aug-2001
STD830	0.009	93.55	6.30	0.116	0.025	1758	2.509	6.37	239.5	11	30	1	10-Jan-1995
STD8PB	0.009	93.55	6.30	0.117	0.025	1755		6.37	239.5	11	30	1	23-Dec-1994
cbnm93_01	0.010	93.53	6.31	0.110	0.040	2150	2.560	6.41	0.6	20	40	0.5	19-Mar-2001
93COAX8K	0.011	93.48	6.31	0.157	0.040	1697	2.512	6.41	6	10	30	2	9-Oct-1993
ISO9CX8K	0.020	92.73	6.89	0.282	0.073	1490	2.570	7.07	11.9	10	30	2	7-May-1994
stdiso09_01	0.019	92.81	6.90	0.202	0.073	2270	2.652	7.07	12	20	40	0.5	
ISO09CX-2001	0.019	92.81	6.90	0.199	0.073	2305	2.656	7.07	11.9	29	40	0.5	8-Aug-2001
2G118CX8	0.025	90.49	9.01	0.374	0.104	3822	2.975	9.25	2.5	10	30	2	23-Oct-1993
PID6_2	0.021	89.48	10.11	0.293	0.094	4148	3.046	10.32	0.4	21	3.2	1	4-Oct-1996
SD4030	0.062	87.34		0.606	0.201	6534	3.638	12.28	869	11	30	1	9-Nov-1994
SD4030PB	0.062	87.34	11.79	0.605	0.201	6543	3.639	12.28	869	11	30	1	21-Nov-1994
2G119CX8	0.036		11.80	0.578	0.168	5919	3.421	12.17	2.5	10	30	2	24-Oct-1993
ISO12C8K	0.055	87.24	11.84	0.645	0.222	4330	3.350	12.35	20.2	10	30	2	8-May-1994
ISO12CX-2001	0.052	87.42	11.85	0.455	0.223	6190	3.544	12.36	20.2	20	40	0.5	9-Aug-2001
PID6_3	0.044	84.88	14.19	0.655	0.235	9569	4.008	14.69	0.4	21	3.2	1	3-Oct-1996
PIDIE6-3-2001	0.043	85.00	14.20	0.519	0.235	10872	4.147	14.70	0.4		17	0.5	6-Aug-2001
84COAX8K	0.067	84.61	14.24	0.724	0.359	5203	3.638	15.01	6	10	30	2	10-Oct-1993
cbnm84_01	0.063	84.80		0.507	0.360	7334	3.859	15.03	0.6	20	40	0.5	21-Mar-2001
ISO15C8K	0.160	82.54	15.48	1.103	0.715	5735	4.290	17.08	12.3	10	30	2	9-May-1994
stdiso15_01	0.152	82.82	15.52	0.794	0.717	8806	4.593	17.11	12	20	40	0.5	27-Mar-2001
ISO15CX-2001	0.152	82.83	15.52	0.780	0.717	8943	4.606	17.11	12.3	26	40	0.5	9-Aug-2001
2G121CX8		82.21	16.53	0.853		7403	3.960	17.27	2.5	10	30	2	3-Nov-1993
LAO225PB	0.058	82.25	16.53	0.809	0.354	7841	4.007	17.27	868.8	11	30	1	15-Dec-1994
LAO22530		82.25	16.53	0.809	0.354	7846	4.008	17.27	868.8	10	30	1	20-Dec-1994
70COAX8K	0.812	74.57	18.60	3.904	2.113	28204	10.722	24.19	6	10	30	2	10-Oct-1989
cbnm70_01	0.776	75.51	18.82	2.759	2.140	40097	11.866	24.37	0.6	20	40	0.5	22-Mar-2001
PID6_4	0.102	78.24	19.89	1.204	0.571	21980	6.047	21.10	0.4	21	6.5	1	4-Dec-1996
PIDIE65	0.123	76.46	21.36	1.352		24409	6.523	22.86		21	15		29-Nov-1996
PIDIE6-5-2001	0.119	76.67	21.41	1.081	0.710	27037	6.798	22.91	0.4	21	26	0.5	7-Aug-2001
PIDIE66	0.884	67.65	24.34		3.627	56522	14.623	32.66	0.4	21		1	30-Nov-1996
61COAX8K	1.154	63.85	25.93	4.791	4.282	34776	13.756	36.03	6	10	30	2	11-Oct-1989
PIDIE67	1.196	63.49	26.20	4.324	4.791	59164	16.779	37.26	0.4	21	29	1	1-Dec-1996
cbnm61_01	1.105	64.83	26.31	3.398	4.349	49504	15.160	36.41	0.6	20	40	0.5	20-Mar-2001
PIDIE6-7-2001	1.164	64.08	26.43	3.482	4.836	68082		37.49	0.4	26	40	0.5	7-Aug-2001

Table F-2. Isotopic Characteristics of Los Alamos Uranium Standards.

Sample	wt %			
	U-234	U-235	U-236	U-238
NBL-0079(93)	0.9800	93.170	0.2937	5.556
C20-8		93.170		
UIISO-91	0.9103	91.336	0.3351	7.419
UIISO-66	0.5781	66.040	0.2590	33.122
NBL-0078 (53)	0.3718	52.488	0.2645	46.876
UIISO-52	0.5306	52.117	0.8676	46.484
UIISO-38	0.2598	37.552	0.2172	61.971
UIISO-27	0.2338	26.752	0.2697	72.745
NBL-0077(20)	0.1486	20.107	0.1973	79.547
UIISO-17	0.1380	17.239	0.1680	82.456
UIISO-13	0.0827	12.954	0.1013	86.862
UIISO-12	0.0719	11.797	0.1152	88.016
A1-323-1	0.0532	10.104	0.0913	89.751
A1-324-1	0.0512	10.086	0.0904	89.772
A1-324-2	0.0522	10.084	0.0904	89.773
NBS-446	0.0359	4.462	0.0069	95.495
A1-1126-2	0.0246	3.027	0.0169	96.931
A1-1126-1	0.0246	3.026	0.0159	96.934
NBS-295	0.0279	2.949	0.0033	97.020
NBS-194	0.0171	1.942	0.0003	98.041
A1-1125-2	0.0157	1.938	0.0089	98.038
A1-1125-1	0.0157	1.937	0.0089	98.039
A1-1127-1	0.0049	0.717	0.0020	99.276
A1-1127-2	0.0049	0.717	0.0020	99.277
A1-408-2	0.0049	0.714	0.0010	99.281
NBS-071	0.0052	0.712	0.0000	99.283
A1-409	0.0049	0.710	0.0010	99.284
NBS-031	0.0020	0.317	0.0146	99.667

Table F-3. Characteristics of the Los Alamos HUA Series of MOX Samples.

Sample	Pu Declared Values (wt %)					ppm <sup>241</sup> Am	mW/gPu	wt % <sup>240</sup> Pu <sub>eff</sub>
	<sup>238</sup> Pu	<sup>239</sup> Pu	<sup>240</sup> Pu	<sup>241</sup> Pu	<sup>242</sup> Pu			
HUA 5062	0.0614	87.397	11.831	0.533	0.178	15864	4.7020	12.284
HUA5065	0.0613	87.399	11.831	0.531	0.178	16062	4.7244	12.284
HUA5069	0.0558	87.554	11.693	0.510	0.187	13960	4.4452	12.147
HUA 5301	0.0464	87.629	11.668	0.472	0.185	8180	3.7306	12.095
HUA 8971	0.0549	87.377	11.826	0.533	0.21	9431	3.9297	12.316

Sample	Pu Mass (g)	U Mass (g)	<sup>235</sup> U (%)	<sup>235</sup> U/Pu	<sup>238</sup> U (%)	<sup>238</sup> U/Pu
HUA 5062	241.6	393.8	0.727	0.0118	99.25	1.618
HUA5065	304.9	438.8	0.769	0.0111	99.21	1.428
HUA5069	113.6	679.4	1.073	0.0642	98.91	5.915
HUA 5301	367.8	805.8	0.225	0.00495	99.77	2.186
HUA 8971	234.8	626	1.022	0.0272	98.96	2.638

Table F-4. Characteristics of ARIES NDA Standards and CALEX.

Sample	(g) Pu Mass	wt % Pu-238	wt % Pu-239	wt % Pu-240	wt % Pu-241	wt % Pu-242	μg/gPu Am-241	mW/gPu P-eff	wt % Pu-240eff
CALEX	400	0.0086	93.97	5.86	0.130	0.029	2430	2.558	5.93
MC-005	3000	0.0133	93.83	5.94	0.168	0.054	1300	2.460	6.06
MC-004	1500	0.0133	93.83	5.94	0.168	0.054	1300	2.460	6.06
MC-003	750	0.0133	93.83	5.94	0.168	0.054	1300	2.460	6.06

This report has been reproduced directly from the best available copy. It is available electronically on the Web (<http://www.doe.gov/bridge>).

Copies are available for sale to U.S. Department of Energy employees and contractors from:

Office of Scientific and Technical Information  
P.O. Box 62  
Oak Ridge, TN 37831  
(865) 576-8401

Copies are available for sale to the public from:

National Technical Information Service  
U.S. Department of Commerce  
5285 Port Royal Road  
Springfield, VA 22616  
(800) 553-6847



---

Los Alamos NM 87545